Validation of MK model for GENIE neutrino generator

Igor Kakorin, Konstantin Kuzmin, Vadim Naumov, Dmitry Shkirmanov

JINR, Dubna, Russia

May 2023

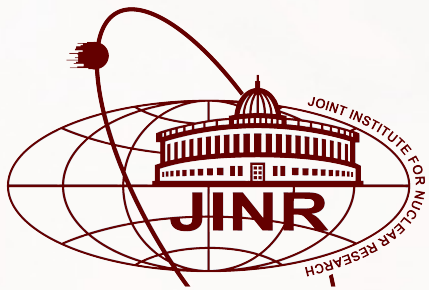

Table of Contents

Next topic

The genealogy of MK-model

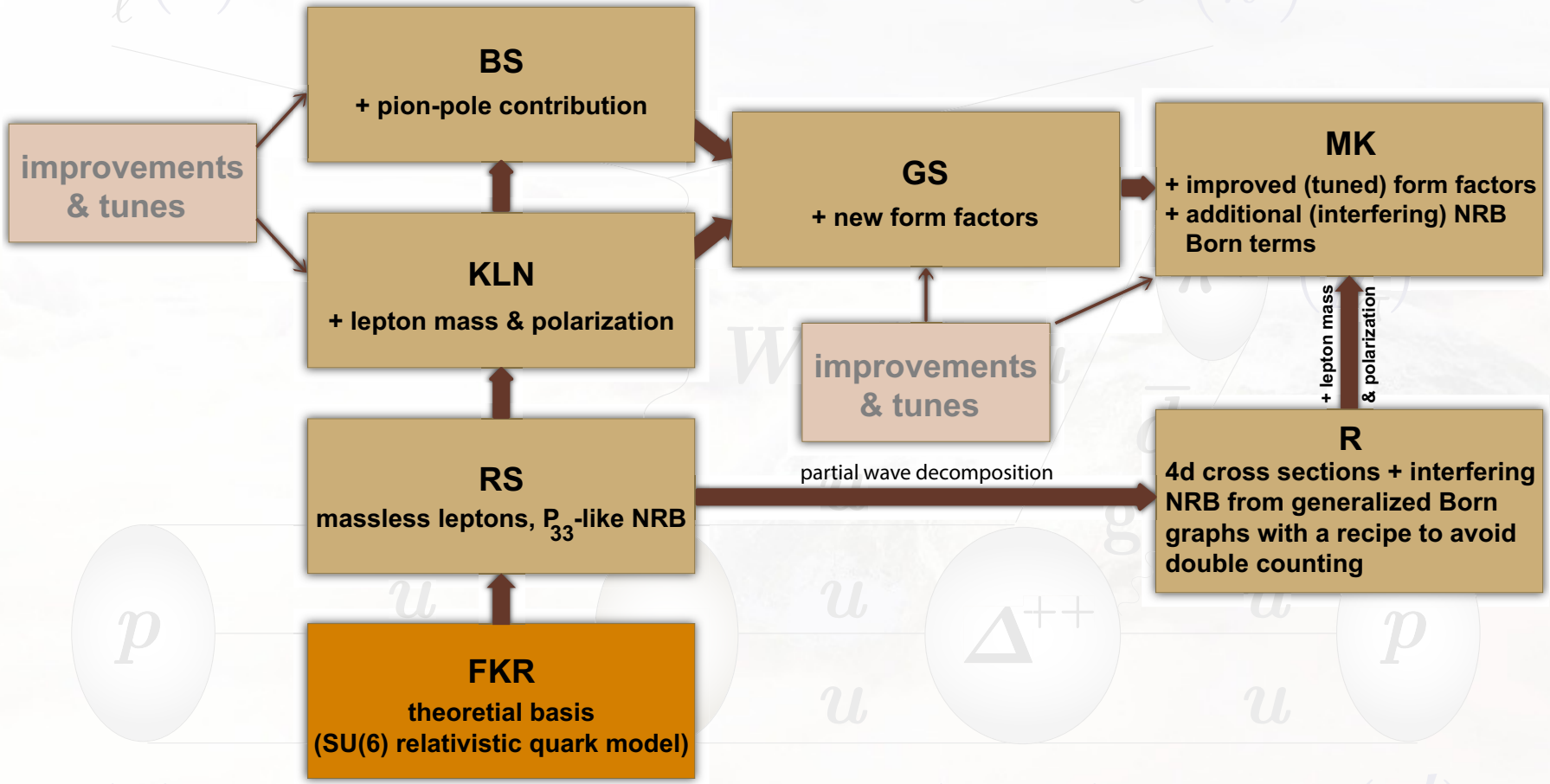

Current status of MK-model

The MK-model is implemented in GENIE according to the last version of code provided by the author. There are some differences between results presented in Ref. [1] and in this document due to differences in the original and current versions of the code:

1. The phases between resonance and non-resonant contributions are eliminated.
2. Vector and axial form factors for resonance contribution are taken according to Ref. [2], while in the previous code a modification of them were used.
3. The adjustable multipliers for vector and axial form factors are depending on resonance are eliminated.
4. The form factor for axial non-resonant part is the same as for vector one.
5. Several mistakes in formulas are fixed.
6. Some problems with signs in the multipole amplitudes are fixed.

However, we suppose that other mistakes are still remain in the model, which requires a more careful study.

χ^2/ndf

To roughly quantify the comparison between the predicted and measured event number distributions, we calculated χ^2 as follows:

$$\frac{\chi^2}{\text{ndf}} = \frac{1}{N-1}\sum_{i=1}^{N}\frac{(T_i - E_i)^2}{E_i},$$

where T_i (E_i) is the number of predicted (measured) events in ith bin and N is the number of bins with $T_i > 0.5$ and $E_i > 0.5$.

- For bins with $E_i = 0$ and $T_i > 0.5$ we substitute $\frac{(T_i - E_i)^2}{E_i} \longmapsto \frac{(T_i - E_i)^2}{T_i}$.
- For the W distributions, the normalization is performed to the region bounded by the condition $W \leqslant 2$ GeV (formal applicability range of all RS-based models). Also the corresponding χ^2 includes only bins with $W \leqslant 2$ GeV. However, we extrapolate the MC model beyond the 2 GeV region to see where it makes sense.

Next topic

Comparison with MK "as is" code in linear bin representation

Below we give a straightforward comparison of the MK code with its implementation in GENIE using **the same** set of input parameters.

- Not a single mistake has been corrected in the MK code, except for a few very obvious and trivial programming bugs (which usually have no noticeable effect on the result).
- We use the linear bin representation of the fourfold differential cross sections, in which the full phase space is devided into

$$N = 12 \times 12 \times 12 \times 12 \times 8 = 165888 \sim 1.6 \times 10^5$$

bins for, respectively,

$$E_\nu \in [\text{Threshold}, 250\ \text{GeV}], \quad W = W_{N\pi}, \quad Q^2, \quad \cos\theta_\pi, \quad \phi_\pi$$

(in the Adler frame for θ_π and ϕ_π) with equidistant separation on a logarithmic scale for the (anti)neutrino energy and linear for the other variables. Other measurable kinematic variables (e.g., $|\mathrm{p}_\pi|$, θ_μ, invariant masses of any pair of secondaries) are functions of the selected ones.

Comparison in linear bin representation

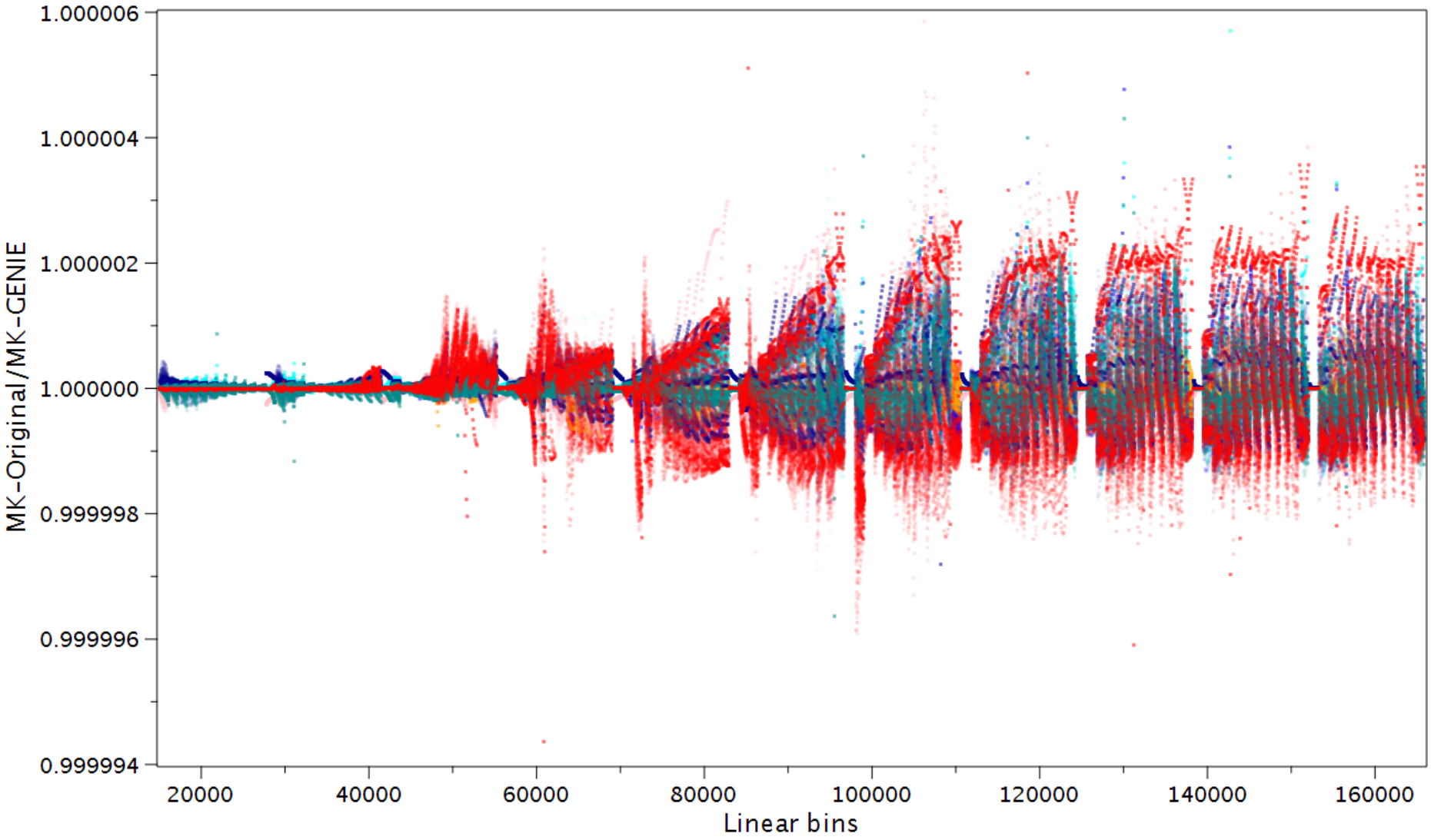

Cross-section ratios for all 7 CC & NC ν_μ induced reactions; same inputs, full phase space.

Comparison in linear bin representation

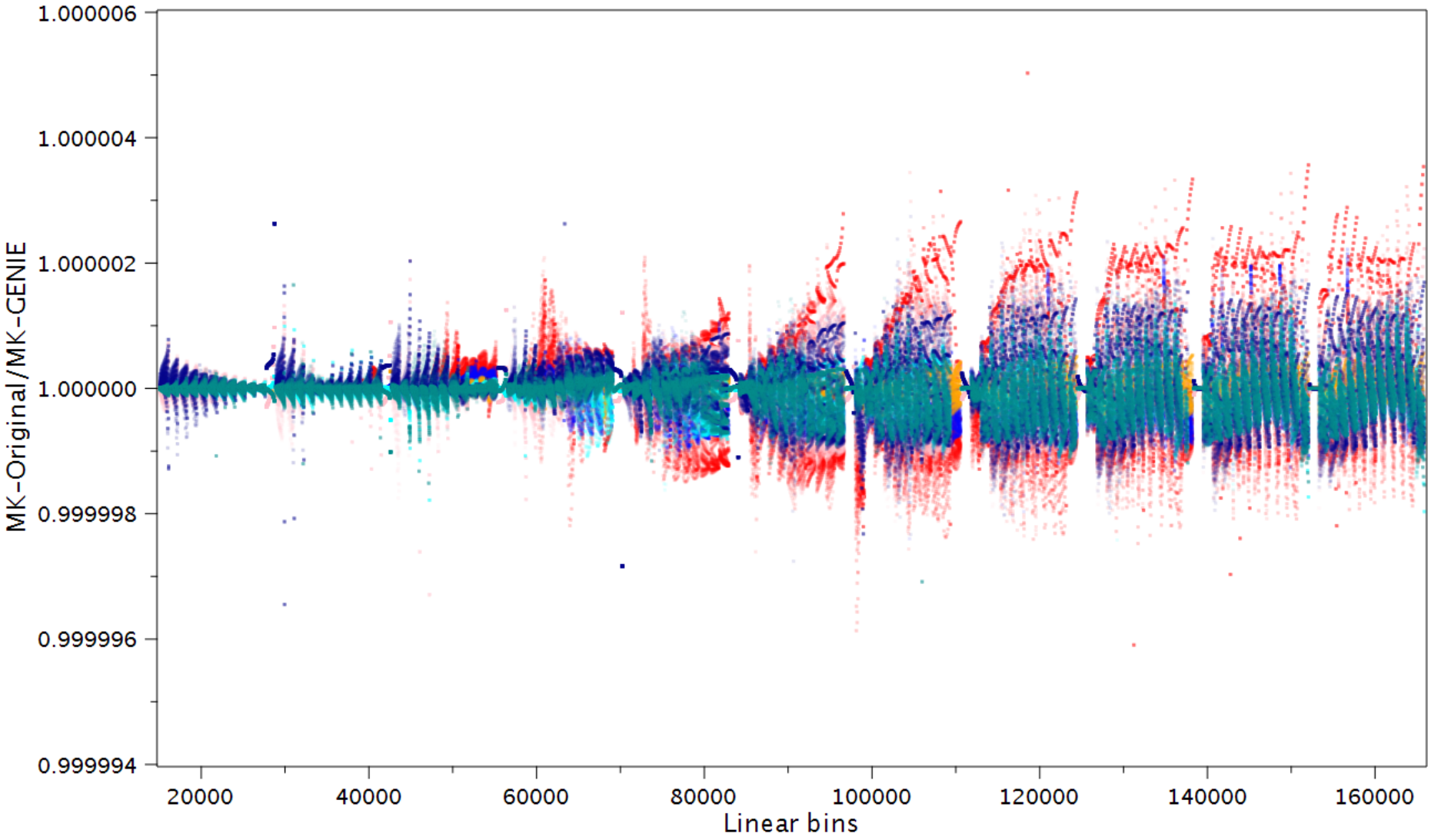

Cross-section ratios for all 7 CC & NC $\overline{\nu}_\mu$ induced reactions; same inputs, full phase space.

Comparison in linear bin representation

CONCLUSIONS:

- The original MK code and its implementation are consistent.
- Slight residual variatios ($\lesssim 5 \times 10^{-6}$) are due to unrecoverable differences in the numbers (like $\sqrt{2}$ and so on) appearing in the MK and GENIE codes.[1]
- Maximum fluctuations occur near kinematic boundaries and special points, such as $\cos\theta_{\mu,\pi} = \pm 1$.

[1] By the way, several years ago we recommended that this issue be unified, but it was not done. This is a minor point, which, however can lead to unnecessary pseudo-problems just in the testing process. Although this will not affect the actual calculations, in the final version of GENIE we would like to correct this matter (if there are no objections).

Next topic

Classification of mistakes in MK

1. Contradictions with the results of the works of Rein-Sehgal, Rein, Kuzmin *et al.*, and Berger-Sehgal.
   Example: the $\nu \longmapsto \overline{\nu}$ transition rules.
2. Obvious bugs, contradictions between the author and himself (in the Ph.D. thesis, the article, the code).
   Example: Phase factors (signs at ϕ in $\exp(\pm i\phi)$).
3. All kinds of checks (such as going beyond the kinematic boundaries and positivity of radicands), which are absent in the source code.

- For a complete list of mistakes and detailed formula output, see **Genie Document 181-v12** and related materials.[2]
- All of these mistakes have been fixed, but we can leave them as an option if necessary for some reasons.
- The main mistakes affect the only type of observables: distributions in ϕ_π.

[2] URL: https://genie-docdb.pp.rl.ac.uk/cgi-bin/private/ShowDocument?docid=181. Corrections that have been agreed upon with the author are noted there.

Classification of mistakes in MK

- In the comparisons below, for total cross sections, only predictions are shown calculated in the corrected version of GENIE, since the corrections do not affect the total and even the ϕ-integrated 3-fold cross sections.
- For the differential cross sections and distributions, we usually present four variants of calculations as explained in the (not too inventive) notation:
  - **All fixed**: Phase factors in the GENIE code are corrected taking into account the formulas from MK thesis and her paper.[3] Transition rules are corrected according to Kuzmin *et al.* and Berger and Sehgal.
  - **Fixed**: Same as above, but without the $F_{17}(1970)$ resonance[4] omitted in the MK code; just to show the (minor) role of the 2* high-mass resonance.
  - **All unfixed**: Phase factors and transition rules remain intact.
  - **Unfixed**: Same as above, but without $F_{17}(1970)$.
- Gray open symbols are for obsolete data.

[3] Recall that the phase factors in the MK code are different for CC and NC channels. The phases for the NC channel are the same as in the thesis and article.

[4] According to RPP-2022 it is $N(1990)\ 7/2^+$, status: ** [*"1* states are a dream, 2* states are a fantasy" (S. Dytman)*], $M_{\mathrm{BW}} \approx 2020$ MeV, $\Gamma_{\mathrm{BW}} \approx 300$ MeV, $\Gamma(N\pi)/\Gamma_{\mathrm{tot}} = 2 - 6\%$.

Next topic

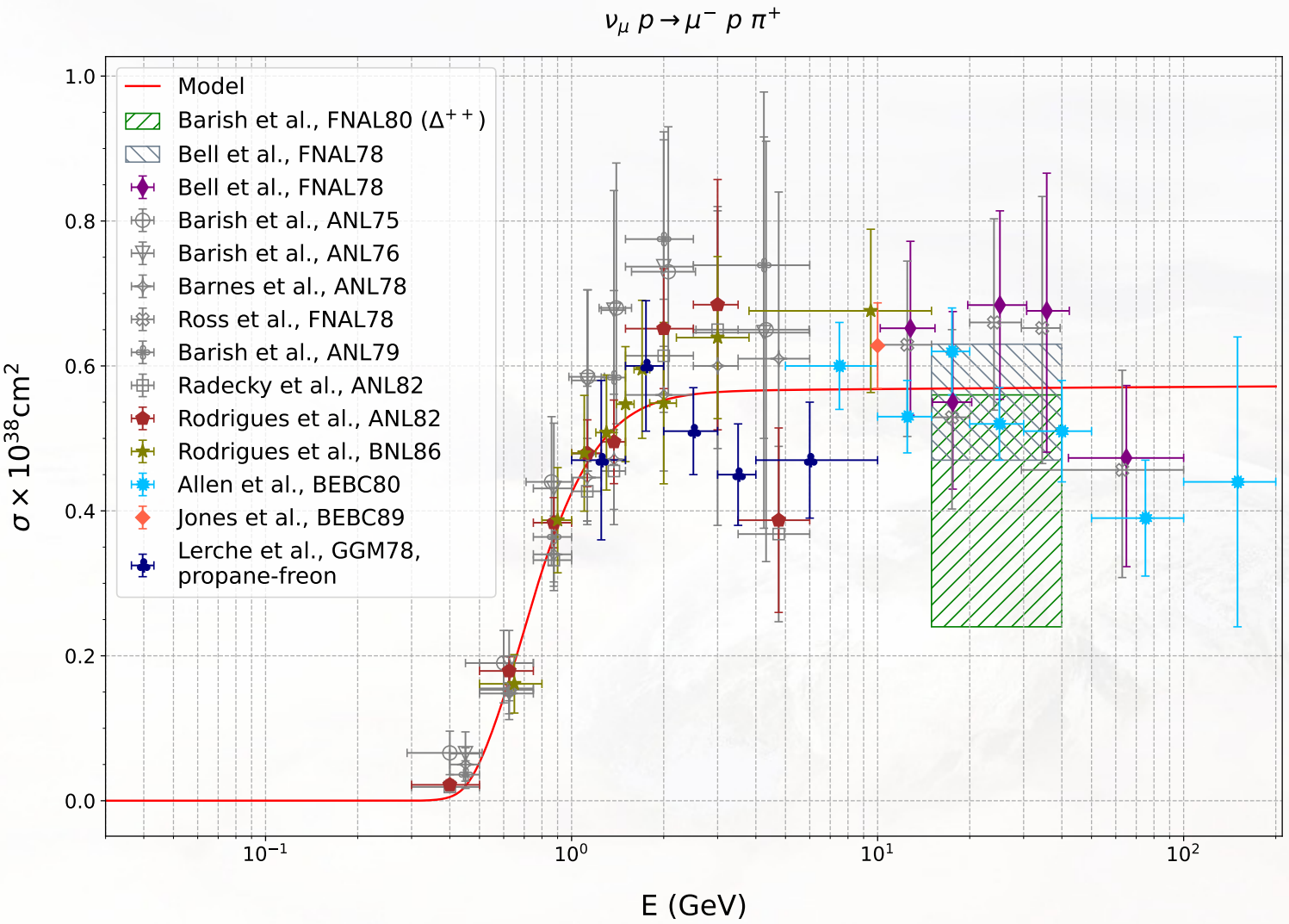

Total cross-section with the invariant hadronic mass $W < 1.4$ GeV. Data are taken from [3–15].

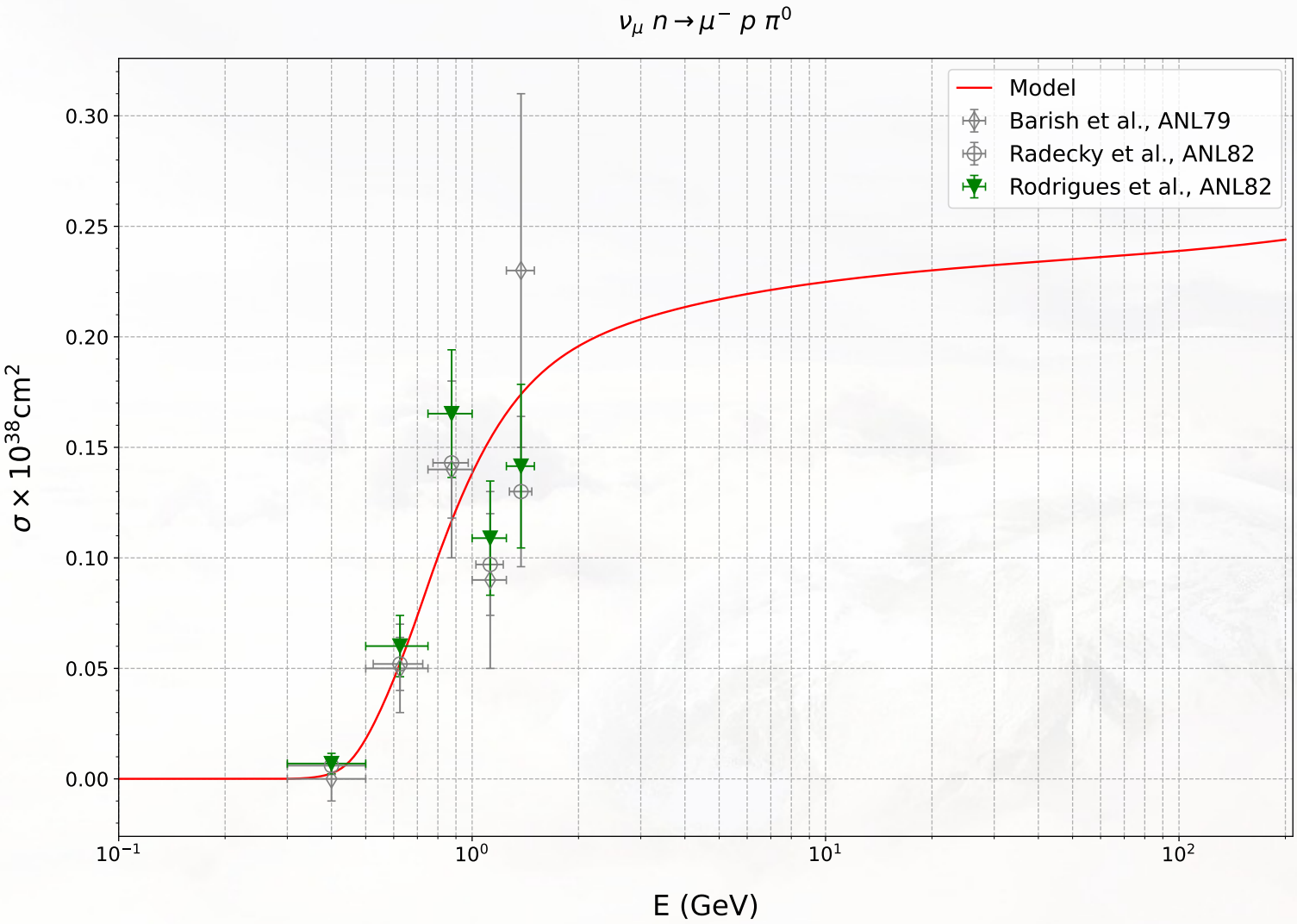

Total cross-section with the invariant hadronic mass $W < 1.4$ GeV. Data are taken from [6, 12, 16].

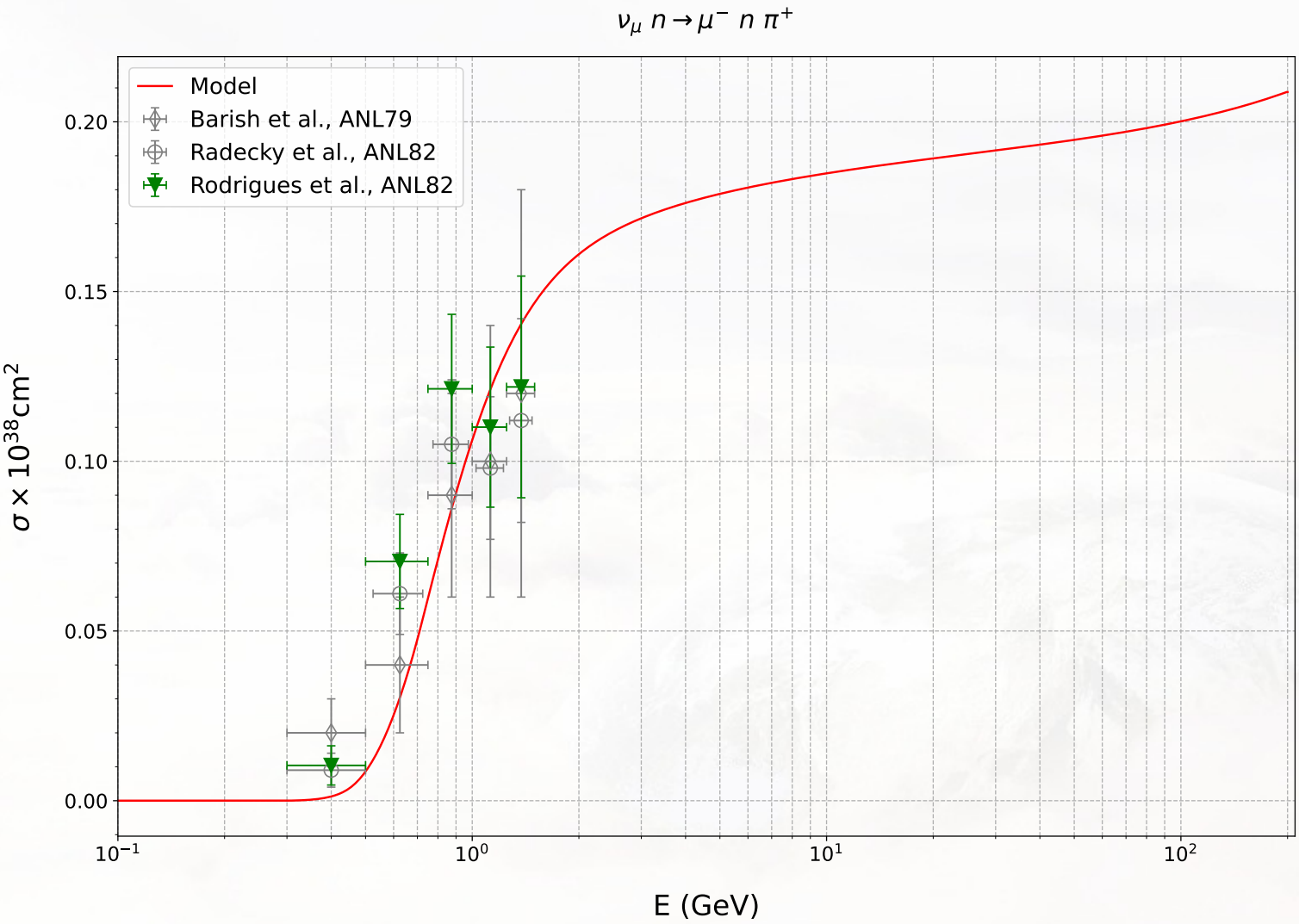

Total cross-section with the invariant hadronic mass $W < 1.4$ GeV. Data are taken from [6, 12, 16].

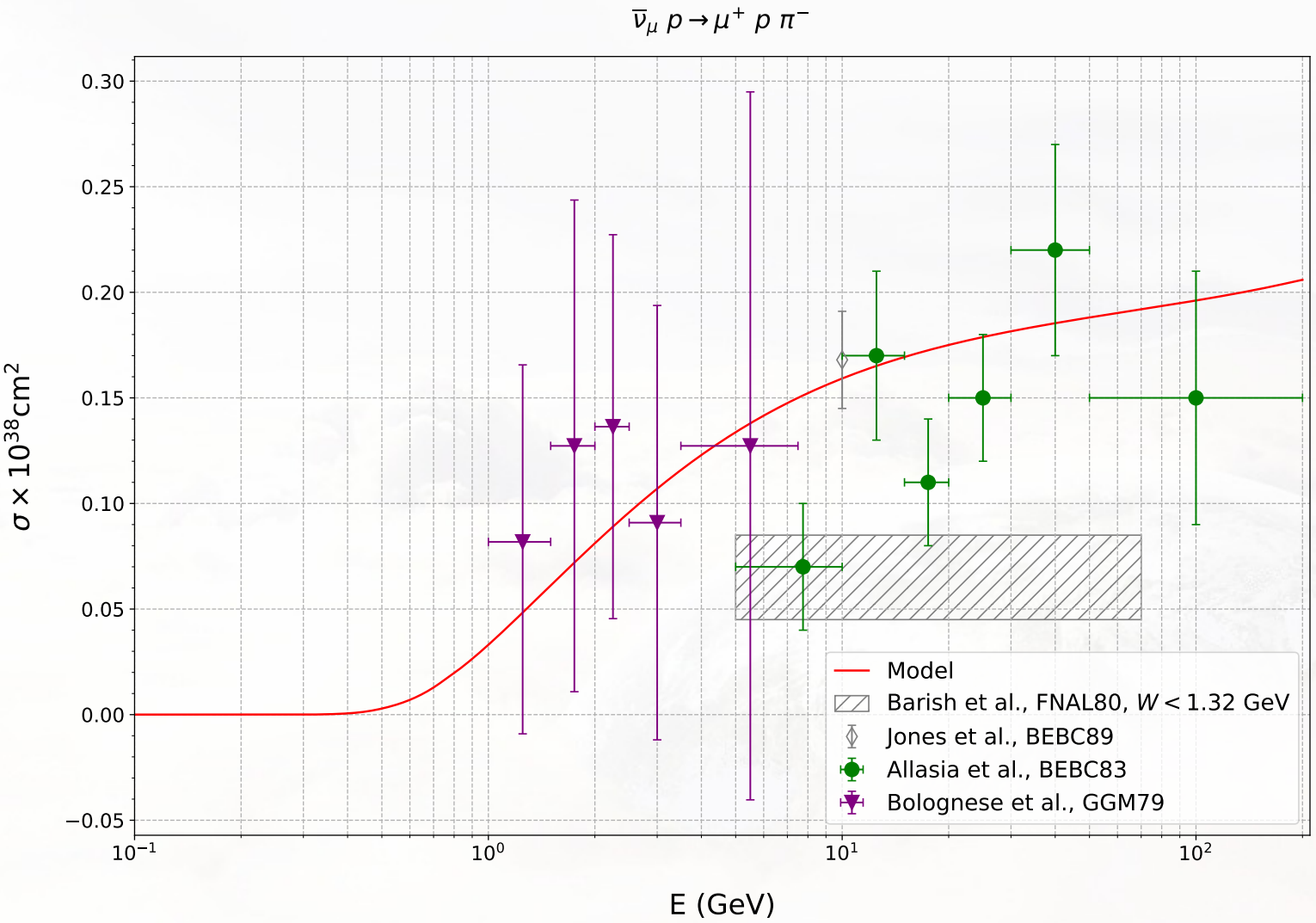

Total cross-section with the invariant hadronic mass $W < 1.4$ GeV. Data are taken from [4, 17–19].

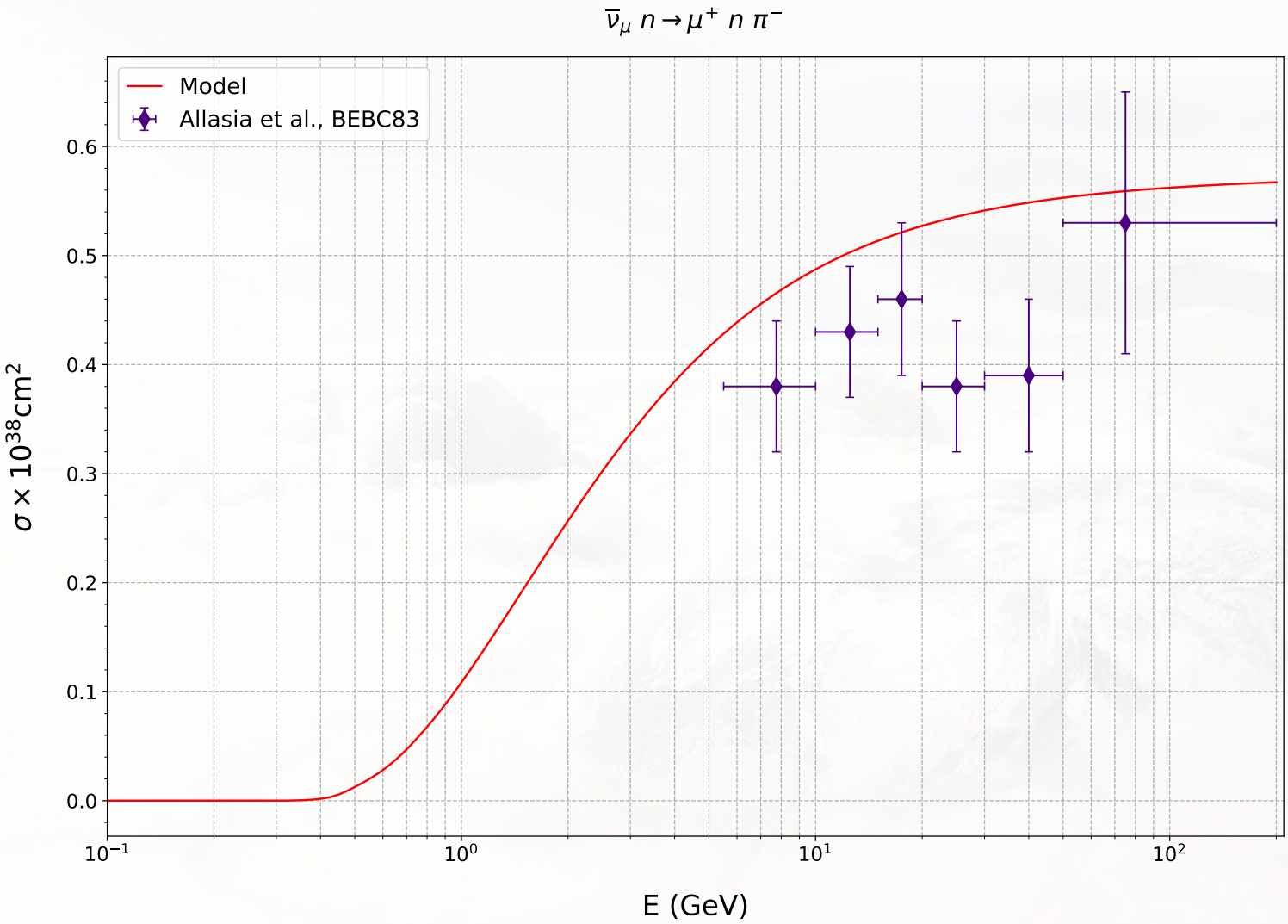

Total cross-section with the invariant hadronic mass $W < 1.4$ GeV. Data are taken from [19].

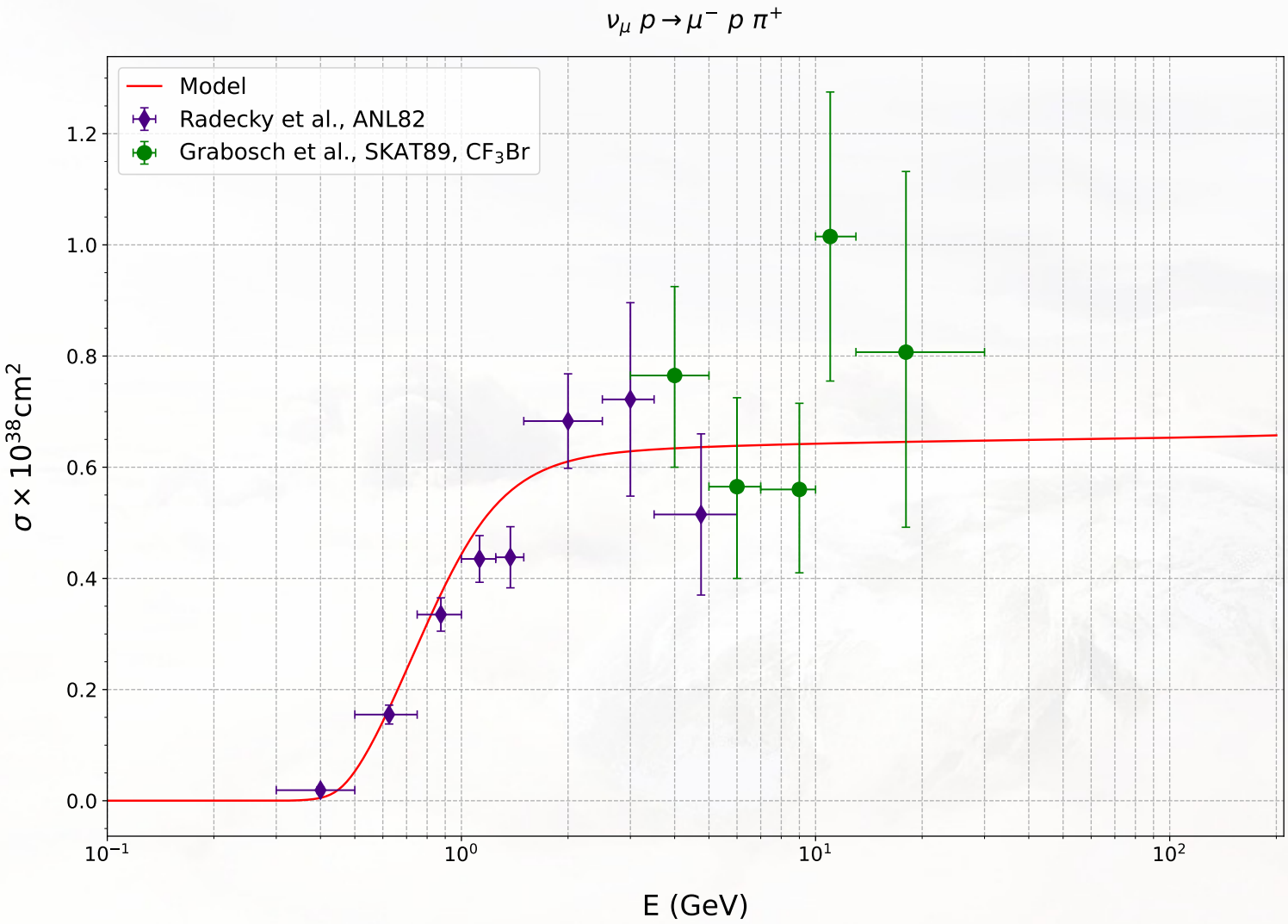

Total cross-section with the invariant hadronic mass $W < 1.6$ GeV. Data are taken from [6, 20].

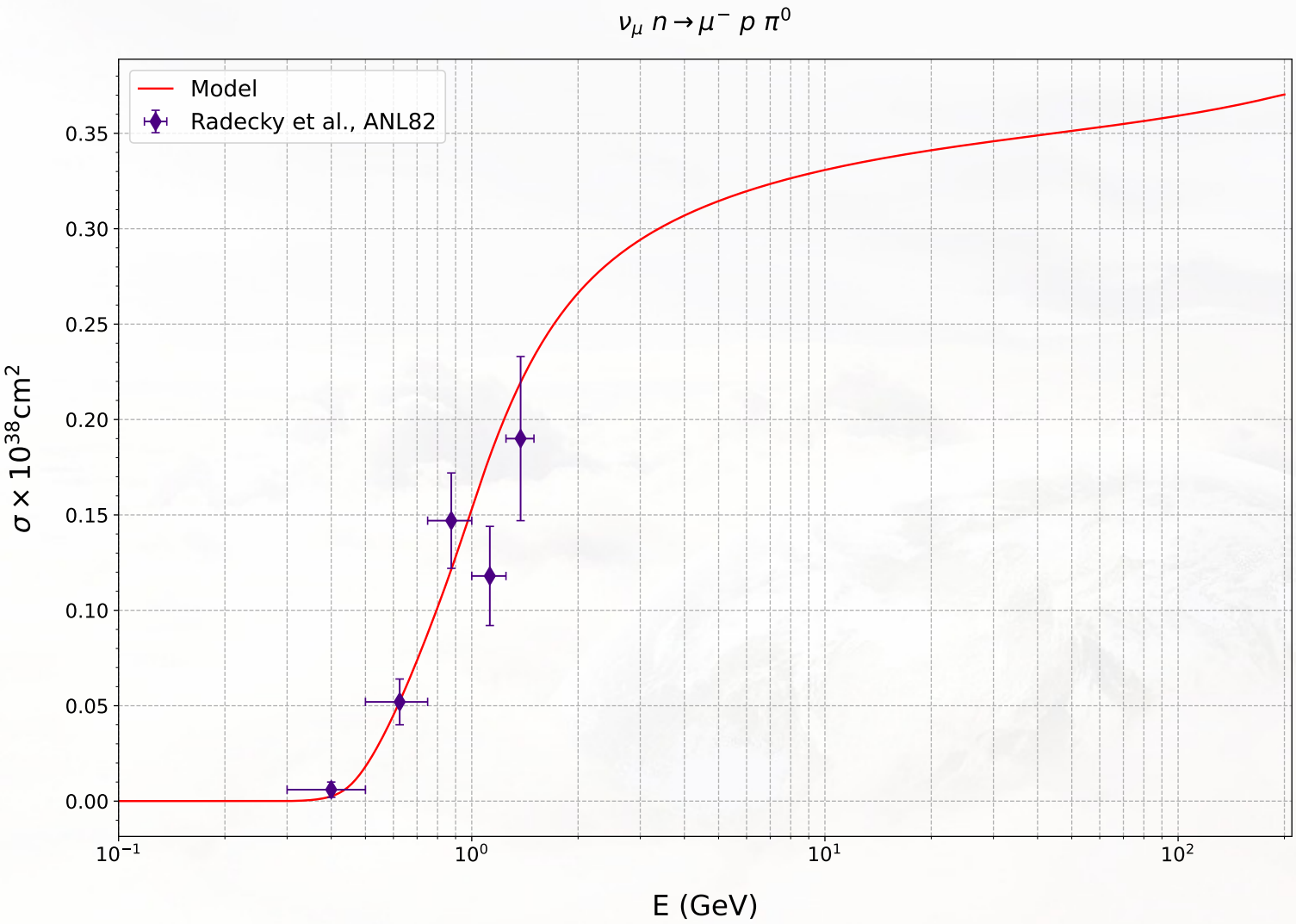

Total cross-section with the invariant hadronic mass $W < 1.6$ GeV. Data are taken from [6].

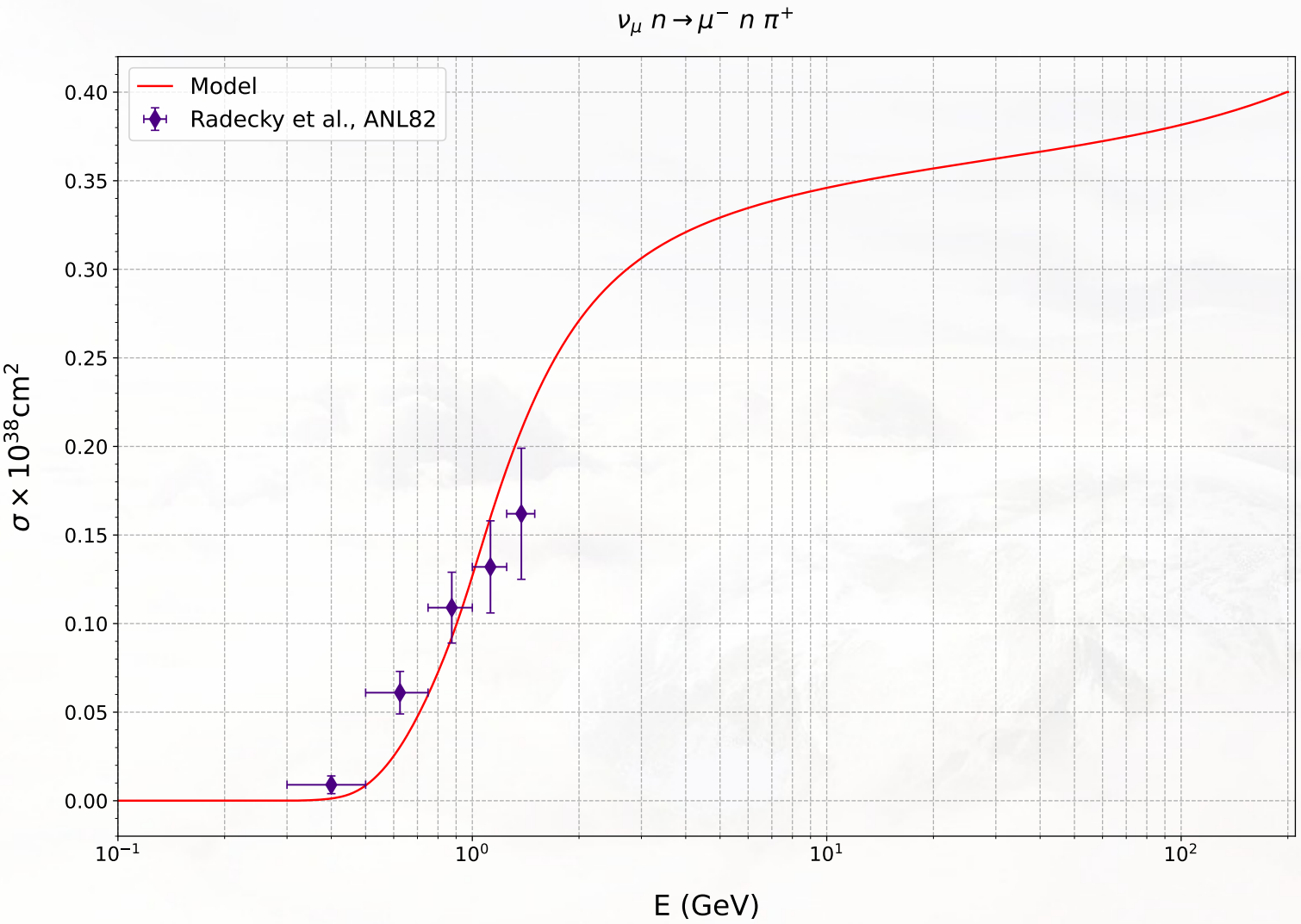

Total cross-section with the invariant hadronic mass $W < 1.6$ GeV. Data are taken from [6].

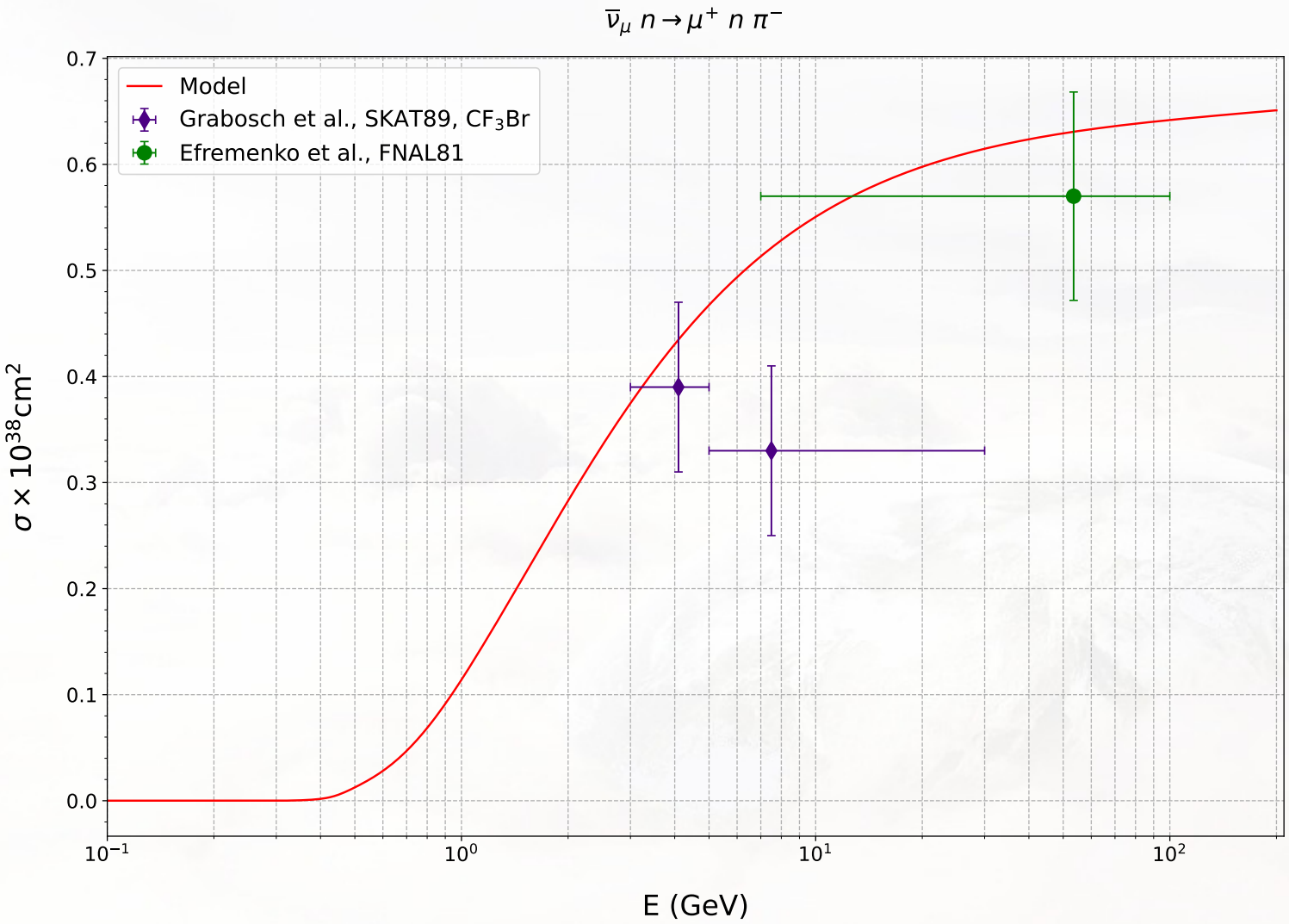

Total cross-section with the invariant hadronic mass $W < 1.6$ GeV. Data are taken from [20, 21].

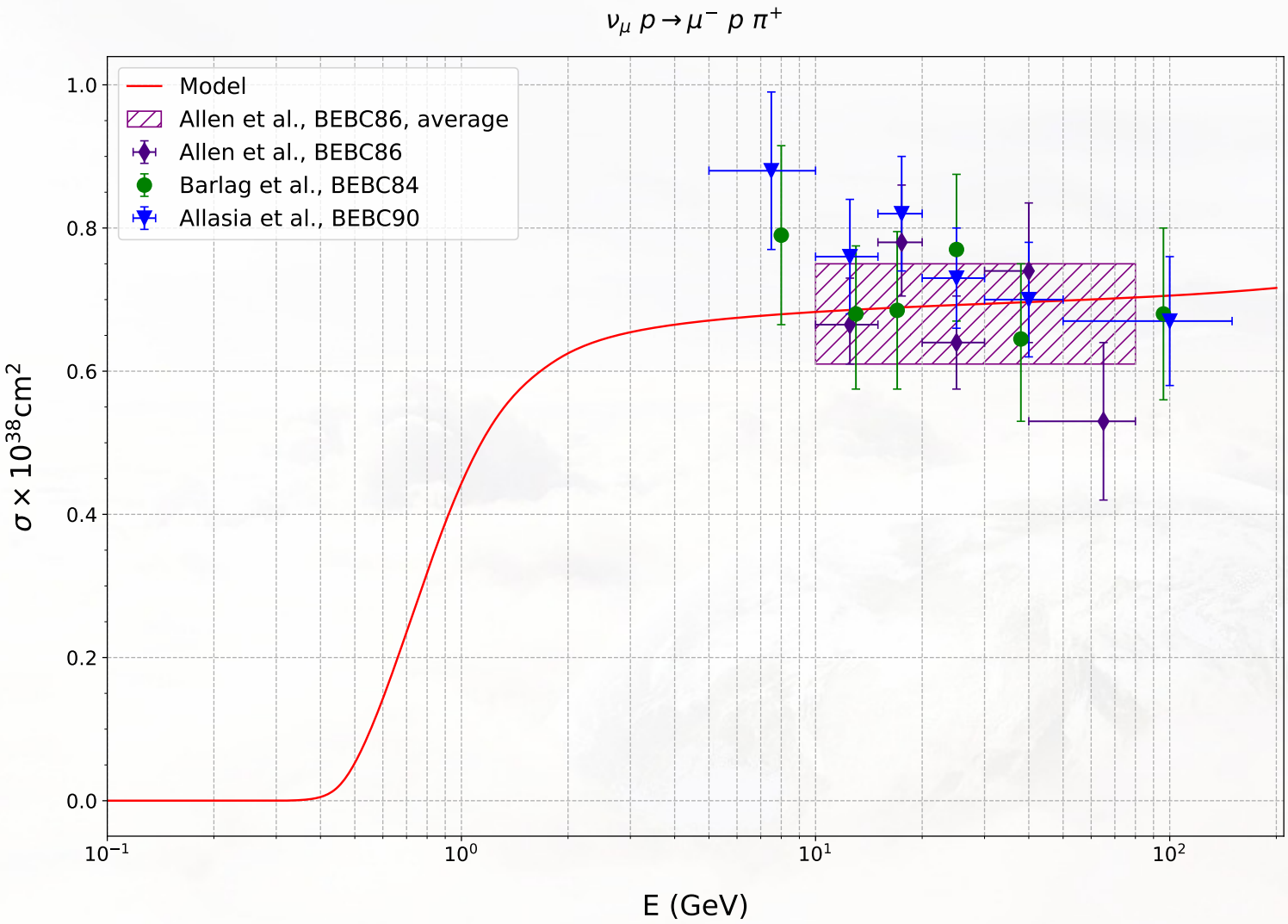

Total cross-section with the invariant hadronic mass $W < 2.0$ GeV. Data are taken from [22–24].

Cf Fig. 5 from Ref. [1]

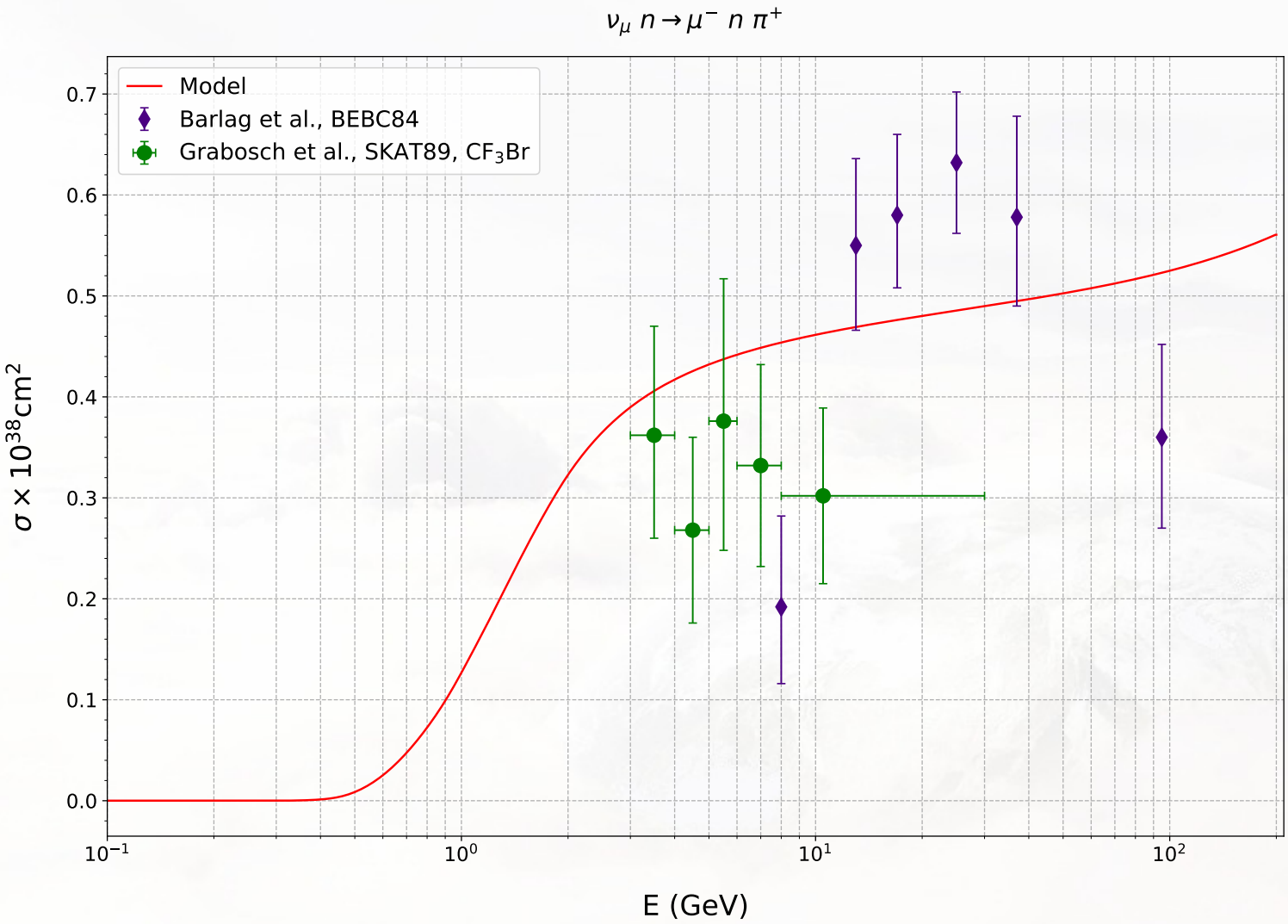

Total cross-section with the invariant hadronic mass $W < 2.0$ GeV. Data are taken from [20, 23]. Cf Fig. 5 from Ref. [1]

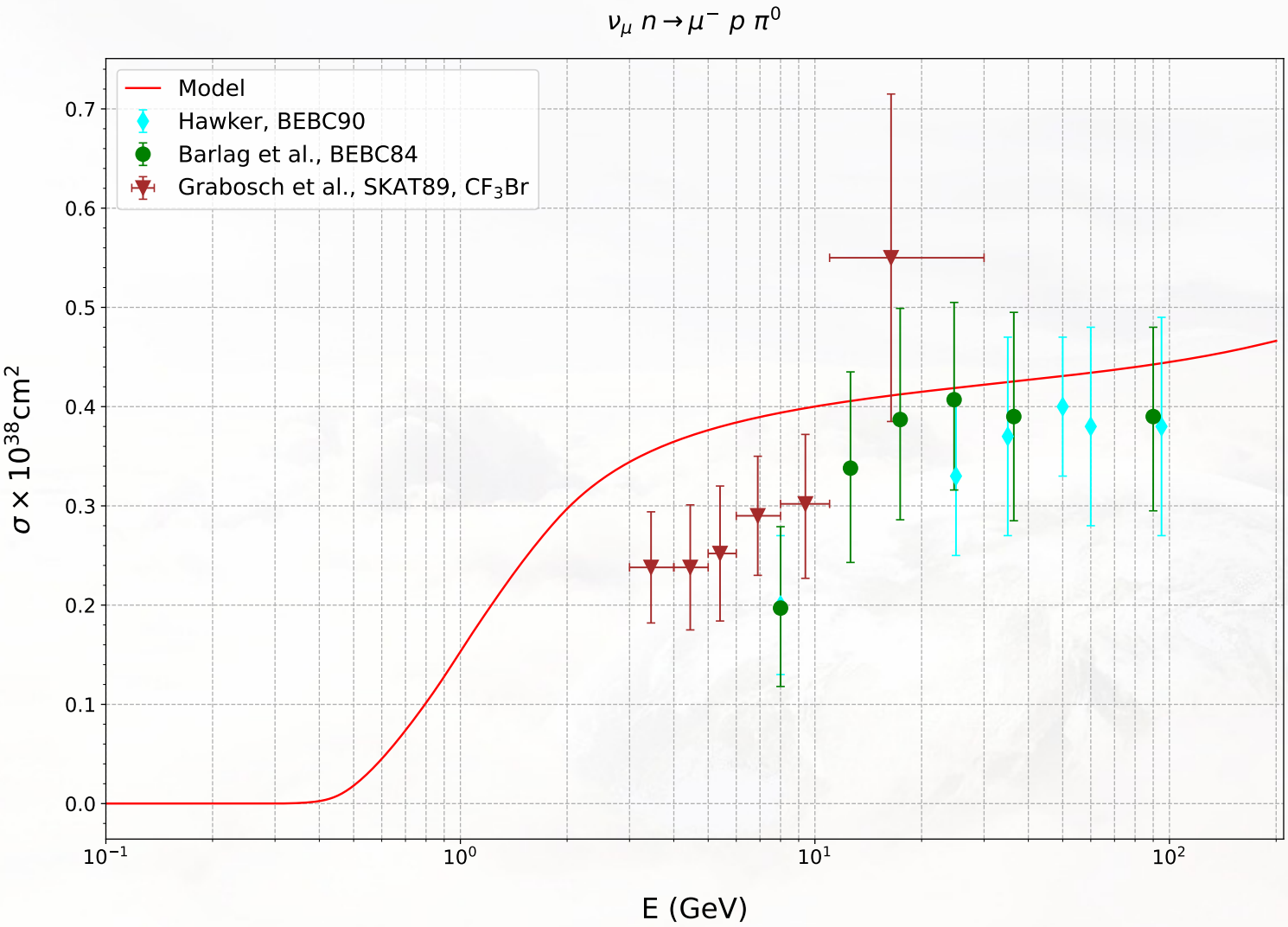

Total cross-section with the invariant hadronic mass $W < 2.0$ GeV. Data are taken from [20, 23, 25]. Cf Fig. 5 from Ref. [1]

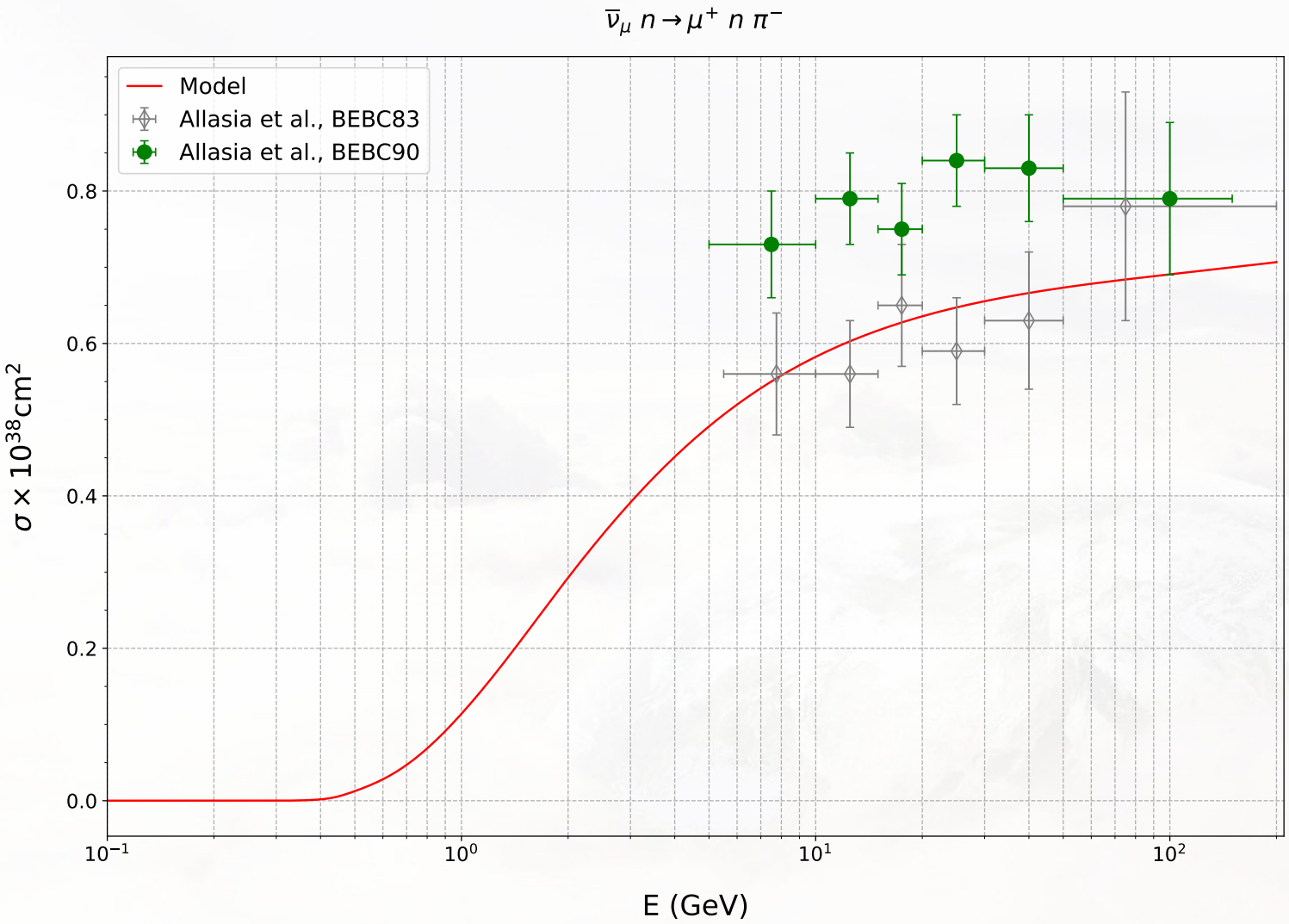

Total cross-section with the invariant hadronic mass $W < 2.0$ GeV. Data are taken from [19, 24]. Cf Fig. 6 from Ref. [1]

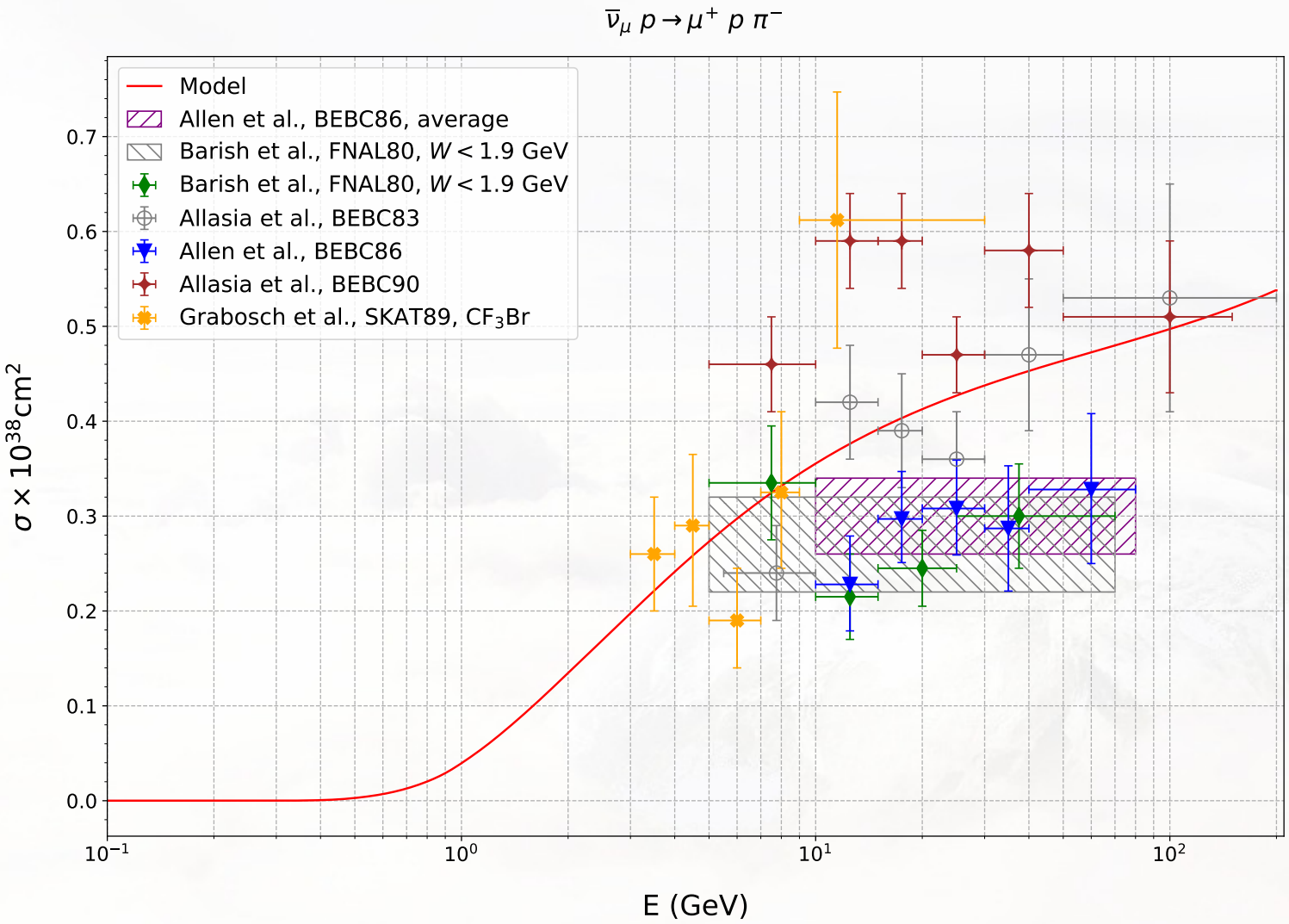

Total cross-section with the invariant hadronic mass $W < 2.0$ GeV. Data are taken from [10, 19, 20, 22, 24]. Cf Fig. 6 from Ref. [1]

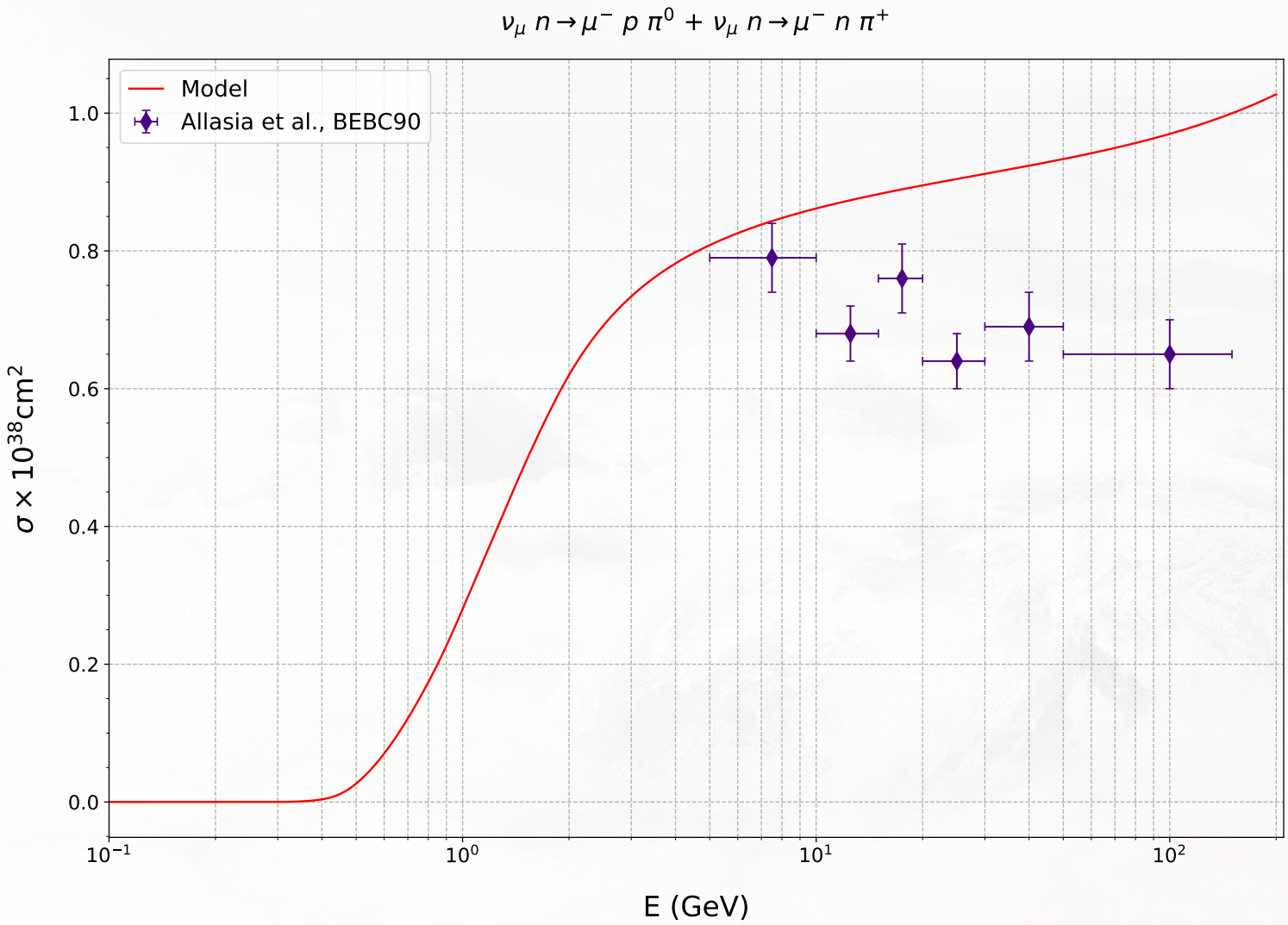

Total cross-section with the invariant hadronic mass $W < 2.0$ GeV. Data are taken from [24].

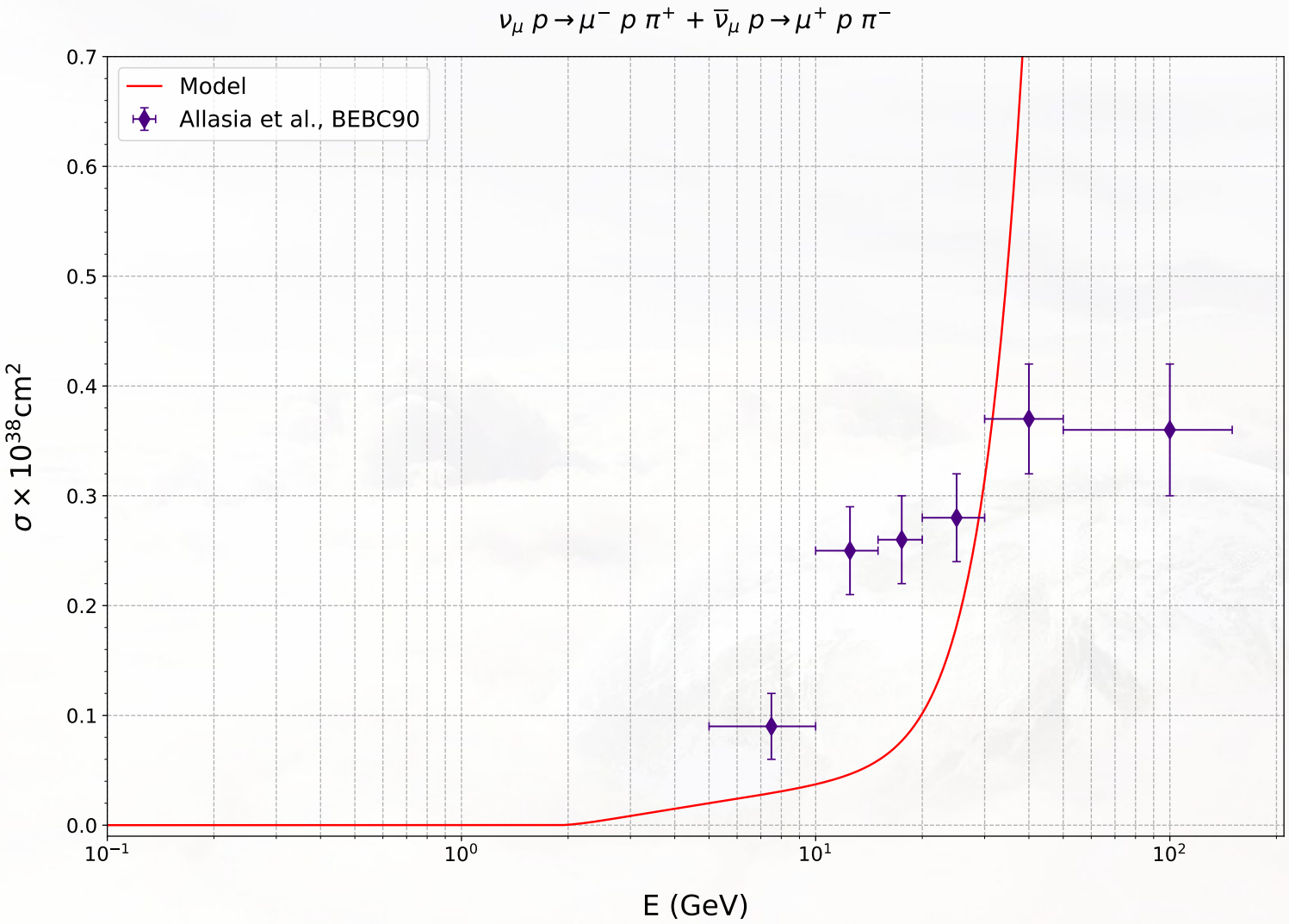

Total cross-section with $W > 2.0$. Data are taken from [24].

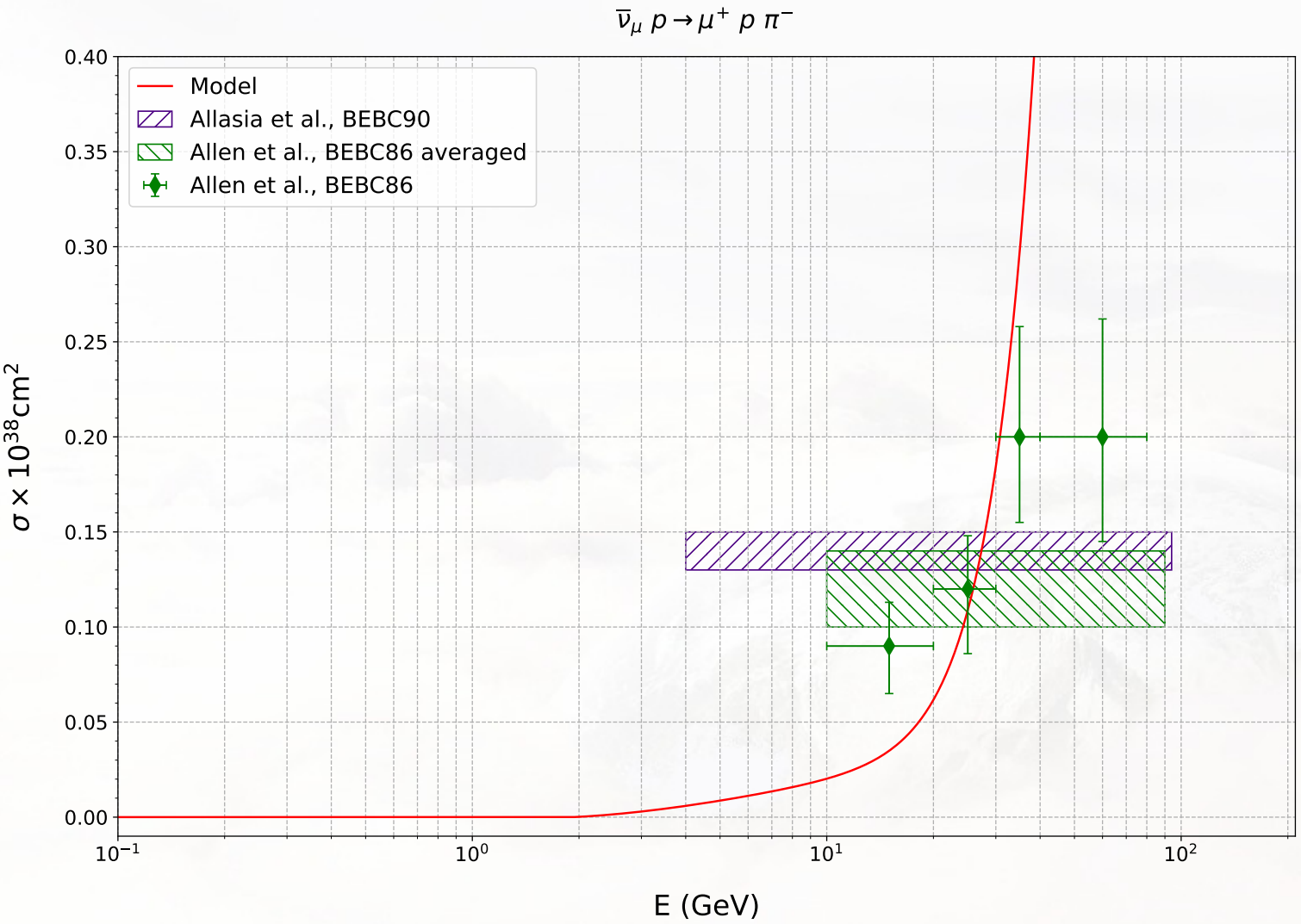

Total cross-section with $W > 2.0$. Data are taken from [22, 24].

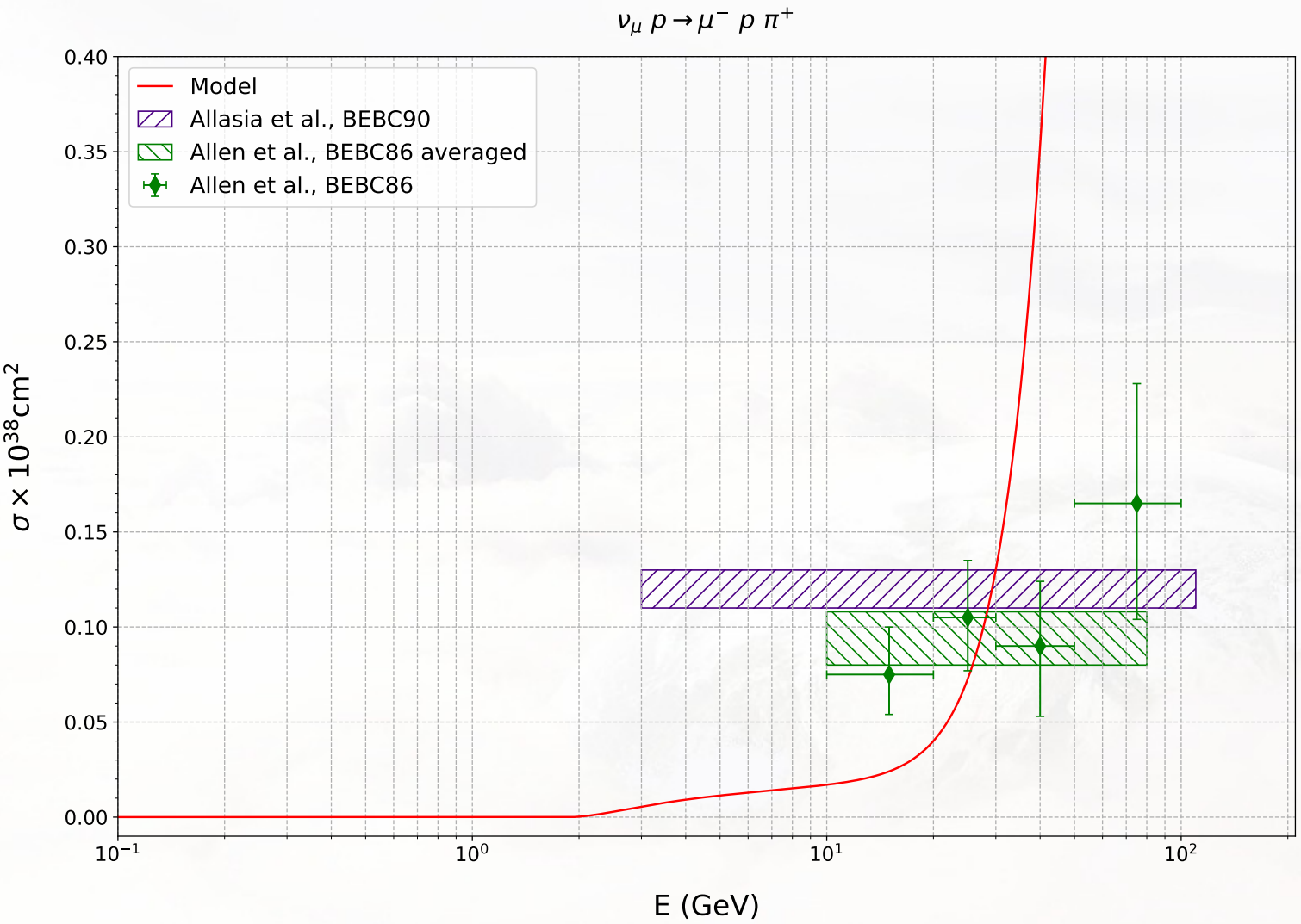

Total cross-section with $W > 2.0$. Data are taken from [22, 24].

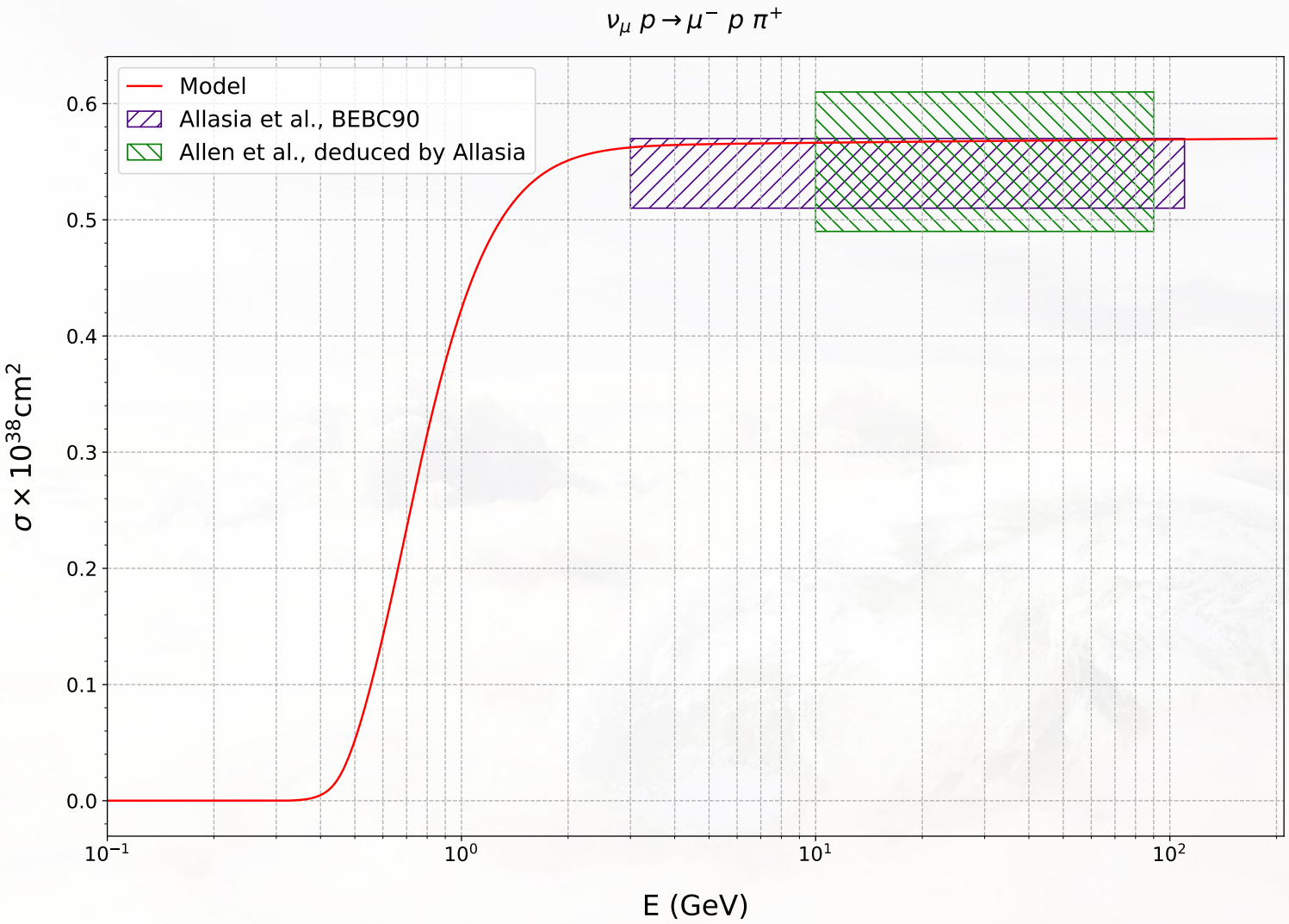

Total cross-section with the invariant hadronic mass $1.1 < W < 1.4$ GeV. Data are taken from [24].

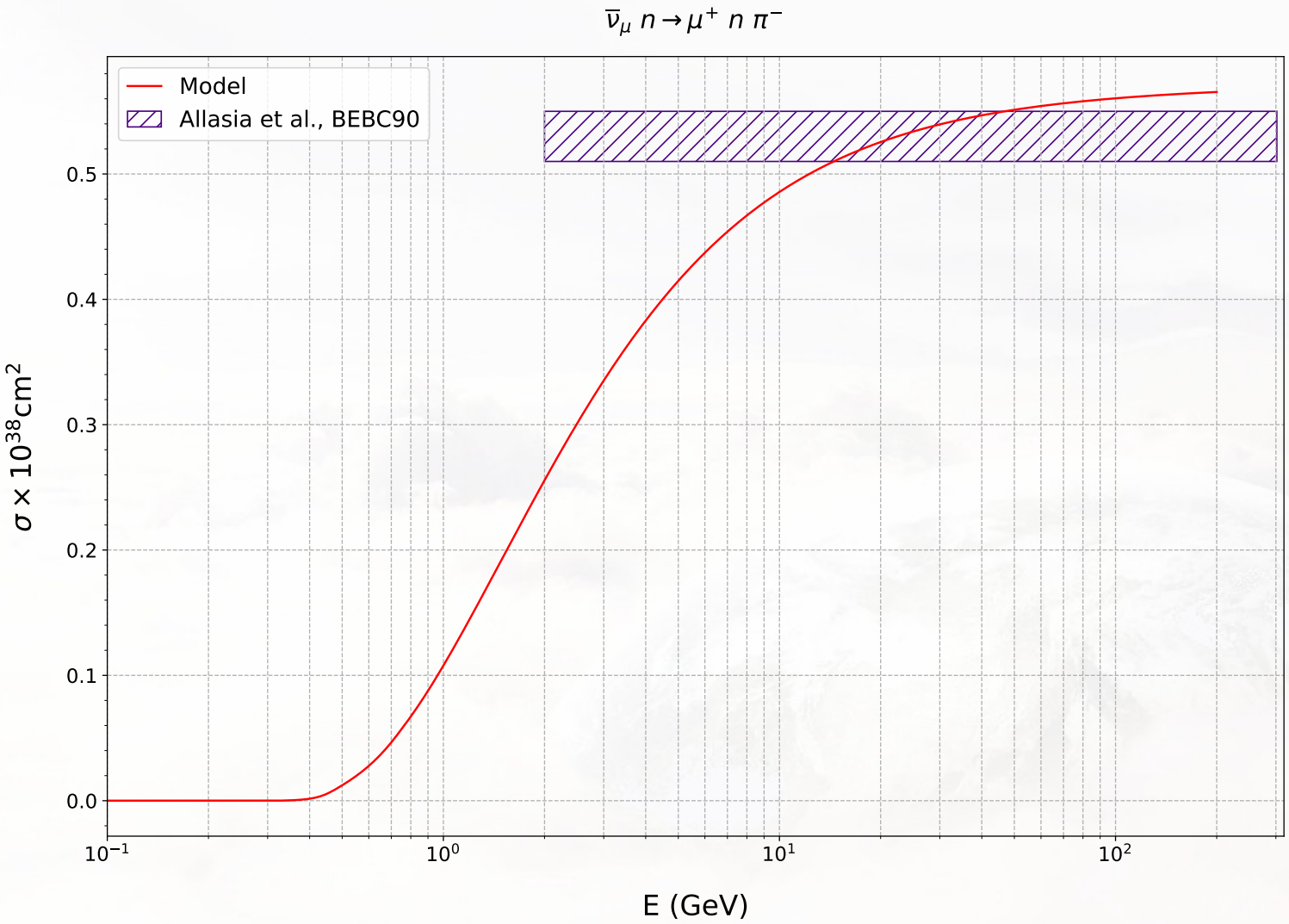

Total cross-section with the invariant hadronic mass $1.1 < W < 1.4$ GeV. Data are taken from [24].

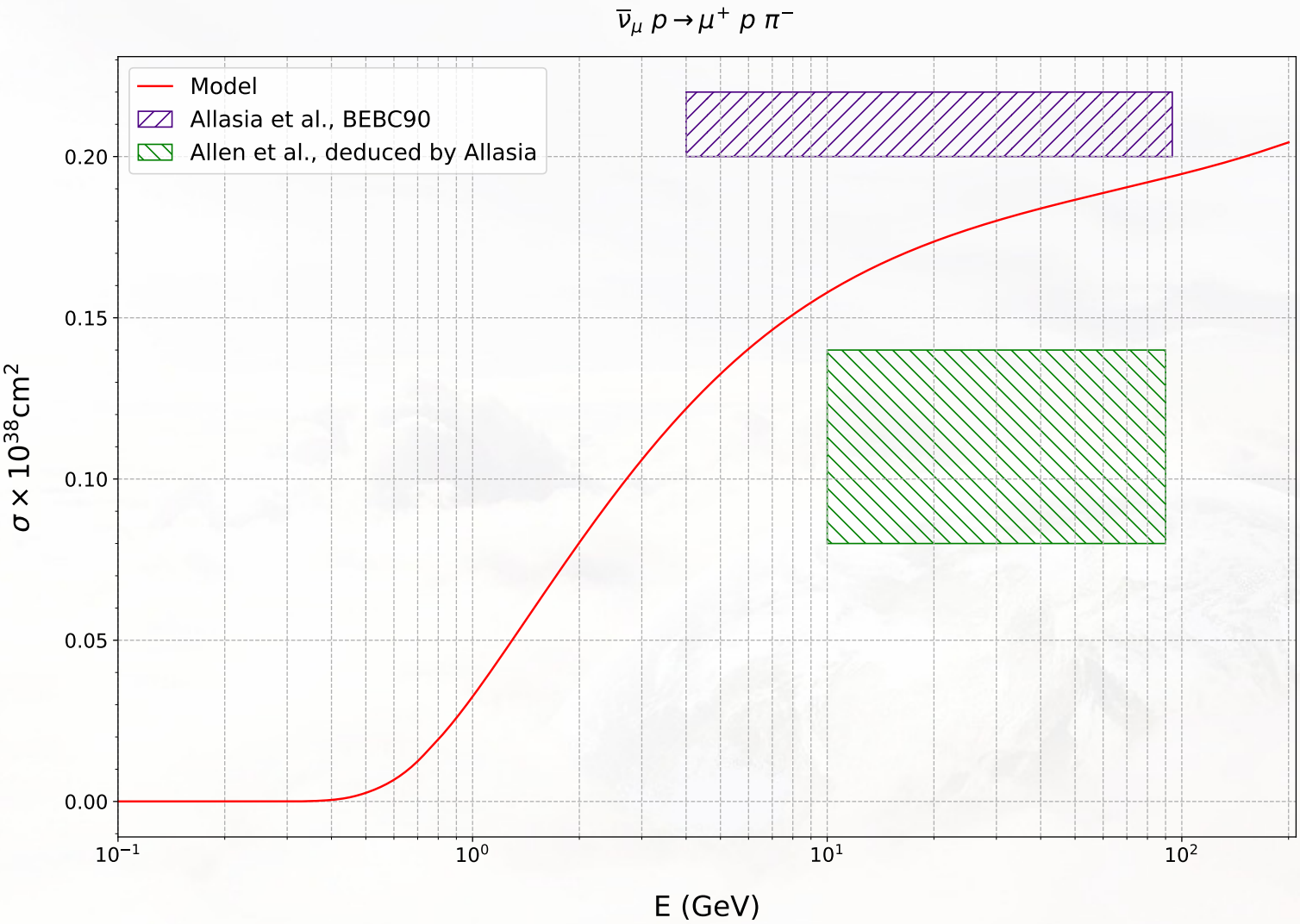

Total cross-section with the invariant hadronic mass $1.1 < W < 1.4$ GeV. Data are taken from [24].

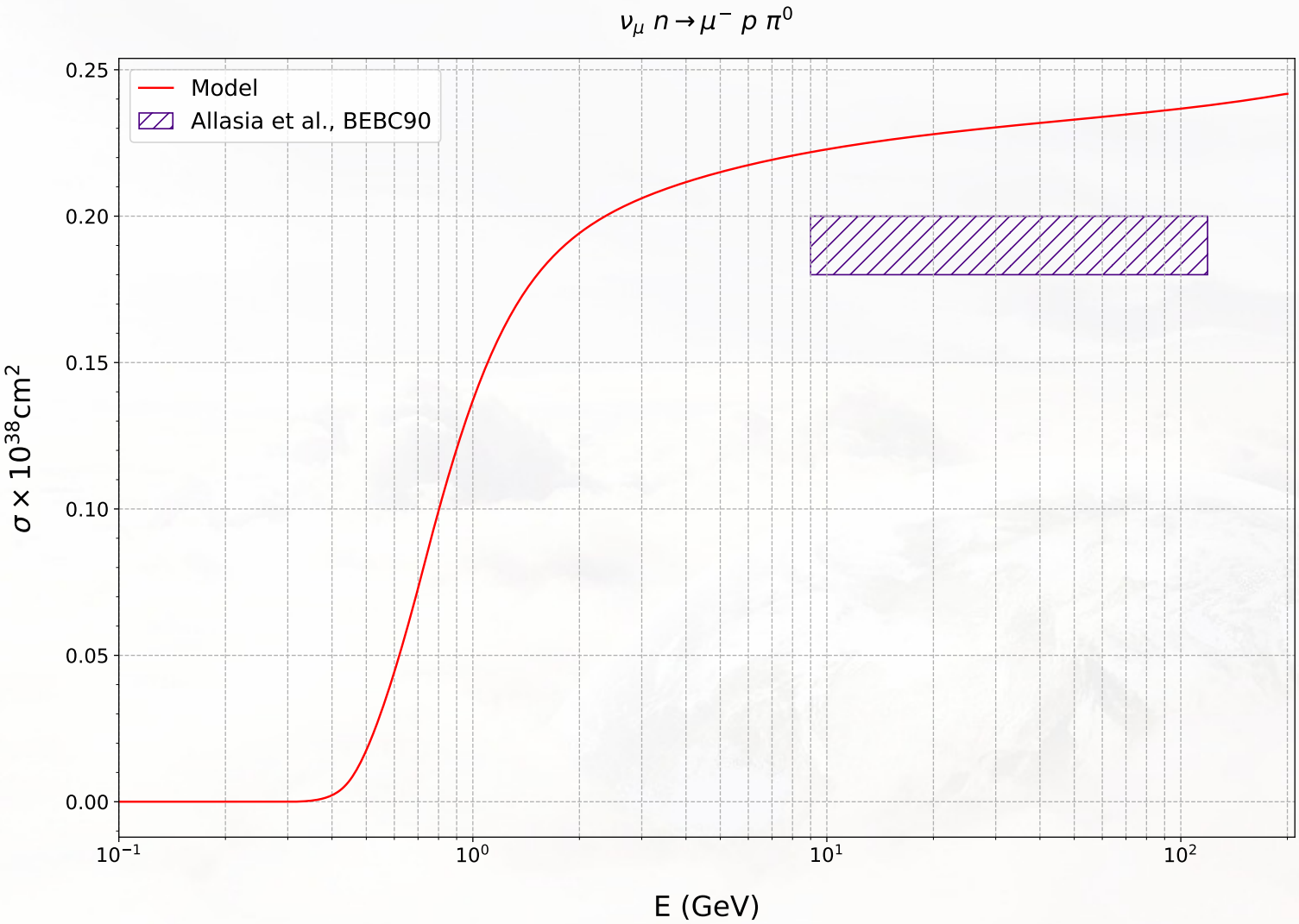

Total cross-section with the invariant hadronic mass $1.1 < W < 1.4$ GeV. Data are taken from [24].

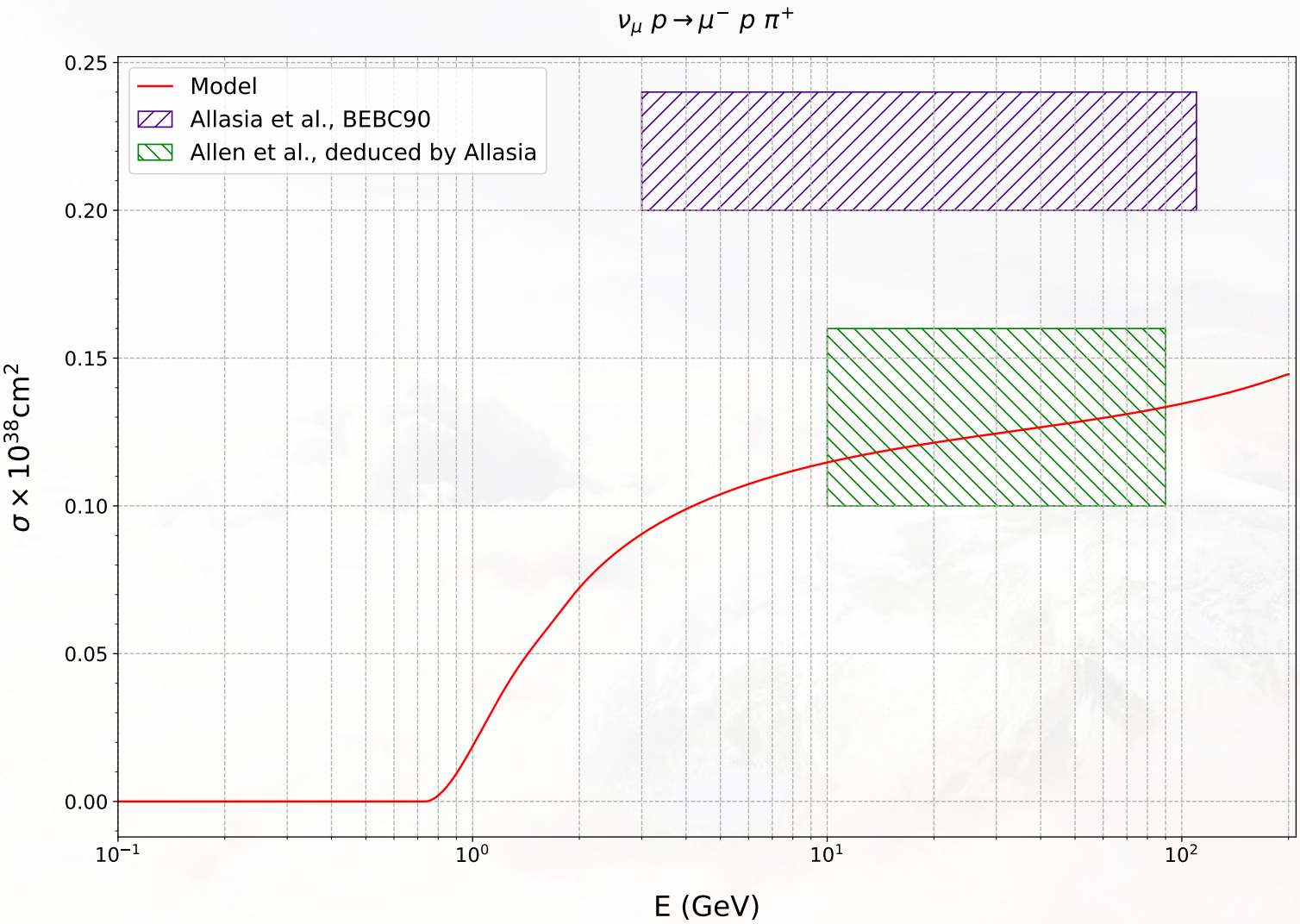

Total cross-section with the invariant hadronic mass $1.4 < W < 2.0$ GeV. Data are taken from [24].

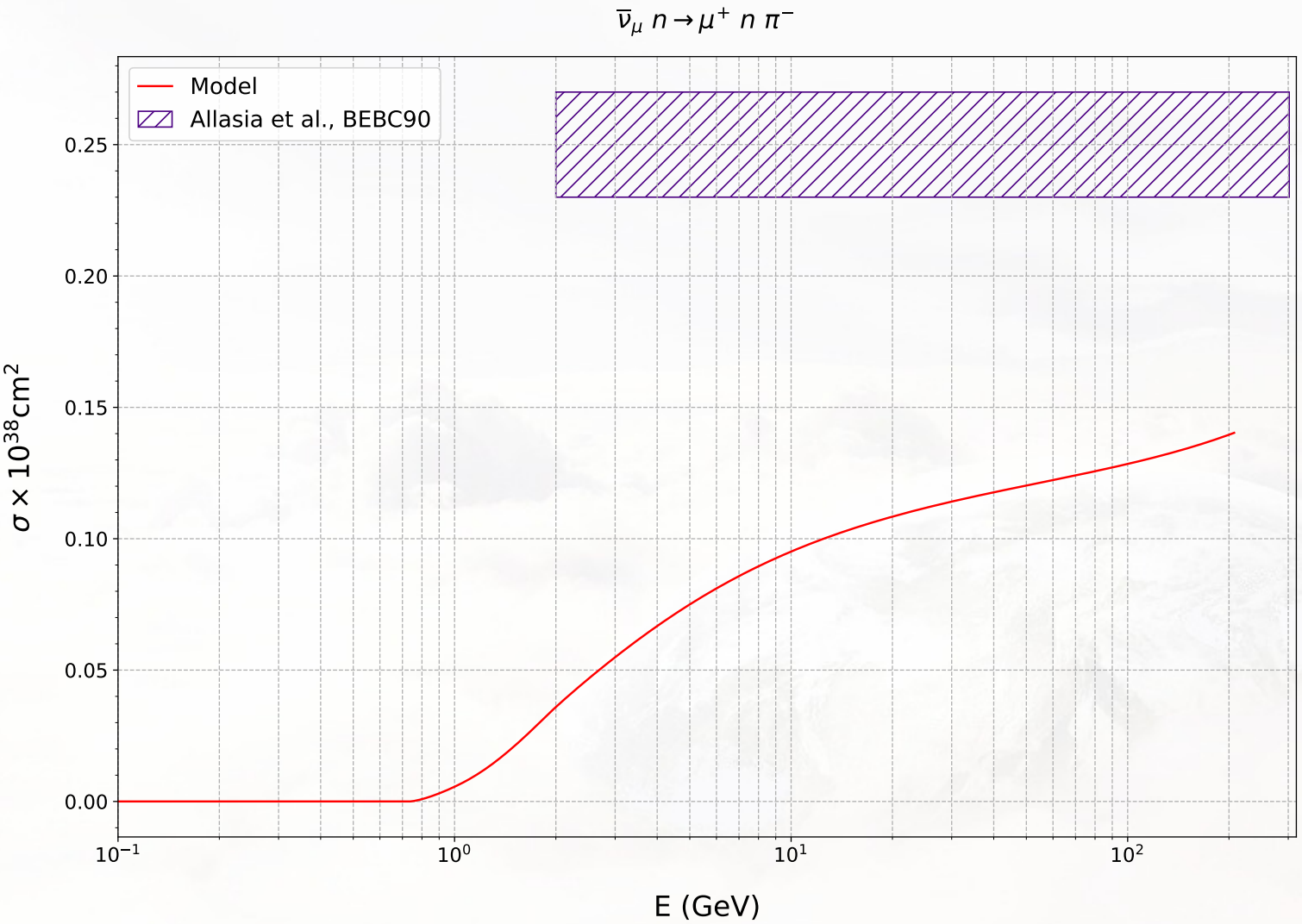

Total cross-section with the invariant hadronic mass $1.4 < W < 2.0$ GeV. Data are taken from [24].

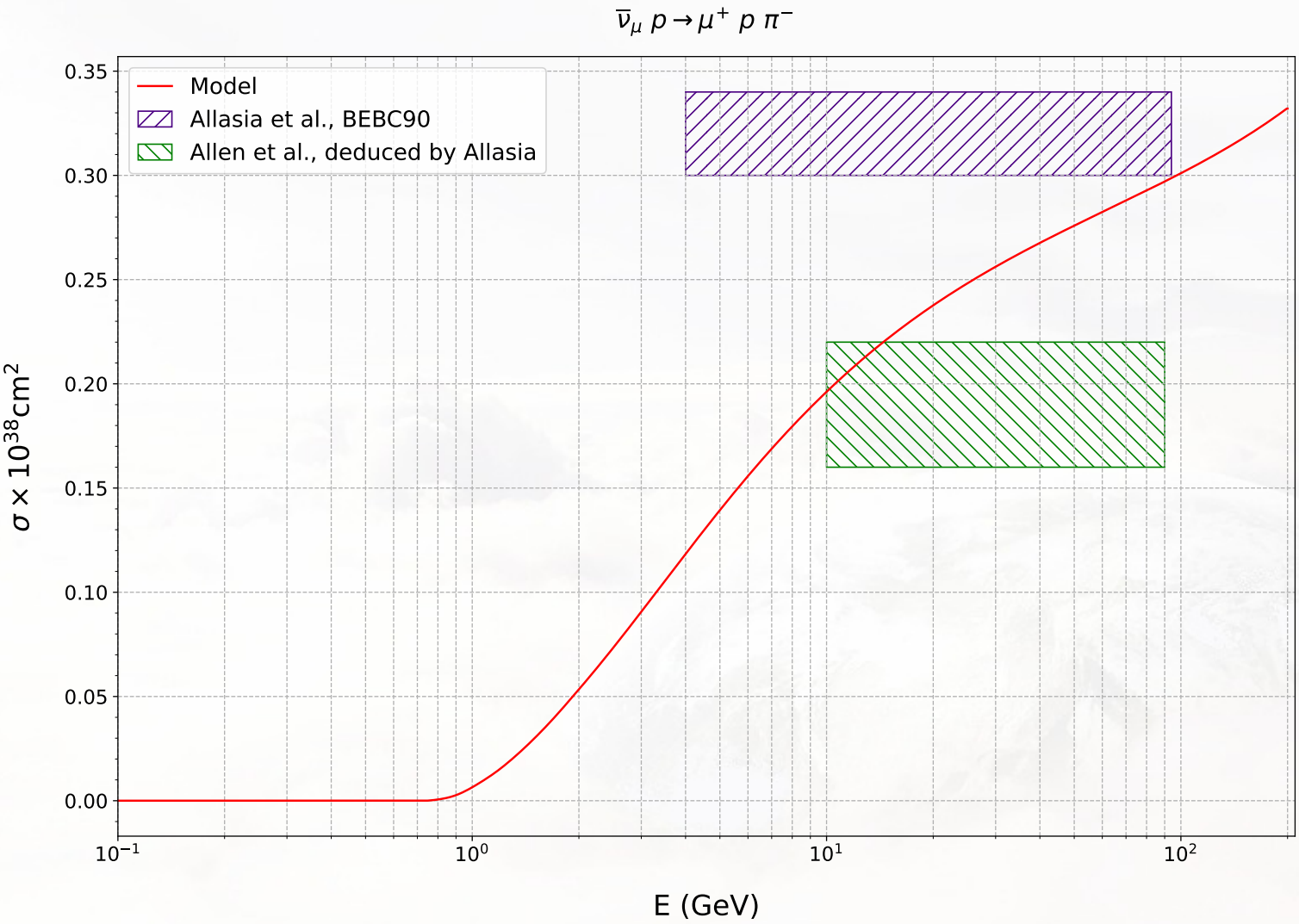

Total cross-section with the invariant hadronic mass $1.4 < W < 2.0$ GeV. Data are taken from [24].

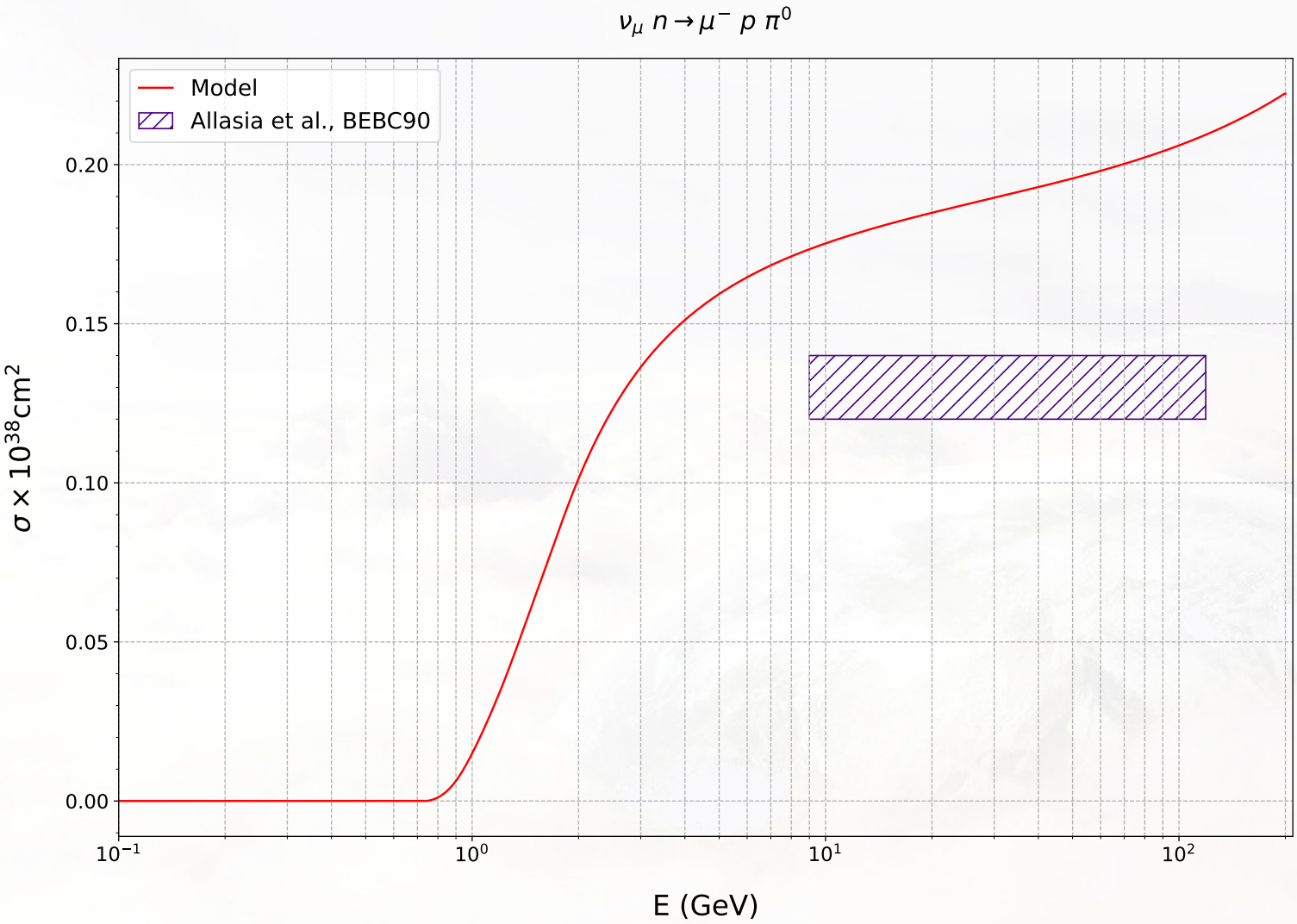

Total cross-section with the invariant hadronic mass $1.4 < W < 2.0$ GeV. Data are taken from [24].

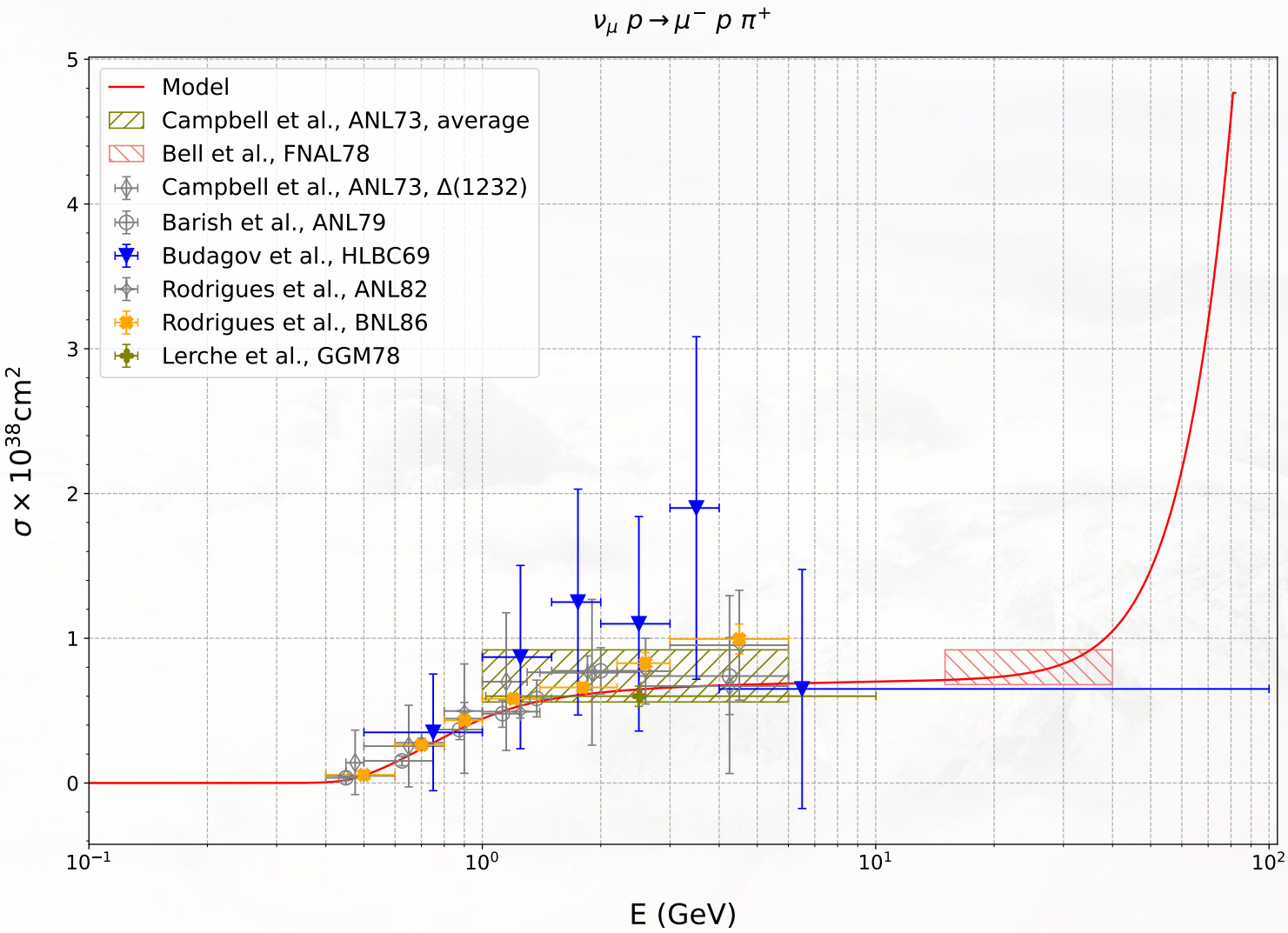

Total cross-section with no W_{cut}. Data are taken from [6, 7, 11, 12, 14, 26, 27].

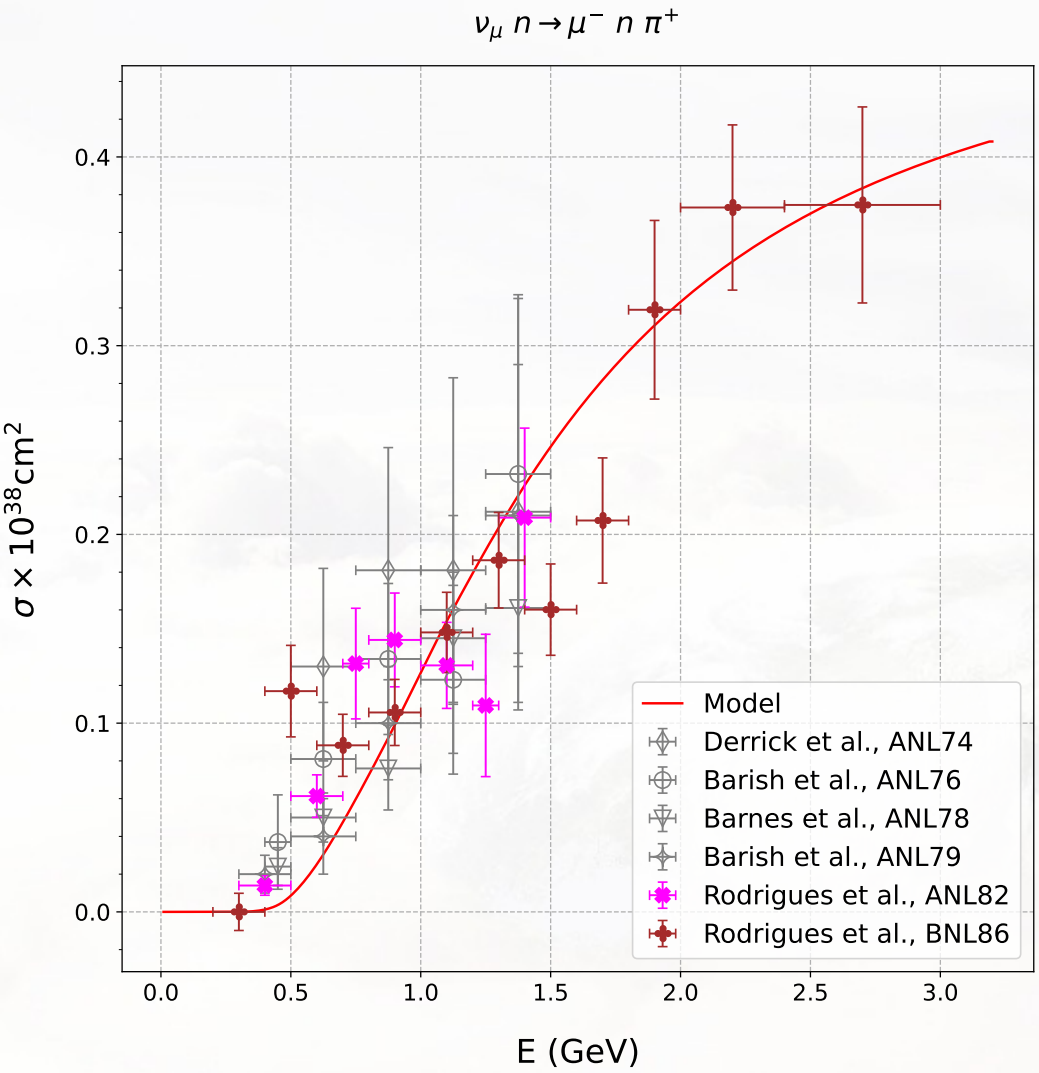

Total cross-section with no W_{cut}. Data are taken from [6, 8, 11, 12, 15, 28].

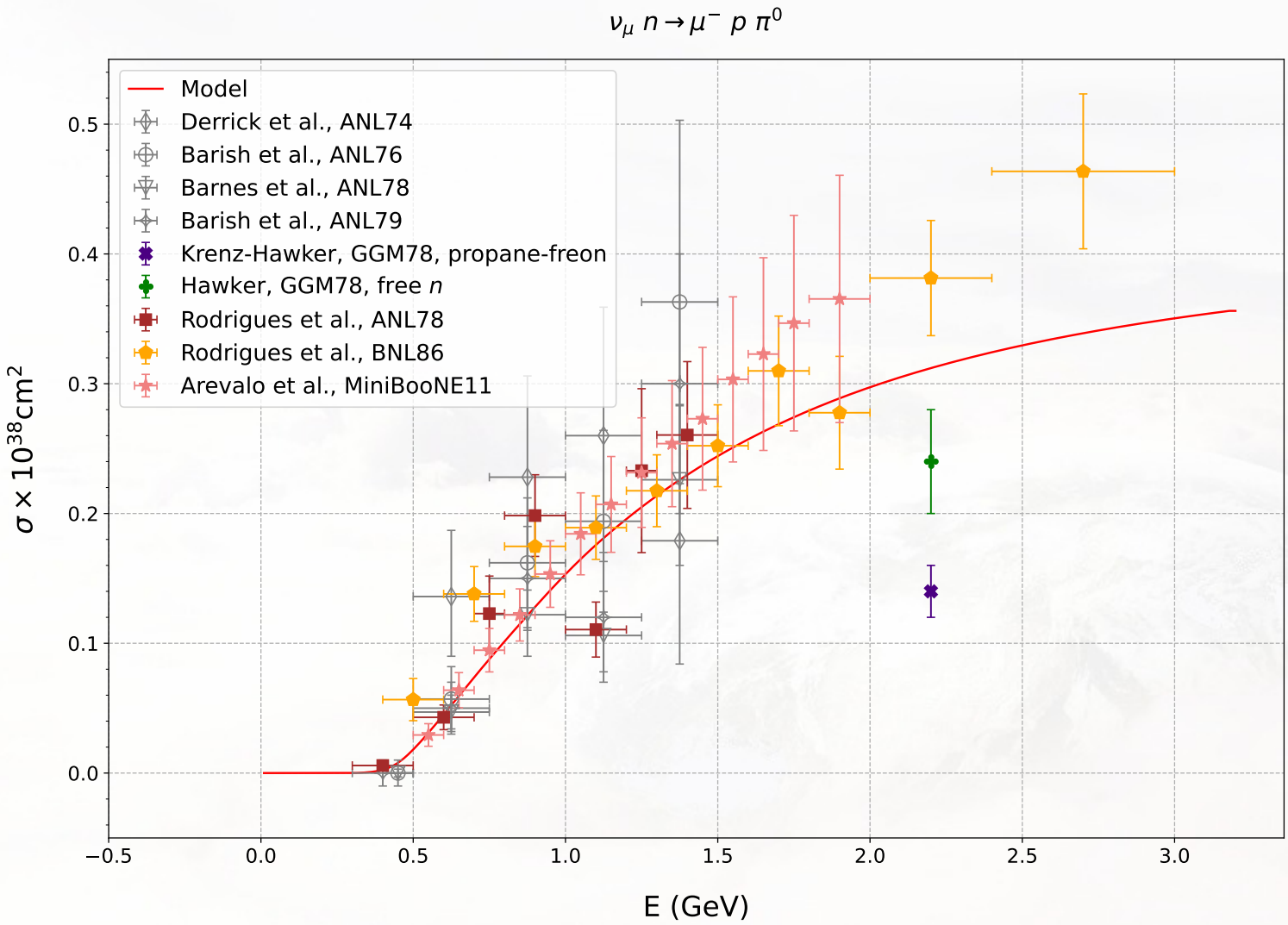

Total cross-section with no W_{cut}. Data are taken from [6, 8, 11, 12, 15, 28–30].

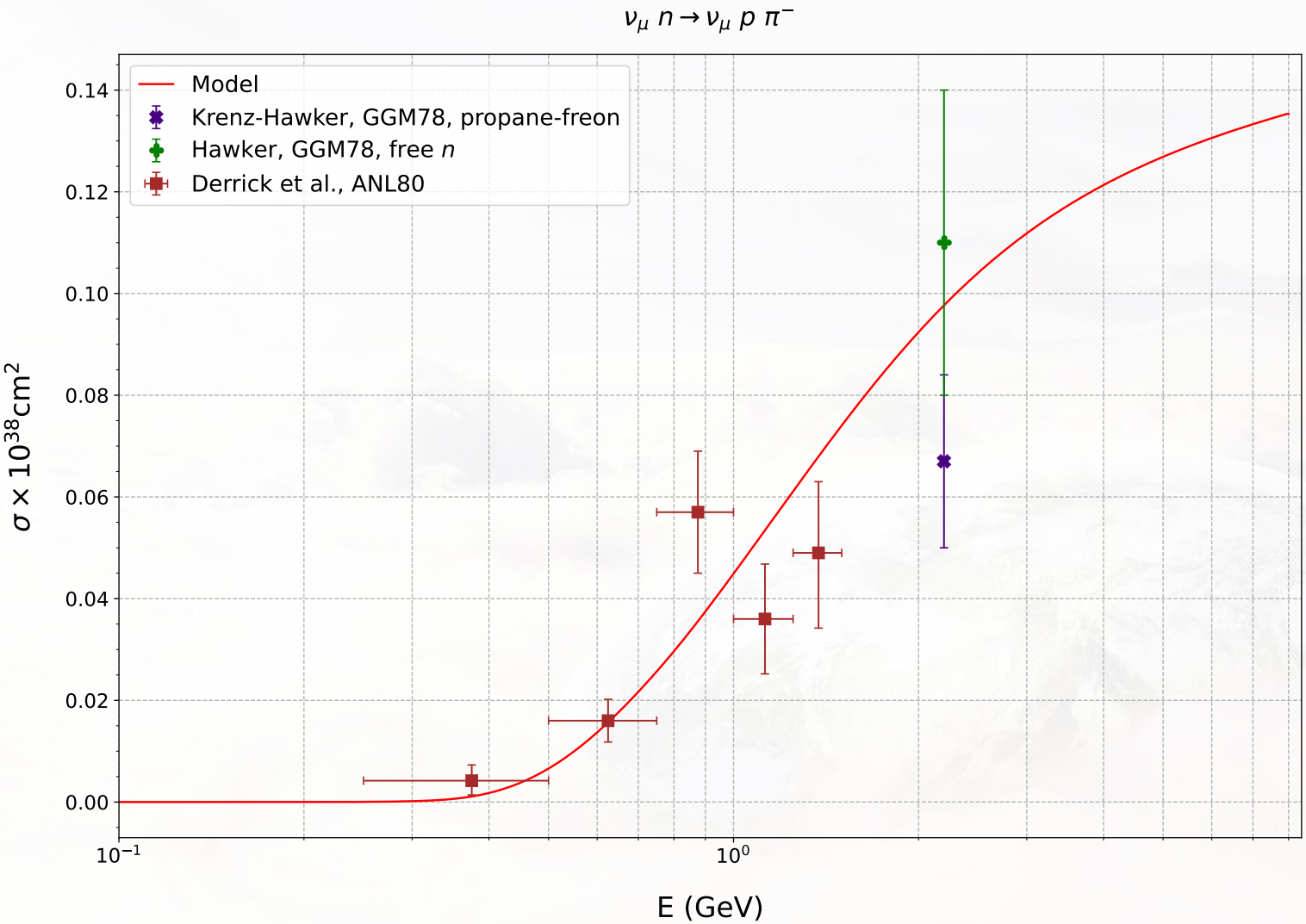

Total cross-section with no W_{cut}. Data are taken from [25, 29, 31]. Cf Fig. 7 from Ref. [1]

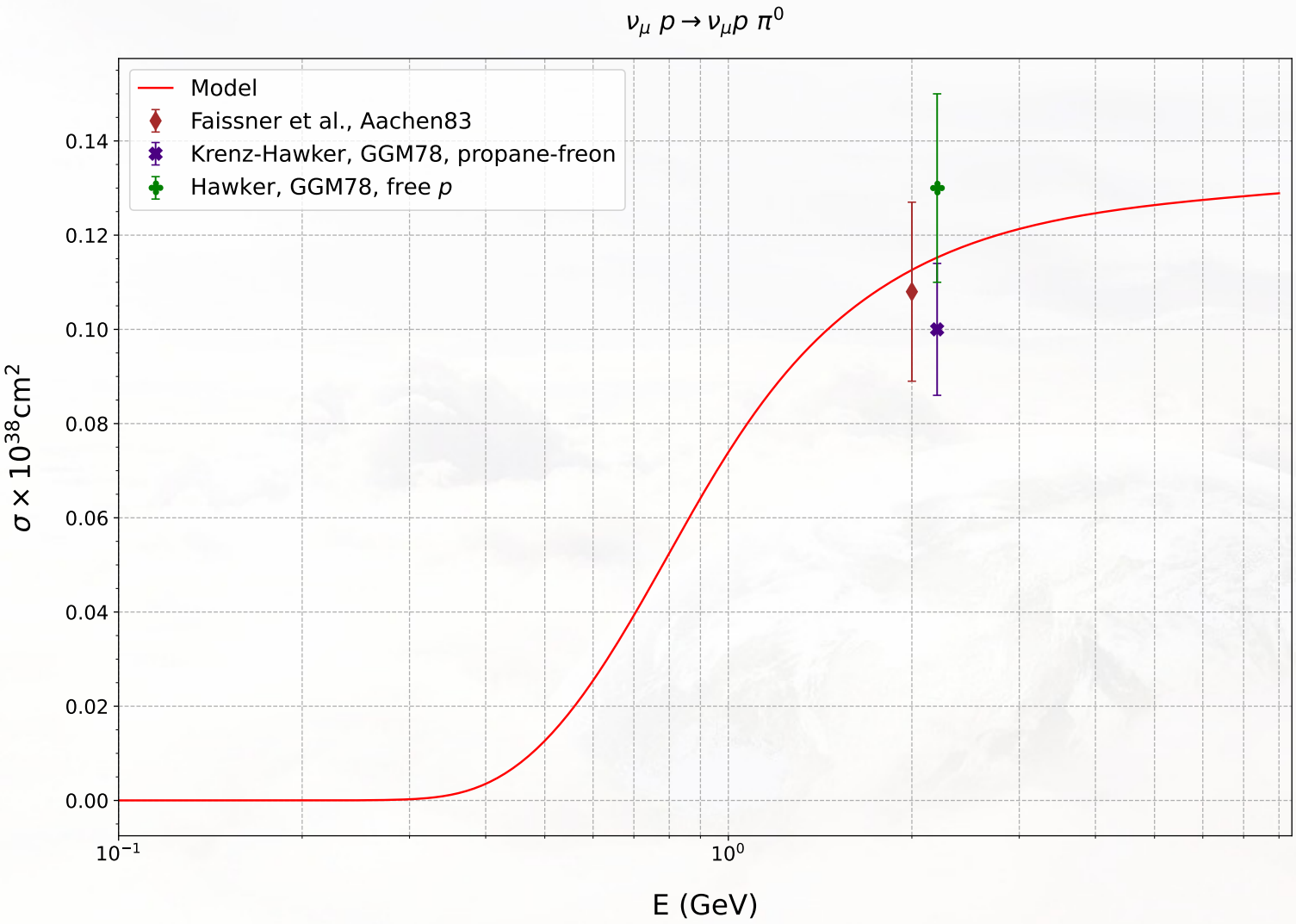

Total cross-section with no W_{cut}. Data are taken from [25, 29, 32]. Cf Fig. 8 from Ref. [1]

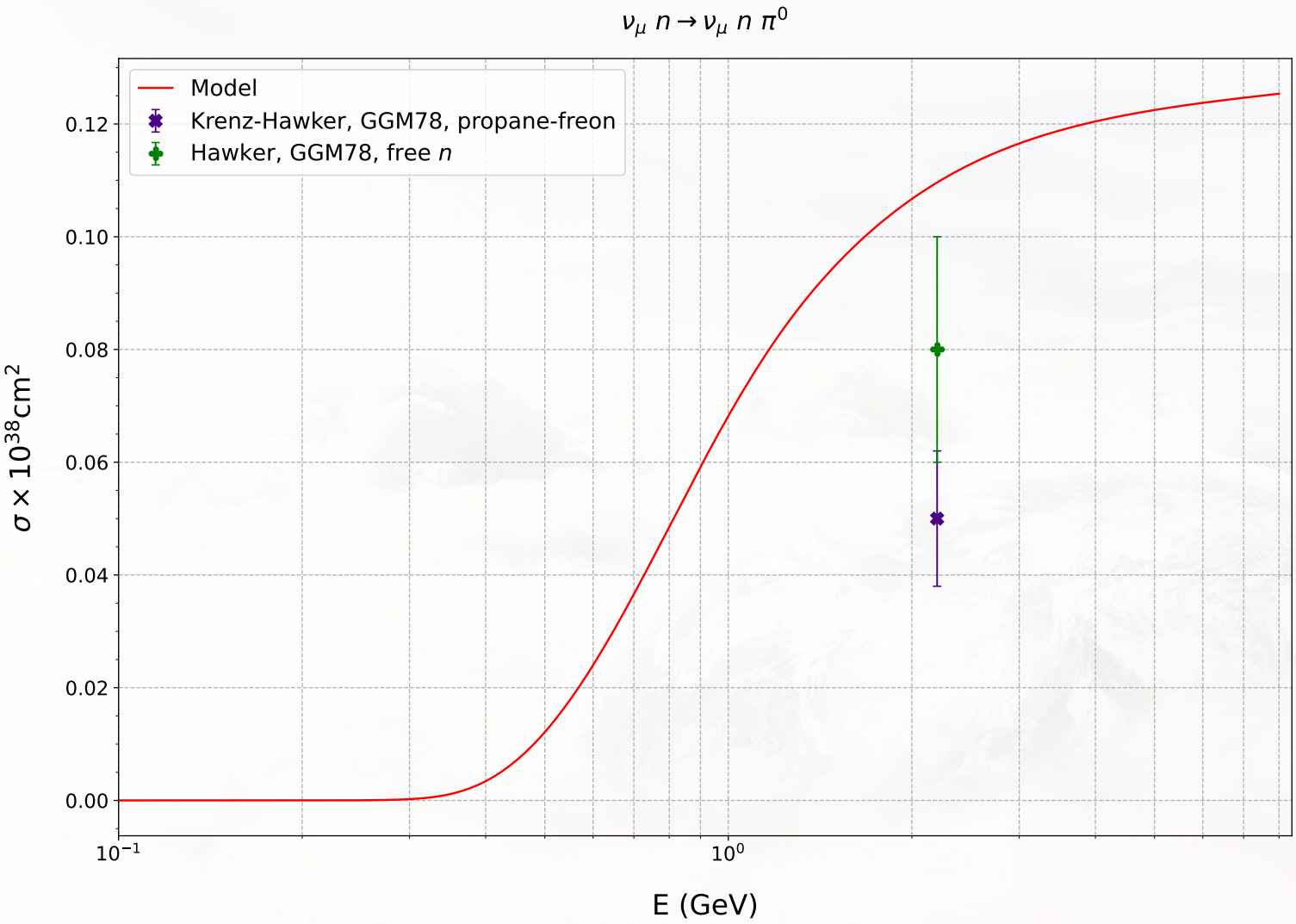

Total cross-section with no W_{cut}. Data are taken from [25, 29]. Cf Fig. 8 from Ref. [1]

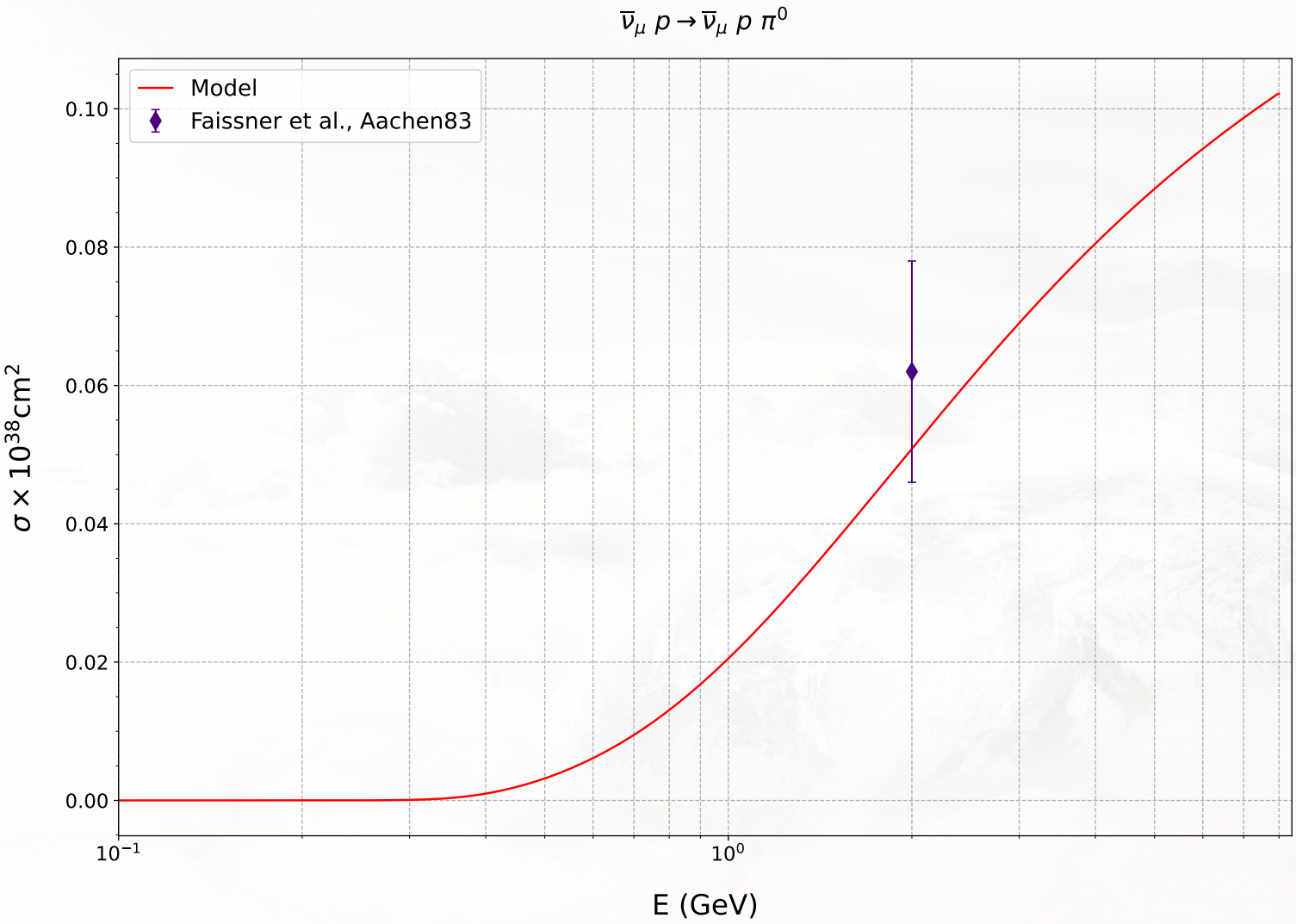

Total cross-section with no W_{cut}. Data are taken from [32]. Cf Fig. 8 from Ref. [1]

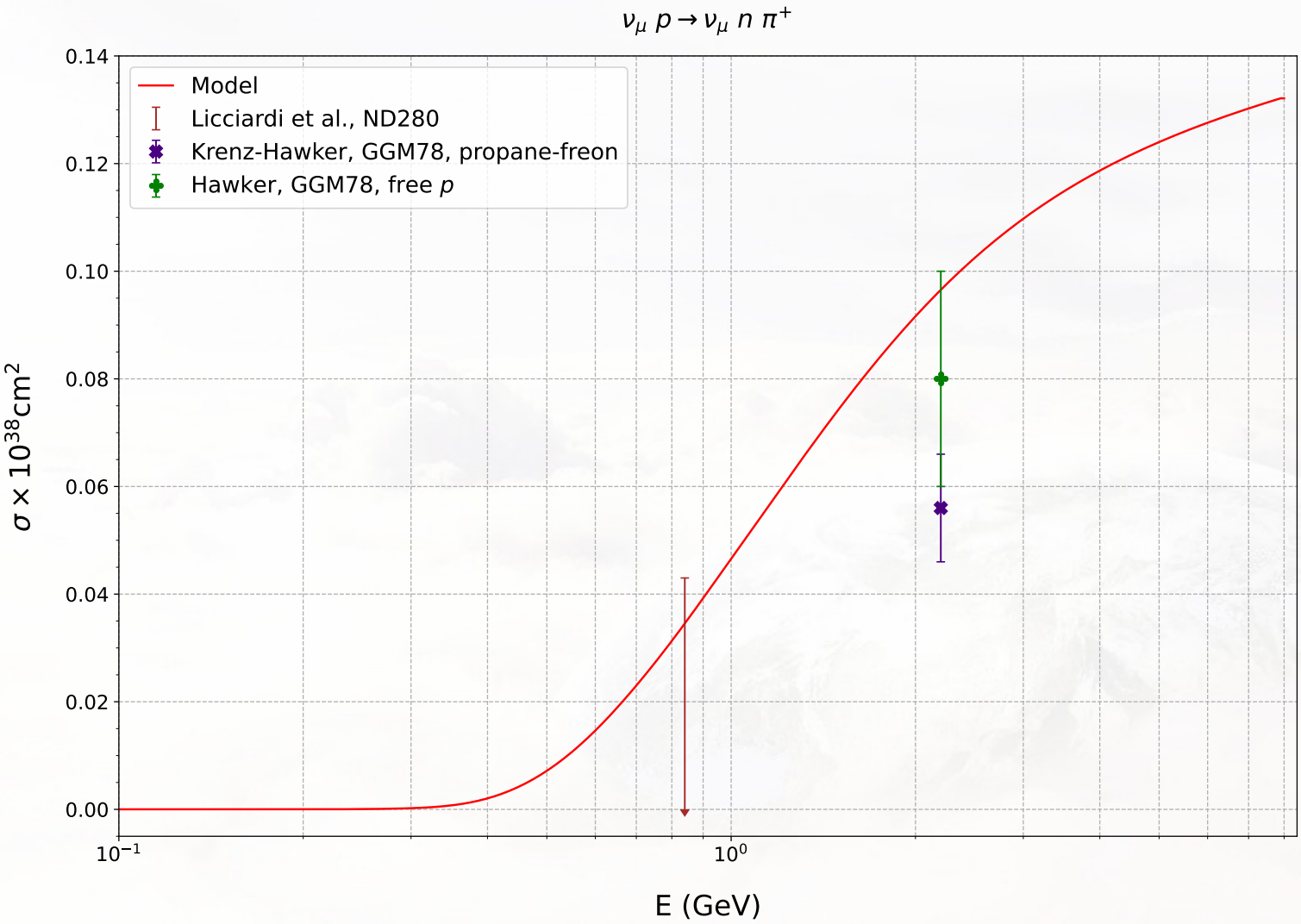

Total cross-section with no W_{cut}. Data are taken from [25, 29, 33]. Cf Fig. 8 from Ref. [1]

Next topic

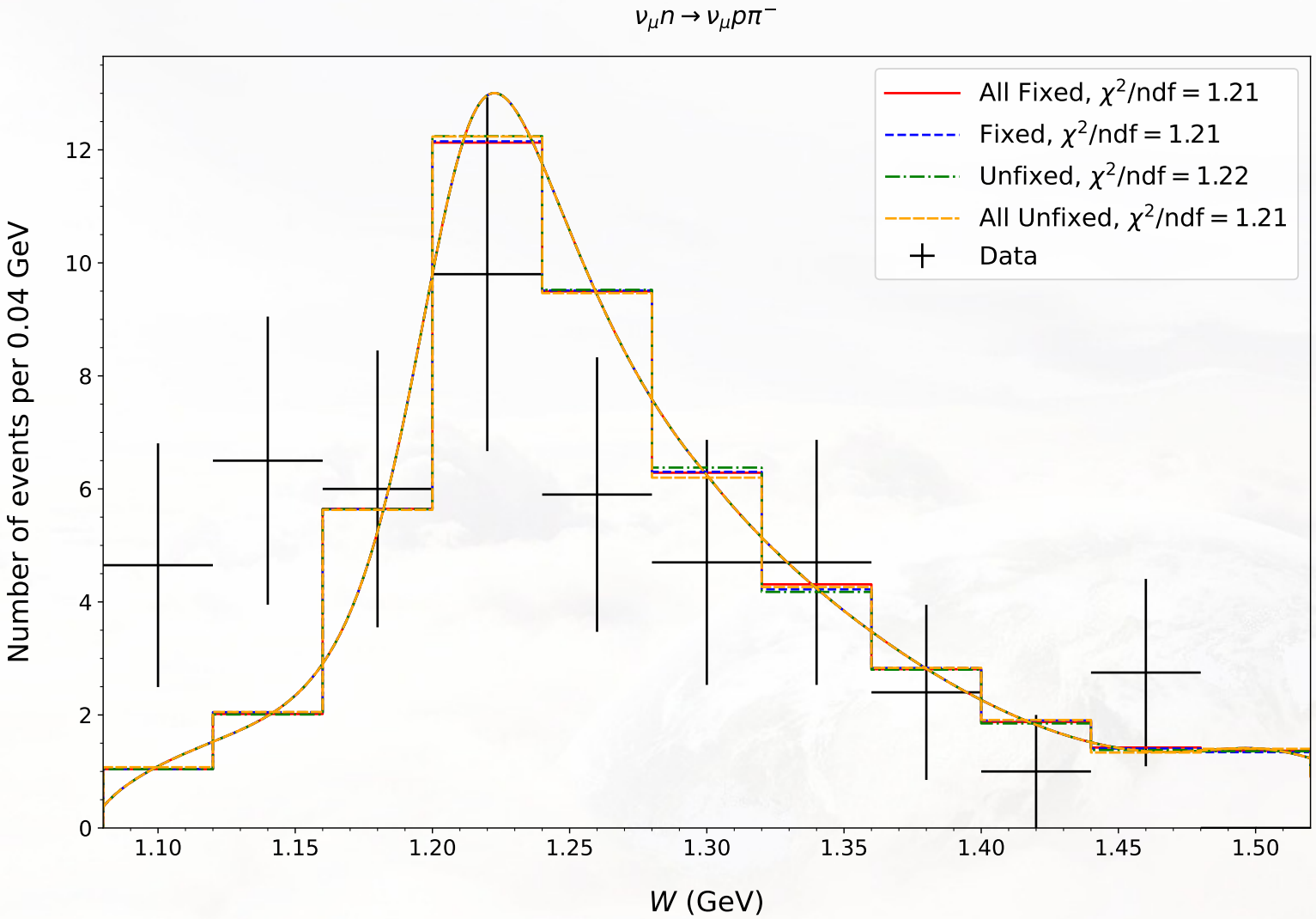

W distribution with no W_{cut}. Neutrino spectrum is restricted by $0.3 < E_\nu < 1.5$ GeV. Model predictions are area-normalized. Predictions with all resonances (All)/without resonance F17(1970) and with fixed and unfixed bugs are shown. Data are taken from Ref. [31]. Neutrino spectrum is taken from [34].

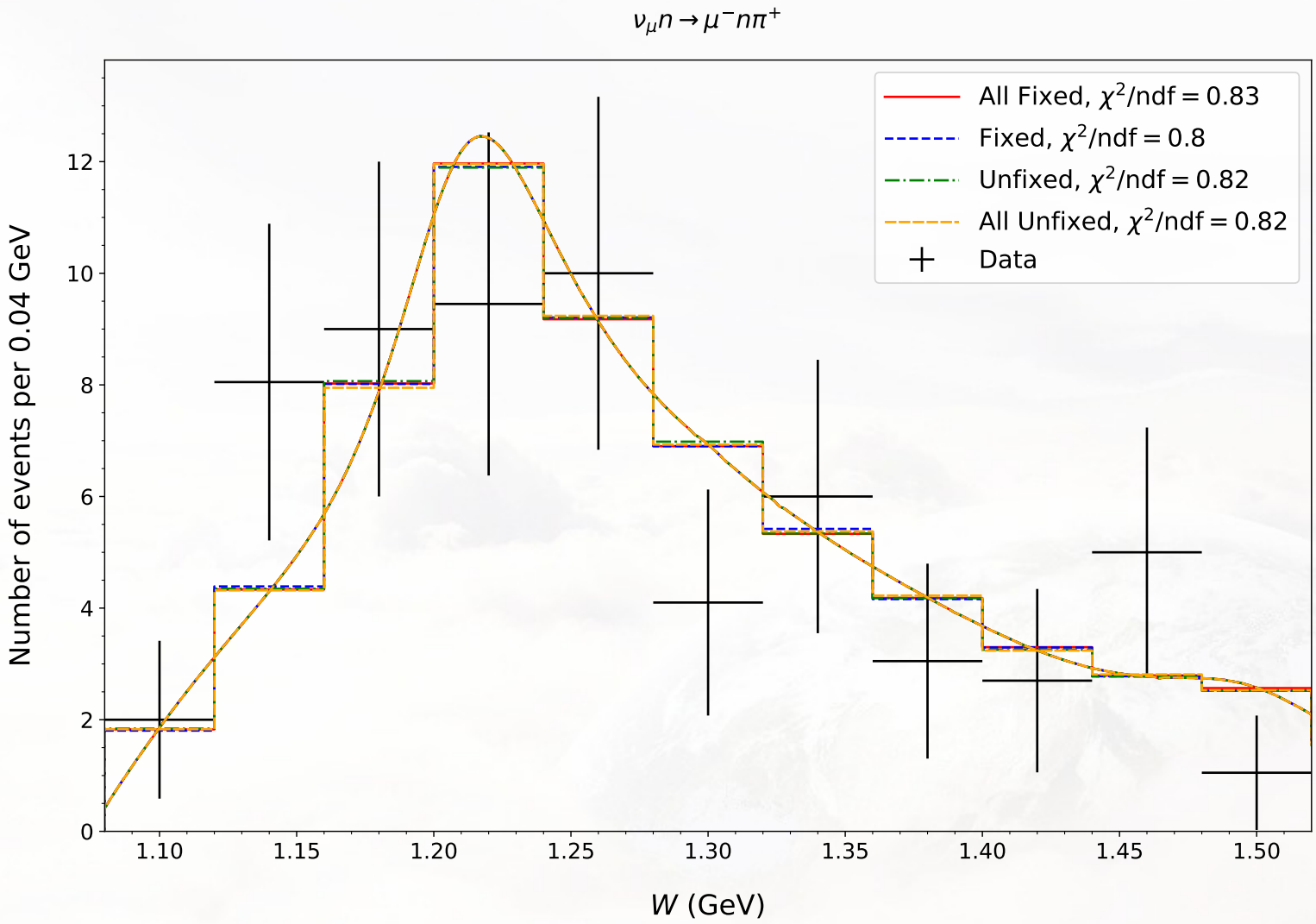

W distribution with no W_{cut}. Neutrino spectrum is restricted by $0.3 < E_\nu < 1.5$ GeV. Model predictions are area-normalized. Predictions with all resonances (All)/without resonance F17(1970) and with fixed and unfixed bugs are shown. Data are taken from Ref. [31]. Neutrino spectrum is taken from [34].

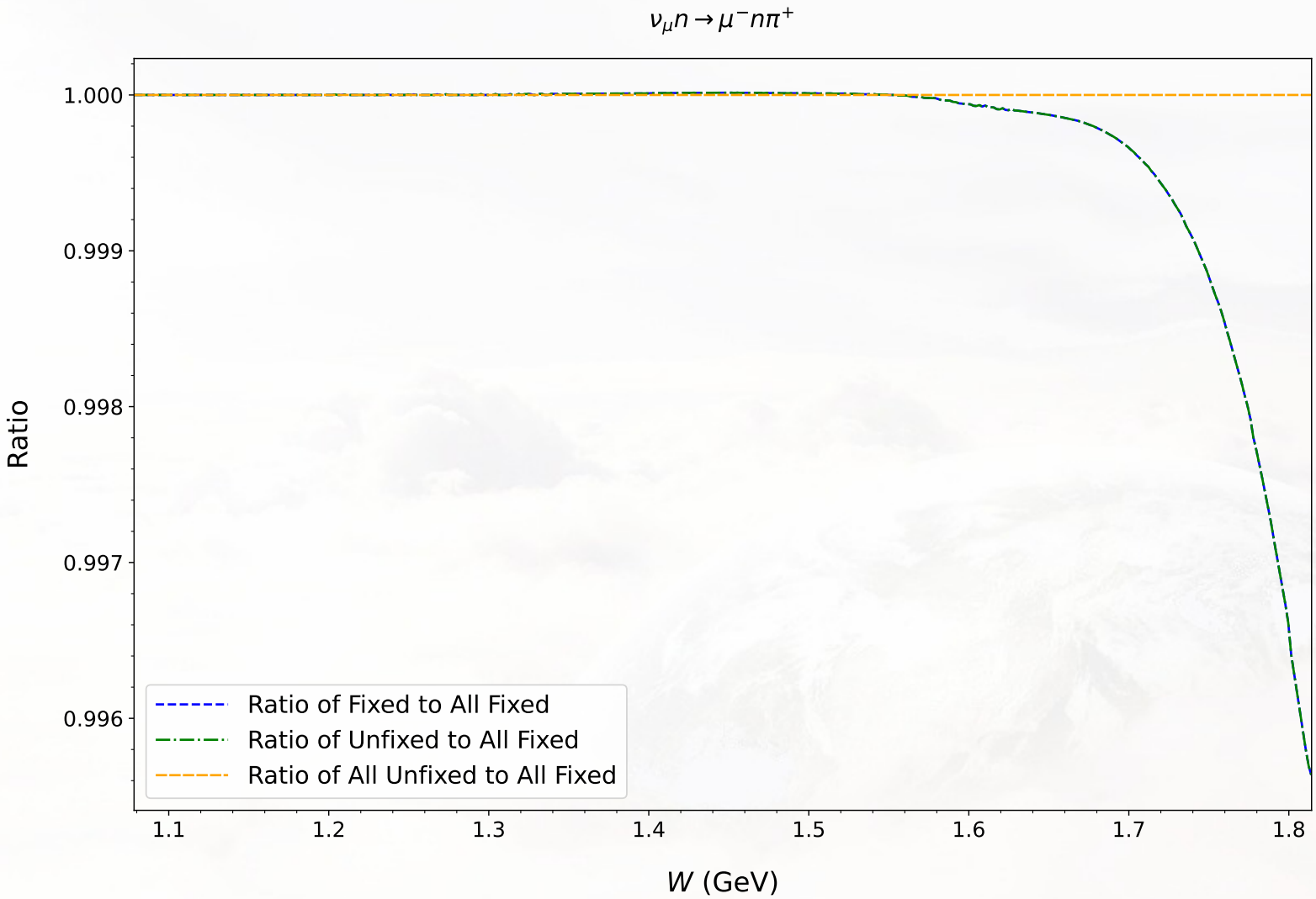

Ratio of $d\sigma/dW$ with no W_{cut}. Neutrino spectrum is restricted by $0.3 < E_\nu < 1.5$ GeV. Data are taken from Ref. [31]. Neutrino spectrum is taken from [34].

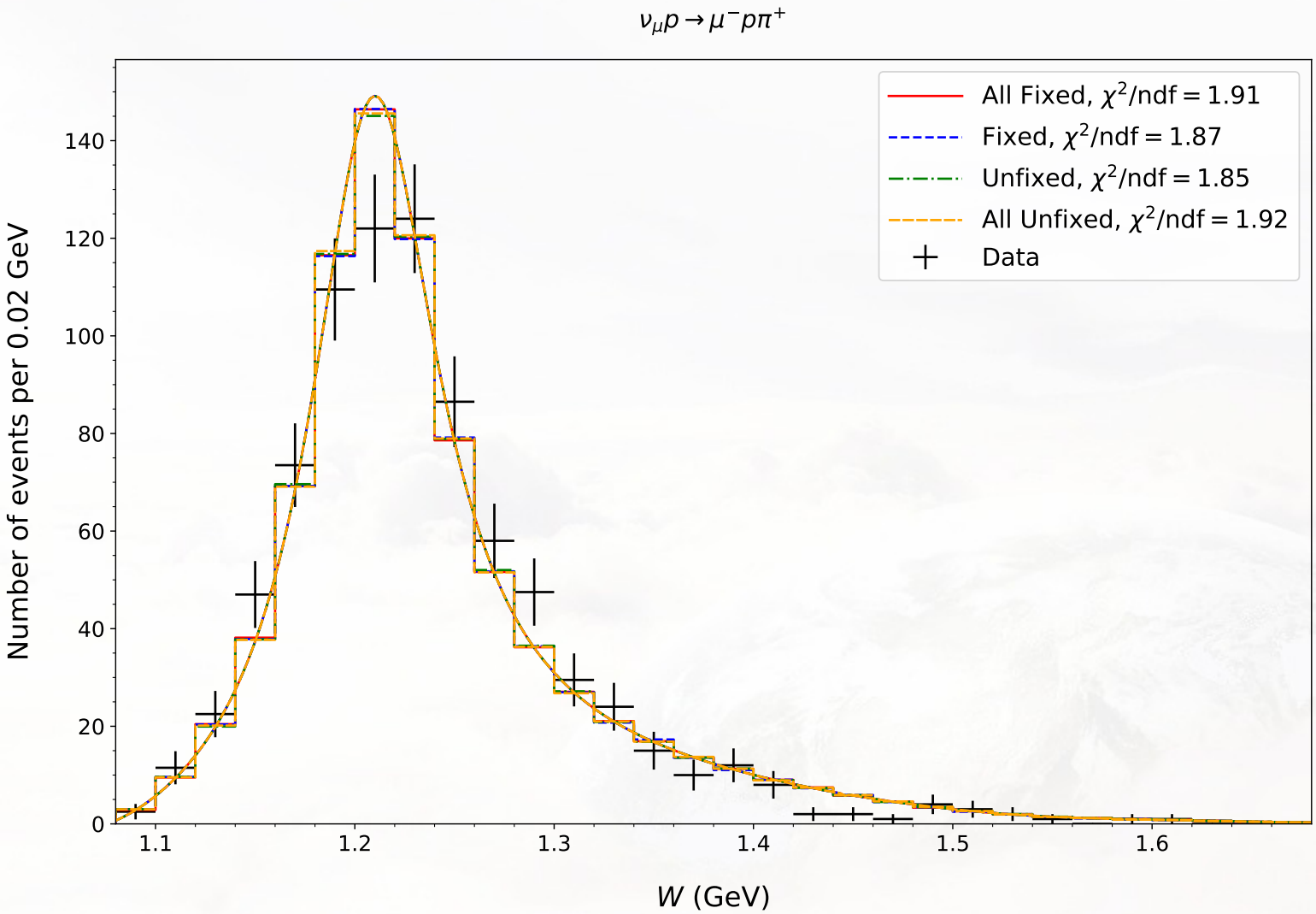

W distribution with no W_{cut}. Neutrino spectrum is restricted by $E_\nu < 6.0$ GeV. Model predictions are area-normalized. Predictions with all resonances (All)/without resonance F17(1970) and with fixed and unfixed bugs are shown. Data are taken from Ref. [6]. Neutrino spectrum is taken from [34]. Cf Fig. 11 top left from Ref. [1]

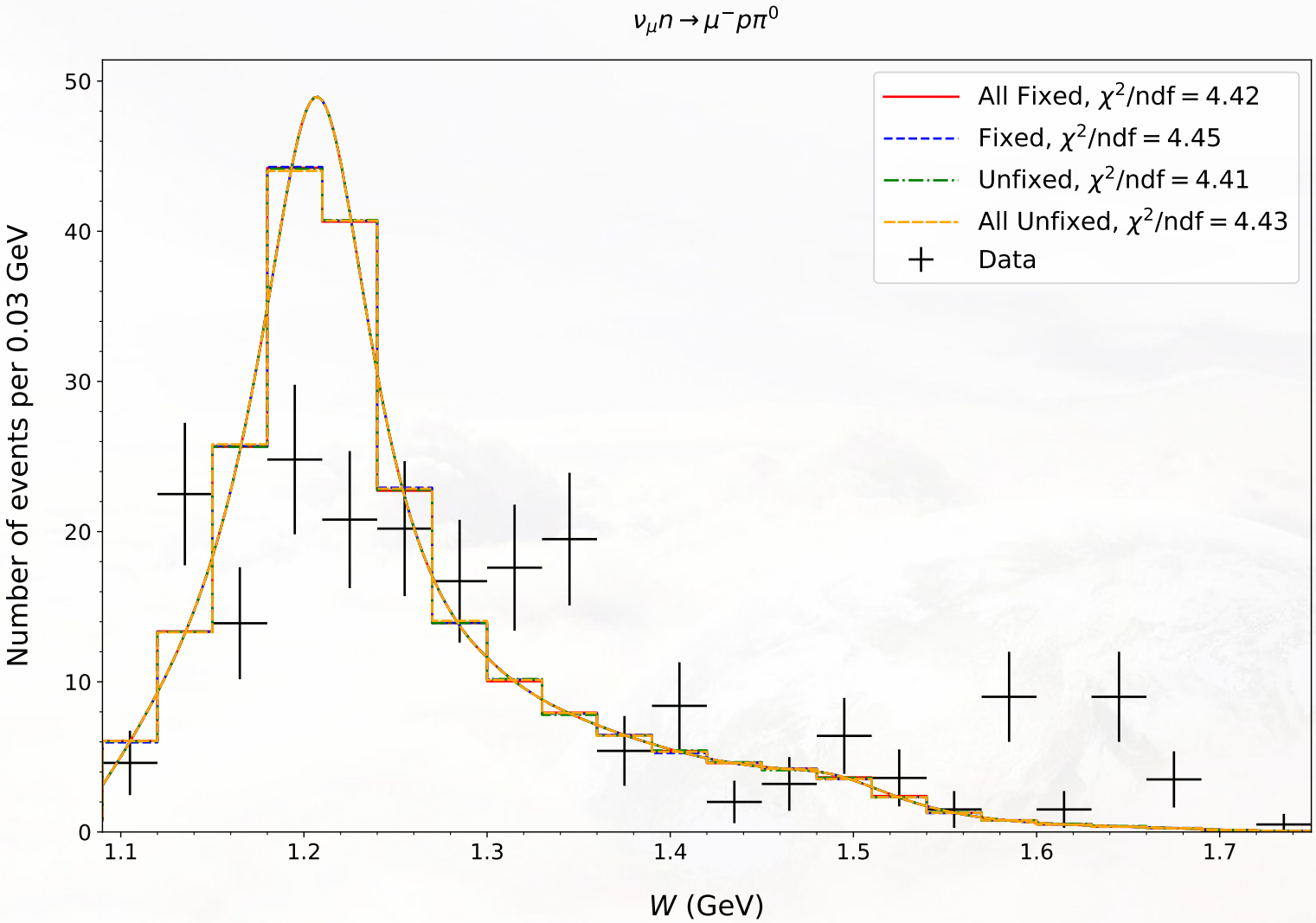

W distribution with no W_{cut}. Neutrino spectrum is restricted by $E_\nu < 1.5$ GeV. Model predictions are area-normalized. Predictions with all resonances (All)/without resonance F17(1970) and with fixed and unfixed bugs are shown. Data are taken from Ref. [6]. Neutrino spectrum is taken from [34]. Cf Fig. 11 bottom from Ref. [1]

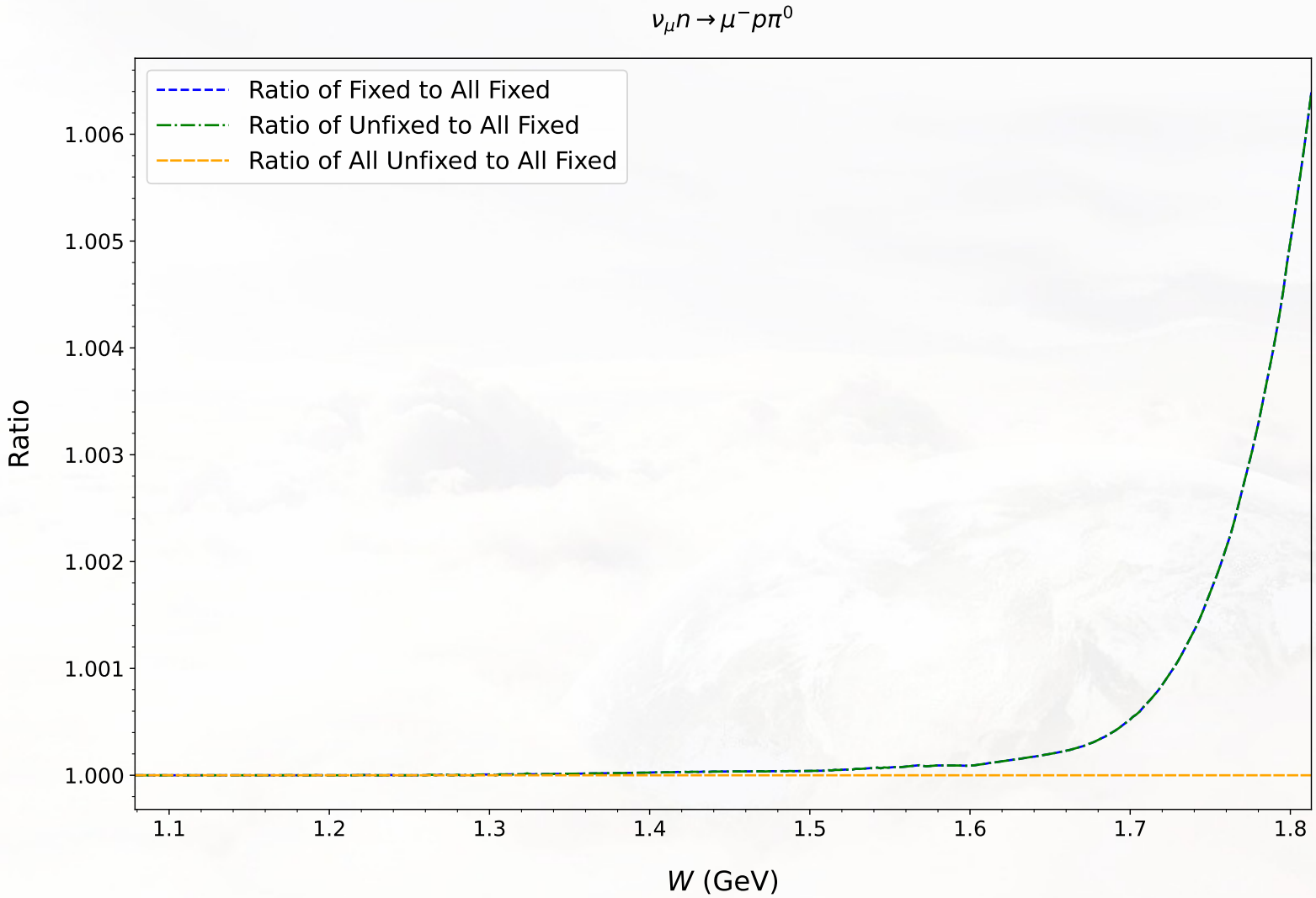

Ratio of $d\sigma/dW$ with no W_{cut}. Neutrino spectrum is restricted by $E_\nu < 1.5$ GeV. Data are taken from Ref. [6]. Neutrino spectrum is taken from [34].

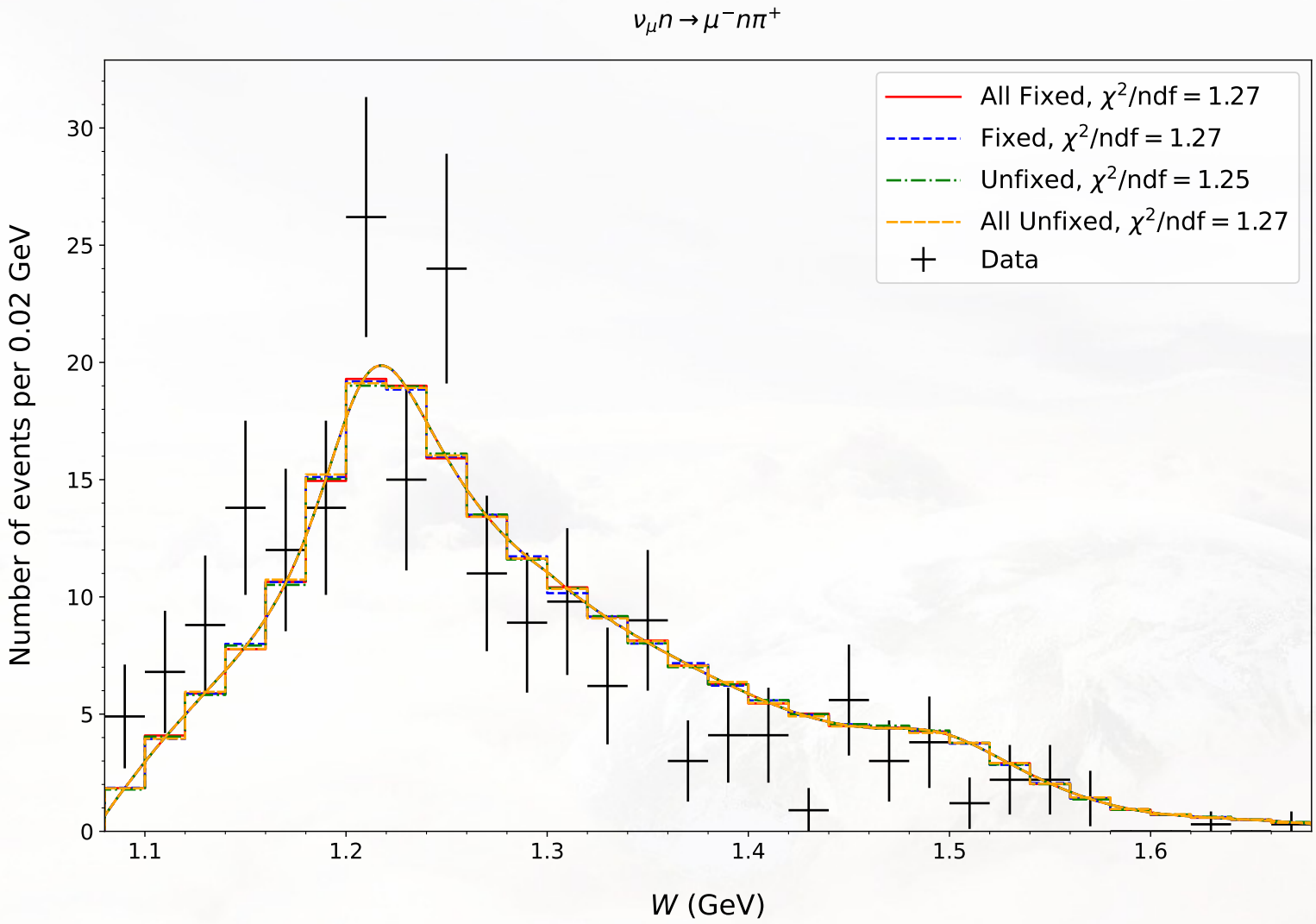

W distribution with no W_{cut}. Neutrino spectrum is restricted by $E_\nu < 1.5$ GeV. Model predictions are area-normalized. Predictions with all resonances (All)/without resonance F17(1970) and with fixed and unfixed bugs are shown. Data are taken from Ref. [6]. Neutrino spectrum is taken from [34]. Cf Fig. 11 top right from Ref. [1]

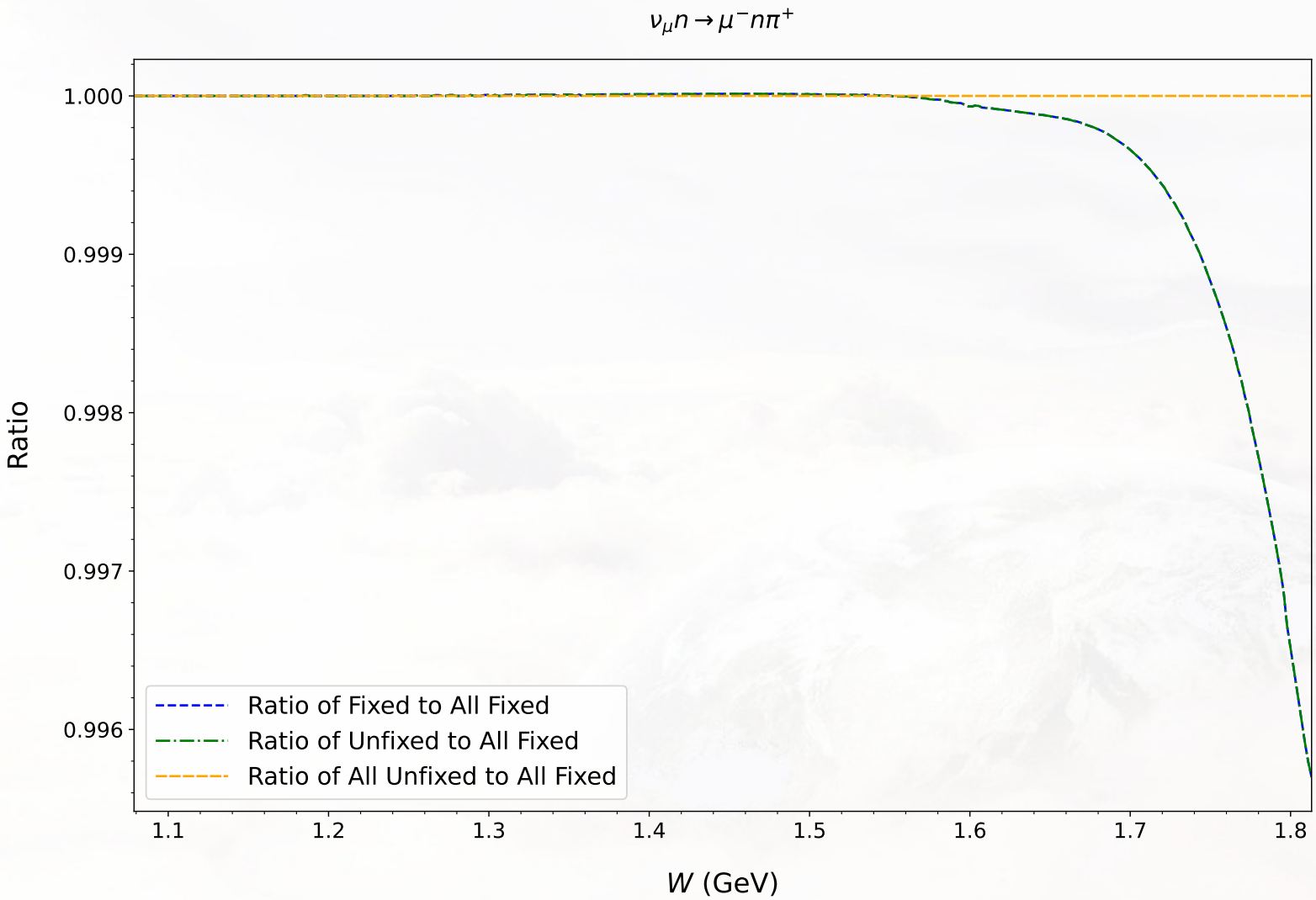

Ratio of $d\sigma/dW$ with no W_{cut}. Neutrino spectrum is restricted by $E_\nu < 1.5$ GeV. Data are taken from Ref. [6]. Neutrino spectrum is taken from [34].

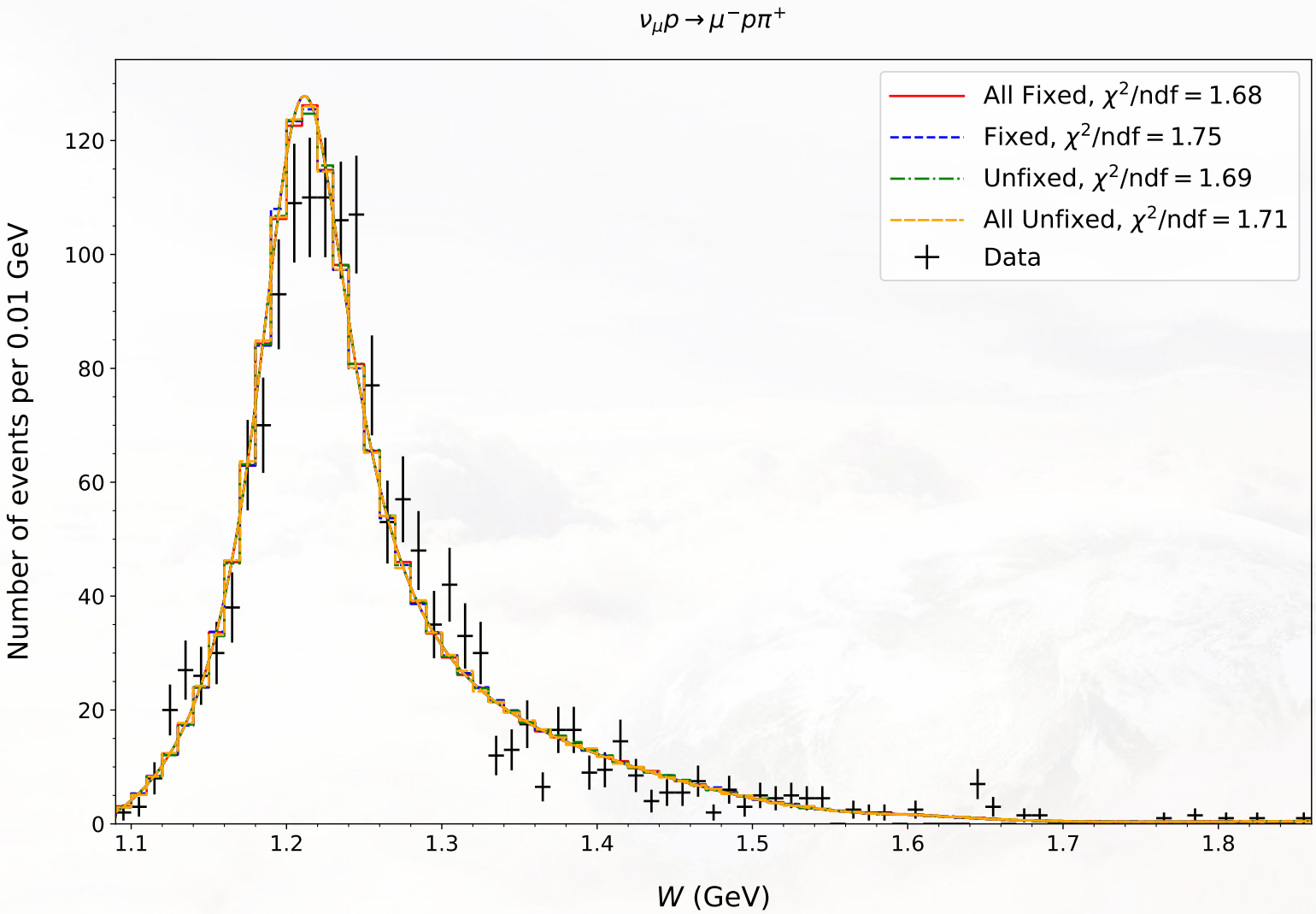

W distribution with no W_{cut}. Neutrino spectrum is restricted by $0.5 < E_\nu < 6.0$ GeV. Model predictions are area-normalized. Predictions with all resonances (All)/without resonance F17(1970) and with fixed and unfixed bugs are shown. Data are taken from Ref. [11]. Neutrino spectrum is taken from [35].

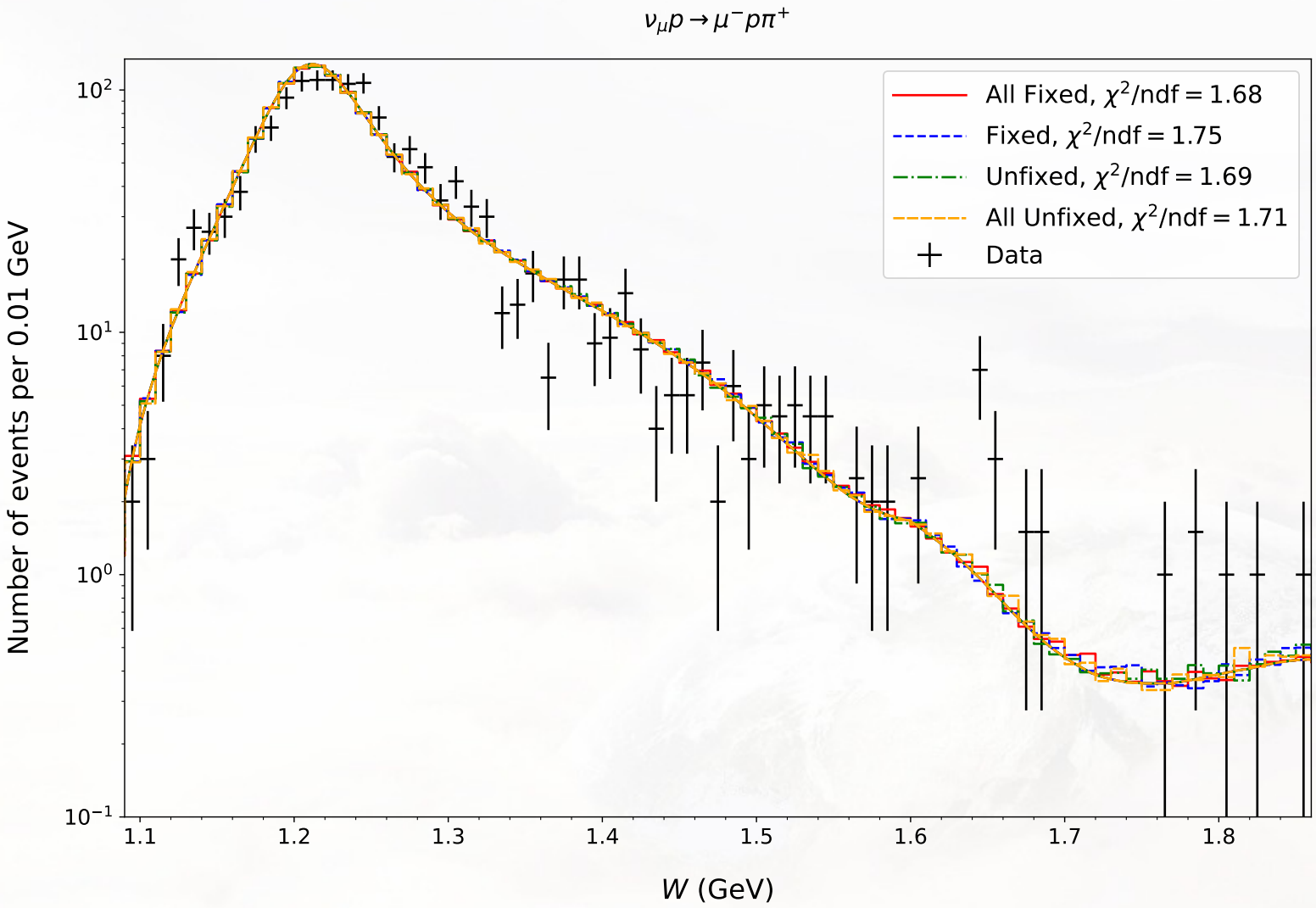

W distribution with no W_{cut}. Neutrino spectrum is restricted by $0.5 < E_\nu < 6.0$ GeV. Model predictions are area-normalized. Predictions with all resonances (All)/without resonance F17(1970) and with fixed and unfixed bugs are shown. Data are taken from Ref. [11]. Neutrino spectrum is taken from [35].

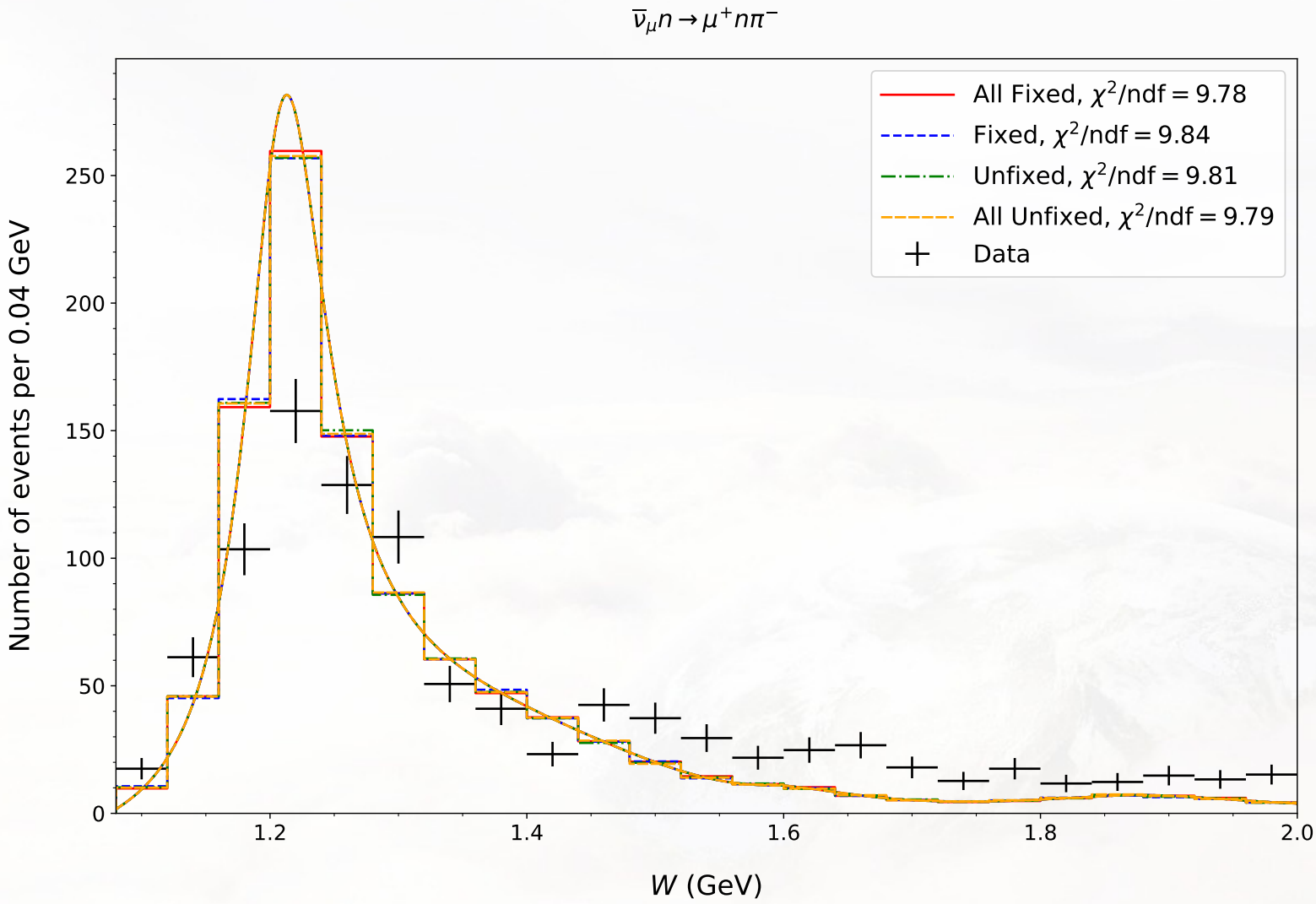

W distribution with no W_{cut}. Neutrino spectrum is restricted by $4.97 < E_\nu < 201$ GeV. Model predictions are area-normalized. Predictions with all resonances (All)/without resonance F17(1970) and with fixed and unfixed bugs are shown. Data are taken from Ref. [24]. Neutrino spectrum is taken from [36].

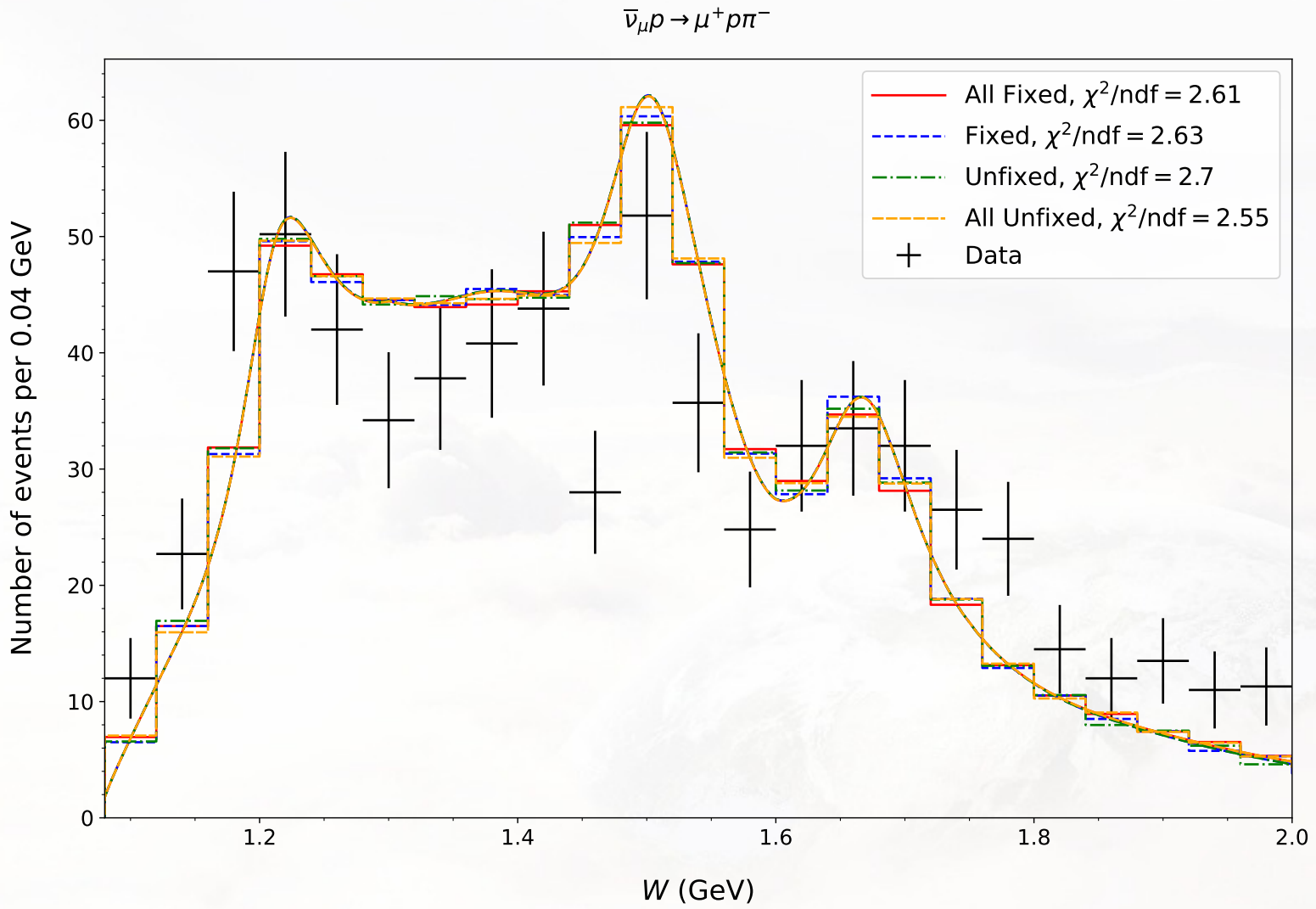

W distribution with no W_{cut}. Neutrino spectrum is restricted by $4.97 < E_\nu < 201$ GeV. Model predictions are area-normalized. Predictions with all resonances (All)/without resonance F17(1970) and with fixed and unfixed bugs are shown. Data are taken from Ref. [24]. Neutrino spectrum is taken from [36]. Cf Fig. 10 bottom right from Ref. [1]

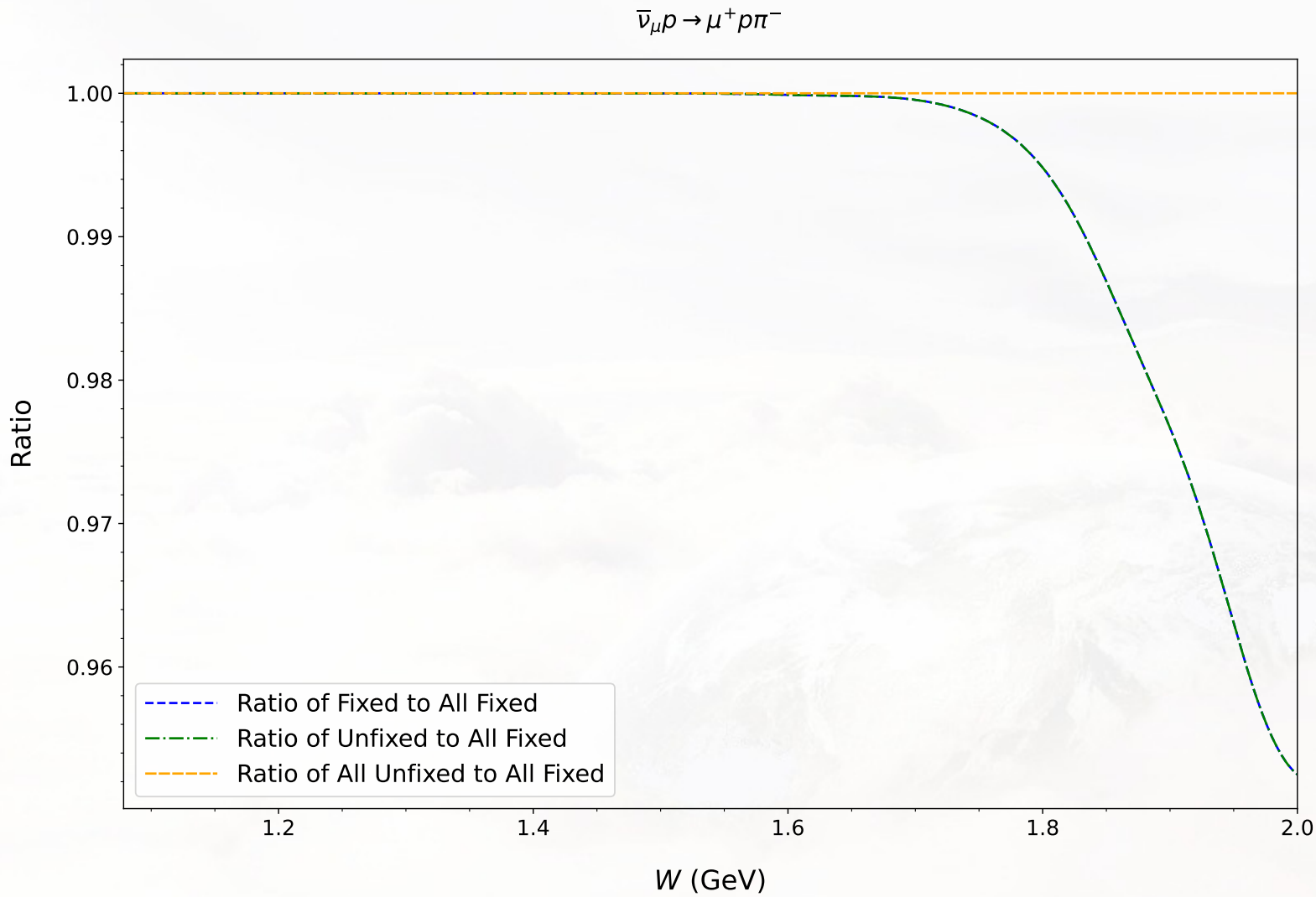

Ratio of $d\sigma/dW$ with no W_{cut}. Neutrino spectrum is restricted by $4.97 < E_\nu < 201$ GeV. Data are taken from Ref. [24]. Neutrino spectrum is taken from [36].

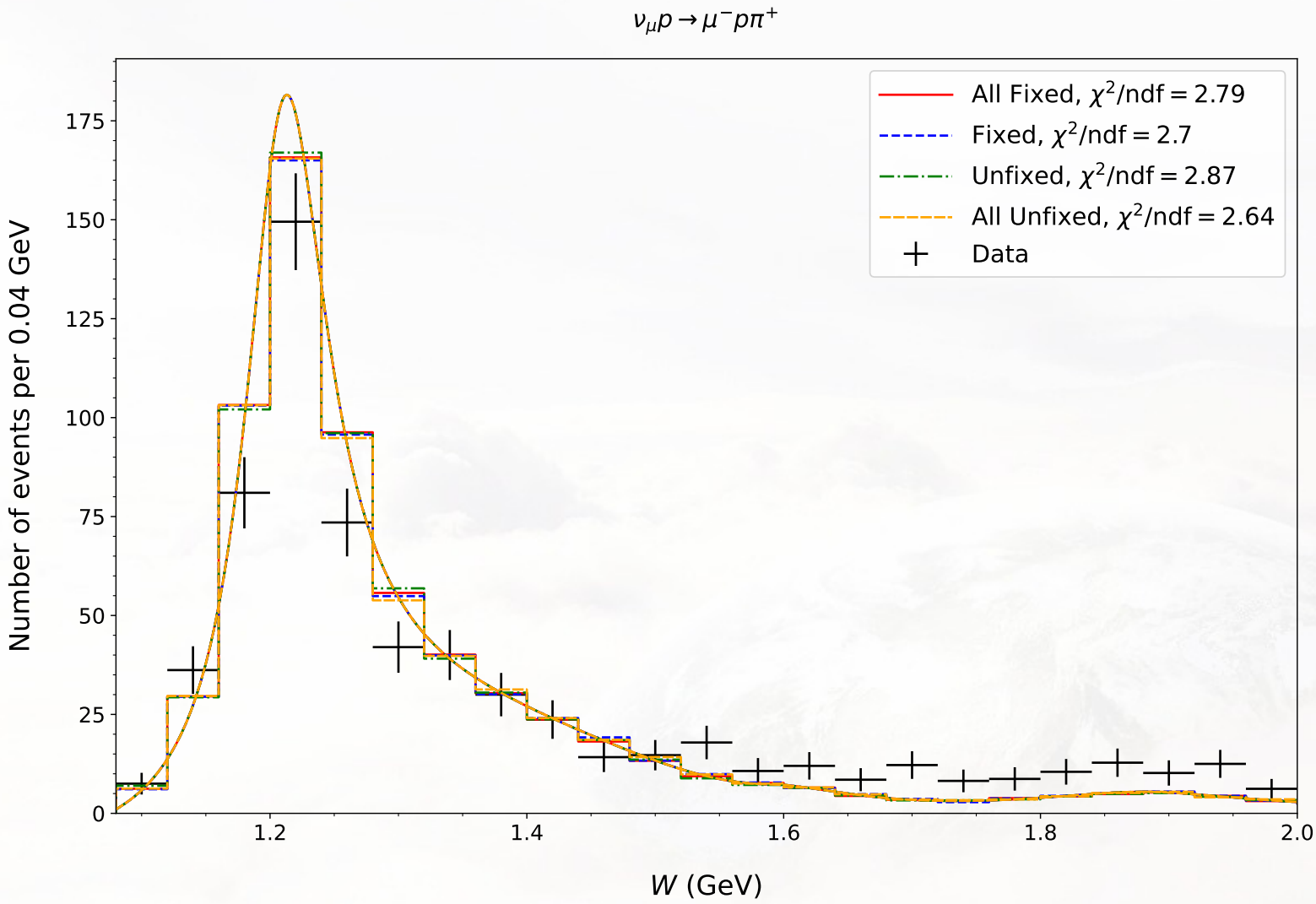

W distribution with no W_{cut}. Neutrino spectrum is restricted by $4.97 < E_\nu < 201$ GeV. Model predictions are area-normalized. Predictions with all resonances (All)/without resonance F17(1970) and with fixed and unfixed bugs are shown. Data are taken from Ref. [24]. Neutrino spectrum is taken from [36]. Cf Fig. 10 top left from Ref. [1]

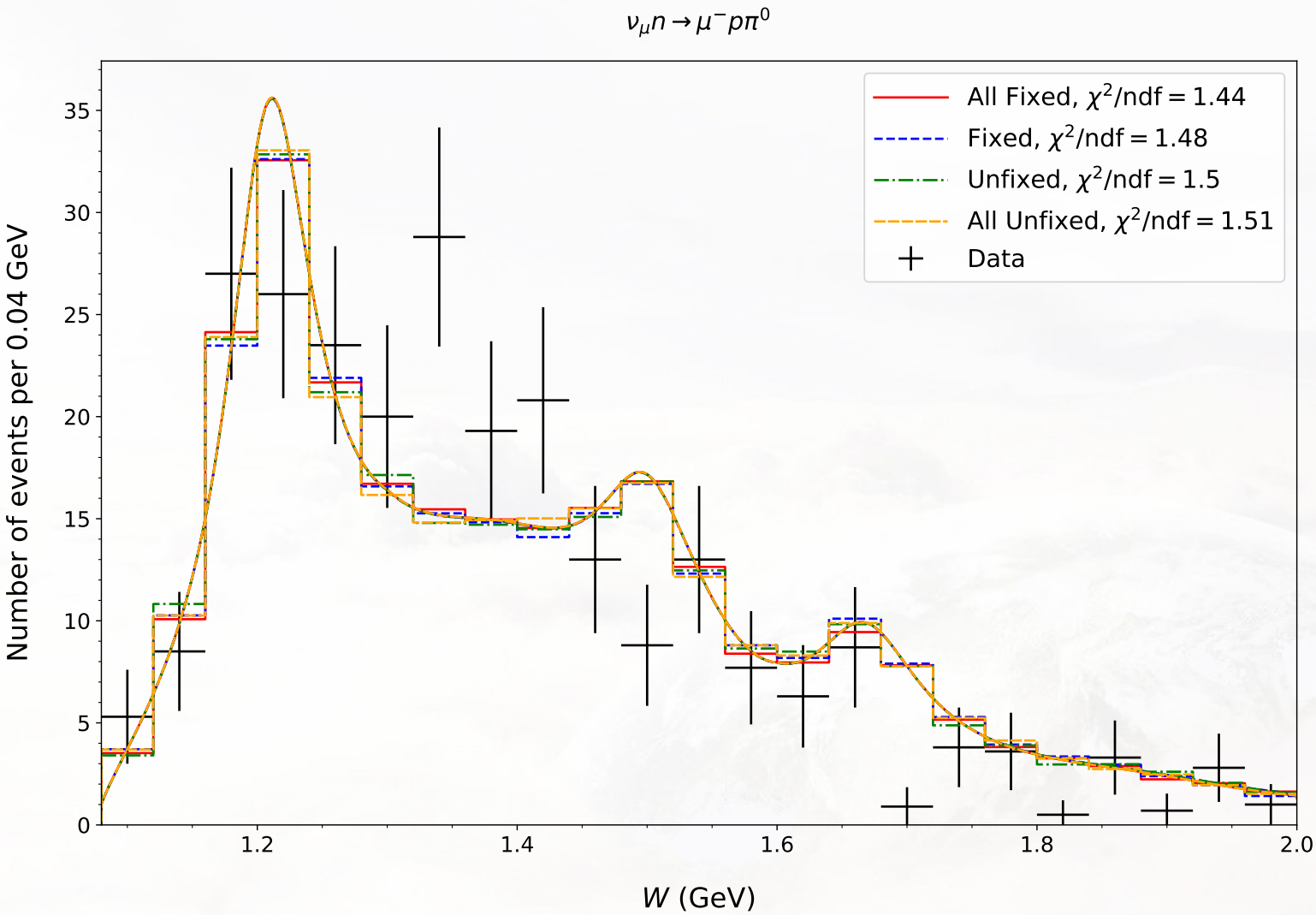

W distribution with no W_{cut}. Neutrino spectrum is restricted by $4.97 < E_\nu < 201$ GeV. Model predictions are area-normalized. Predictions with all resonances (All)/without resonance F17(1970) and with fixed and unfixed bugs are shown. Data are taken from Ref. [24]. Neutrino spectrum is taken from [36]. Cf Fig. 10 top right from Ref. [1]

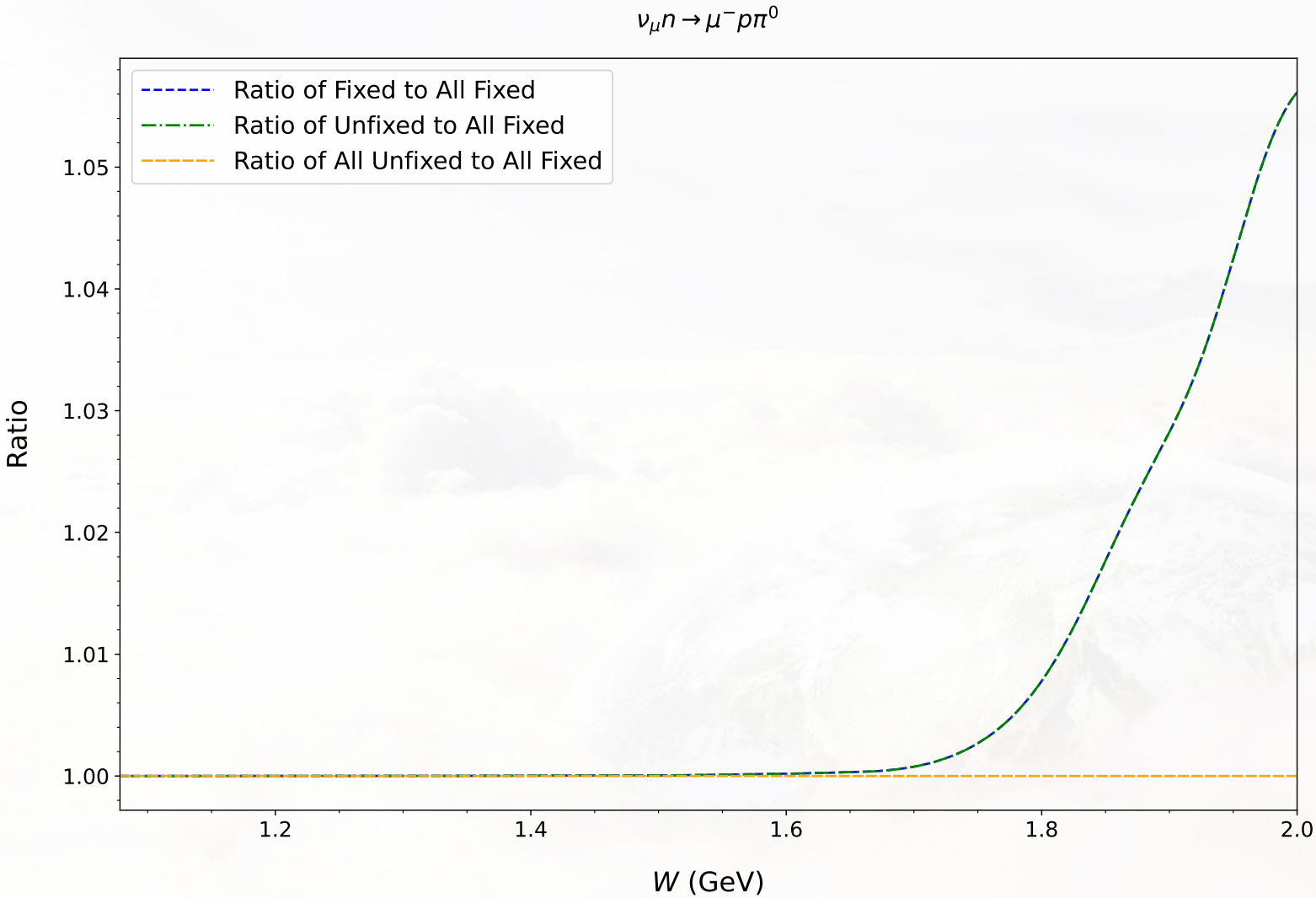

Ratio of $d\sigma/dW$ with no W_{cut}. Neutrino spectrum is restricted by $4.97 < E_\nu < 201$ GeV. Data are taken from Ref. [24]. Neutrino spectrum is taken from [36].

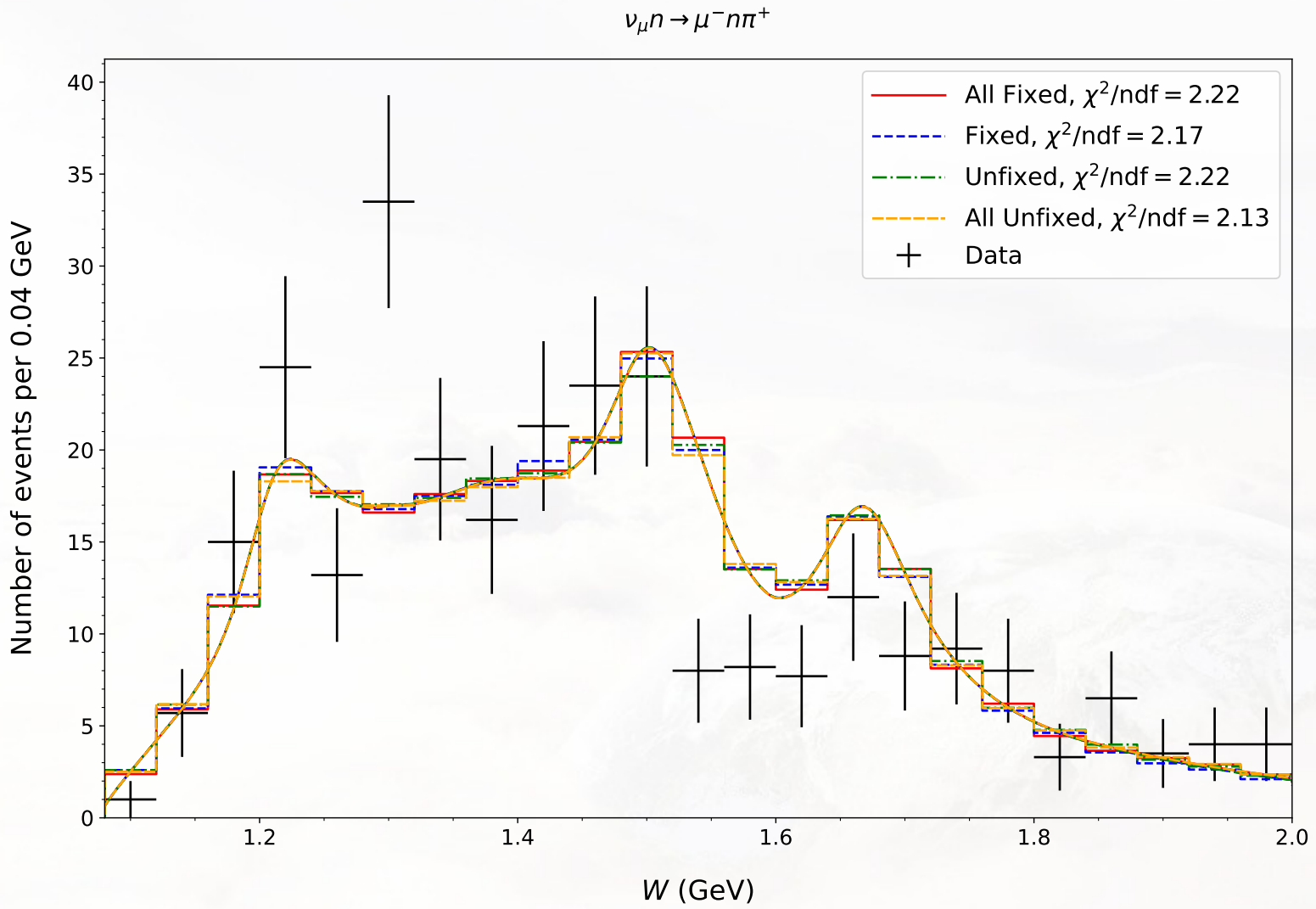

W distribution with no W_{cut}. Neutrino spectrum is restricted by $4.97 < E_\nu < 201$ GeV. Model predictions are area-normalized. Predictions with all resonances (All)/without resonance F17(1970) and with fixed and unfixed bugs are shown. Data are taken from Ref. [24]. Neutrino spectrum is taken from [36]. Cf Fig. 10 bottom left from Ref. [1]

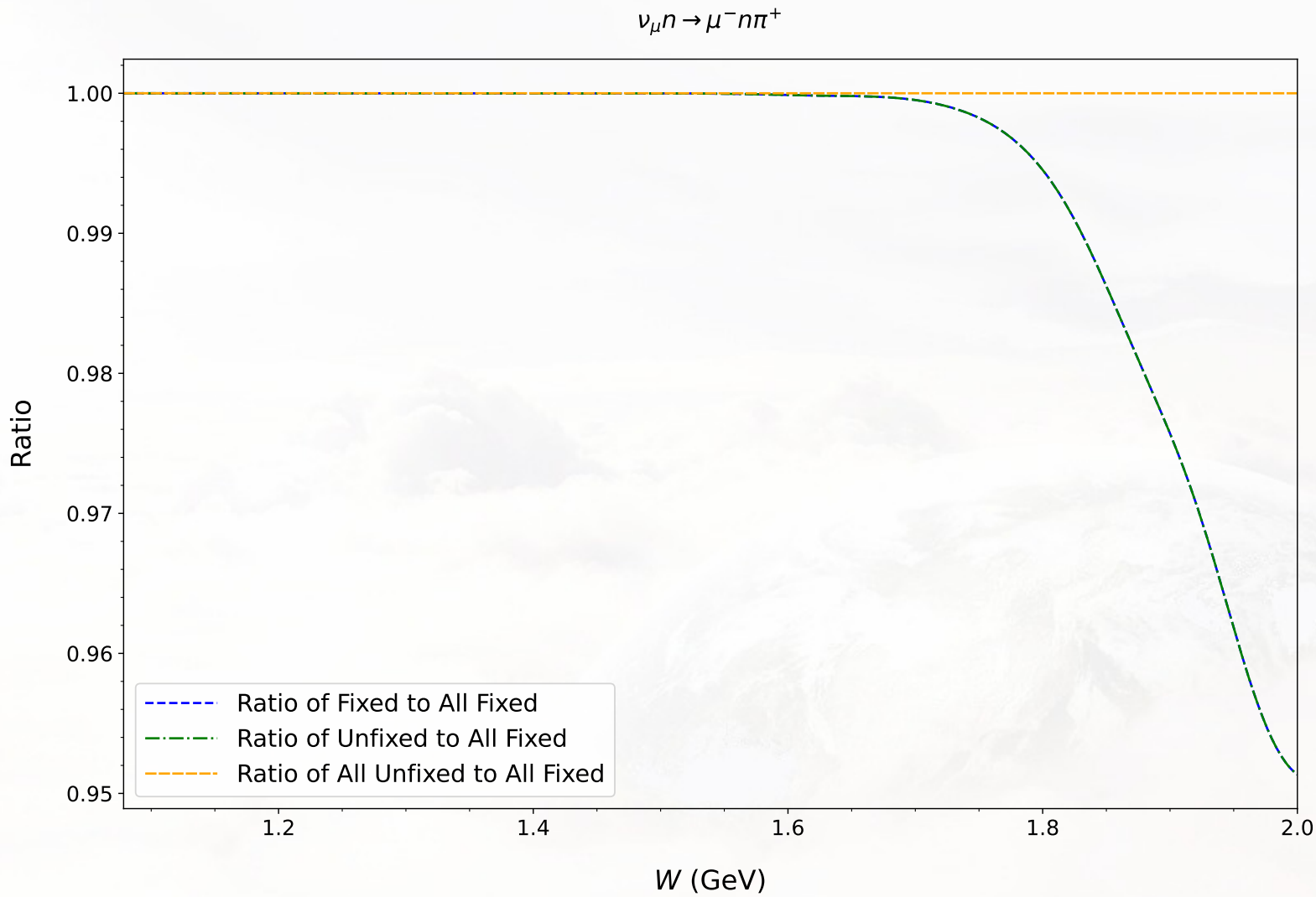

Ratio of $d\sigma/dW$ with no W_{cut}. Neutrino spectrum is restricted by $4.97 < E_\nu < 201$ GeV. Data are taken from Ref. [24]. Neutrino spectrum is taken from [36].

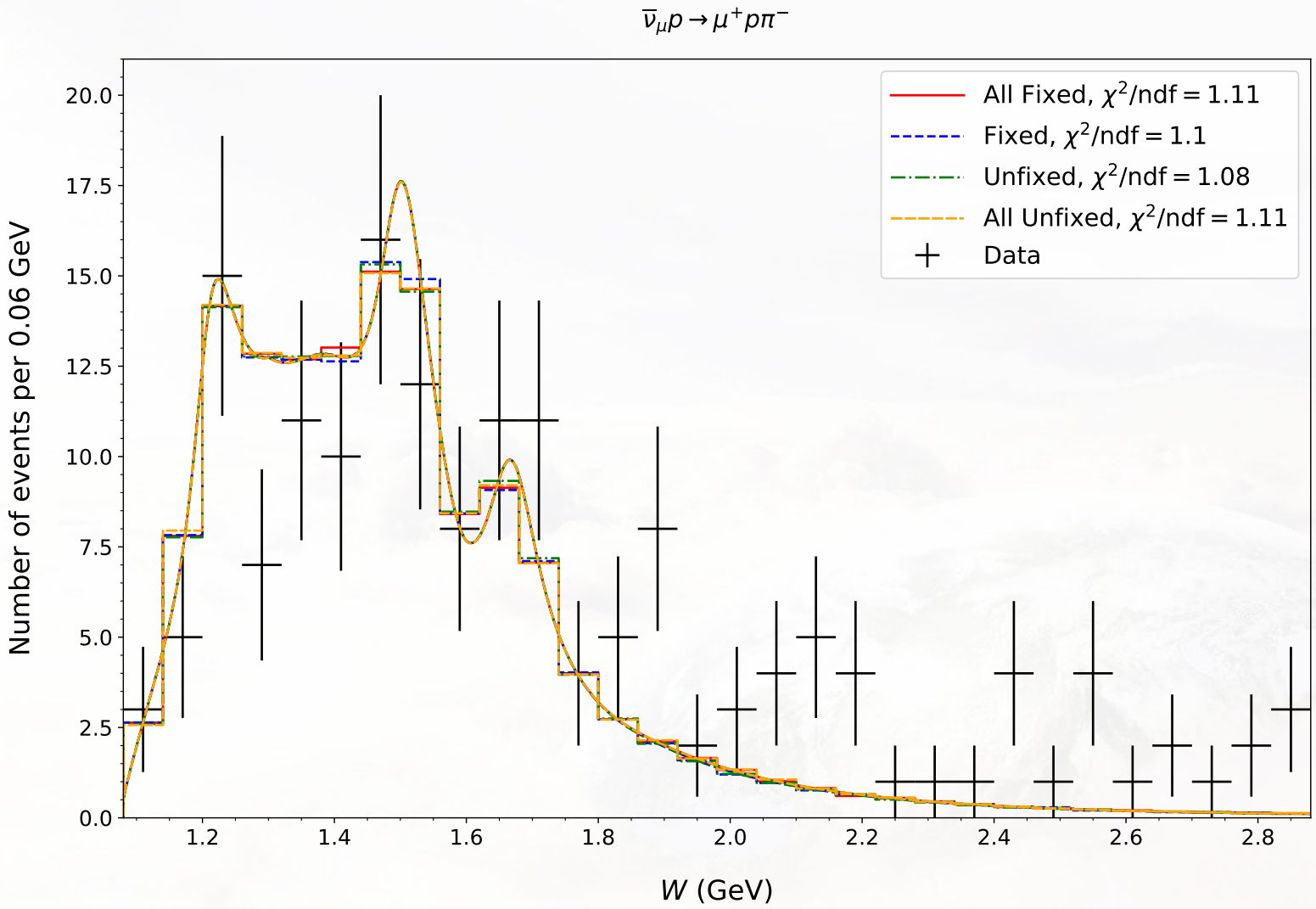

W distribution with no W_{cut}. Neutrino spectrum is restricted by $5.0 < E_\nu < 155.0$ GeV. Model predictions are area-normalized. Predictions with all resonances (All)/without resonance F17(1970) and with fixed and unfixed bugs are shown. Data are taken from Ref. [10]. Only $W < 1.98$ GeV used for area renormalization calculation. Neutrino spectrum is taken from [17] (Stefanski-White spectrum model).

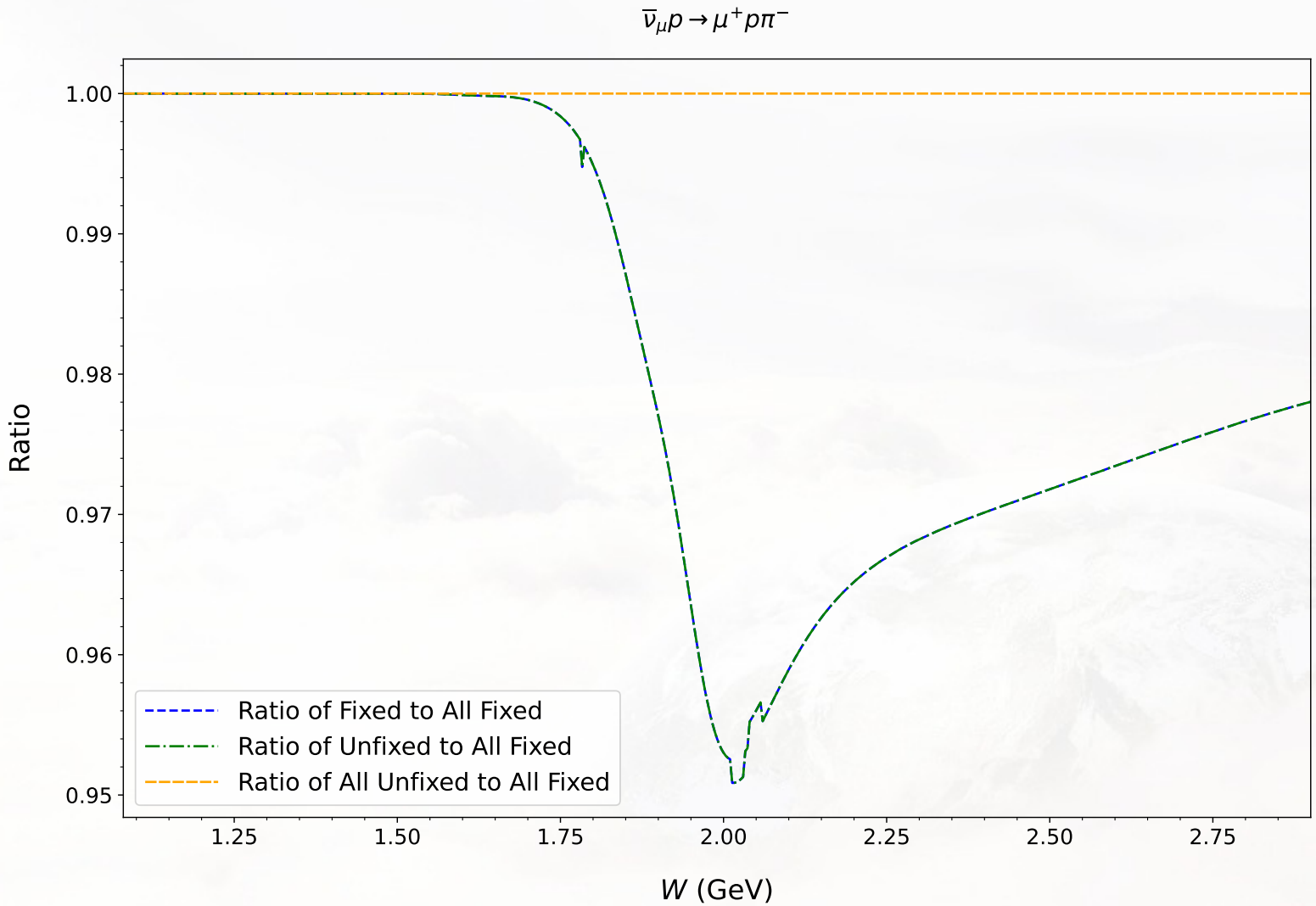

Ratio of $d\sigma/dW$ with no W_{cut}. Neutrino spectrum is restricted by $5.0 < E_\nu < 155.0$ GeV. Data are taken from Ref. [10]. Neutrino spectrum is taken from [17] (Stefanski-White spectrum model).

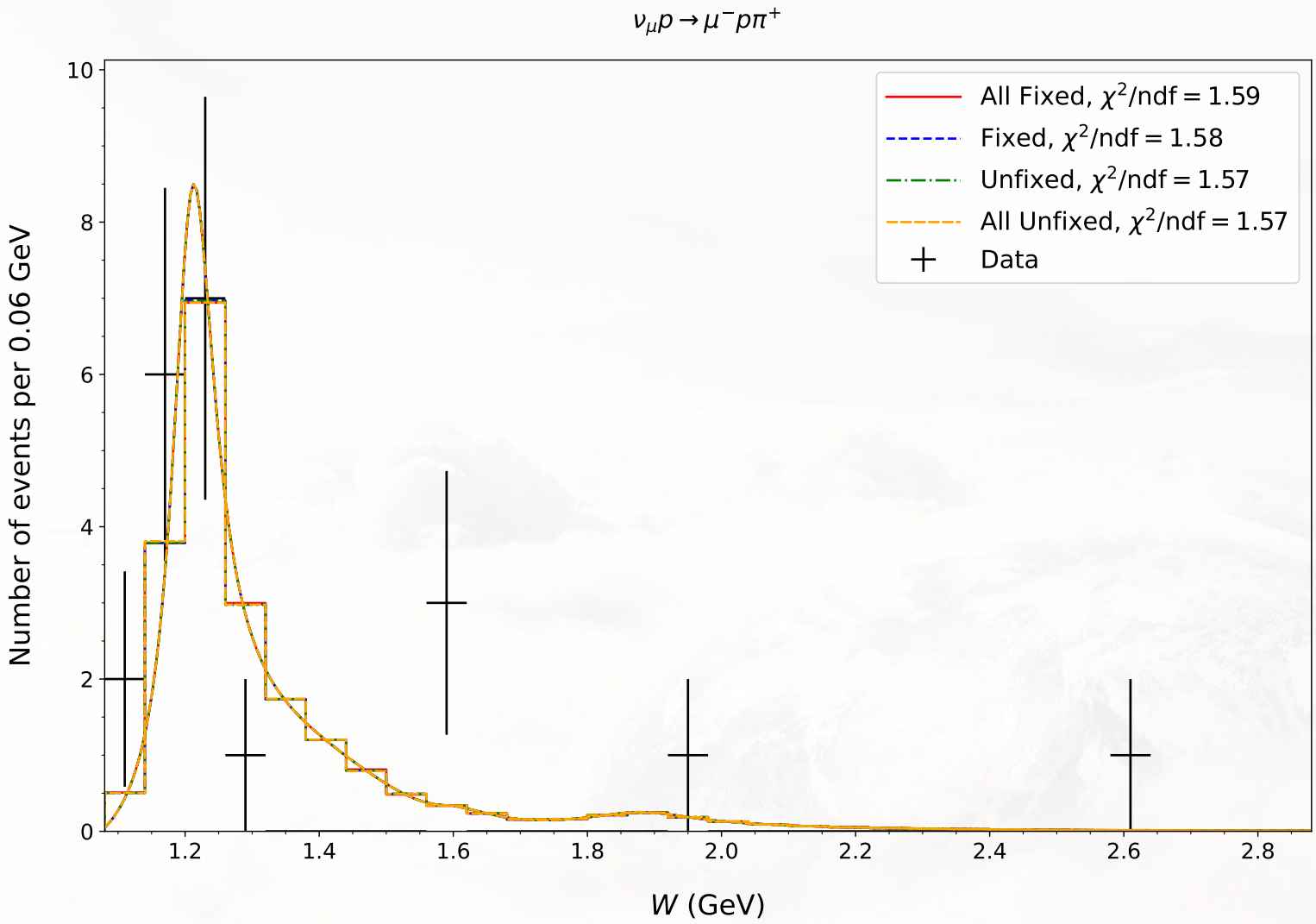

W distribution with no W_{cut}. Neutrino spectrum is restricted by $5.0 < E_\nu < 155.0$ GeV. Model predictions are area-normalized. Predictions with all resonances (All)/without resonance F17(1970) and with fixed and unfixed bugs are shown. Data are taken from Ref. [10]. Only $W < 1.98$ GeV used for area renormalization calculation. Neutrino spectrum is taken from [17] (Stefanski-White spectrum model).

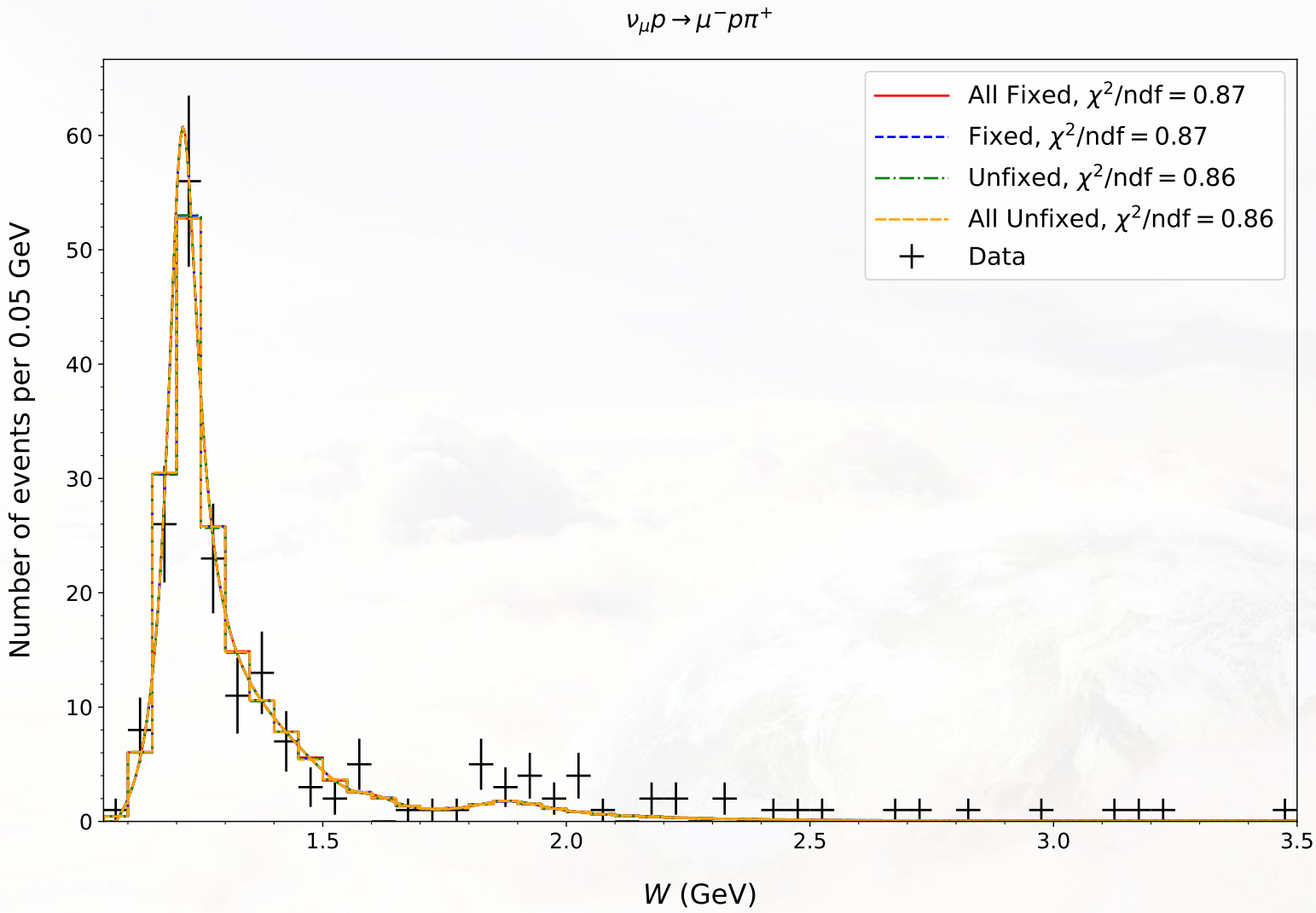

W distribution with no W_{cut}. Neutrino spectrum is restricted by $5.0 < E_\nu < 155.0$ GeV. Model predictions are area-normalized. Predictions with all resonances (All)/without resonance F17(1970) and with fixed and unfixed bugs are shown. Data are taken from Ref. [14]. Only $W < 2.0$ GeV used for area renormalization calculation. Neutrino spectrum is taken from [17] (Stefanski-White spectrum model).

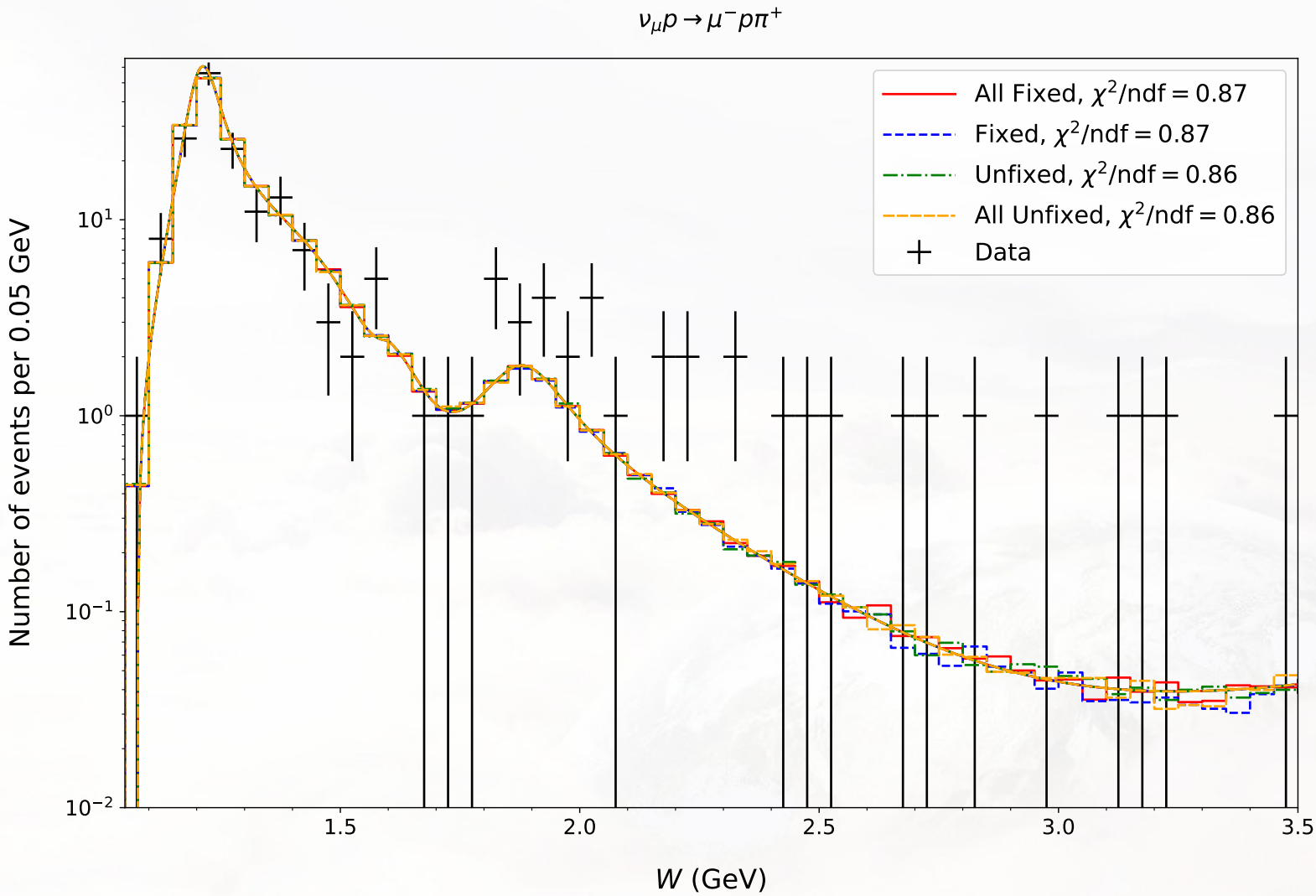

W distribution with no W_{cut}. Neutrino spectrum is restricted by $5.0 < E_\nu < 155.0$ GeV. Model predictions are area-normalized. Predictions with all resonances (All)/without resonance F17(1970) and with fixed and unfixed bugs are shown. Data are taken from Ref. [14]. Only $W < 2.0$ GeV used for area renormalization calculation. Neutrino spectrum is taken from [17] (Stefanski-White spectrum model).

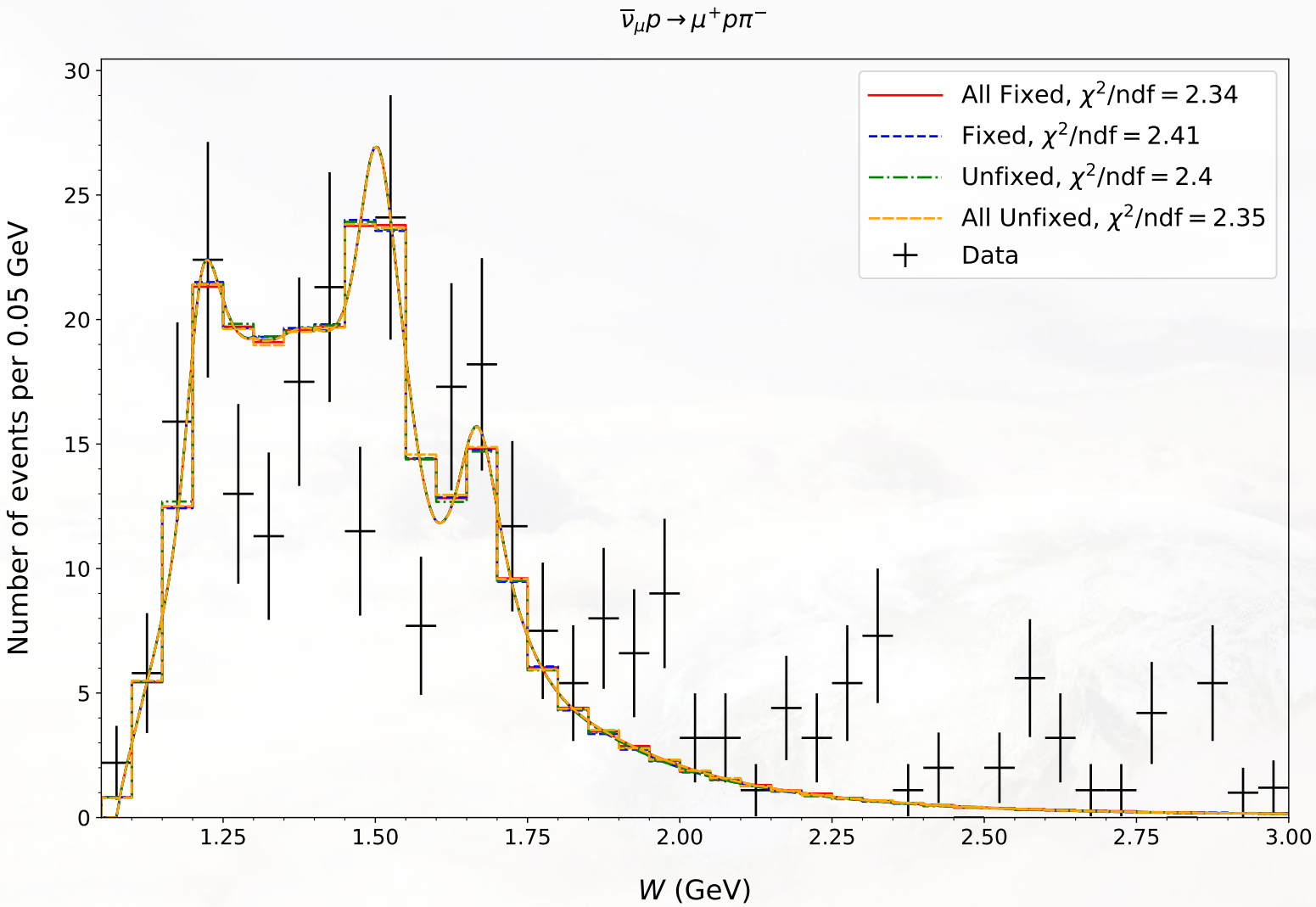

W distribution with no W_{cut}. Neutrino spectrum is restricted by $5.0 < E_\nu < 200.0$ GeV. Model predictions are area-normalized. Predictions with all resonances (All)/without resonance F17(1970) and with fixed and unfixed bugs are shown. Data are taken from Ref. [19]. Only $W < 2.0$ GeV used for area renormalization calculation. Neutrino spectrum is taken from [36].

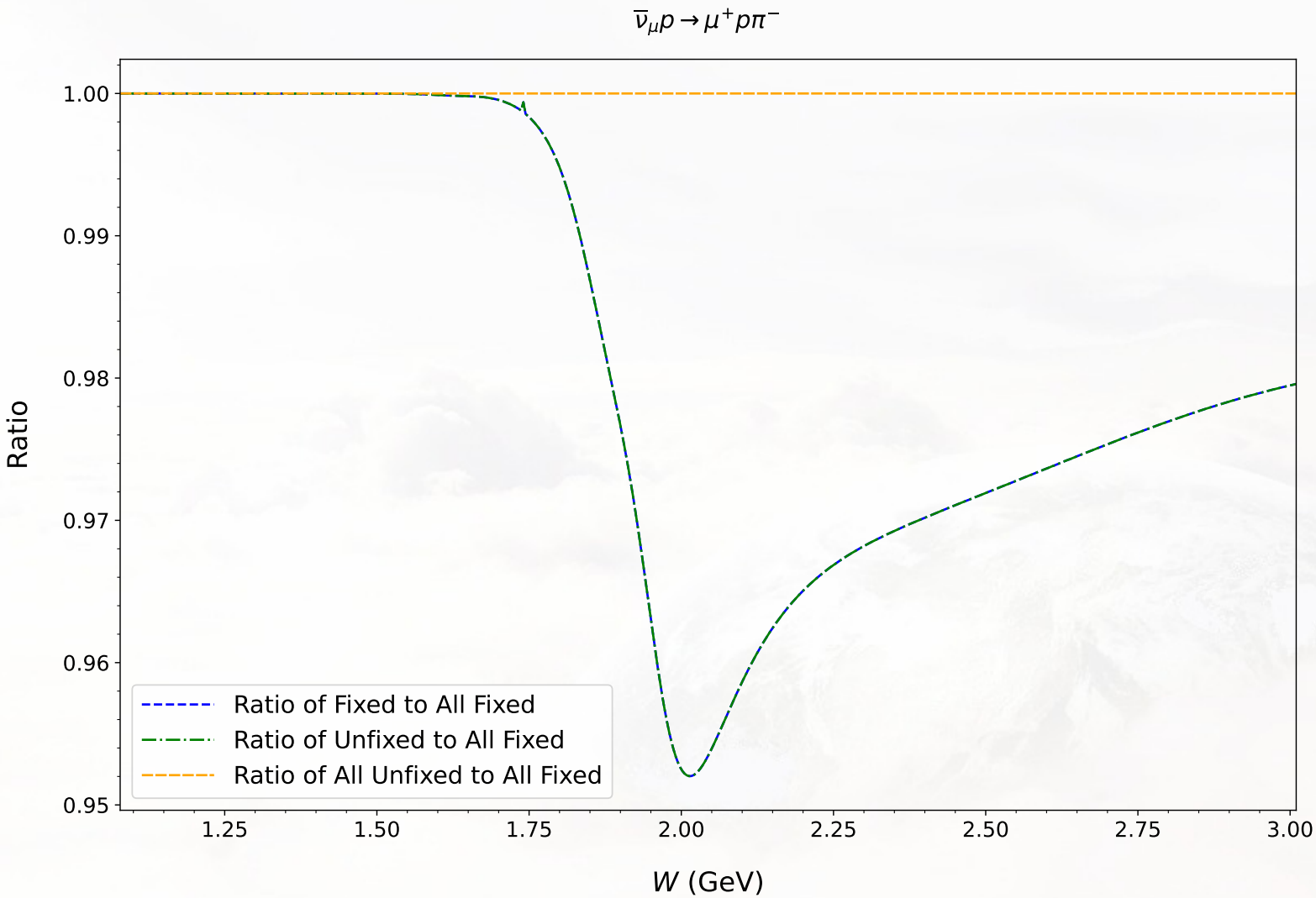

Ratio of $d\sigma/dW$ with no W_{cut}. Neutrino spectrum is restricted by $5.0 < E_\nu < 200.0$ GeV. Data are taken from Ref. [19]. Neutrino spectrum is taken from [36].

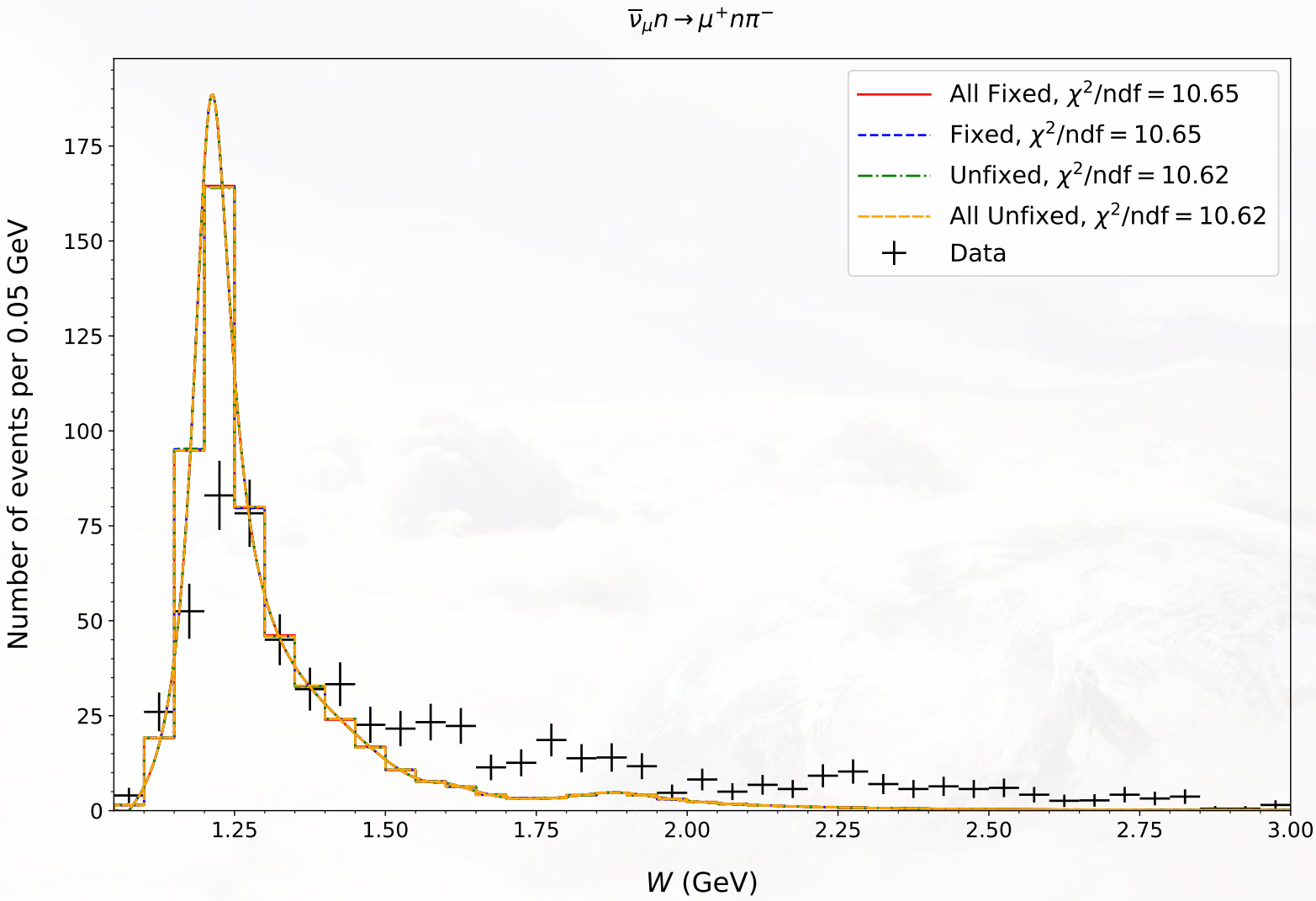

W distribution with no W_{cut}. Neutrino spectrum is restricted by $5.0 < E_\nu < 200.0$ GeV. Model predictions are area-normalized. Predictions with all resonances (All)/without resonance F17(1970) and with fixed and unfixed bugs are shown. Data are taken from Ref. [19]. Only $W < 2.0$ GeV used for area renormalization calculation. Neutrino spectrum is taken from [36].

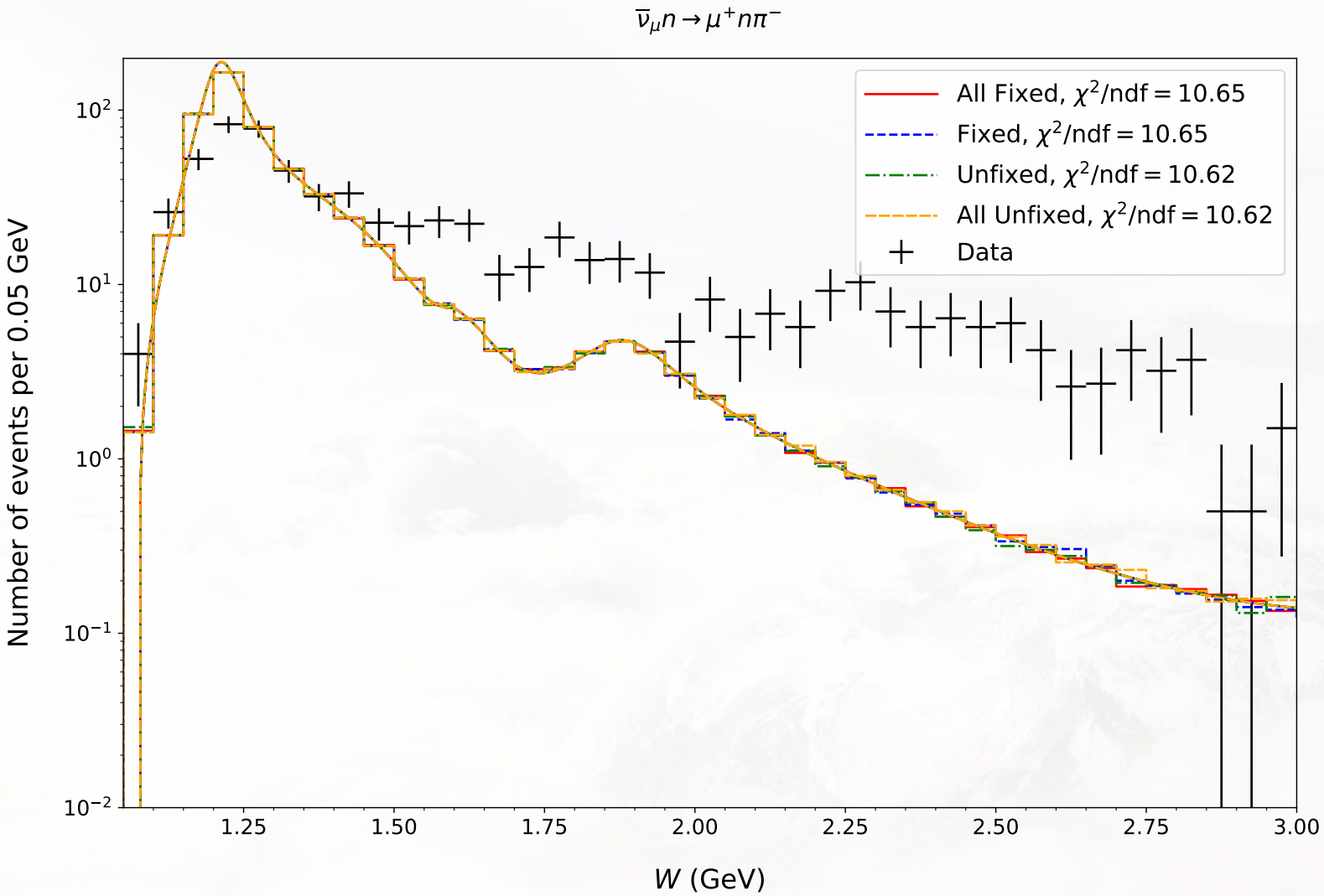

W distribution with no W_{cut}. Neutrino spectrum is restricted by $5.0 < E_\nu < 200.0$ GeV. Model predictions are area-normalized. Predictions with all resonances (All)/without resonance F17(1970) and with fixed and unfixed bugs are shown. Data are taken from Ref. [19]. Only $W < 2.0$ GeV used for area renormalization calculation. Neutrino spectrum is taken from [36].

Next topic

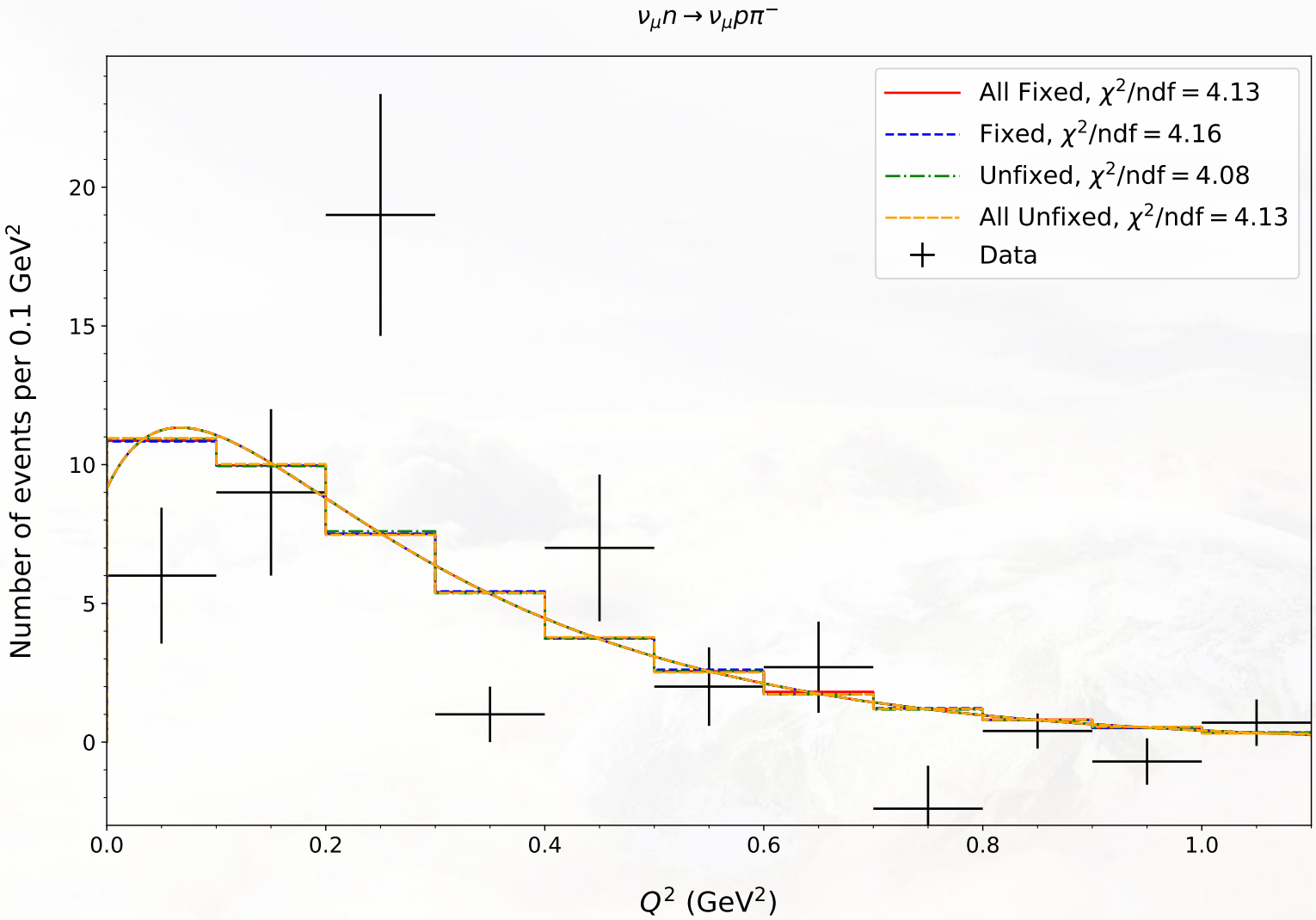

Q^2 distribution with no W_{cut}. Neutrino spectrum is restricted by $0.3 < E_\nu < 1.5$ GeV. Model predictions are area-normalized. Predictions with all resonances (All)/without resonance F17(1970) and with fixed and unfixed bugs are shown. Data are taken from Ref. [31]. Neutrino spectrum is taken from [34].

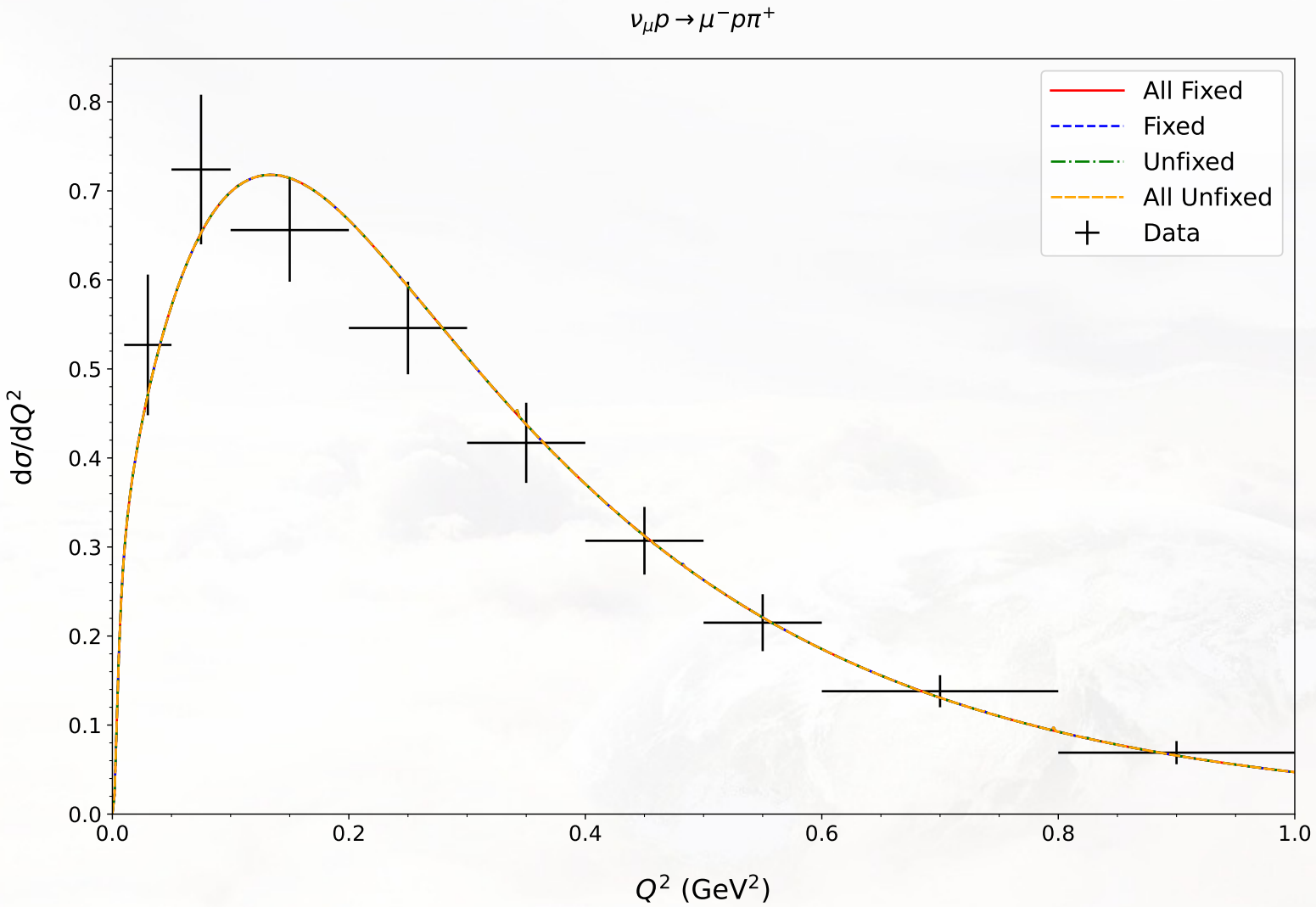

Q^2 distribution with $W < 1.4$ GeV. Neutrino spectrum is restricted by $0.5 < E_\nu < 6.0$ GeV. Predictions with all resonances (All)/without resonance F17(1970) and with fixed and unfixed bugs are shown. Data are taken from Ref. [6]. Neutrino spectrum is taken from [34].

Cf Fig. 4 from Ref. [1]

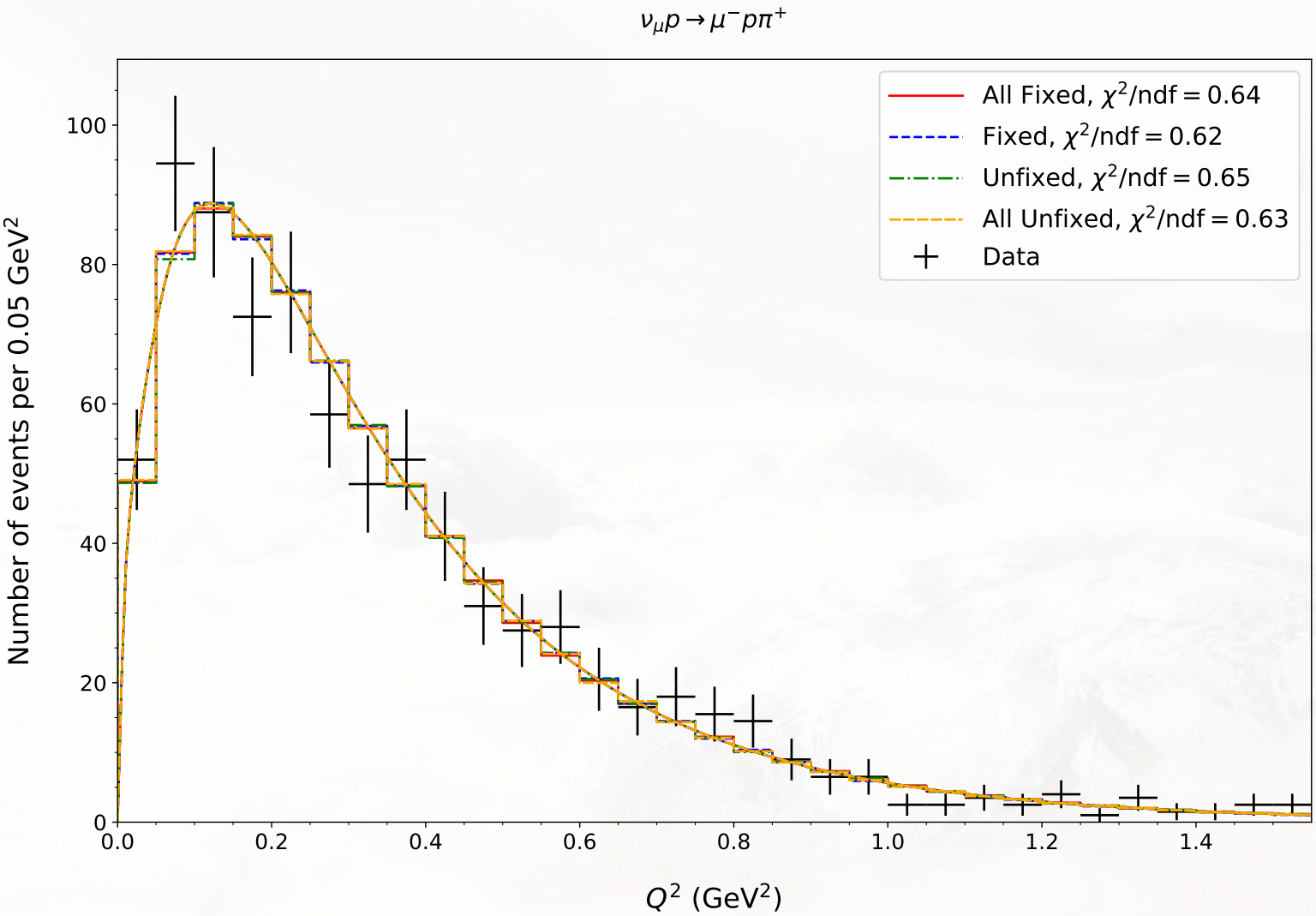

Q^2 distribution with $W < 1.4$ GeV. Neutrino spectrum is restricted by $E_\nu < 6.0$ GeV. Model predictions are area-normalized. Predictions with all resonances (All)/without resonance F17(1970) and with fixed and unfixed bugs are shown. Data are taken from Ref. [6]. Neutrino spectrum is taken from [34].

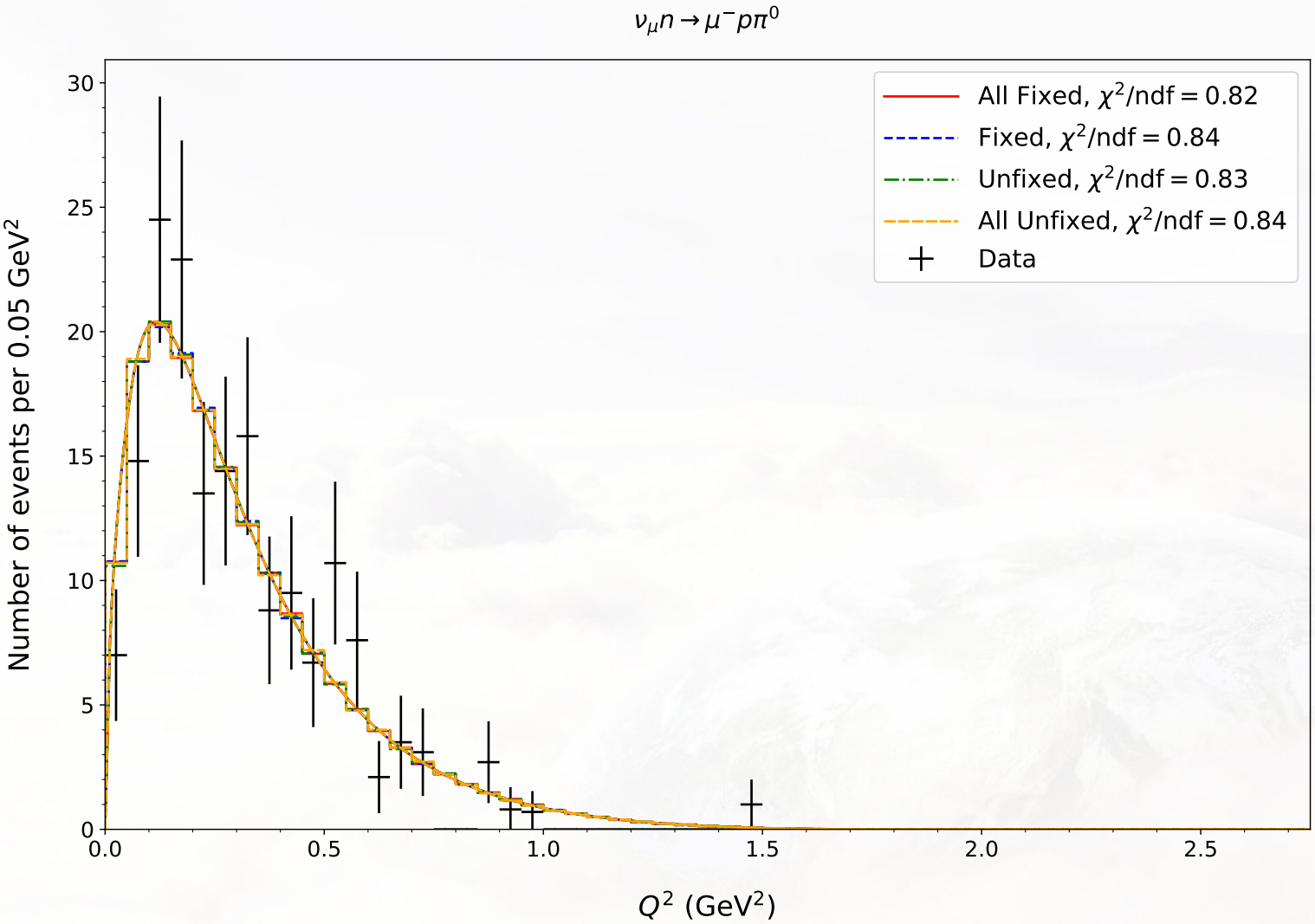

Q^2 distribution with $W < 1.4$ GeV. Neutrino spectrum is restricted by $E_\nu < 1.5$ GeV. Model predictions are area-normalized. Predictions with all resonances (All)/without resonance F17(1970) and with fixed and unfixed bugs are shown. Data are taken from Ref. [6]. Neutrino spectrum is taken from [34].

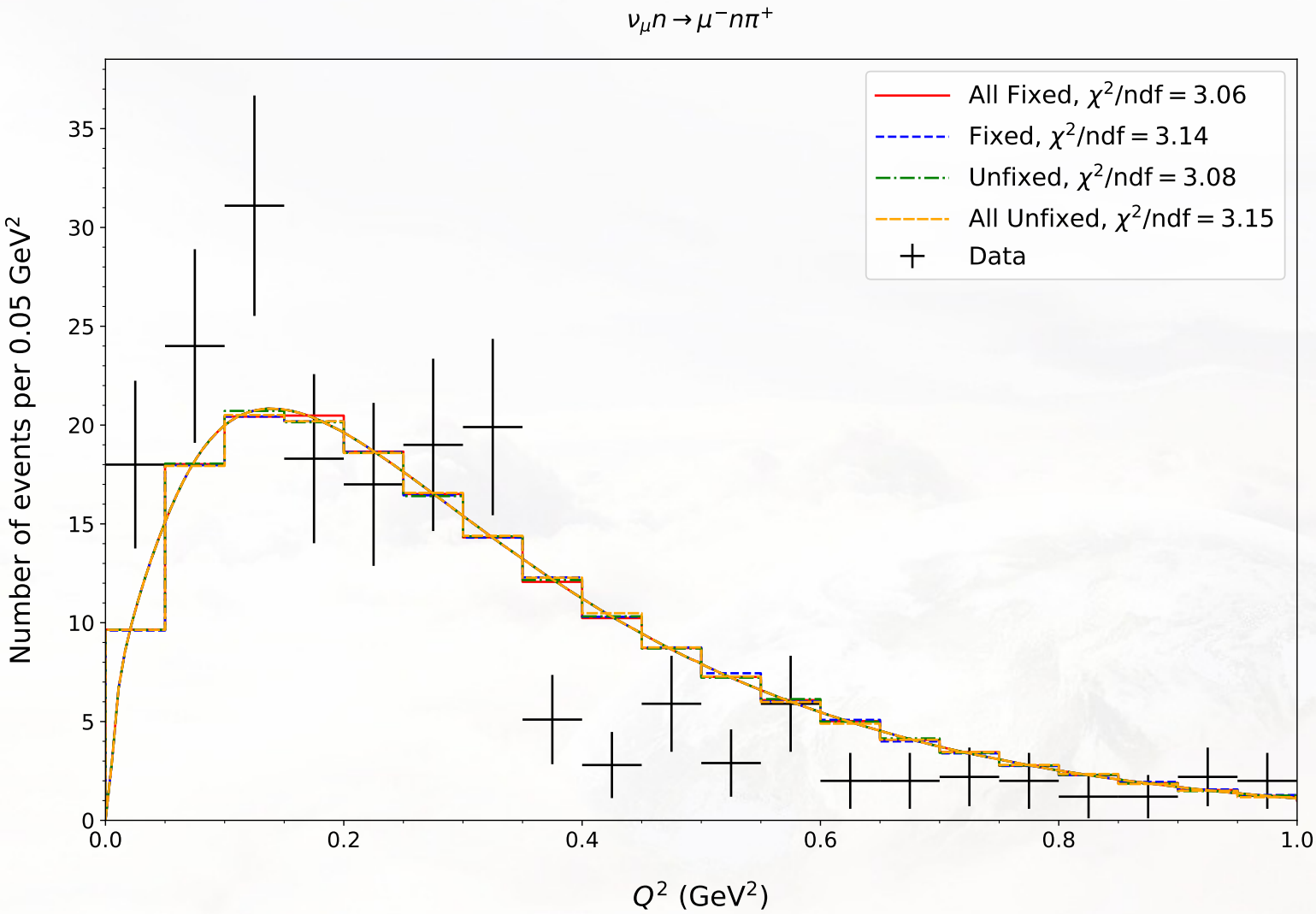

Q^2 distribution with $W < 1.4$ GeV. Neutrino spectrum is restricted by $E_\nu < 1.5$ GeV. Model predictions are area-normalized. Predictions with all resonances (All)/without resonance F17(1970) and with fixed and unfixed bugs are shown. Data are taken from Ref. [6]. Neutrino spectrum is taken from [34].

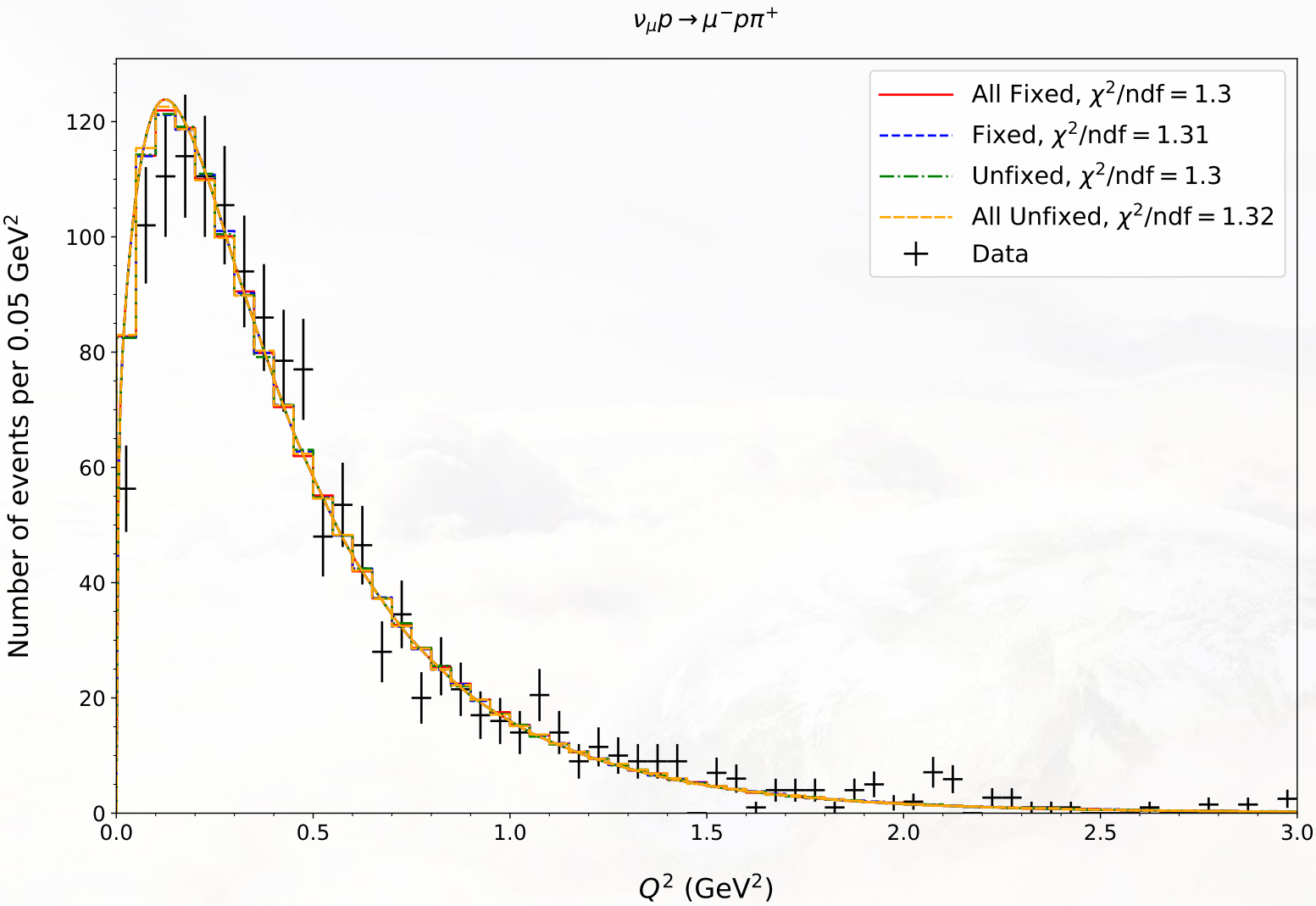

Q^2 distribution with $W < 1.4$ GeV. Neutrino spectrum is restricted by $0.5 < E_\nu < 6.0$ GeV. Model predictions are area-normalized. Predictions with all resonances (All)/without resonance F17(1970) and with fixed and unfixed bugs are shown. Data are taken from Ref. [11]. Neutrino spectrum is taken from [35].

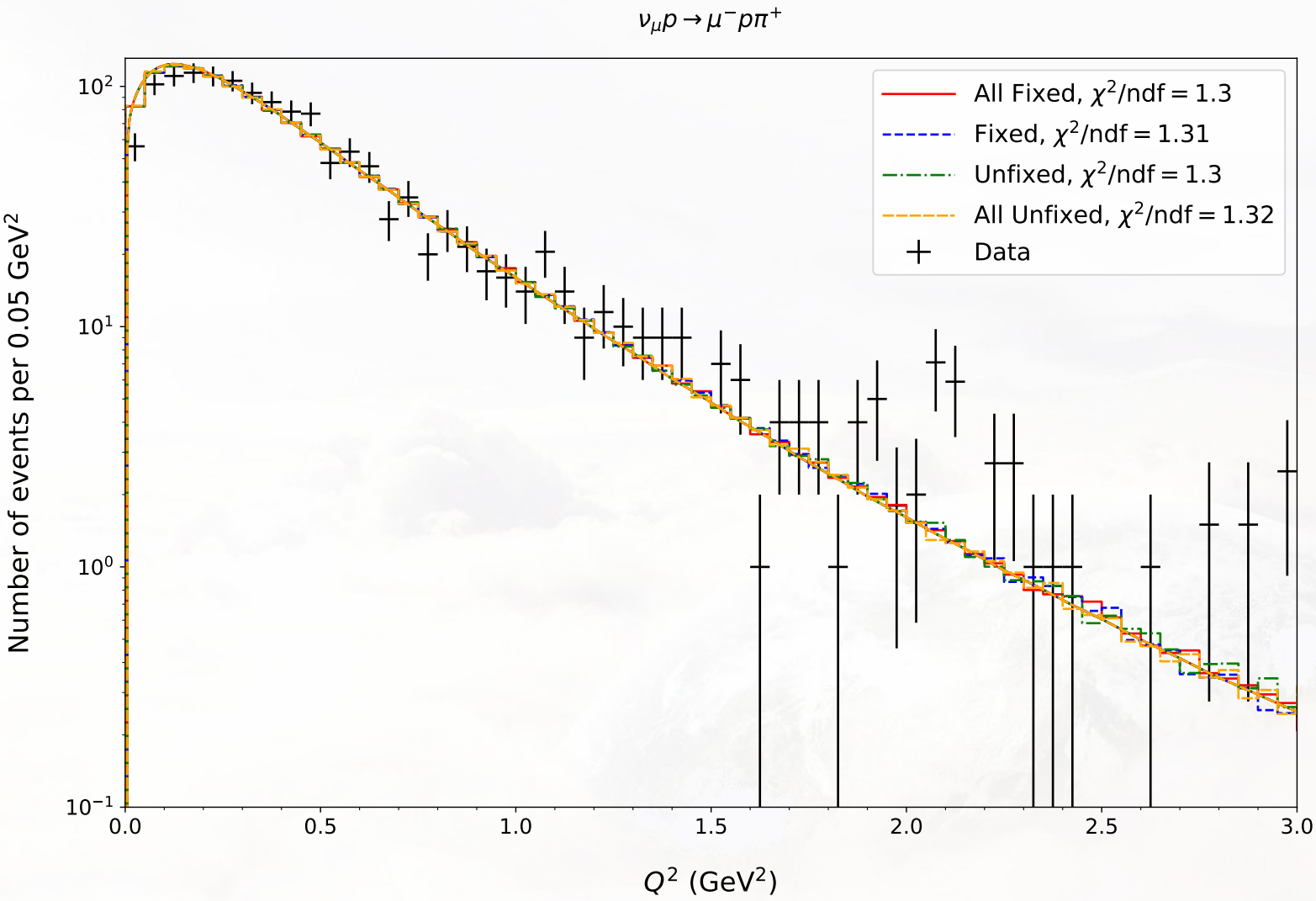

Q^2 distribution with $W < 1.4$ GeV. Neutrino spectrum is restricted by $0.5 < E_\nu < 6.0$ GeV. Model predictions are area-normalized. Predictions with all resonances (All)/without resonance F17(1970) and with fixed and unfixed bugs are shown. Data are taken from Ref. [11]. Neutrino spectrum is taken from [35].

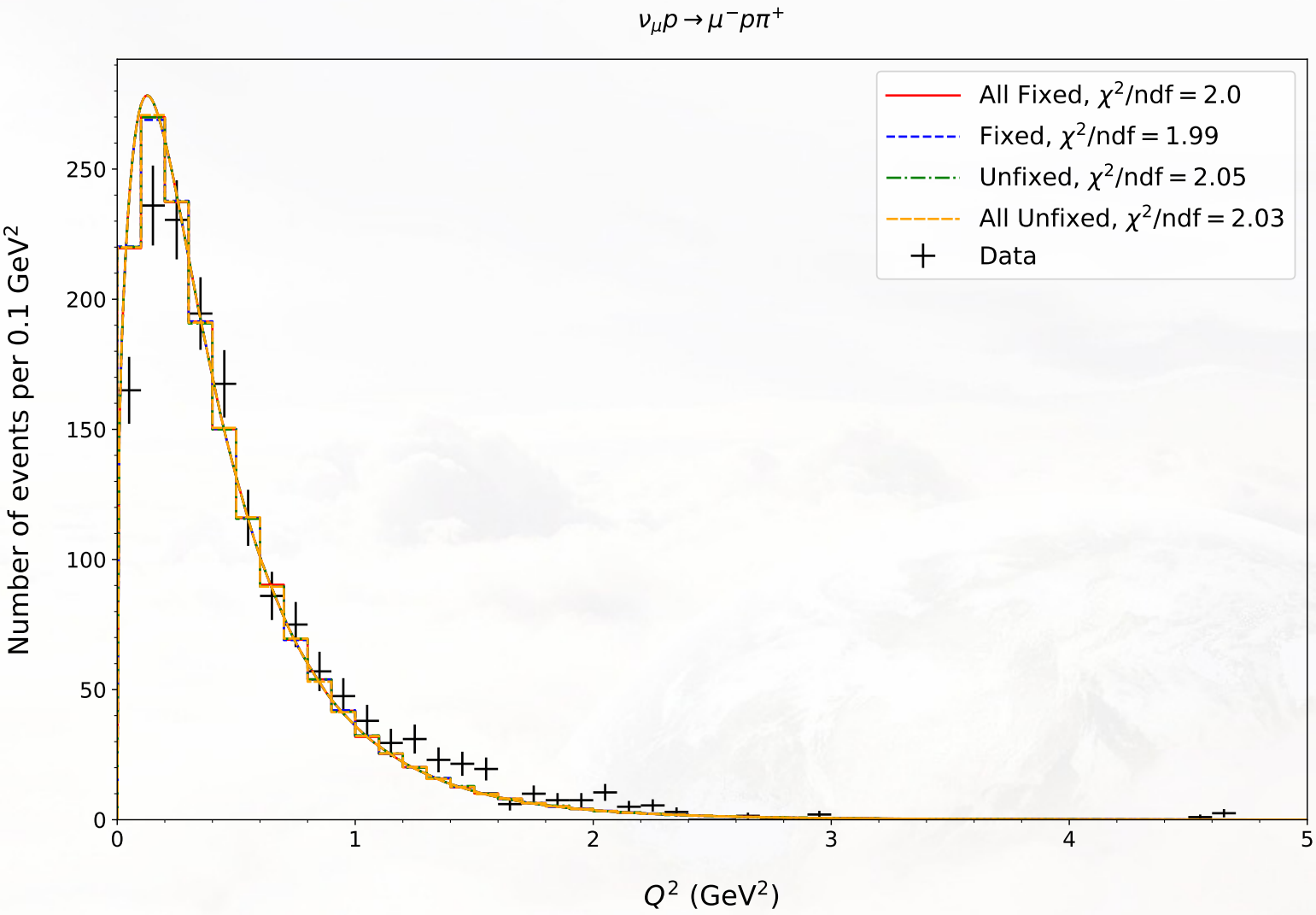

Q^2 distribution with no W_{cut}. Neutrino spectrum is restricted by $E_\nu < 6.0$ GeV. Model predictions are area-normalized. Predictions with all resonances (All)/without resonance F17(1970) and with fixed and unfixed bugs are shown. Data are taken from Ref. [11]. Neutrino spectrum is taken from [35].

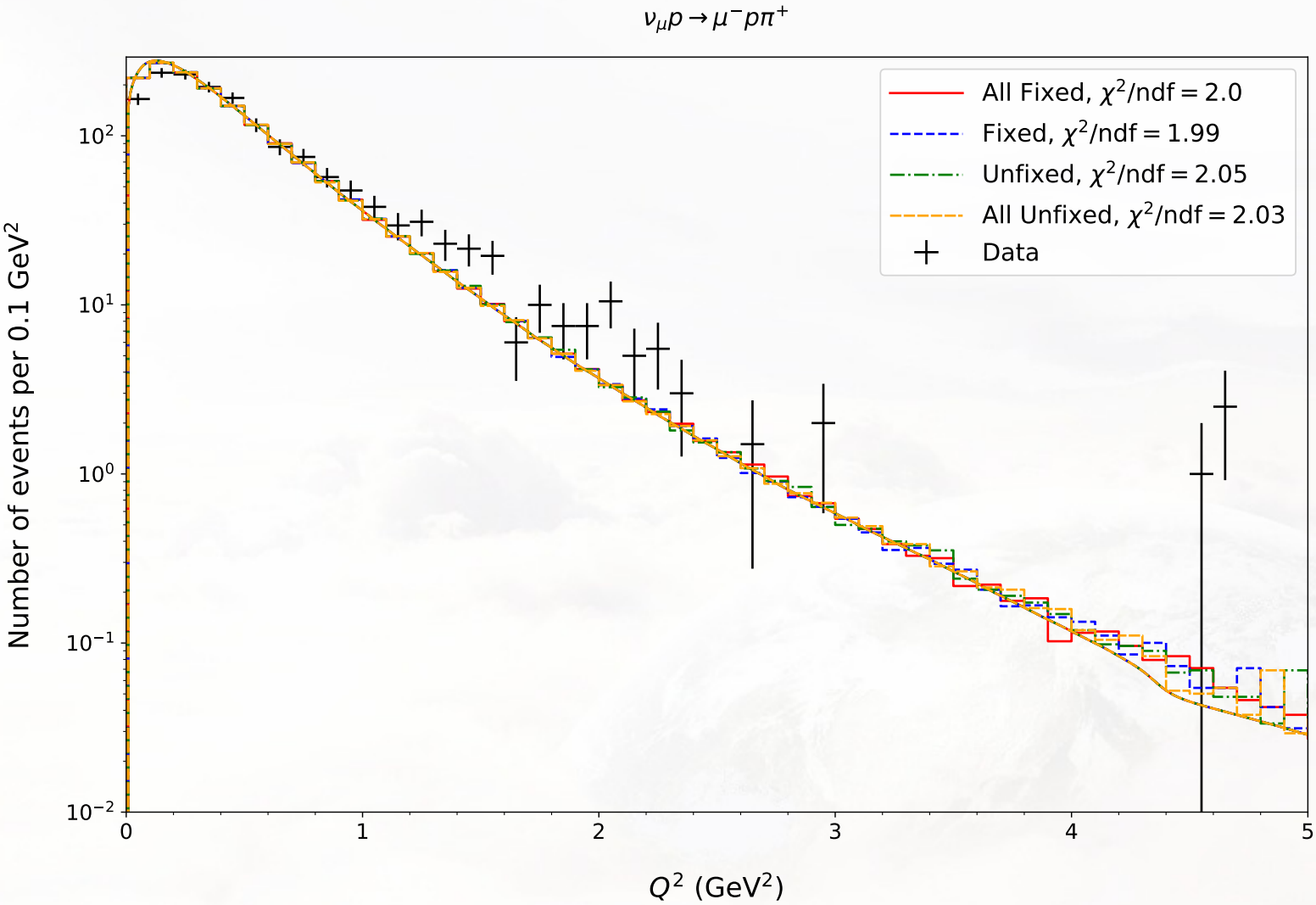

Q^2 distribution with no W_{cut}. Neutrino spectrum is restricted by $E_\nu < 6.0$ GeV. Model predictions are area-normalized. Predictions with all resonances (All)/without resonance F17(1970) and with fixed and unfixed bugs are shown. Data are taken from Ref. [11]. Neutrino spectrum is taken from [35].

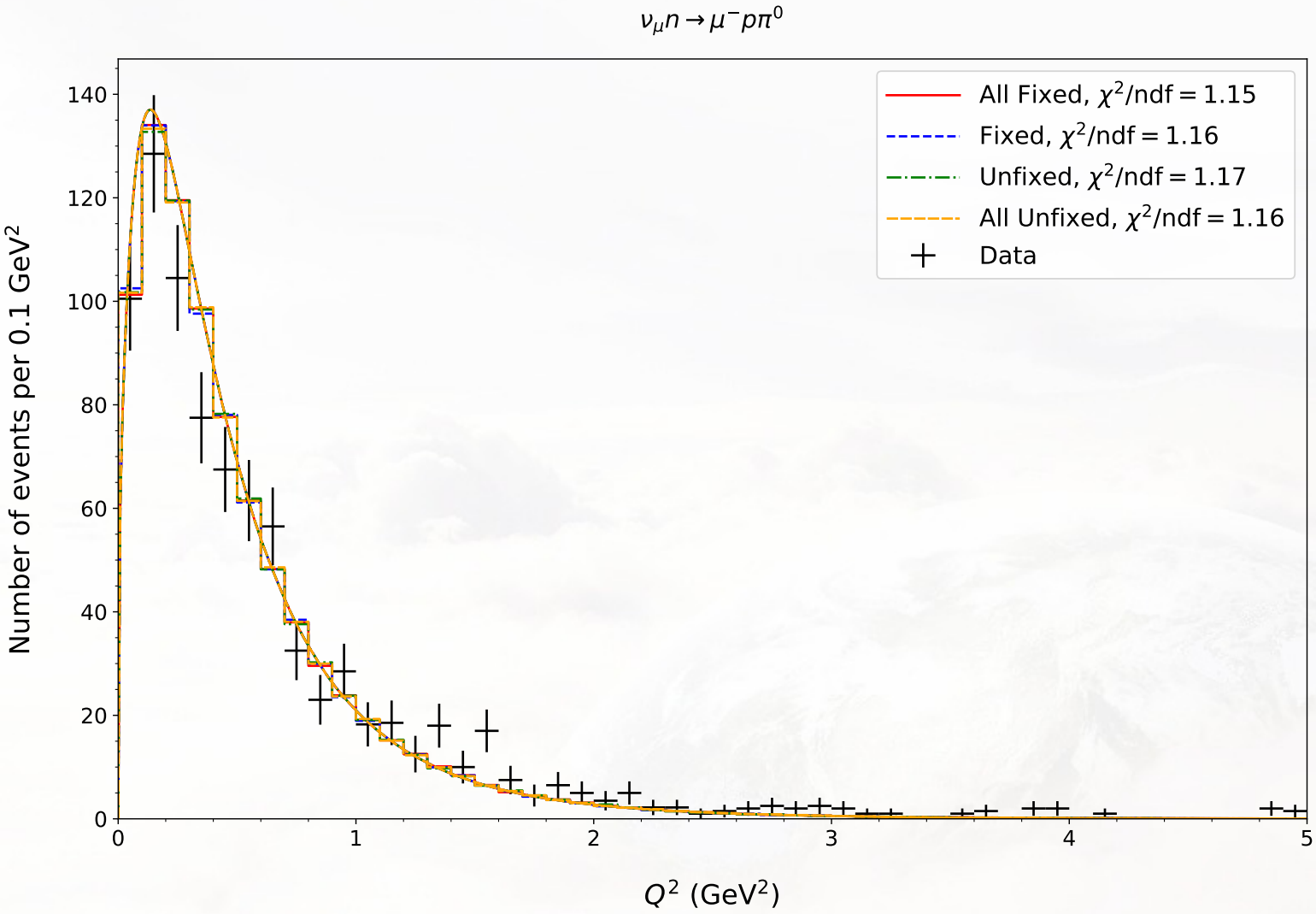

Q^2 distribution with no W_{cut}. Neutrino spectrum is restricted by $E_\nu < 6.0$ GeV. Model predictions are area-normalized. Predictions with all resonances (All)/without resonance F17(1970) and with fixed and unfixed bugs are shown. Data are taken from Ref. [11]. Neutrino spectrum is taken from [35].

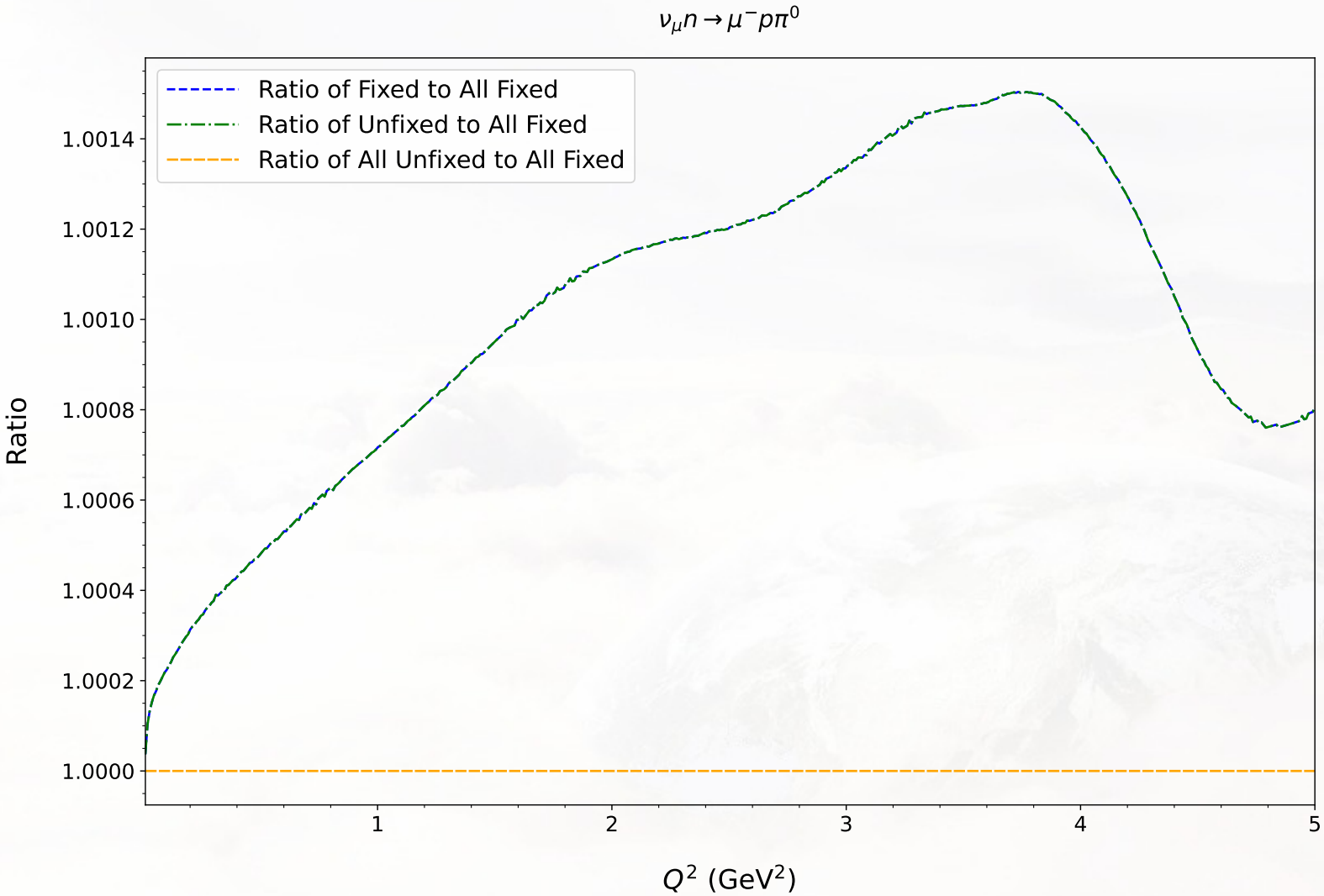

Ratio of $d\sigma/dQ^2$ with no W_{cut}. Neutrino spectrum is restricted by $E_\nu < 6.0$ GeV. Data are taken from Ref. [11]. Neutrino spectrum is taken from [35].

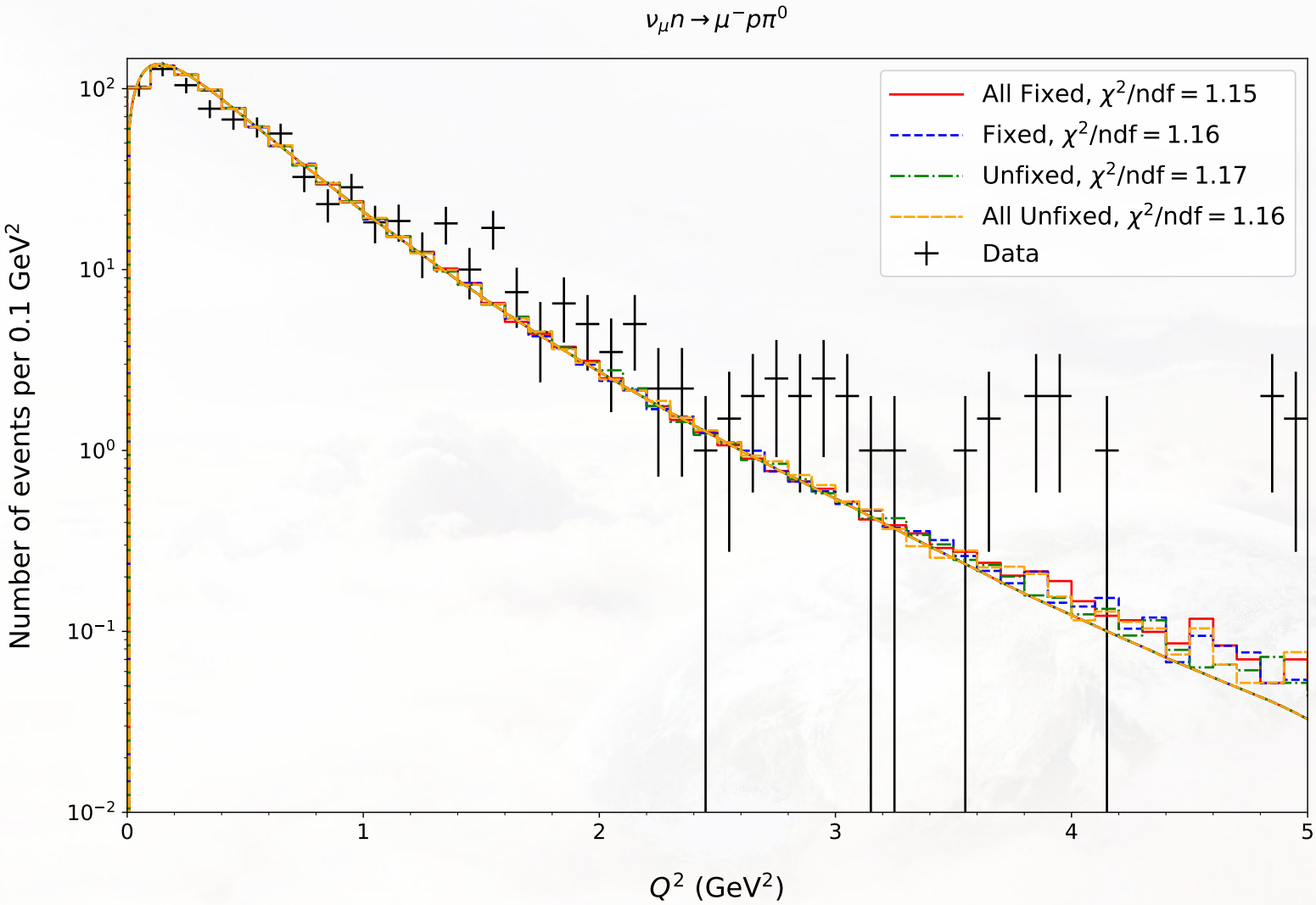

Q^2 distribution with no W_{cut}. Neutrino spectrum is restricted by $E_\nu < 6.0$ GeV. Model predictions are area-normalized. Predictions with all resonances (All)/without resonance F17(1970) and with fixed and unfixed bugs are shown. Data are taken from Ref. [11]. Neutrino spectrum is taken from [35].

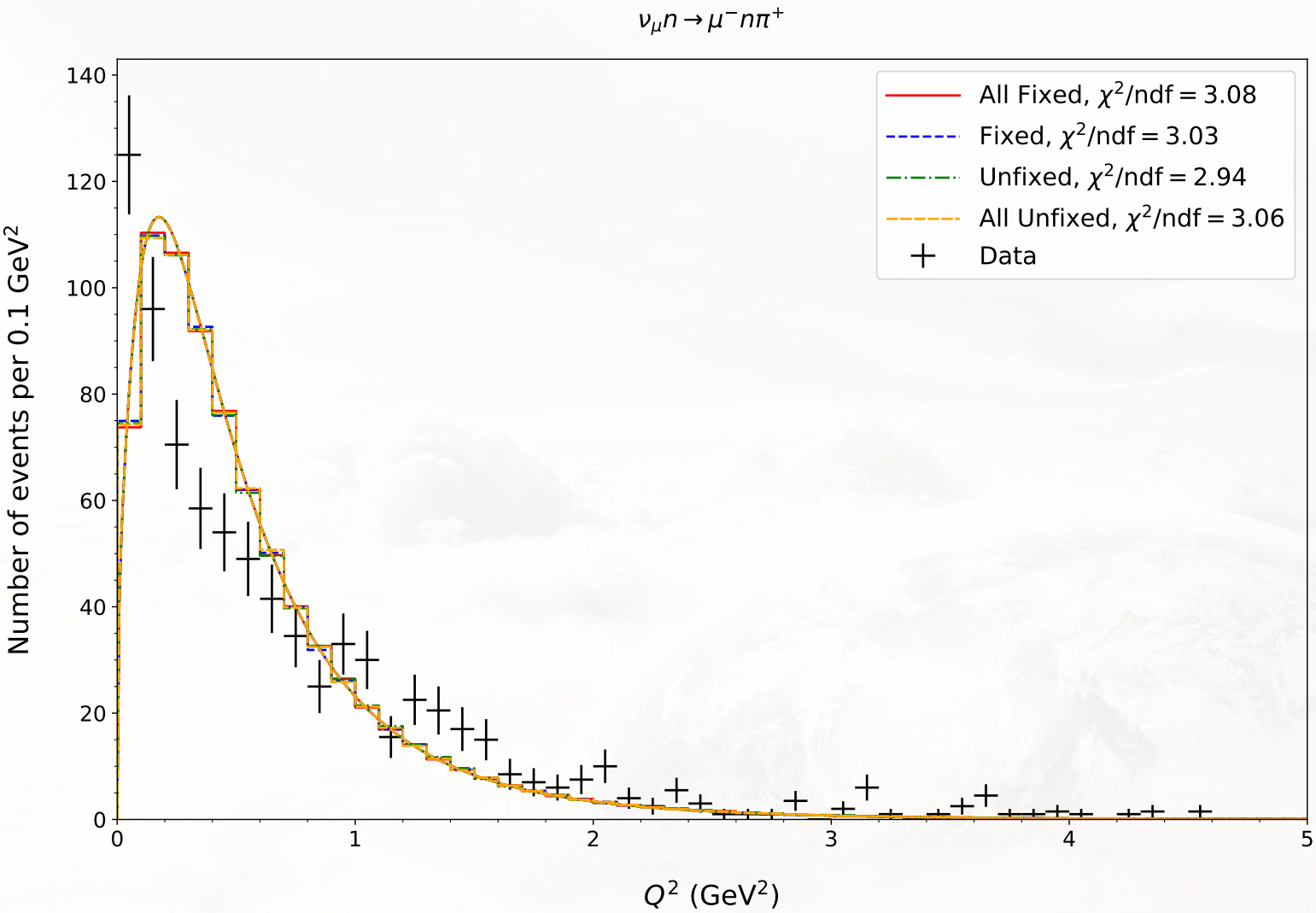

Q^2 distribution with no W_{cut}. Neutrino spectrum is restricted by $E_\nu < 6.0$ GeV. Model predictions are area-normalized. Predictions with all resonances (All)/without resonance F17(1970) and with fixed and unfixed bugs are shown. Data are taken from Ref. [11]. Neutrino spectrum is taken from [35].

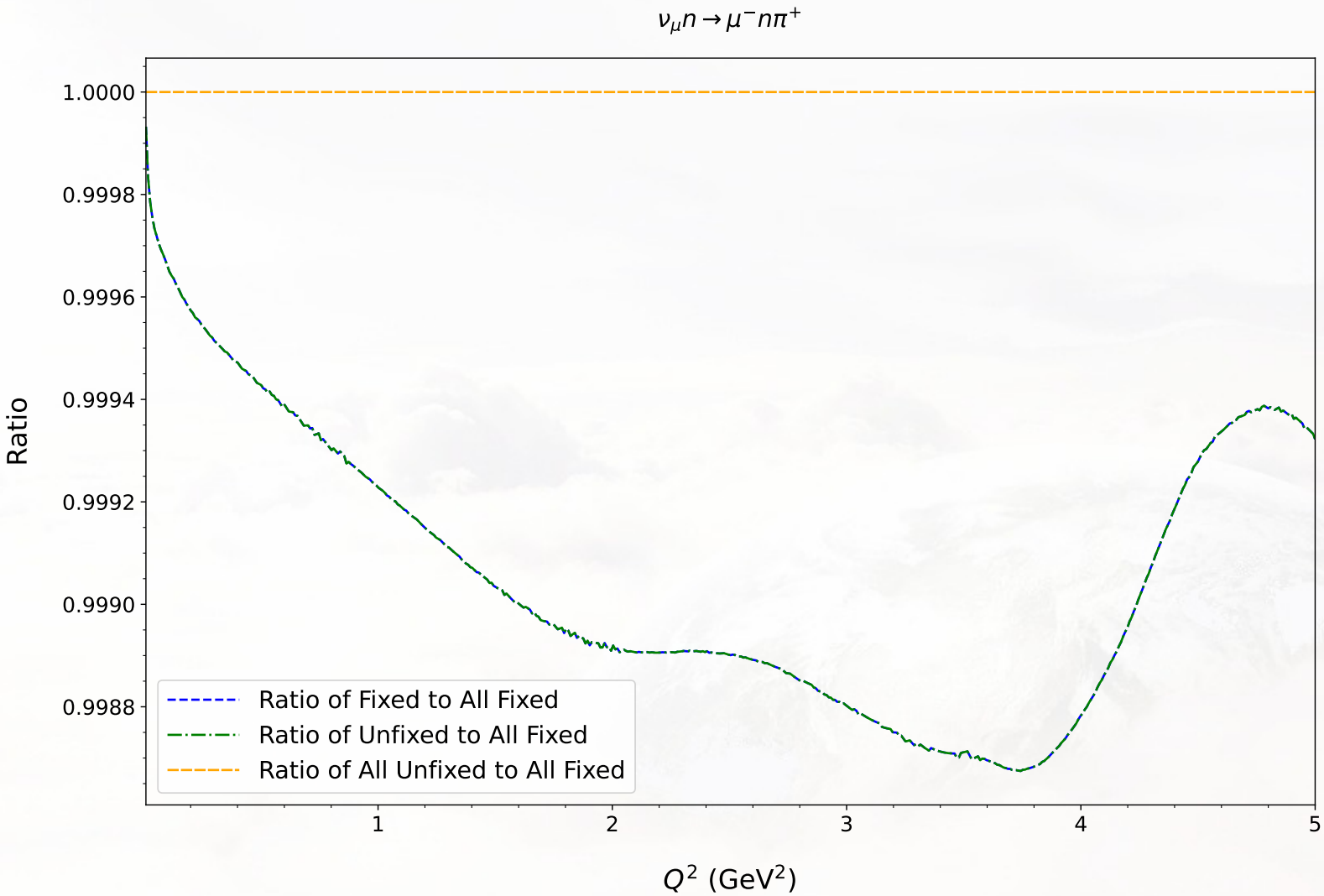

Ratio of $d\sigma/dQ^2$ with no W_{cut}. Neutrino spectrum is restricted by $E_\nu < 6.0$ GeV. Data are taken from Ref. [11]. Neutrino spectrum is taken from [35].

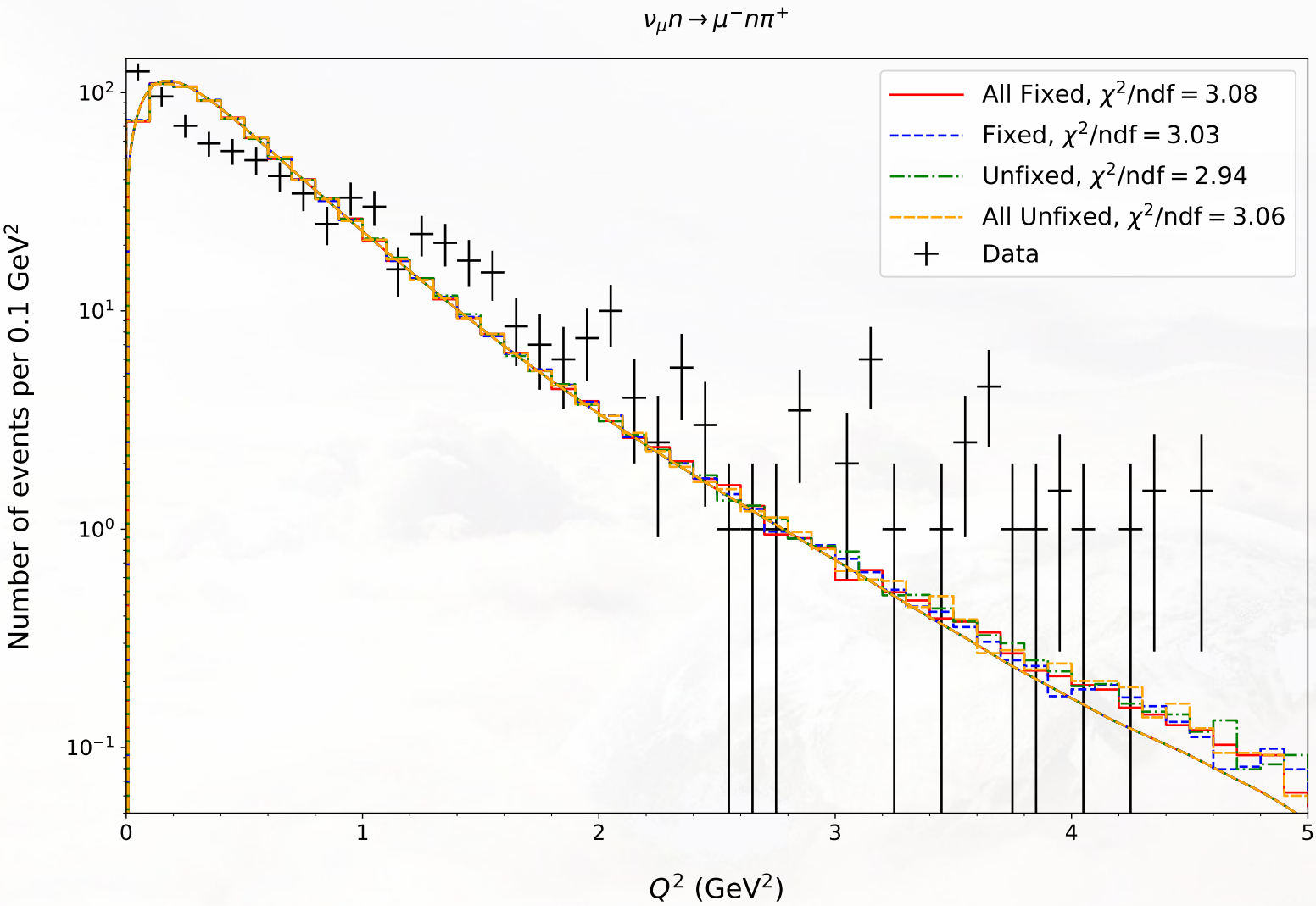

Q^2 distribution with no W_{cut}. Neutrino spectrum is restricted by $E_\nu < 6.0$ GeV. Model predictions are area-normalized. Predictions with all resonances (All)/without resonance F17(1970) and with fixed and unfixed bugs are shown. Data are taken from Ref. [11]. Neutrino spectrum is taken from [35].

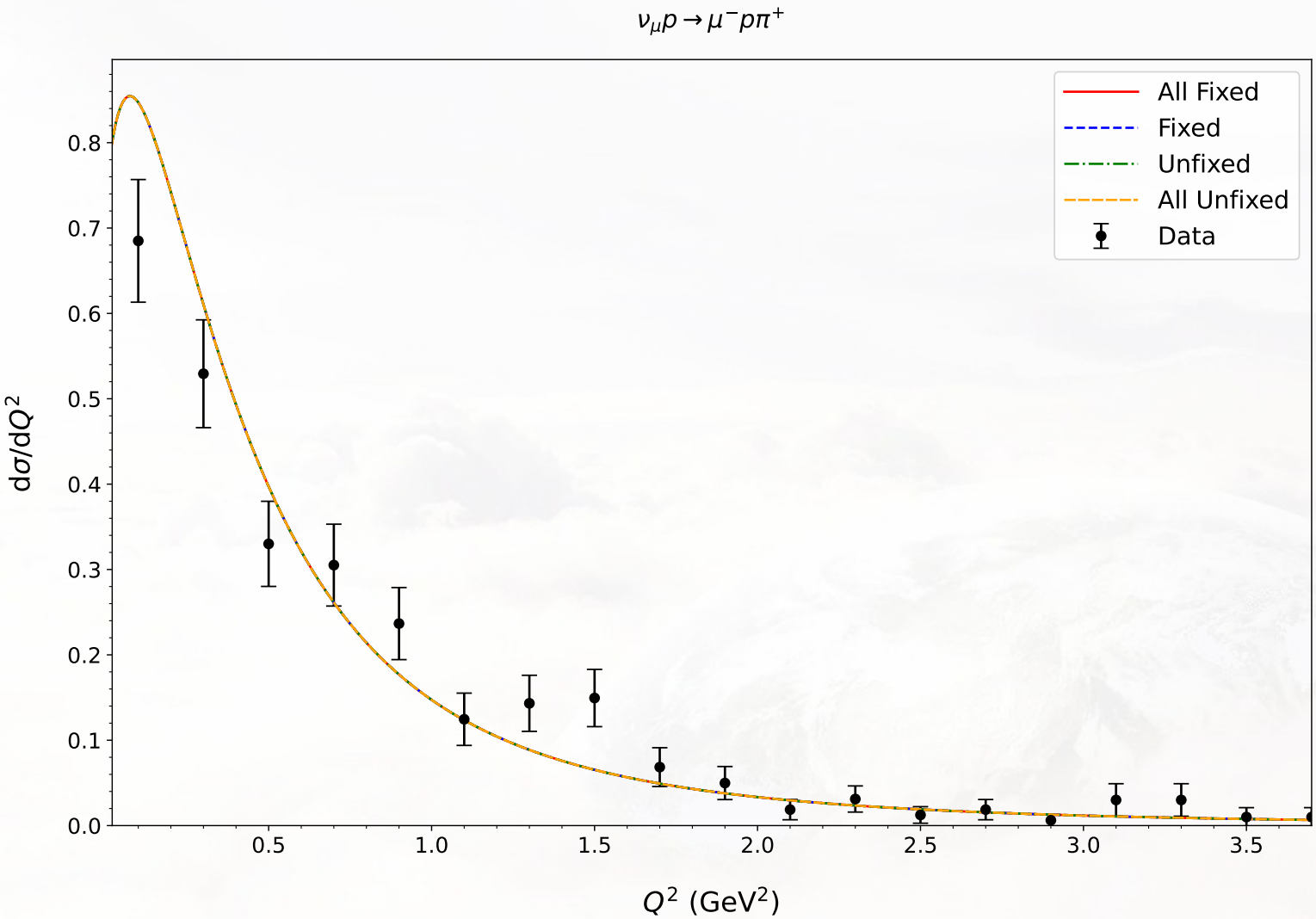

Q^2 distribution with $1.1 < W < 1.4$ GeV. Neutrino spectrum is restricted by $5.0 < E_\nu < 200.0$ GeV. Predictions with all resonances (All)/without resonance F17(1970) and with fixed and unfixed bugs are shown. Data are taken from Ref. [24]. Neutrino spectrum is taken from [35].

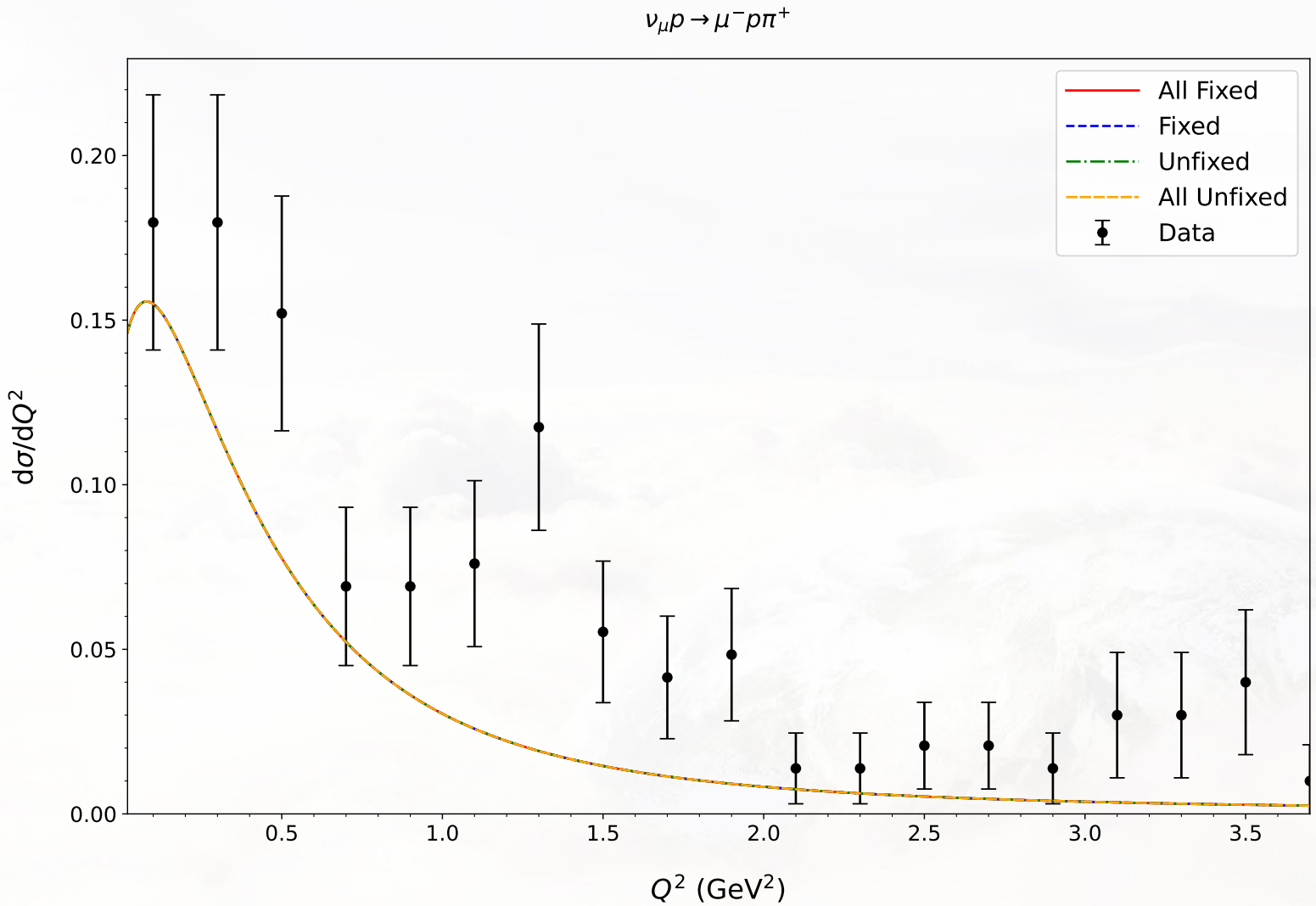

Q^2 distribution with $1.4 < W < 2.0$ GeV. Neutrino spectrum is restricted by $5.0 < E_\nu < 200.0$ GeV. Predictions with all resonances (All)/without resonance F17(1970) and with fixed and unfixed bugs are shown. Data are taken from Ref. [24]. Neutrino spectrum is taken from [35].

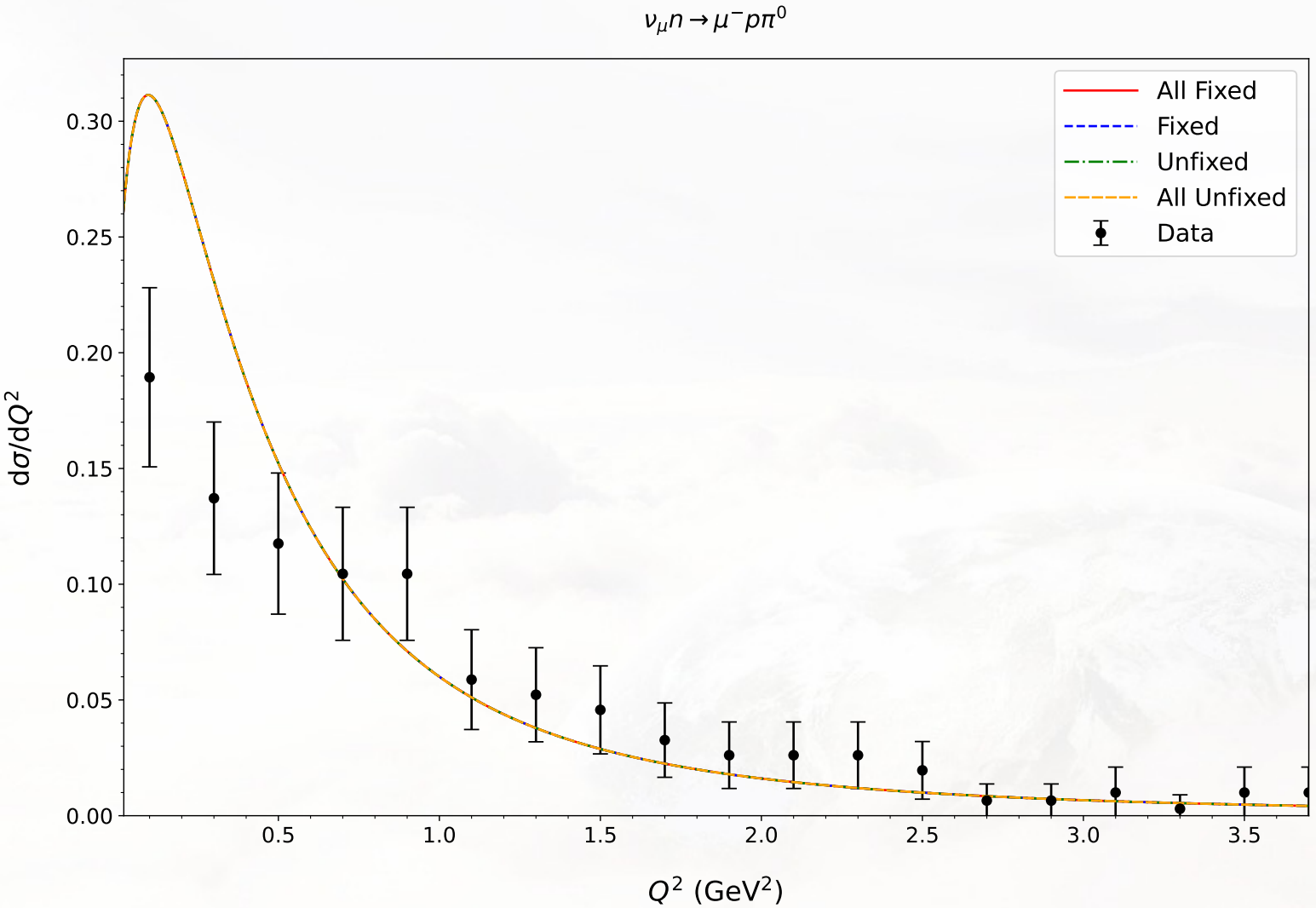

Q^2 distribution with $1.1 < W < 1.4$ GeV. Neutrino spectrum is restricted by $5.0 < E_\nu < 200.0$ GeV. Predictions with all resonances (All)/without resonance F17(1970) and with fixed and unfixed bugs are shown. Data are taken from Ref. [24]. Neutrino spectrum is taken from [35].

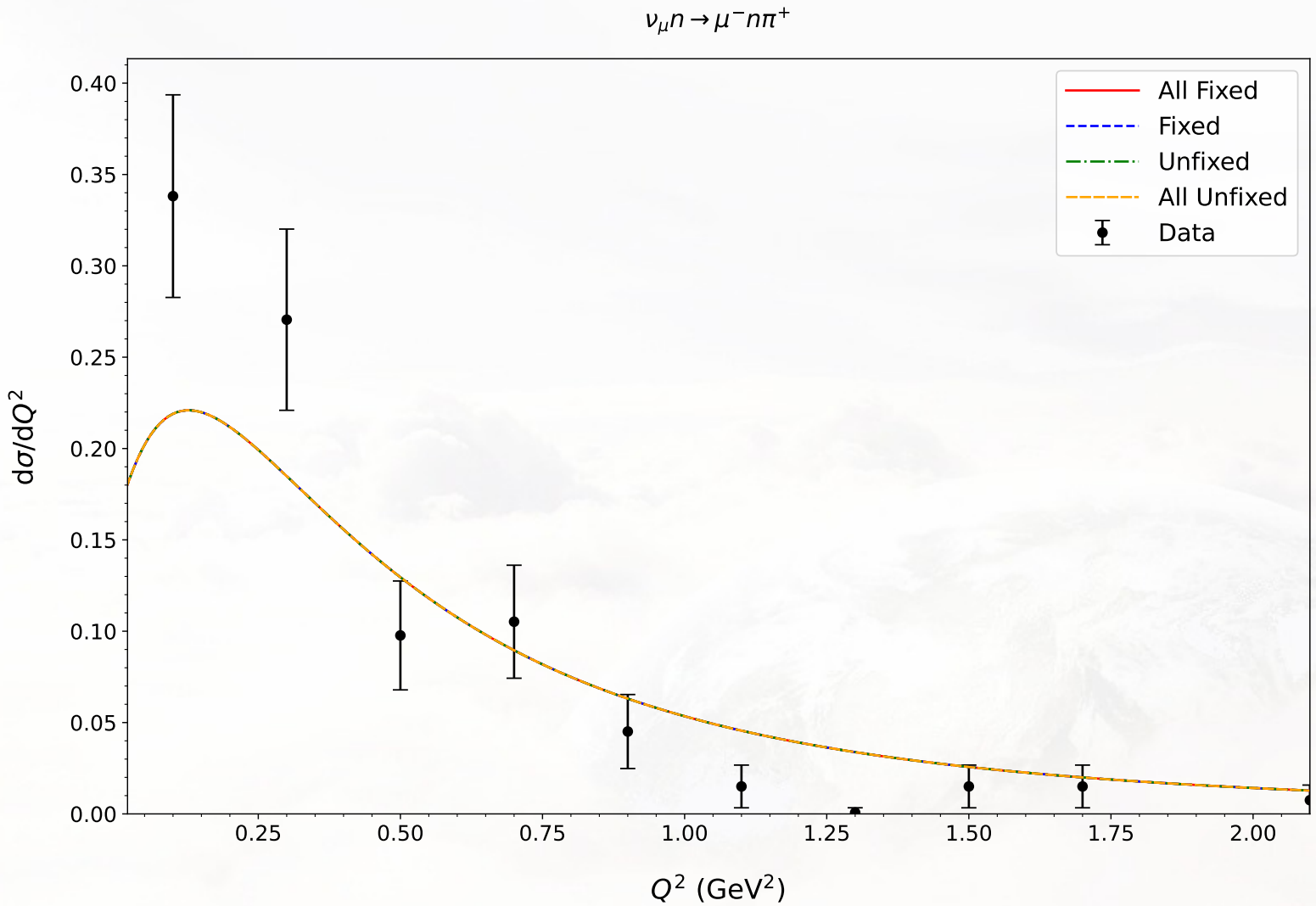

Q^2 distribution with $1.1 < W < 1.4$ GeV. Neutrino spectrum is restricted by $5.0 < E_\nu < 200.0$ GeV. Predictions with all resonances (All)/without resonance F17(1970) and with fixed and unfixed bugs are shown. Data are taken from Ref. [24]. Neutrino spectrum is taken from [35].

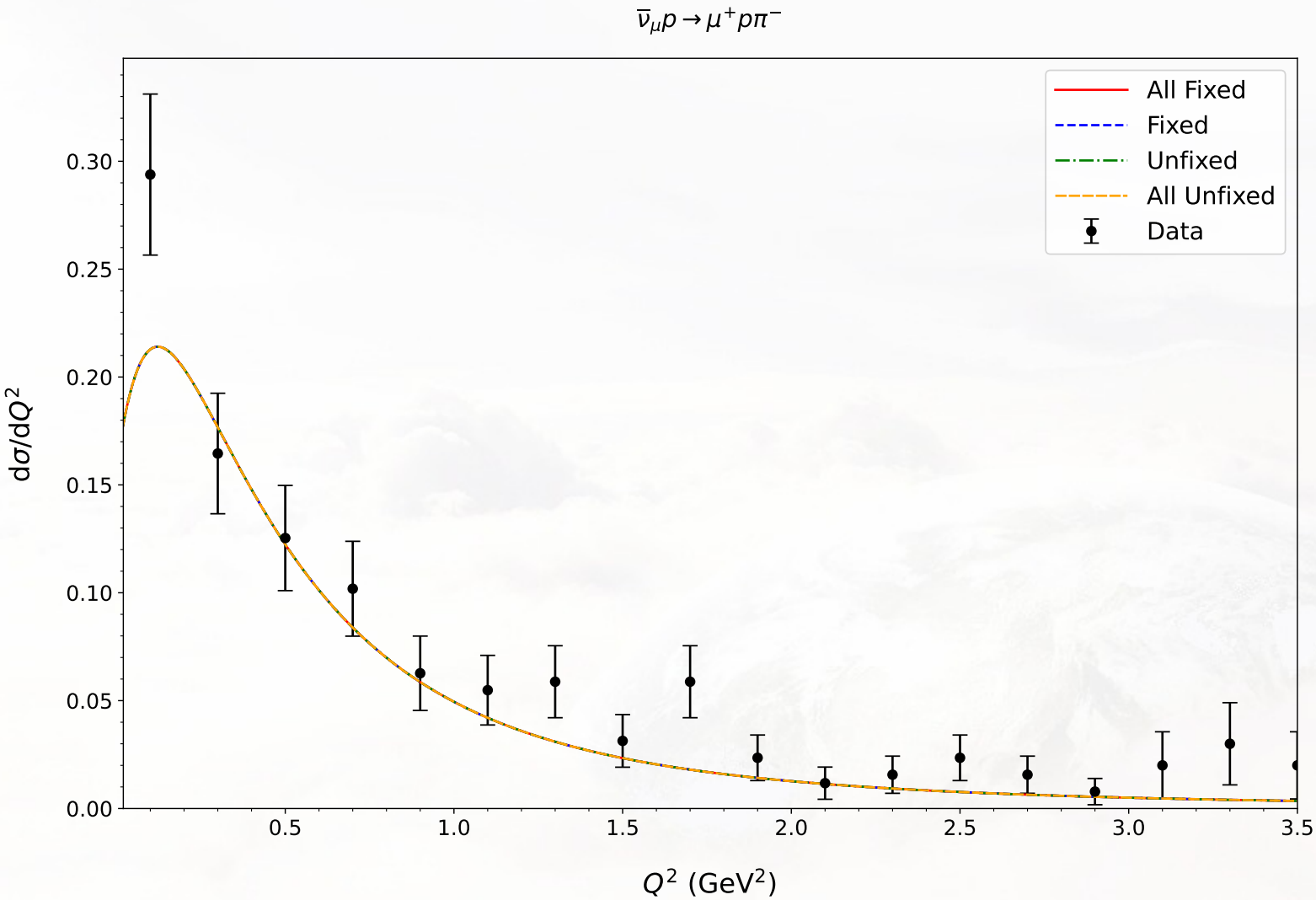

Q^2 distribution with $1.1 < W < 1.4$ GeV. Neutrino spectrum is restricted by $5.0 < E_\nu < 200.0$ GeV. Predictions with all resonances (All)/without resonance F17(1970) and with fixed and unfixed bugs are shown. Data are taken from Ref. [24]. Neutrino spectrum is taken from [35].

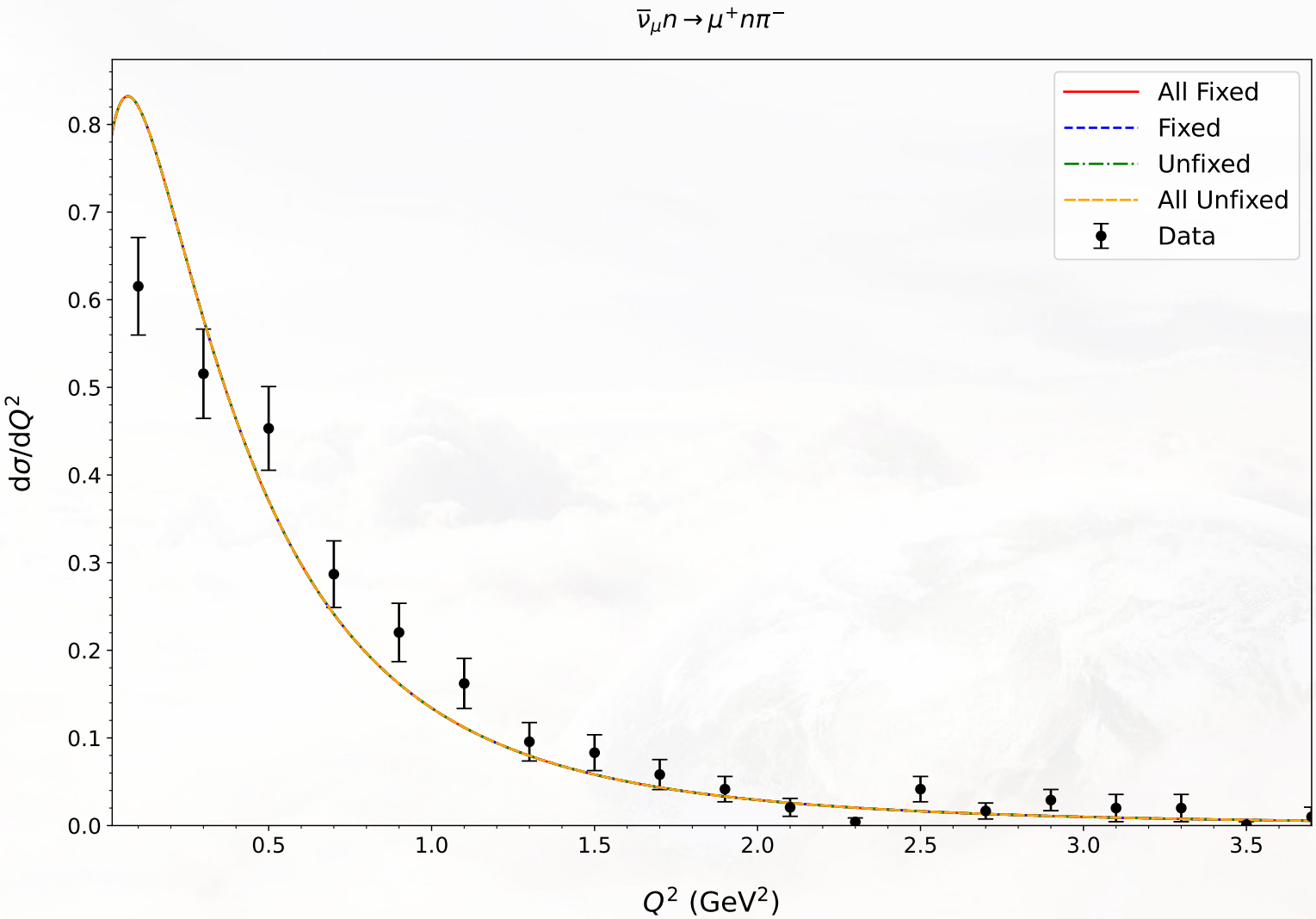

Q^2 distribution with $1.1 < W < 1.4$ GeV. Neutrino spectrum is restricted by $5.0 < E_\nu < 200.0$ GeV. Predictions with all resonances (All)/without resonance F17(1970) and with fixed and unfixed bugs are shown. Data are taken from Ref. [24]. Neutrino spectrum is taken from [35].

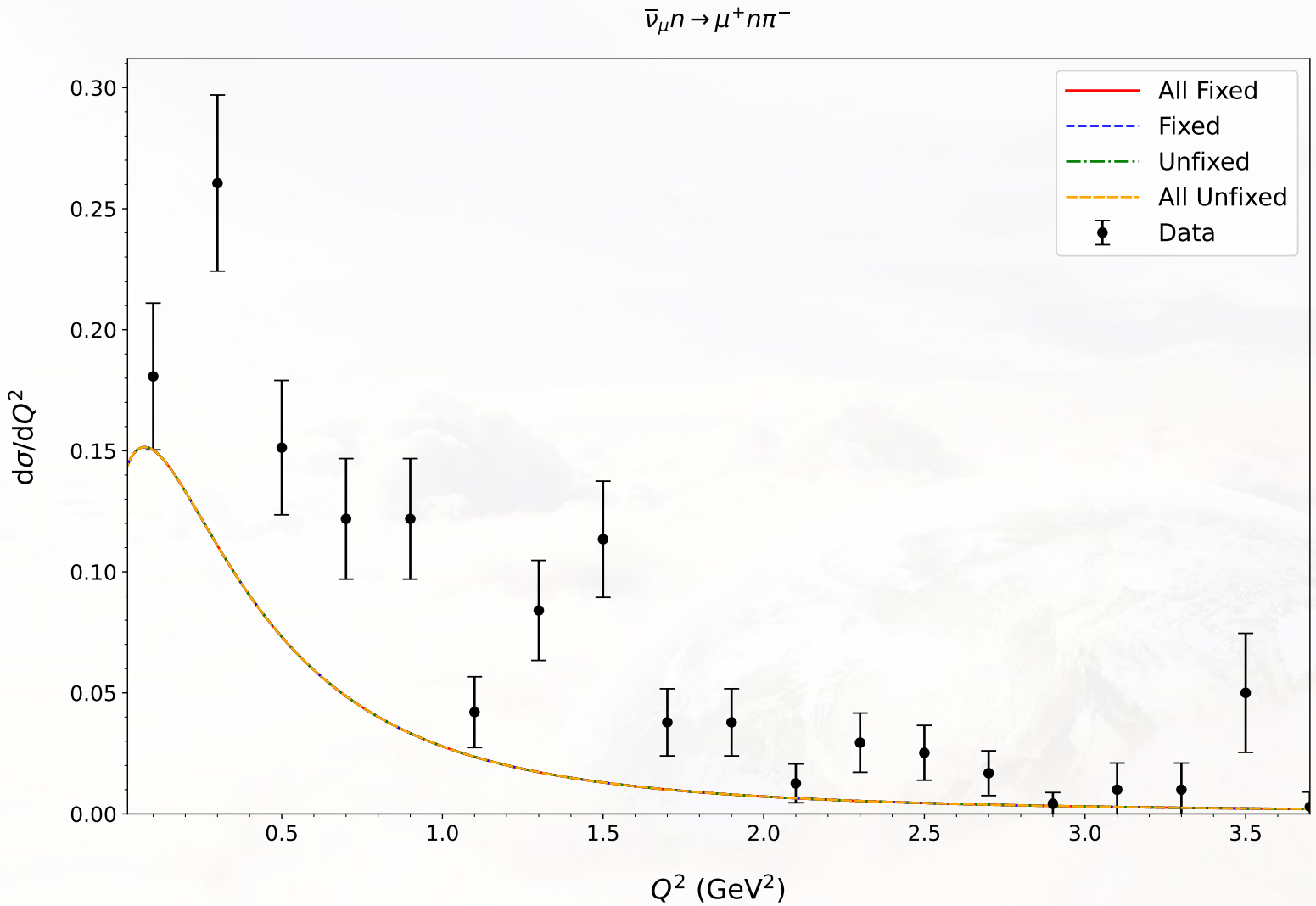

Q^2 distribution with $1.4 < W < 2.0$ GeV. Neutrino spectrum is restricted by $5.0 < E_\nu < 200.0$ GeV. Predictions with all resonances (All)/without resonance F17(1970) and with fixed and unfixed bugs are shown. Data are taken from Ref. [24]. Neutrino spectrum is taken from [35].

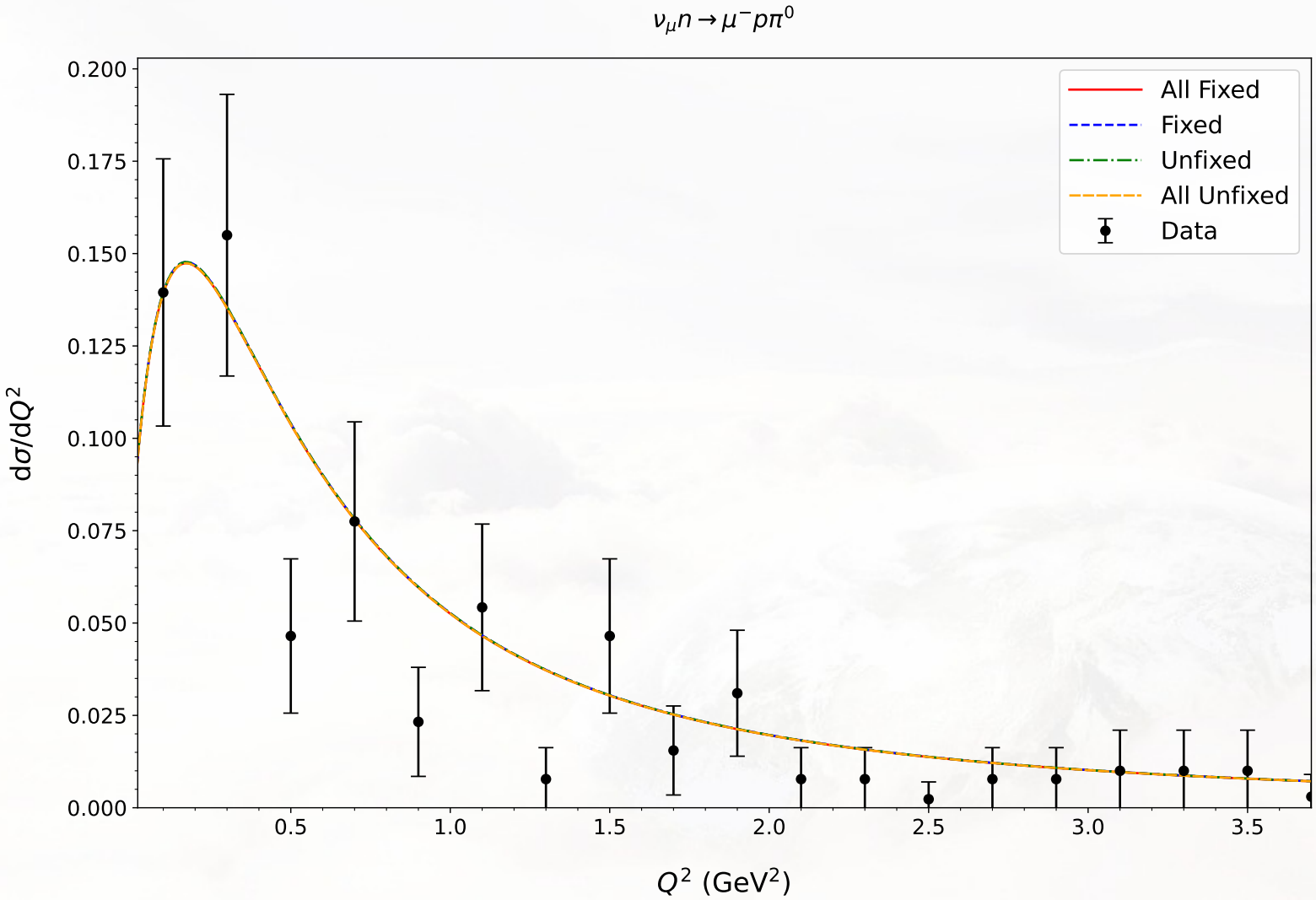

Q^2 distribution with $1.4 < W < 2.0$ GeV. Neutrino spectrum is restricted by $5.0 < E_\nu < 200.0$ GeV. Predictions with all resonances (All)/without resonance F17(1970) and with fixed and unfixed bugs are shown. Data are taken from Ref. [24]. Neutrino spectrum is taken from [35].

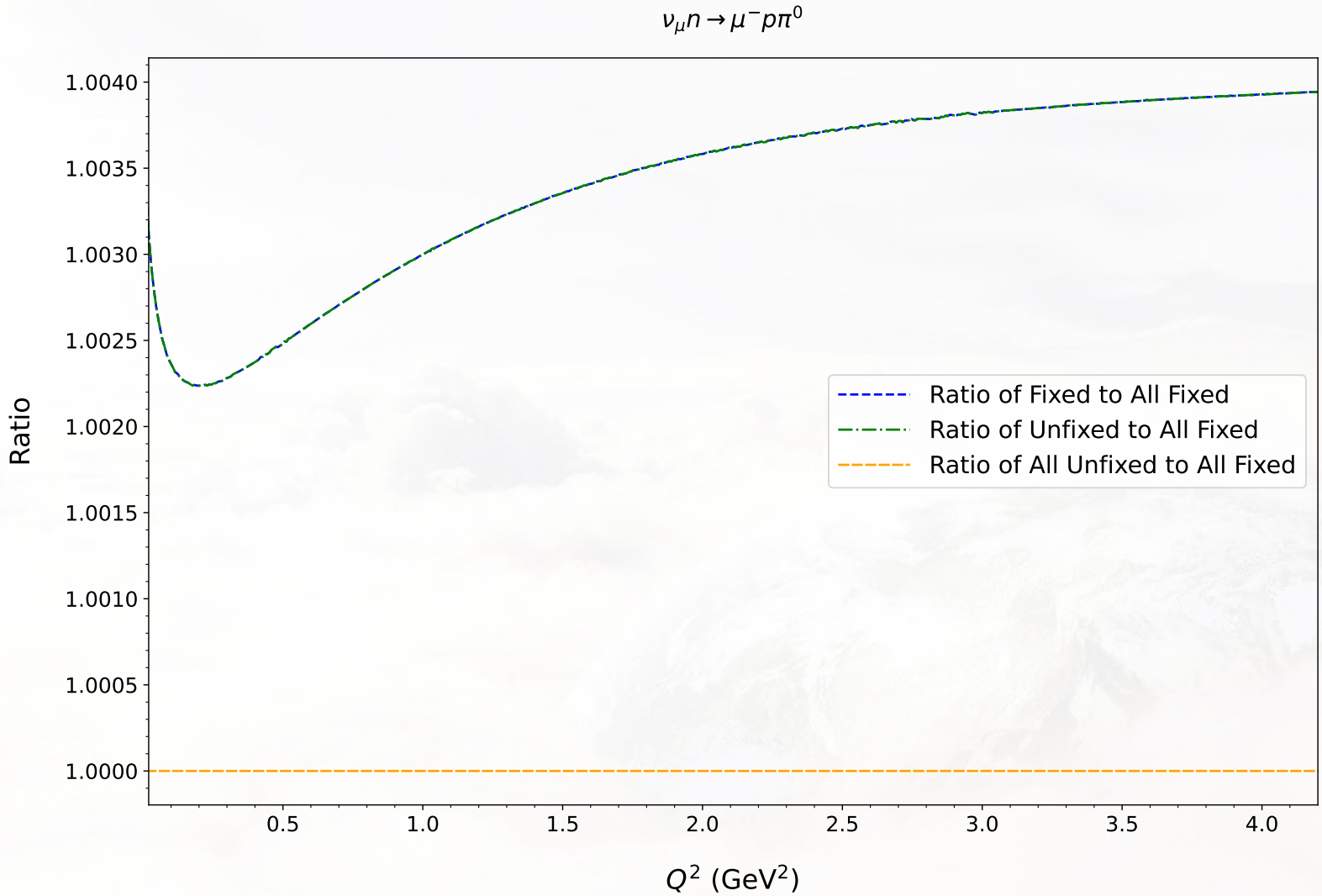

Ratio of $d\sigma/dQ^2$ with $1.4 < W < 2.0$ GeV. Neutrino spectrum is restricted by $5.0 < E_\nu < 200.0$ GeV. Data are taken from Ref. [24]. Neutrino spectrum is taken from [35].

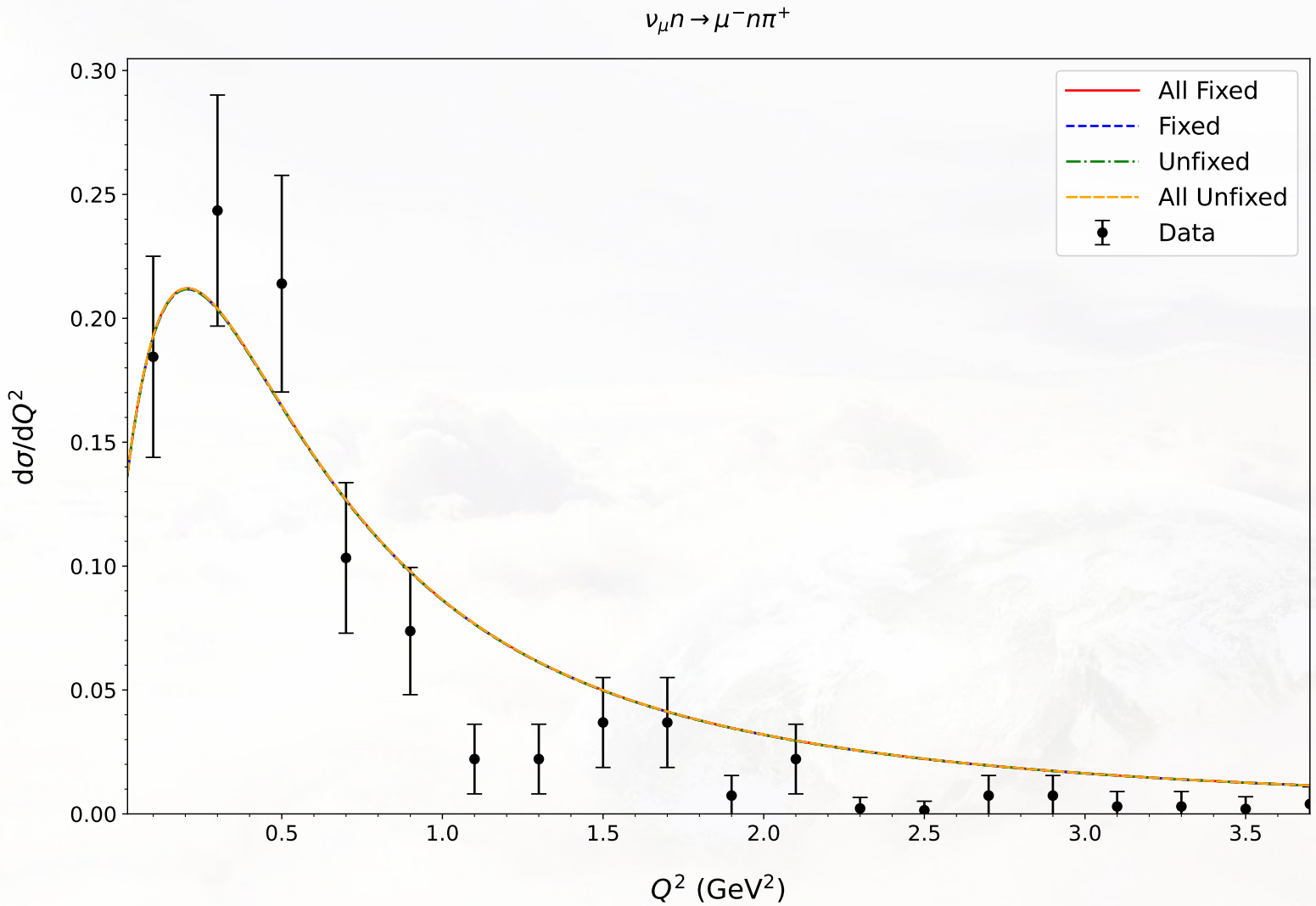

Q^2 distribution with $1.4 < W < 2.0$ GeV. Neutrino spectrum is restricted by $5.0 < E_\nu < 200.0$ GeV. Predictions with all resonances (All)/without resonance F17(1970) and with fixed and unfixed bugs are shown. Data are taken from Ref. [24]. Neutrino spectrum is taken from [35].

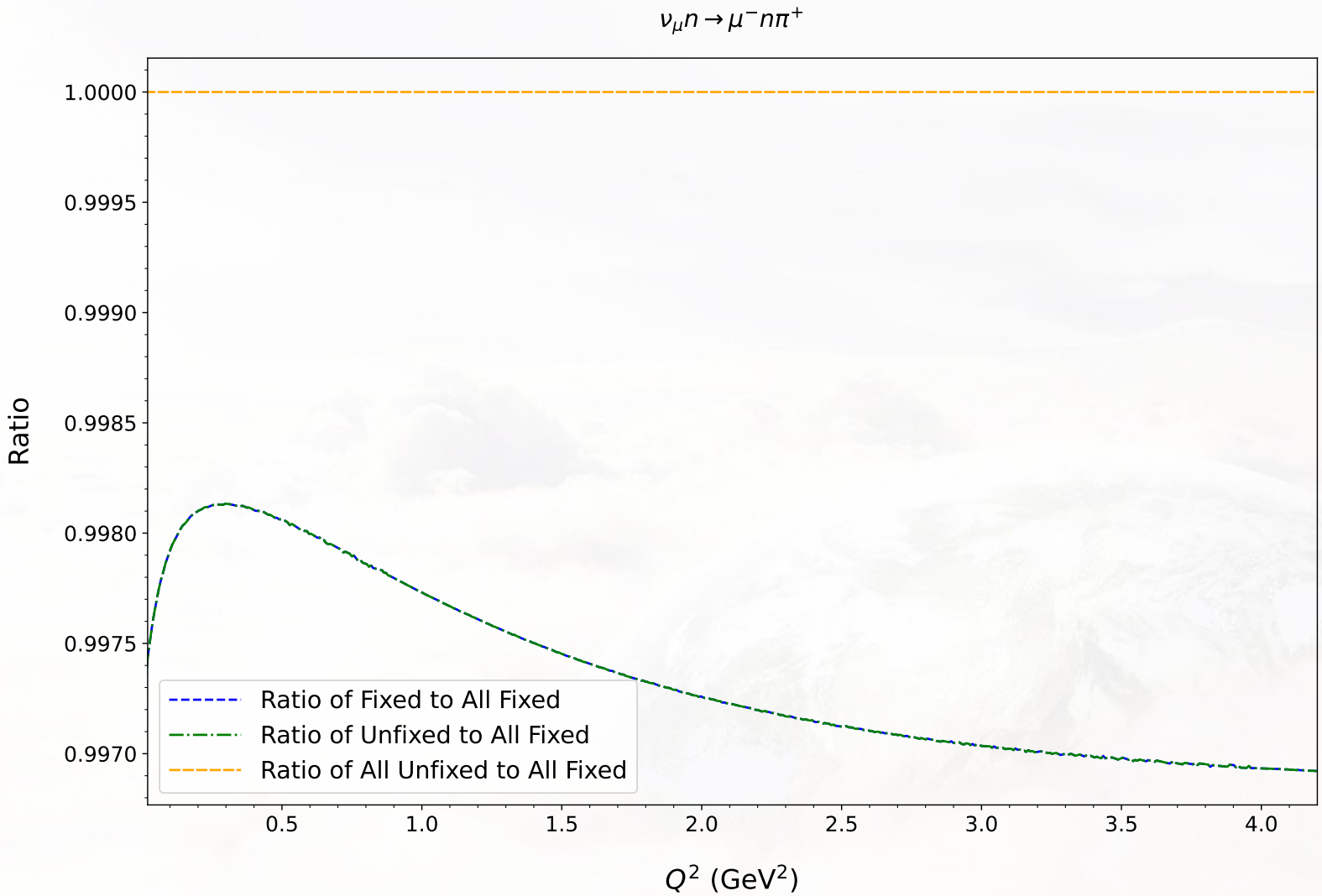

Ratio of $d\sigma/dQ^2$ with $1.4 < W < 2.0$ GeV. Neutrino spectrum is restricted by $5.0 < E_\nu < 200.0$ GeV. Data are taken from Ref. [24]. Neutrino spectrum is taken from [35].

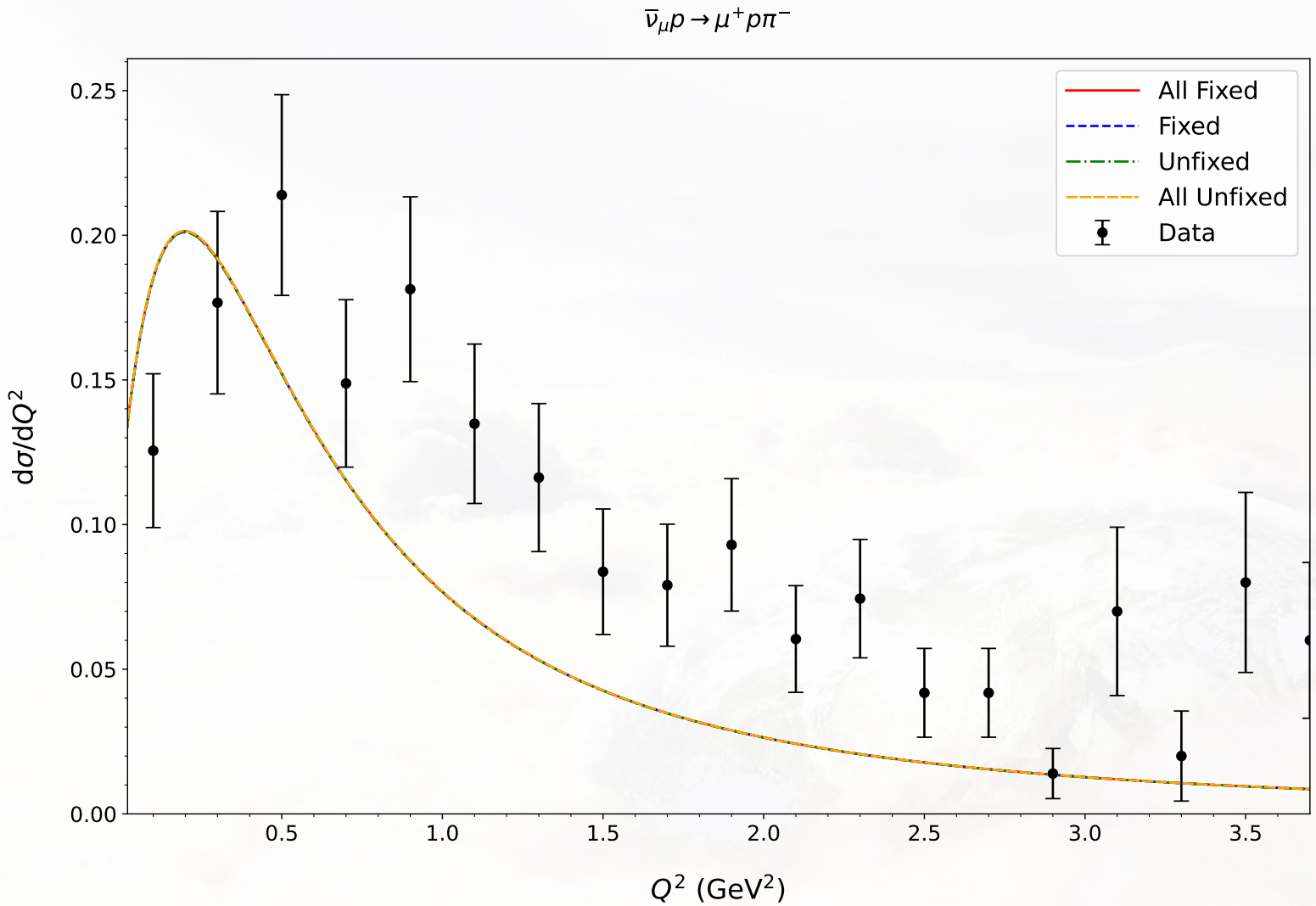

Q^2 distribution with $1.4 < W < 2.0$ GeV. Neutrino spectrum is restricted by $5.0 < E_\nu < 200.0$ GeV. Predictions with all resonances (All)/without resonance F17(1970) and with fixed and unfixed bugs are shown. Data are taken from Ref. [24]. Neutrino spectrum is taken from [35].

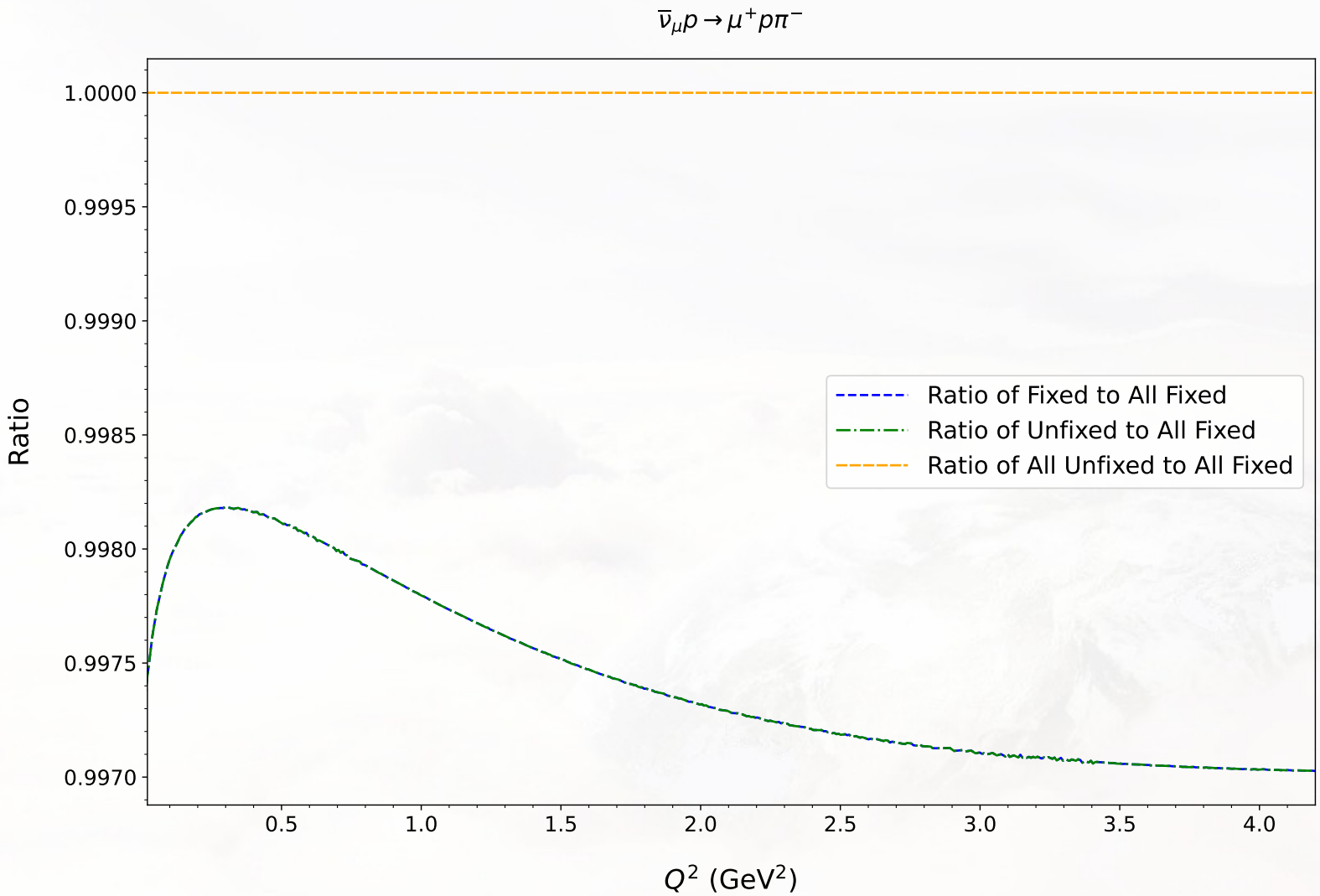

Ratio of $d\sigma/dQ^2$ with $1.4 < W < 2.0$ GeV. Neutrino spectrum is restricted by $5.0 < E_\nu < 200.0$ GeV. Data are taken from Ref. [24]. Neutrino spectrum is taken from [35].

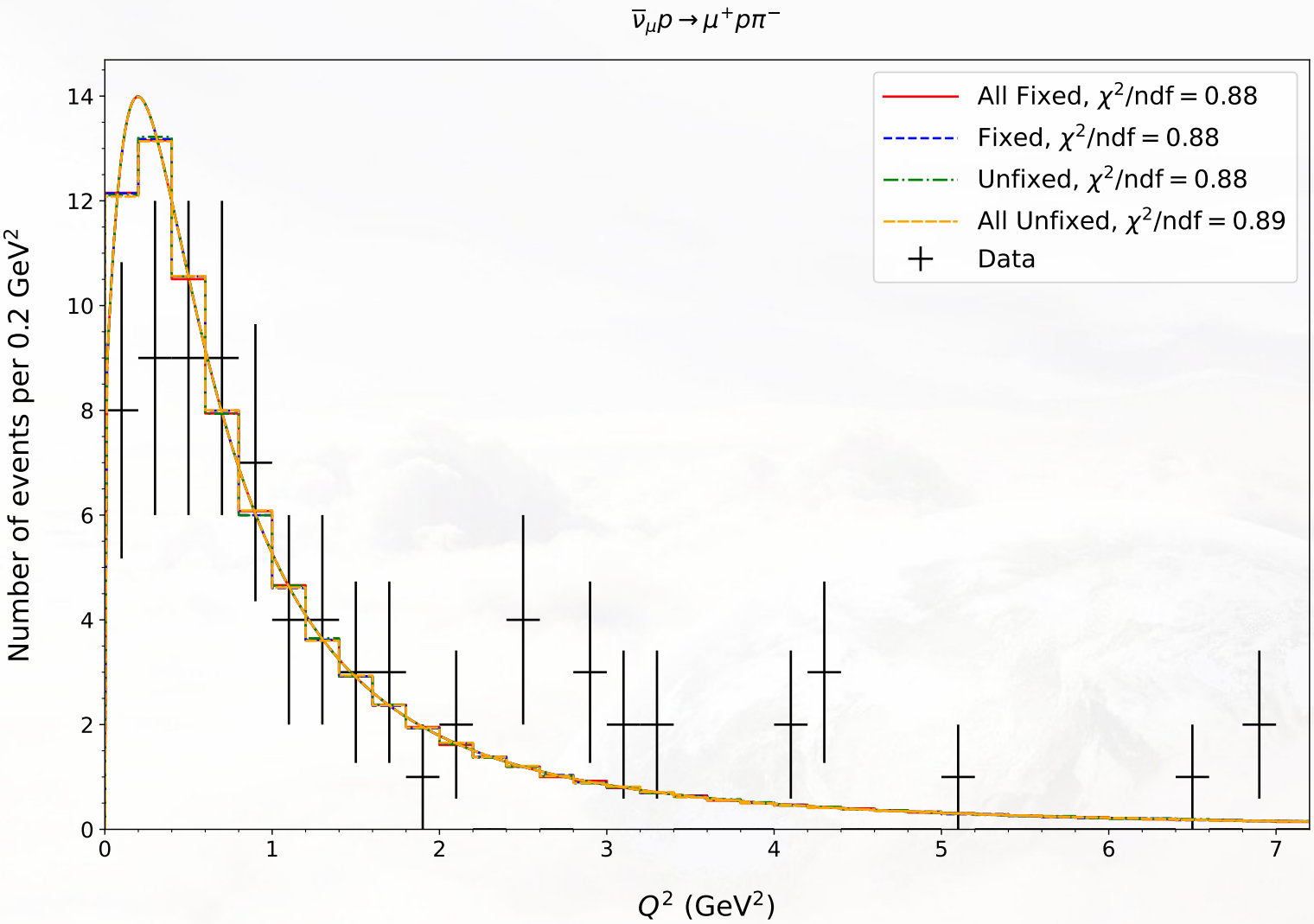

Q^2 distribution with $1.4 < W < 1.9$ GeV. Neutrino spectrum is restricted by $5.0 < E_\nu < 155.0$ GeV. Model predictions are area-normalized. Predictions with all resonances (All)/without resonance F17(1970) and with fixed and unfixed bugs are shown. Data are taken from Ref. [10]. Neutrino spectrum is taken from [17] (Stefanski-White spectrum model).

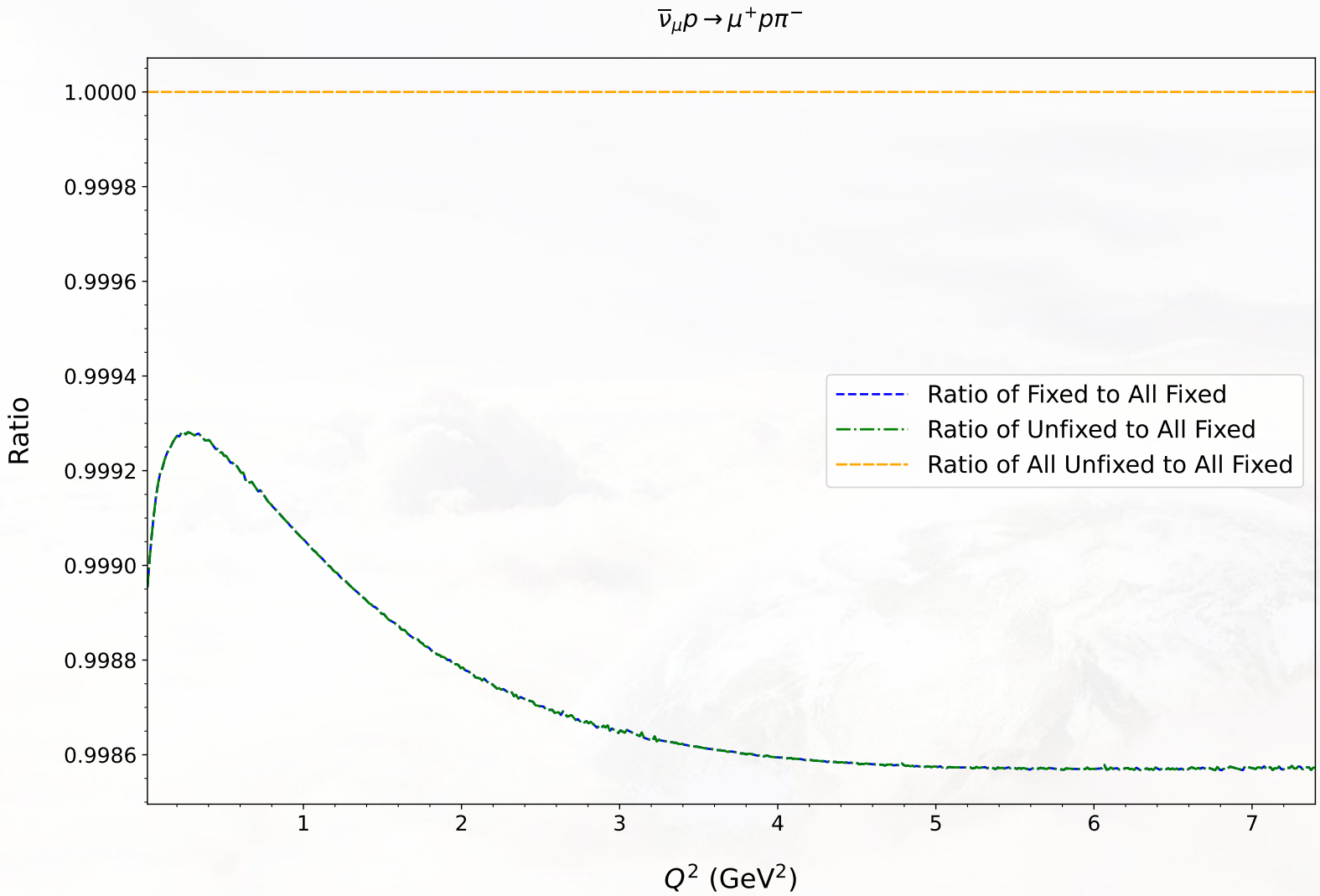

Ratio of $d\sigma/dQ^2$ with $1.4 < W < 1.9$ GeV. Neutrino spectrum is restricted by $5.0 < E_\nu < 155.0$ GeV. Data are taken from Ref. [10]. Neutrino spectrum is taken from [17] (Stefanski-White spectrum model).

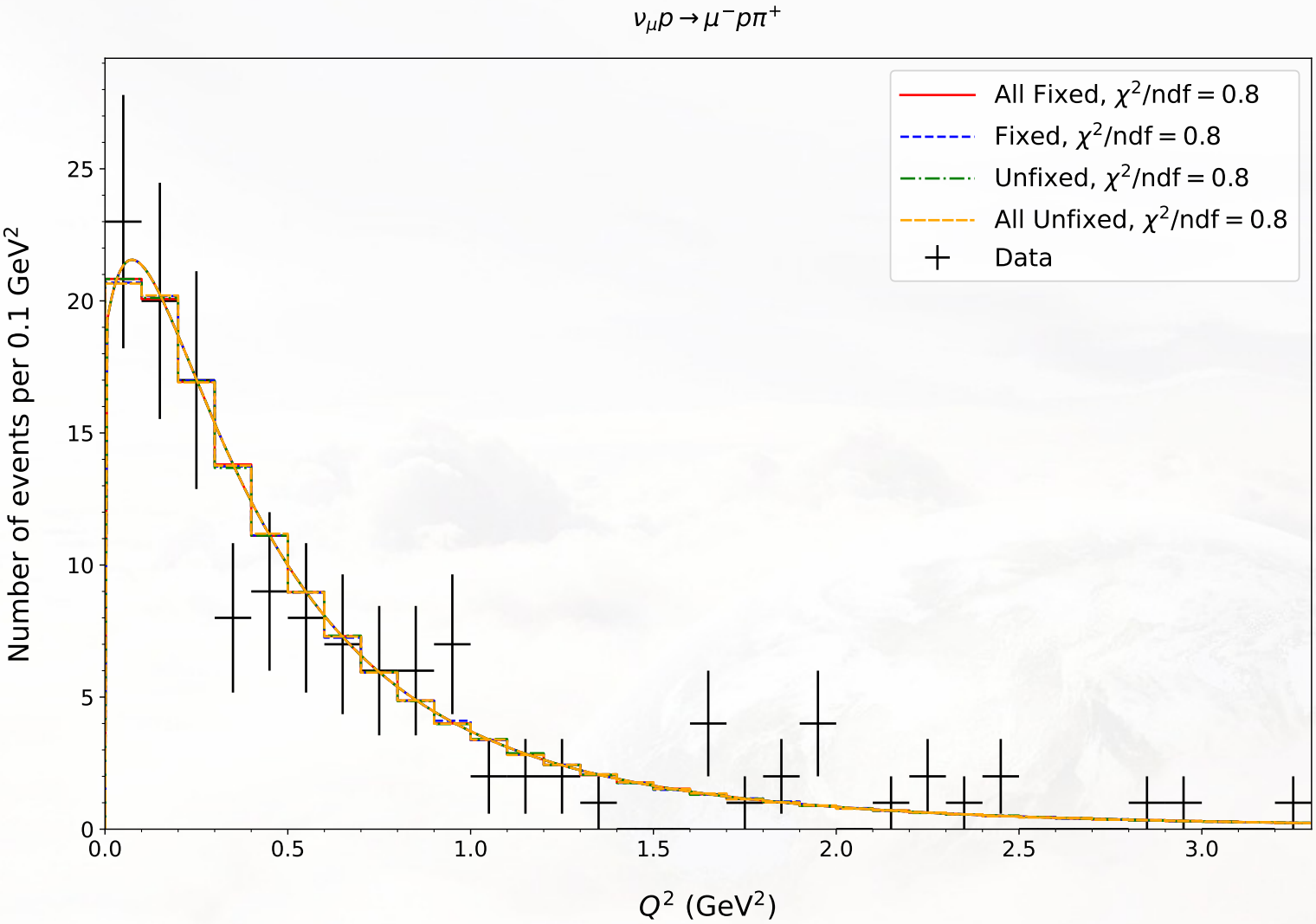

Q^2 distribution with $W < 1.4$ GeV. Neutrino spectrum is restricted by $5.0 < E_\nu < 155.0$ GeV. Model predictions are area-normalized. Predictions with all resonances (All)/without resonance F17(1970) and with fixed and unfixed bugs are shown. Data are taken from Ref. [14]. Neutrino spectrum is taken from [17] (Stefanski-White spectrum model).

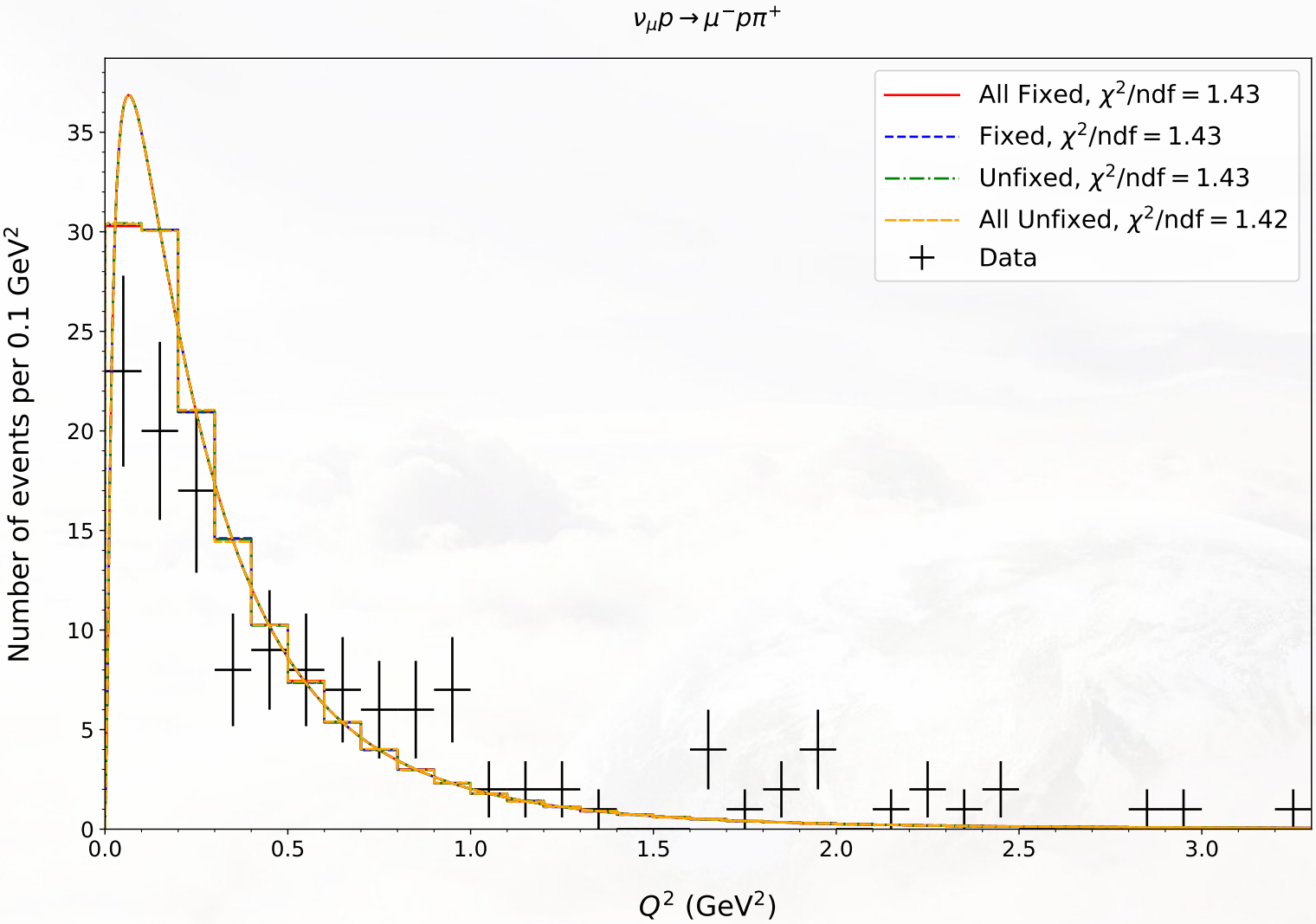

Q^2 distribution with no W_{cut}. Neutrino spectrum is restricted by $5.0 < E_\nu < 155.0$ GeV. Model predictions are area-normalized. Predictions with all resonances (All)/without resonance F17(1970) and with fixed and unfixed bugs are shown. Data are taken from Ref. [14]. Neutrino spectrum is taken from [17] (Stefanski-White spectrum model).

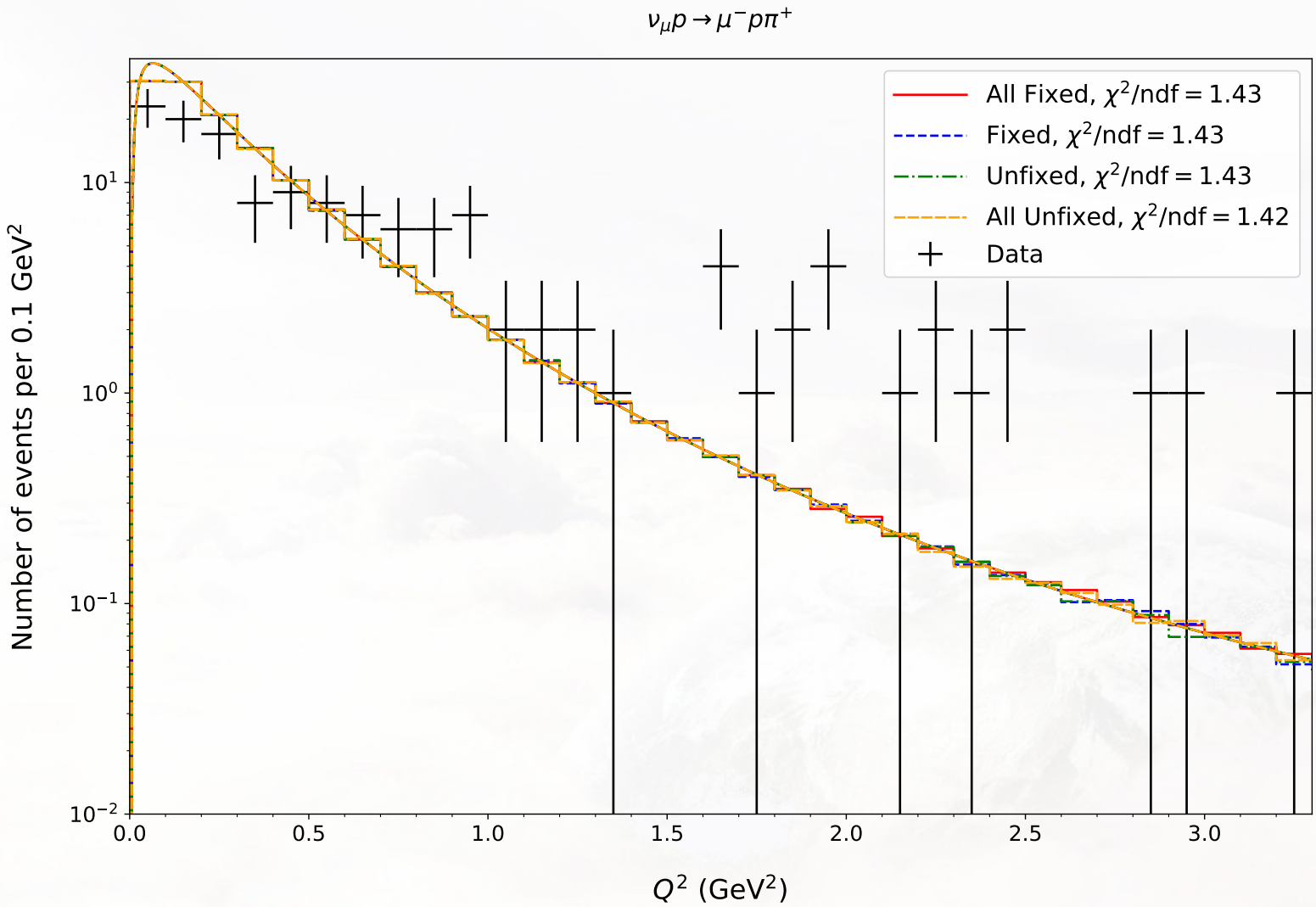

Q^2 distribution with no W_{cut}. Neutrino spectrum is restricted by $5.0 < E_\nu < 155.0$ GeV. Model predictions are area-normalized. Predictions with all resonances (All)/without resonance F17(1970) and with fixed and unfixed bugs are shown. Data are taken from Ref. [14]. Neutrino spectrum is taken from [17] (Stefanski-White spectrum model).

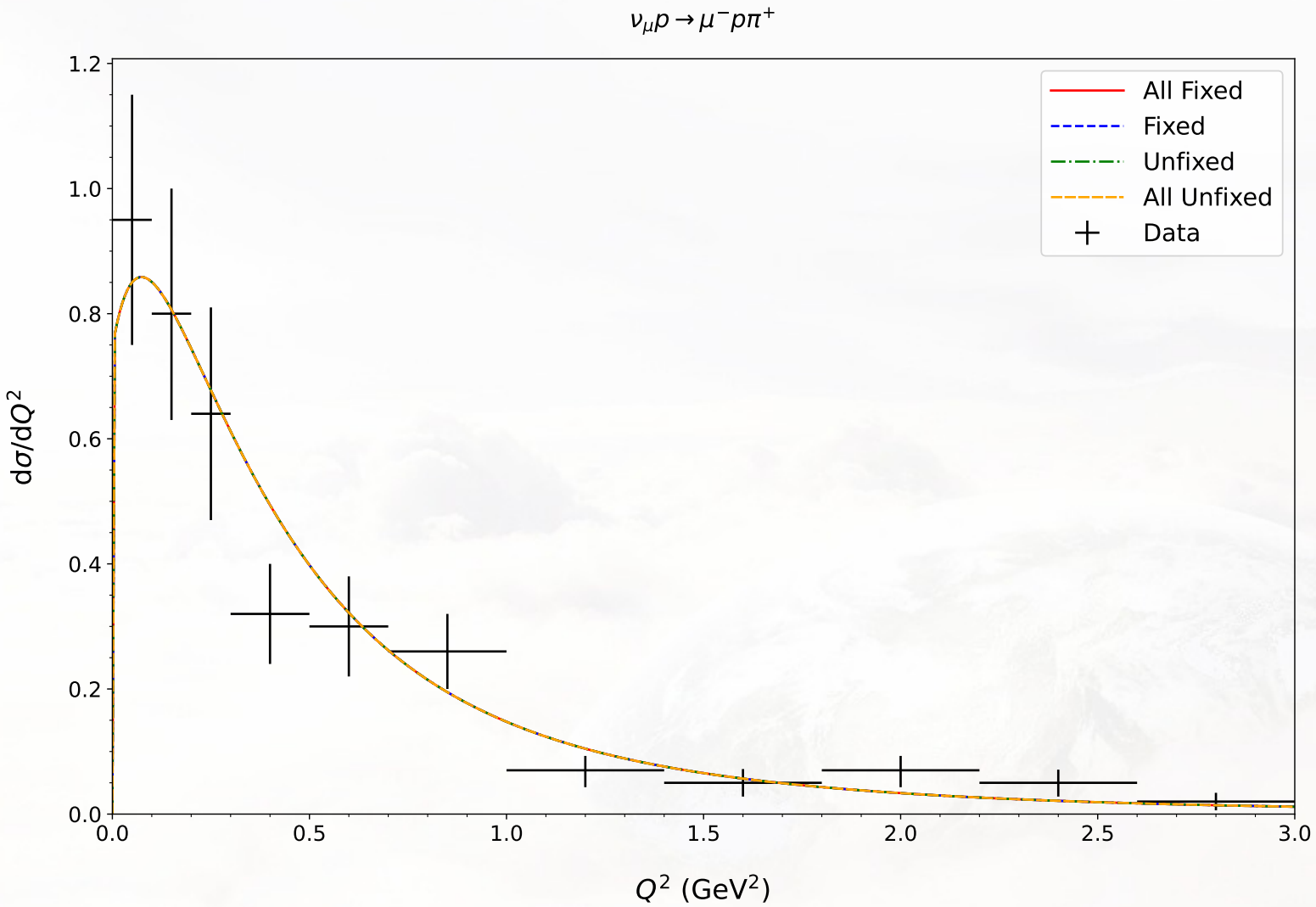

Q^2 distribution with $W < 1.4$ GeV. Neutrino spectrum is restricted by $5.0 < E_\nu < 155.0$ GeV. Predictions with all resonances (All)/without resonance F17(1970) and with fixed and unfixed bugs are shown. Data are taken from Ref. [37]. Neutrino spectrum is taken from [17] (Stefanski-White spectrum model).

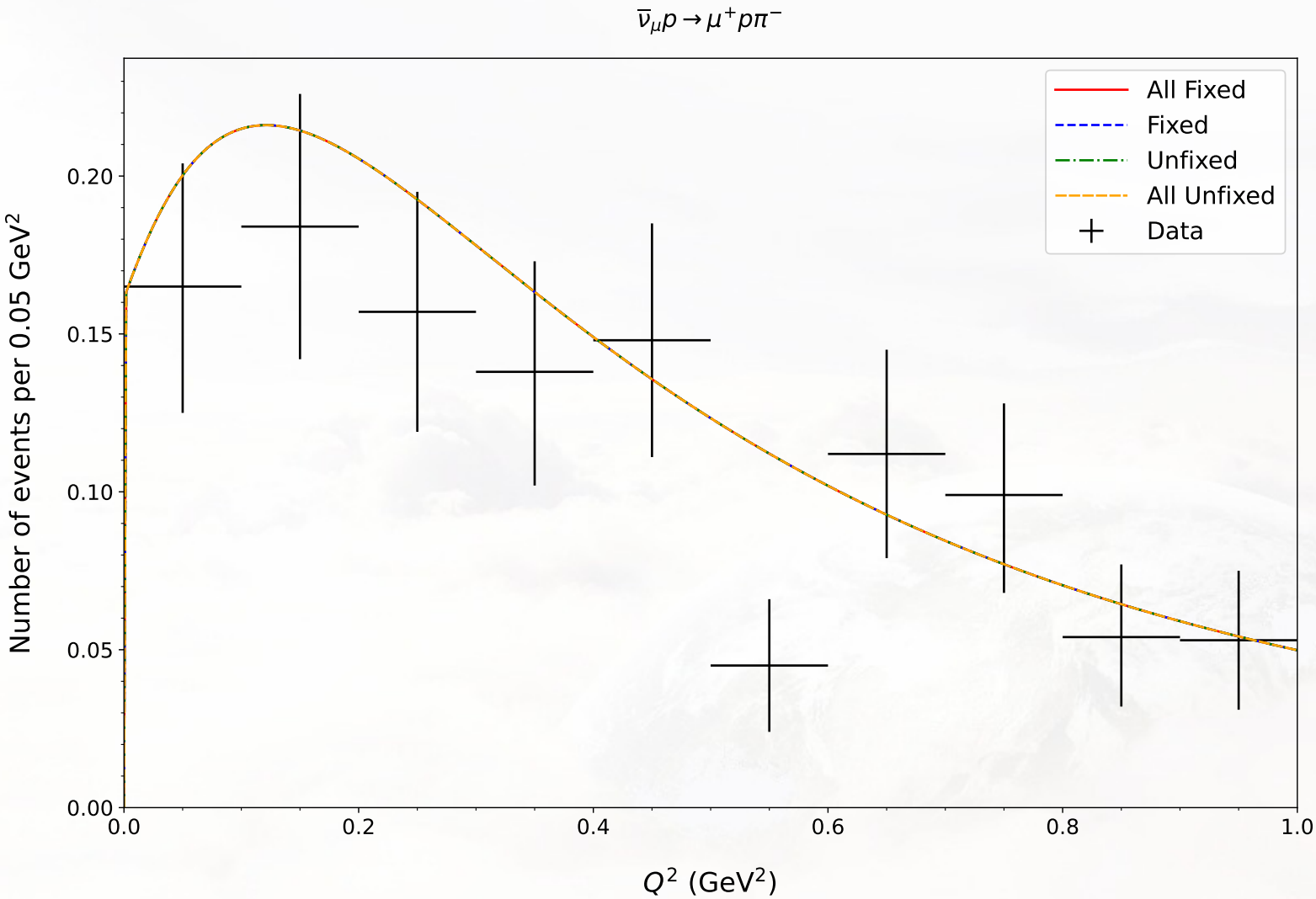

Q^2 distribution with $W < 1.4$ GeV. Neutrino spectrum is restricted by $4.97 < E_\nu < 201$ GeV. Predictions with all resonances (All)/without resonance F17(1970) and with fixed and unfixed bugs are shown. Data are taken from Ref. [38]. Neutrino spectrum is taken from [36].

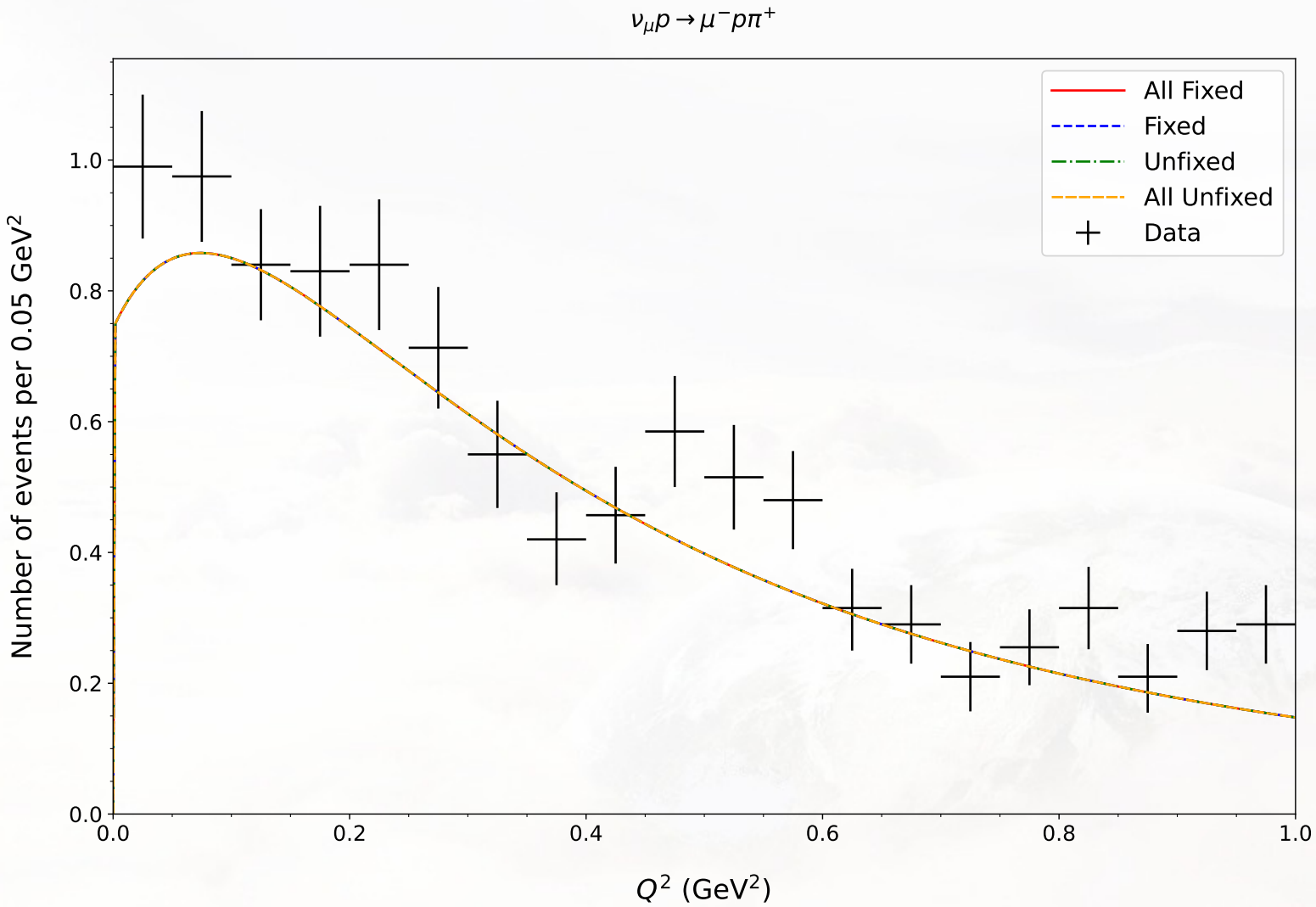

Q^2 distribution with $W < 1.4$ GeV. Neutrino spectrum is restricted by $4.97 < E_\nu < 201$ GeV. Predictions with all resonances (All)/without resonance F17(1970) and with fixed and unfixed bugs are shown. Data are taken from Ref. [38]. Neutrino spectrum is taken from [36].

Next topic

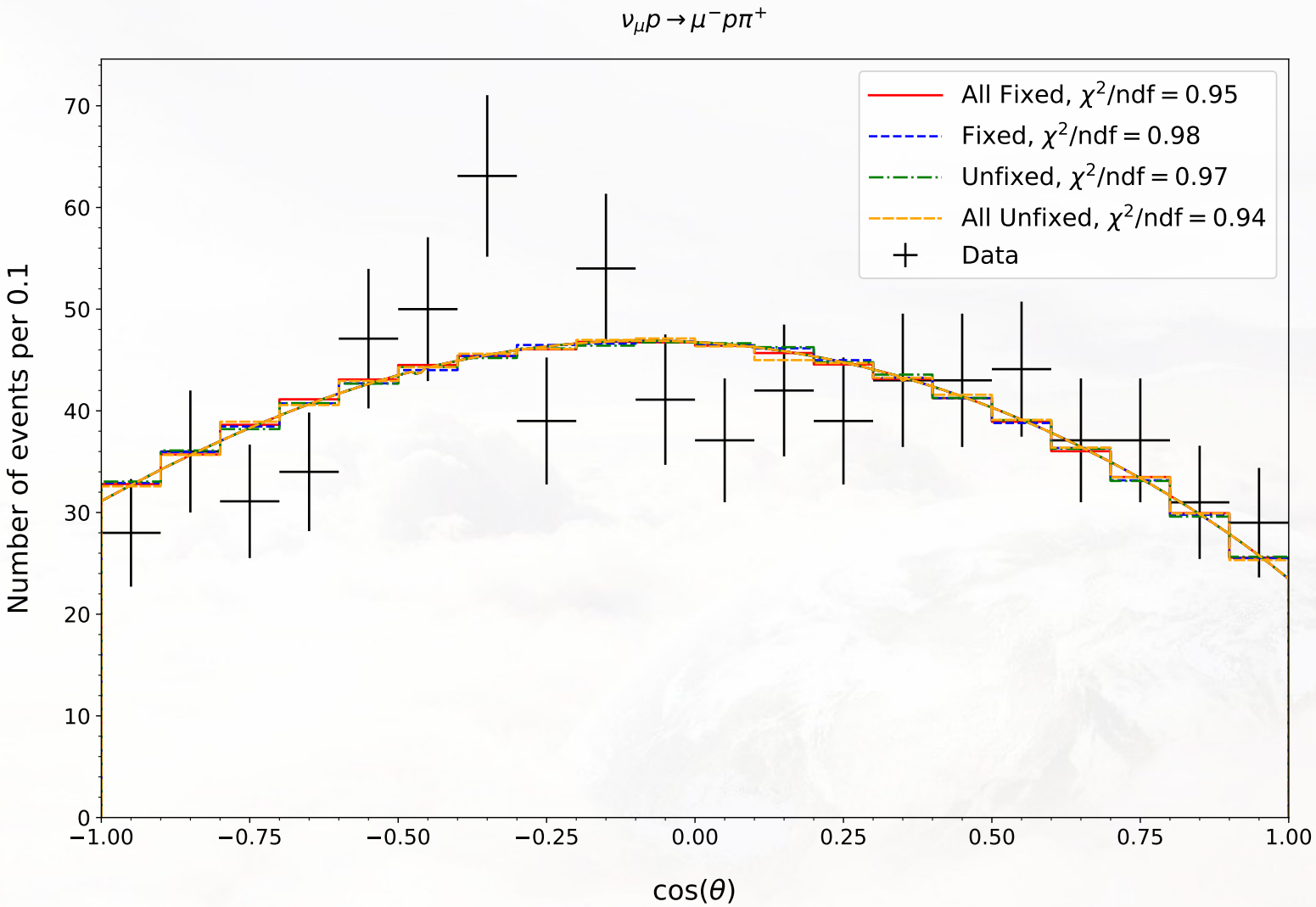

Distribution of cosine of pion zenith angle in Adler frame with $W < 1.4$ GeV. Neutrino spectrum is restricted by $E_\nu < 6.0$ GeV. Model predictions are area-normalized. Predictions with all resonances (All)/without resonance F17(1970) and with fixed and unfixed bugs are shown. Data are taken from Ref. [6]. Neutrino spectrum is taken from [34]. Cf Fig. 12 left from Ref. [1]

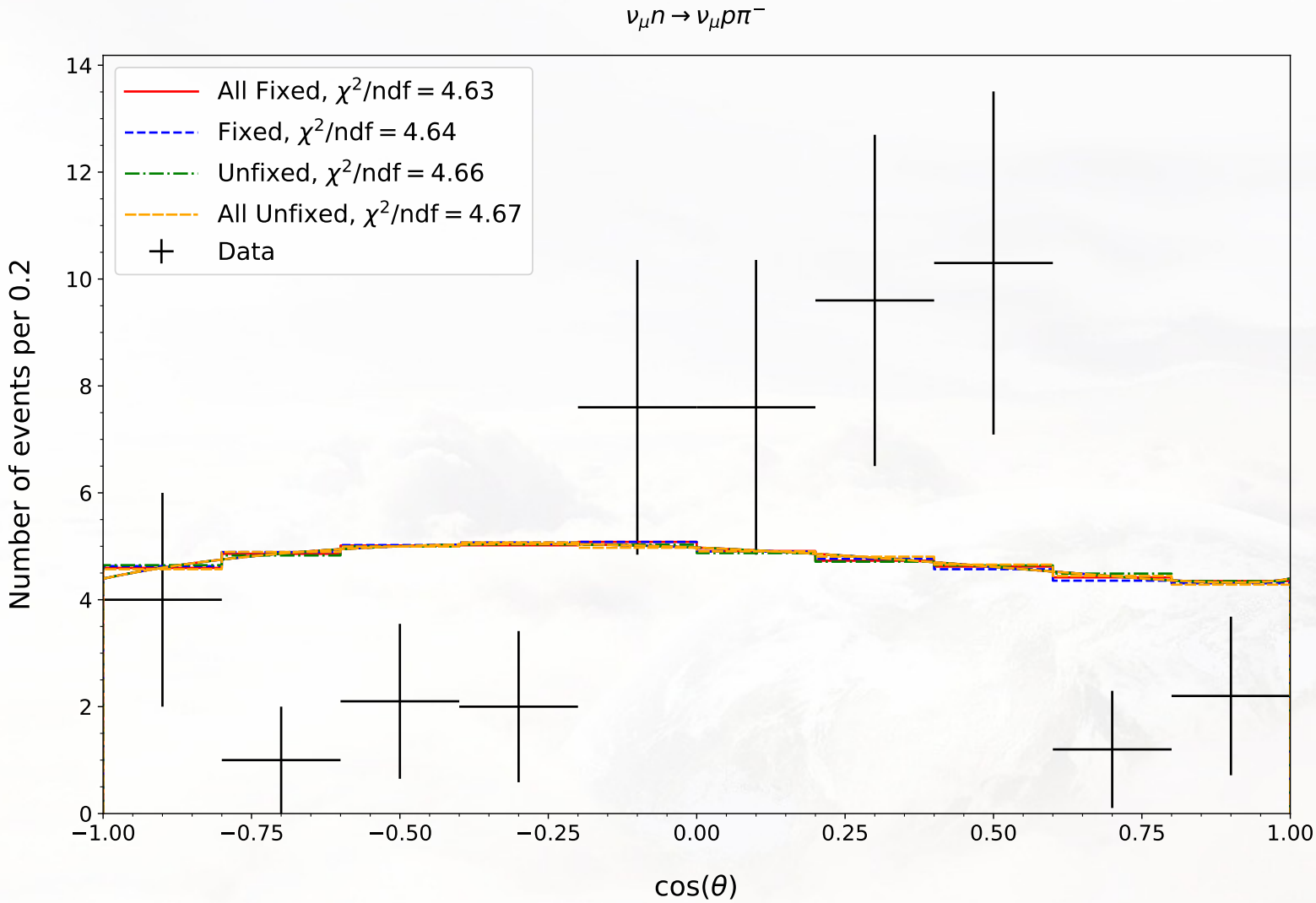

Distribution of cosine of pion zenith angle in Adler frame with no W_{cut}. Neutrino spectrum is restricted by $0.3 < E_\nu < 1.5$ GeV. Model predictions are area-normalized. Predictions with all resonances (All)/without resonance F17(1970) and with fixed and unfixed bugs are shown. Data are taken from Ref. [31]. Neutrino spectrum is taken from [34].

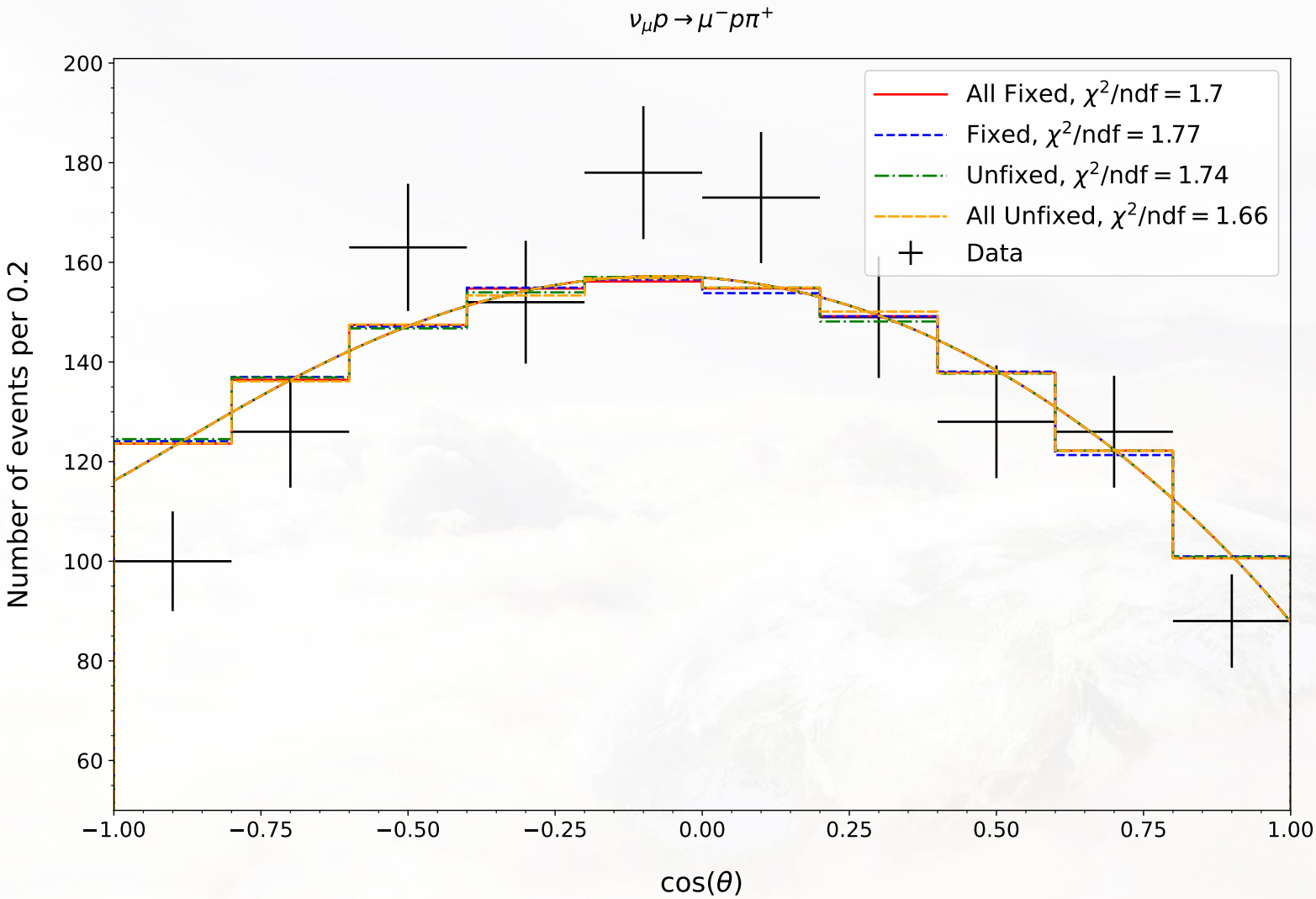

Distribution of cosine of pion zenith angle in Adler frame with $W < 1.4$ GeV. Neutrino spectrum is restricted by $0.5 < E_\nu < 6.0$ GeV. Model predictions are area-normalized. Predictions with all resonances (All)/without resonance F17(1970) and with fixed and unfixed bugs are shown. Data are taken from Ref. [11]. Neutrino spectrum is taken from [35]. Cf Fig. 12 right from Ref. [1]

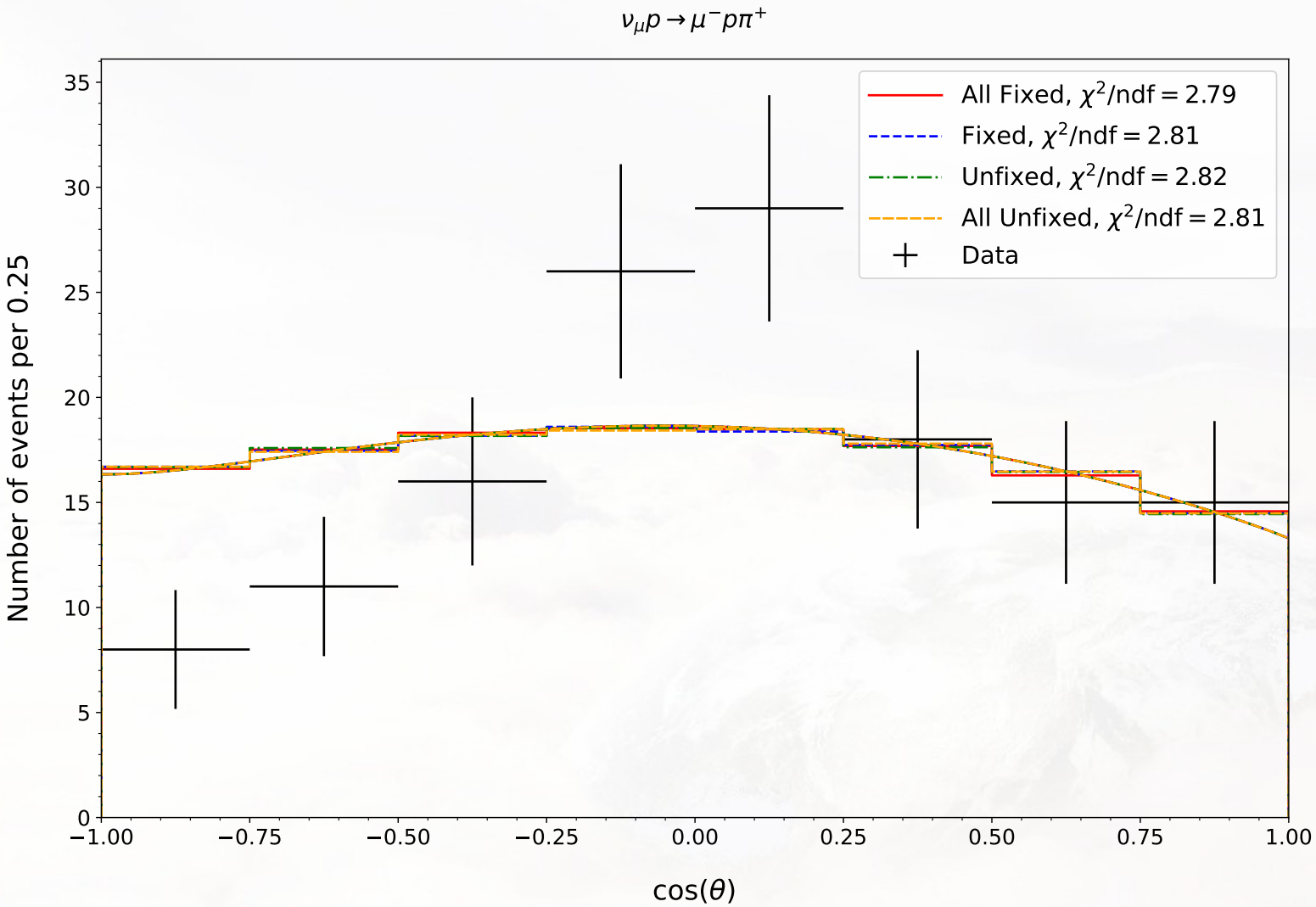

Distribution of cosine of pion zenith angle in Adler frame with $W < 1.4$ GeV. Neutrino spectrum is restricted by $5.0 < E_\nu < 155.0$ GeV. Model predictions are area-normalized. Predictions with all resonances (All)/without resonance F17(1970) and with fixed and unfixed bugs are shown. Data are taken from Ref. [37]. Neutrino spectrum is taken from [17] (Stefanski-White spectrum model).

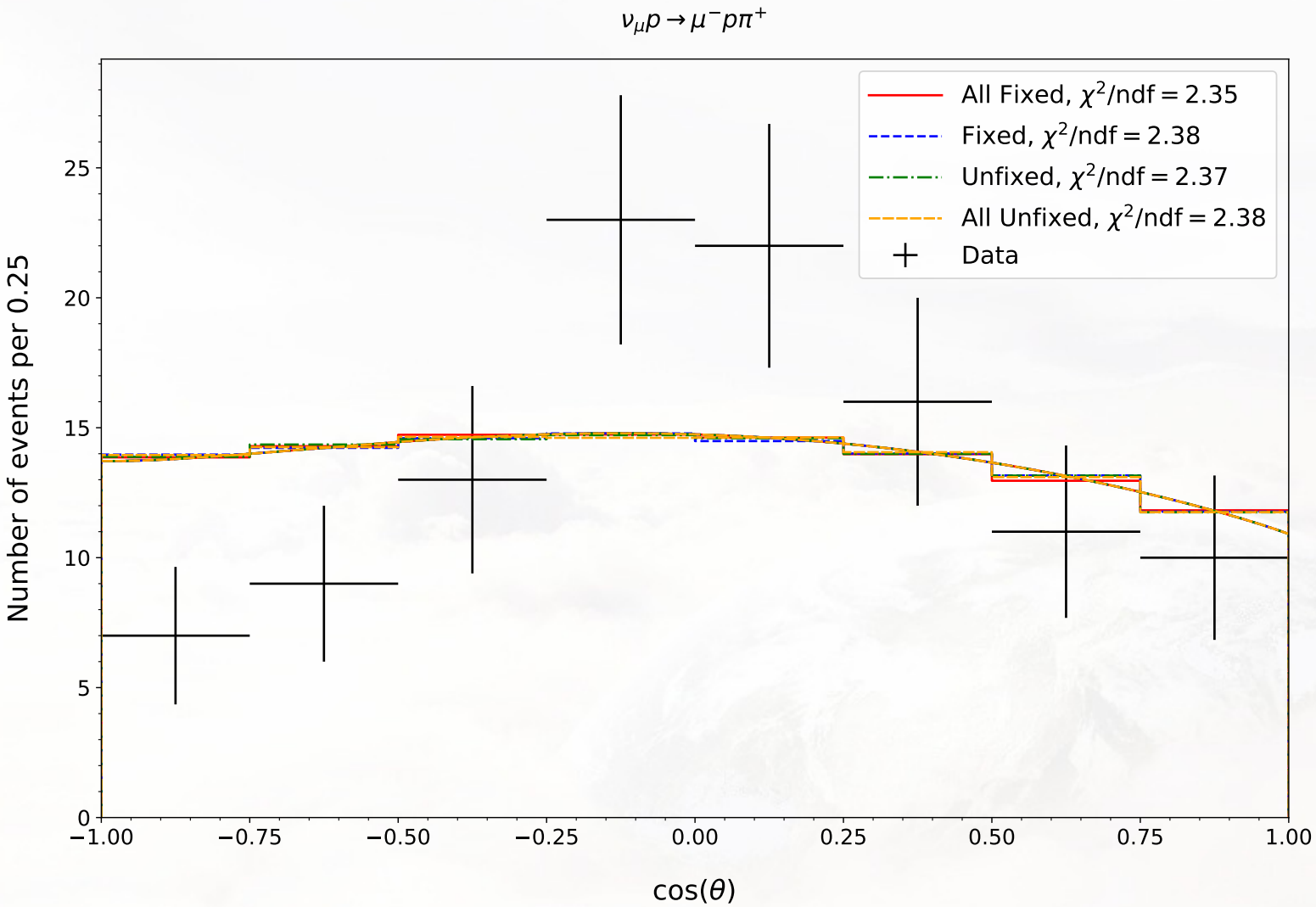

Distribution of cosine of pion zenith angle in Adler frame with $W < 1.4$ GeV, $Q^2 < 1.0$ GeV. Neutrino spectrum is restricted by $5.0 < E_\nu < 155.0$ GeV. Model predictions are area-normalized. Predictions with all resonances (All)/without resonance F17(1970) and with fixed and unfixed bugs are shown. Data are taken from Ref. [37]. Neutrino spectrum is taken from [17] (Stefanski-White spectrum model).

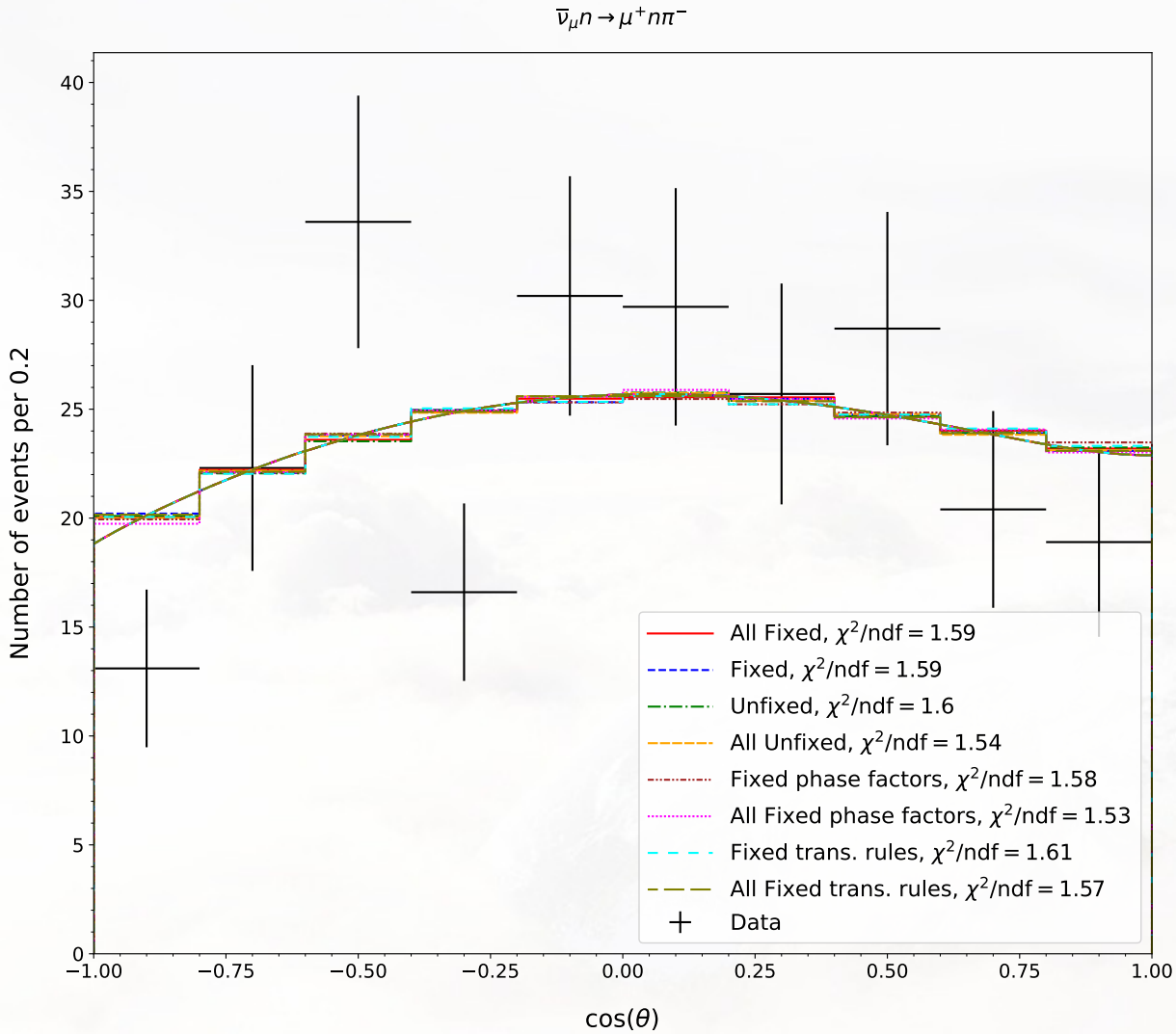

Distribution of cosine of pion zenith angle in Jackson frame with $W < 1.4$ GeV. Neutrino spectrum is restricted by $5.0 < E_\nu < 200.0$ GeV. Model predictions are area-normalized. Predictions with all resonances (All)/without resonance F17(1970) with fixed phase factor and with fixed neutrino to antineutrino transition rules. Data are taken from Ref. [19]. Neutrino spectrum is taken from [36].

Next topic

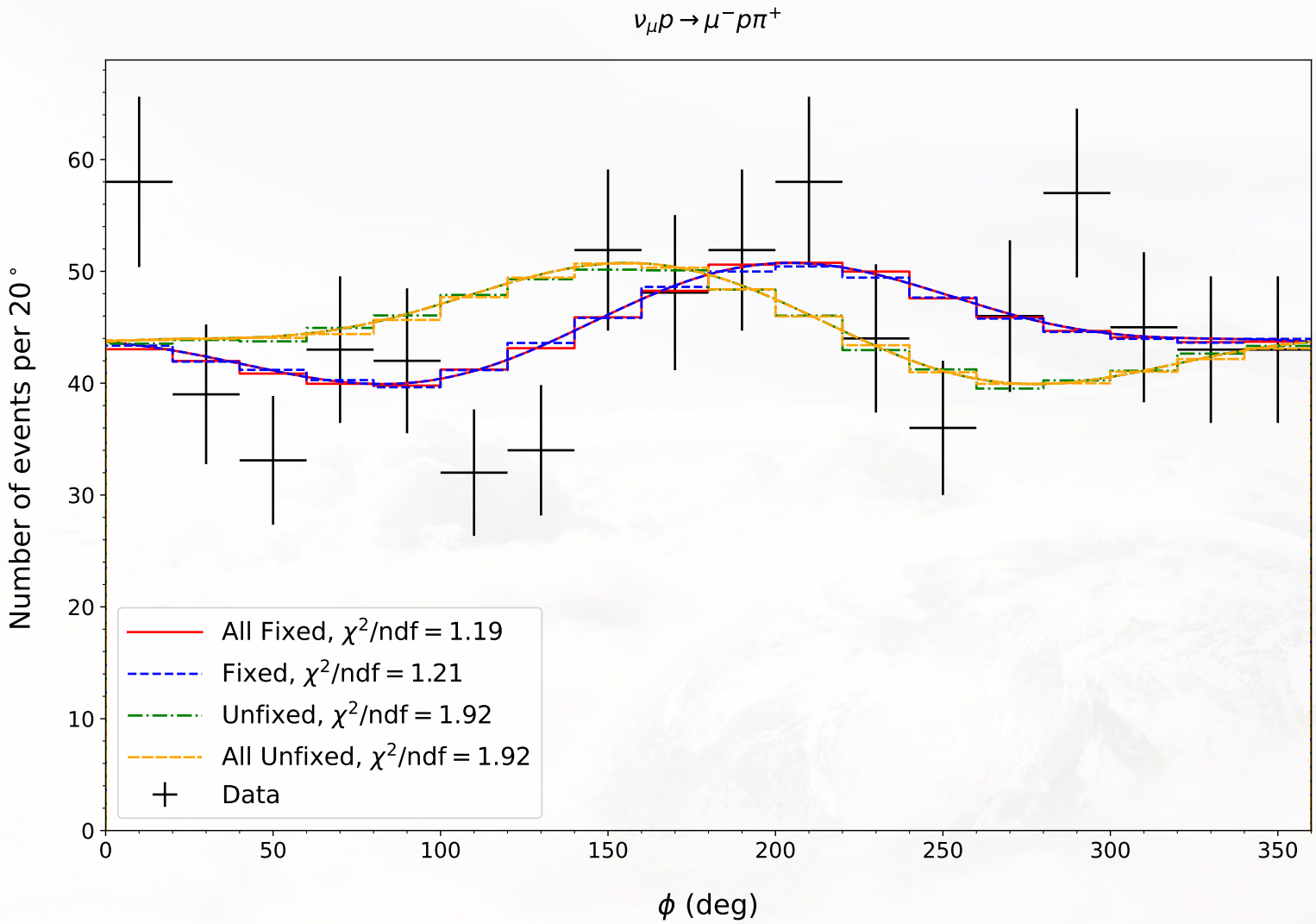

Distribution of pion azimuthal angle in Adler frame with $W < 1.4$ GeV. Neutrino spectrum is restricted by $E_\nu < 6.0$ GeV. Model predictions are area-normalized. Predictions with all resonances (All)/without resonance F17(1970) and with fixed and unfixed bugs are shown. Data are taken from Ref. [6]. Neutrino spectrum is taken from [34]. Cf Fig. 14 left from Ref. [1]

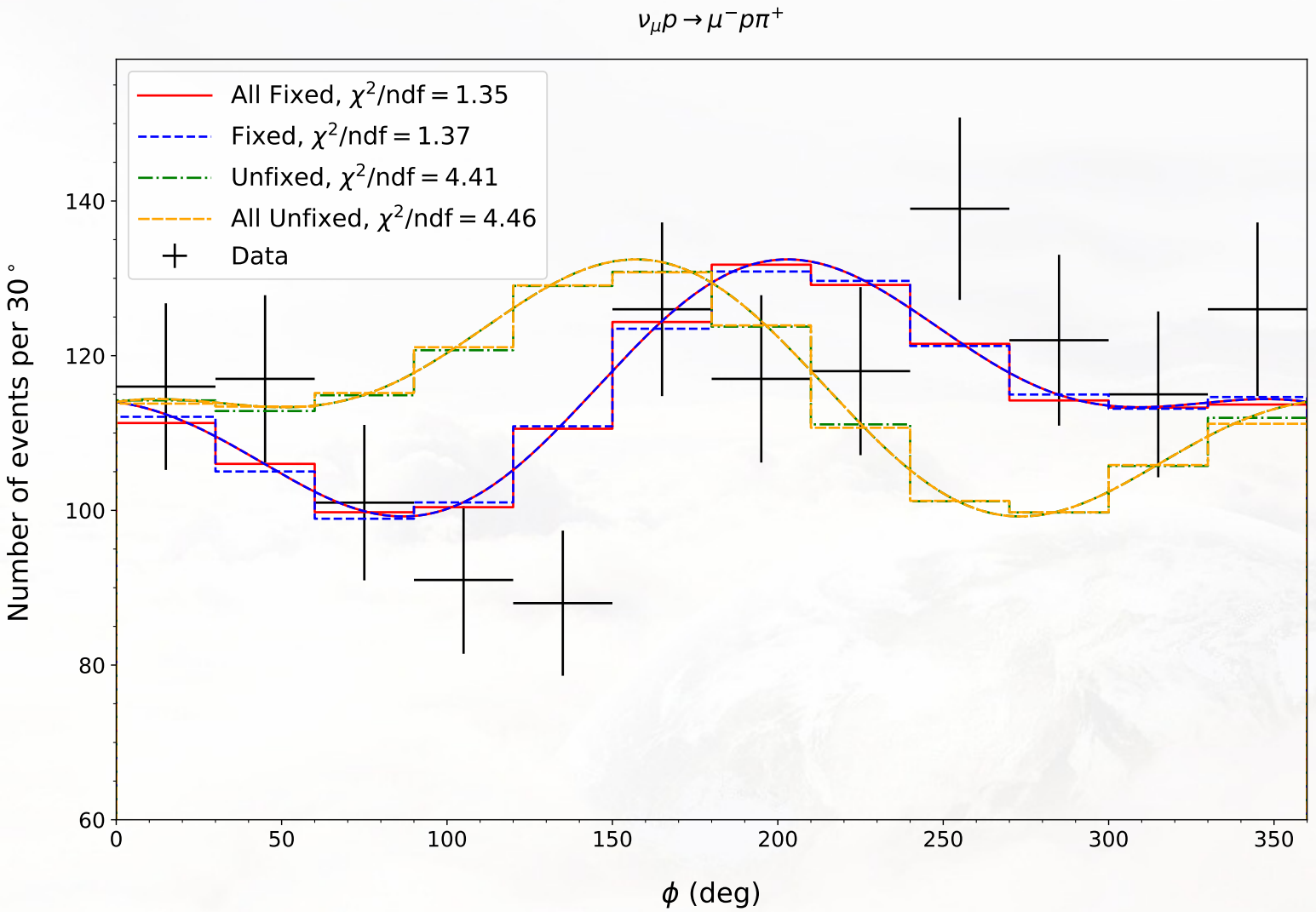

Distribution of pion azimuthal angle in Adler frame with $W < 1.4$ GeV. Neutrino spectrum is restricted by $0.5 < E_\nu < 6.0$ GeV. Model predictions are area-normalized. Predictions with all resonances (All)/without resonance F17(1970) and with fixed and unfixed bugs are shown. Data are taken from Ref. [11]. Neutrino spectrum is taken from [35]. Cf Fig. 14 right from Ref. [1]

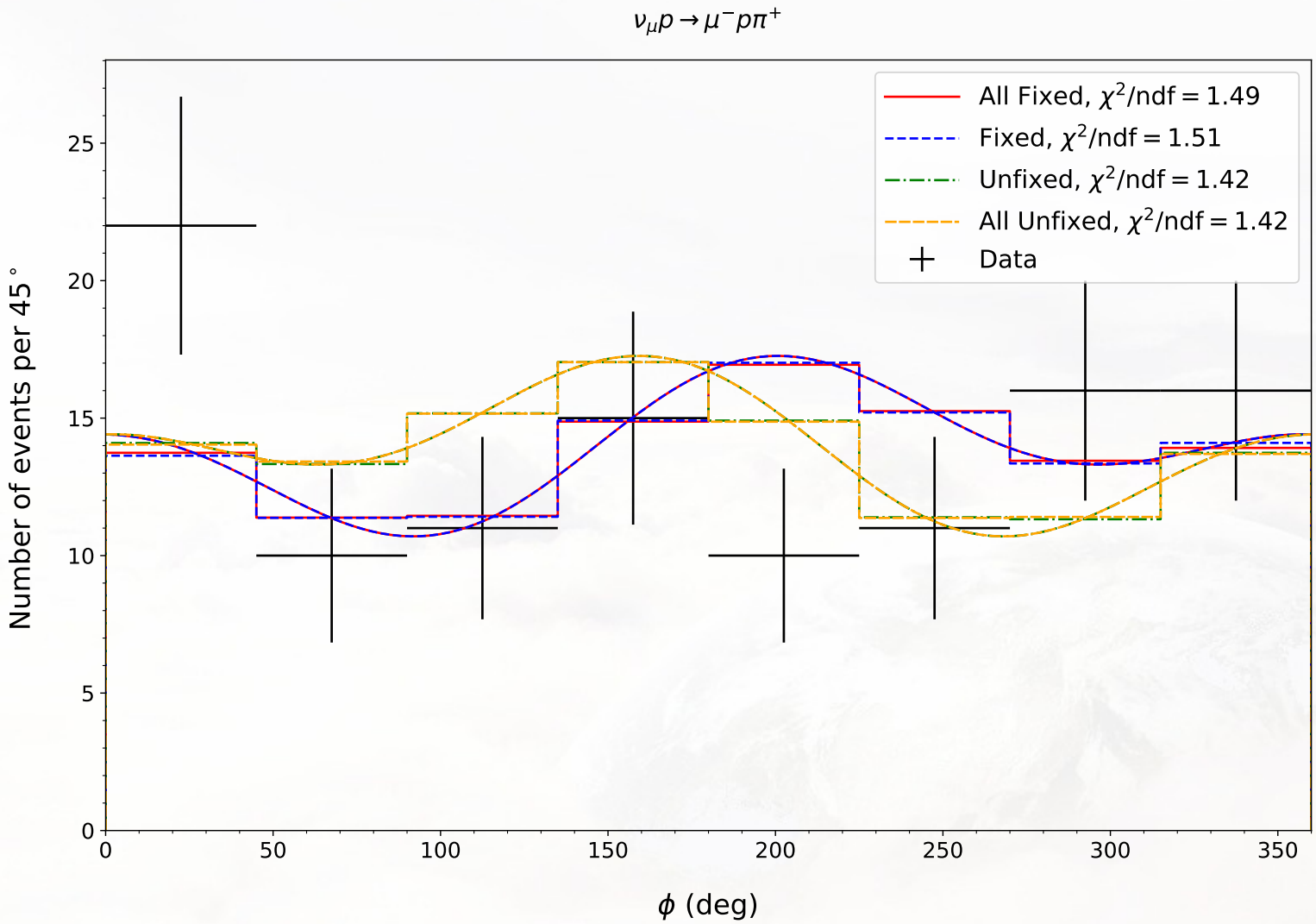

Distribution of pion azimuthal angle in Adler frame with $W < 1.4$ GeV, $Q^2 < 1.0$ GeV. Neutrino spectrum is restricted by $5.0 < E_\nu < 155.0$ GeV. Model predictions are area-normalized. Predictions with all resonances (All)/without resonance F17(1970) and with fixed and unfixed bugs are shown. Data are taken from Ref. [37]. Neutrino spectrum is taken from [17] (Stefanski-White spectrum model).

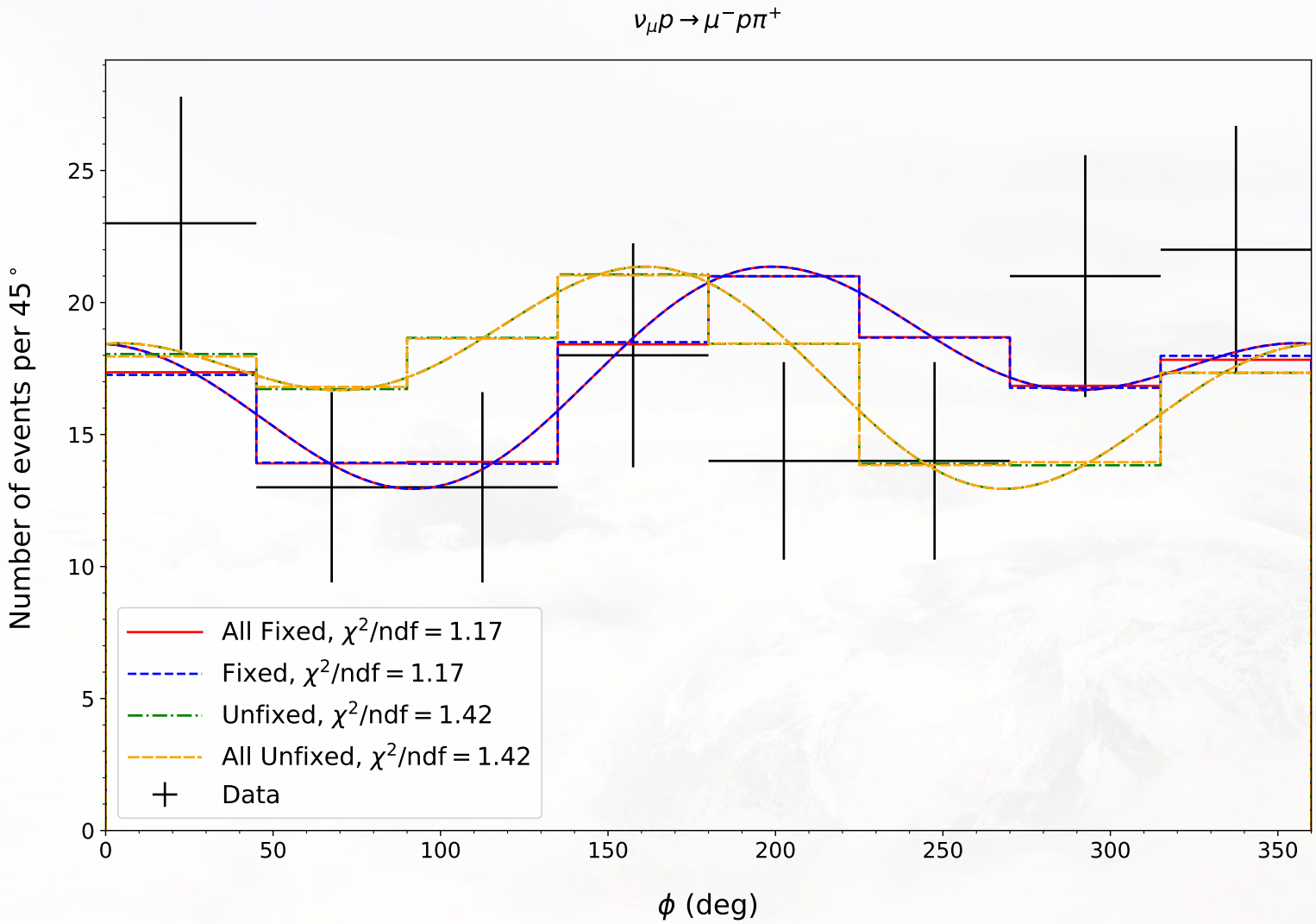

Distribution of pion azimuthal angle in Adler frame with $W < 1.4$ GeV. Neutrino spectrum is restricted by $5.0 < E_\nu < 155.0$ GeV. Model predictions are area-normalized. Predictions with all resonances (All)/without resonance F17(1970) and with fixed and unfixed bugs are shown. Data are taken from Ref. [37]. Neutrino spectrum is taken from [17] (Stefanski-White spectrum model).

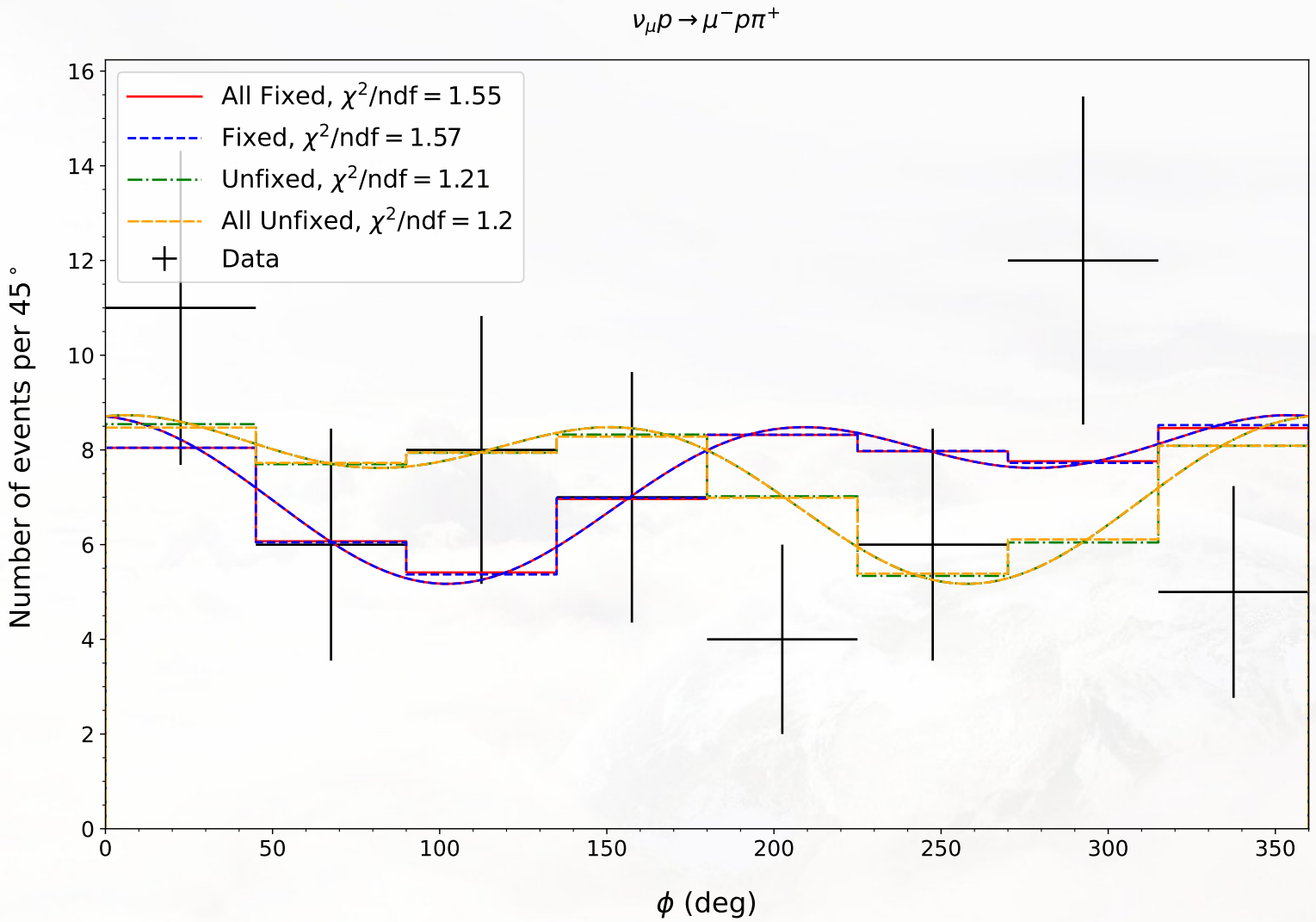

Distribution of pion azimuthal angle in Adler frame with $W < 1.4$ GeV, $Q^2 < 1.0$ GeV, $0.0 < \cos(\theta)$. Neutrino spectrum is restricted by $5.0 < E_\nu < 155.0$ GeV. Model predictions are area-normalized. Predictions with all resonances (All)/without resonance F17(1970) and with fixed and unfixed bugs are shown. Data are taken from Ref. [37]. Neutrino spectrum is taken from [17] (Stefanski-White spectrum model).

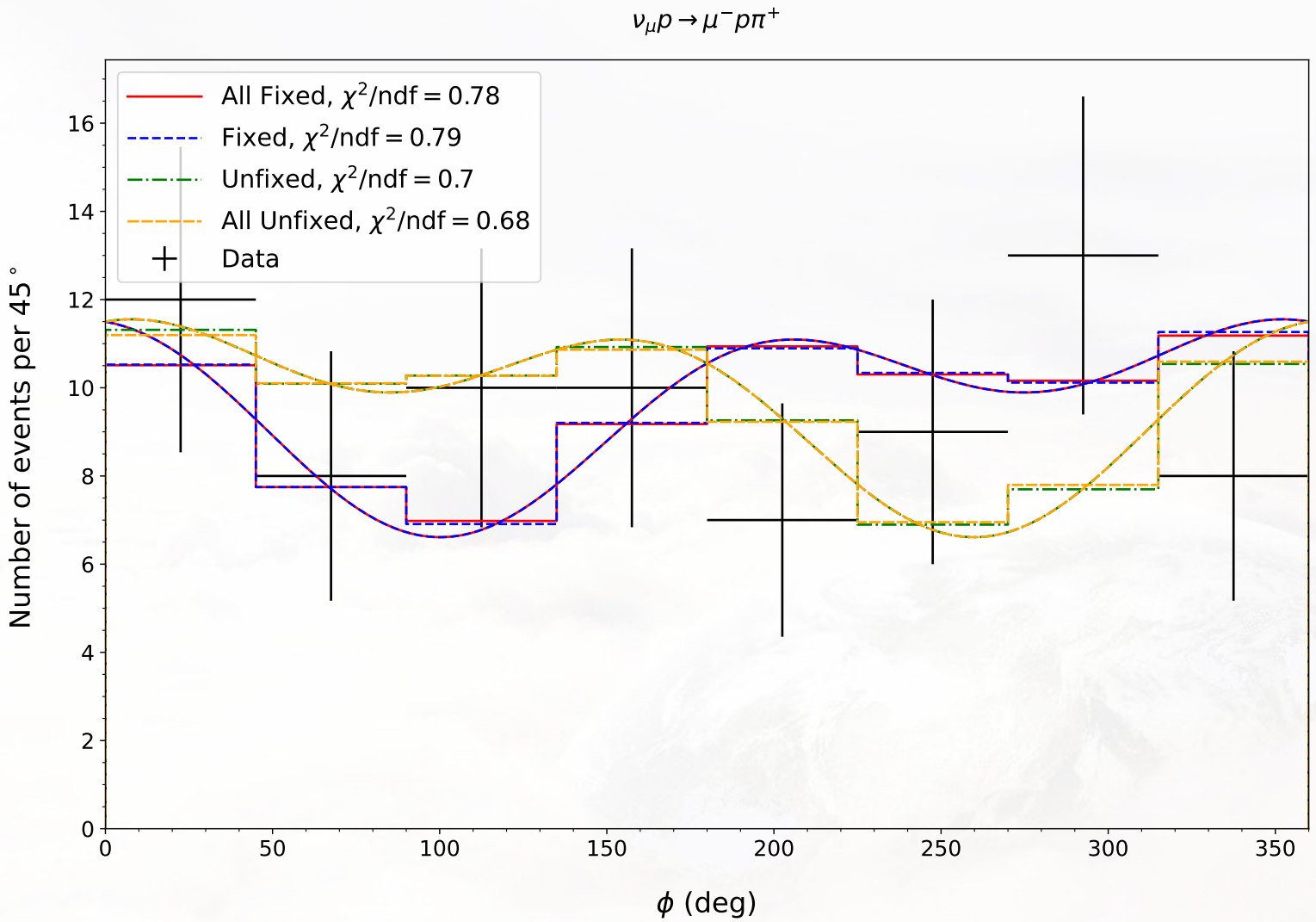

Distribution of pion azimuthal angle in Adler frame with $W < 1.4$ GeV, $0.0 < \cos(\theta)$. Neutrino spectrum is restricted by $5.0 < E_\nu < 155.0$ GeV. Model predictions are area-normalized. Predictions with all resonances (All)/without resonance F17(1970) and with fixed and unfixed bugs are shown. Data are taken from Ref. [37]. Neutrino spectrum is taken from [17] (Stefanski-White spectrum model).

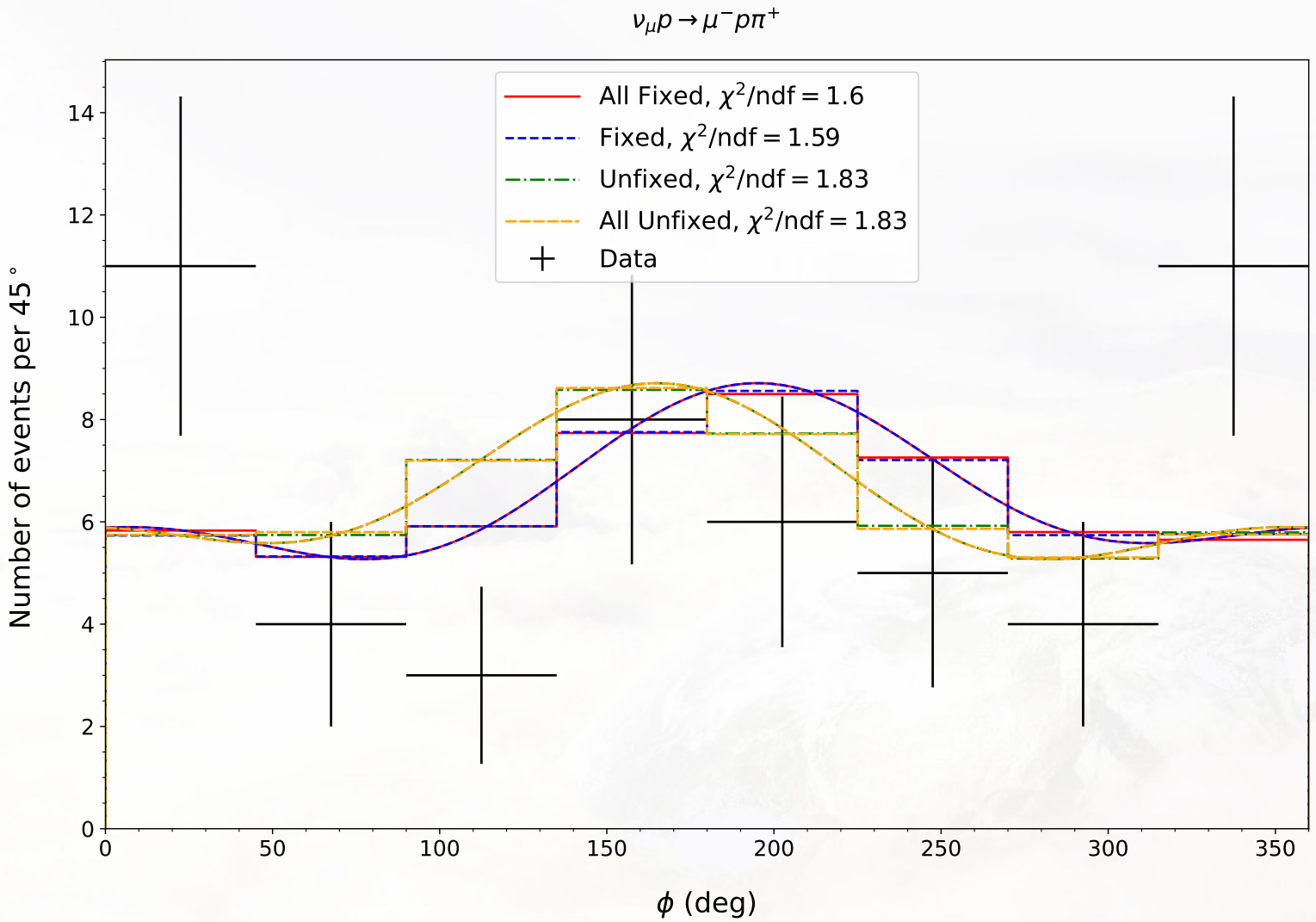

Distribution of pion azimuthal angle in Adler frame with $W < 1.4$ GeV, $Q^2 < 1.0$ GeV, $\cos(\theta) < 0.0$. Neutrino spectrum is restricted by $5.0 < E_\nu < 155.0$ GeV. Model predictions are area-normalized. Predictions with all resonances (All)/without resonance F17(1970) and with fixed and unfixed bugs are shown. Data are taken from Ref. [37]. Neutrino spectrum is taken from [17] (Stefanski-White spectrum model).

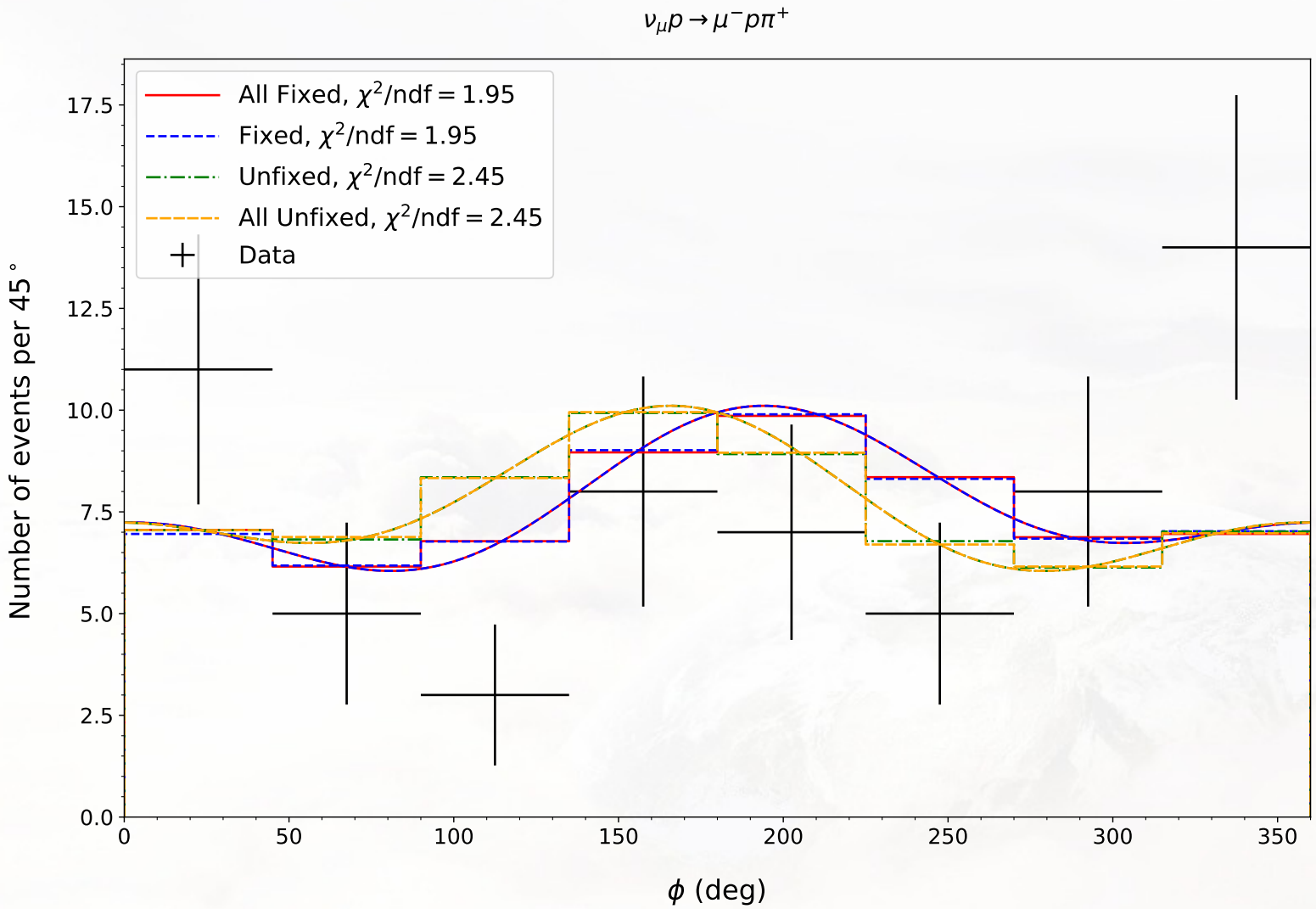

Distribution of pion azimuthal angle in Adler frame with $W < 1.4$ GeV, $\cos(\theta) < 0.0$. Neutrino spectrum is restricted by $5.0 < E_\nu < 155.0$ GeV. Model predictions are area-normalized. Predictions with all resonances (All)/without resonance F17(1970) and with fixed and unfixed bugs are shown. Data are taken from Ref. [37]. Neutrino spectrum is taken from [17] (Stefanski-White spectrum model).

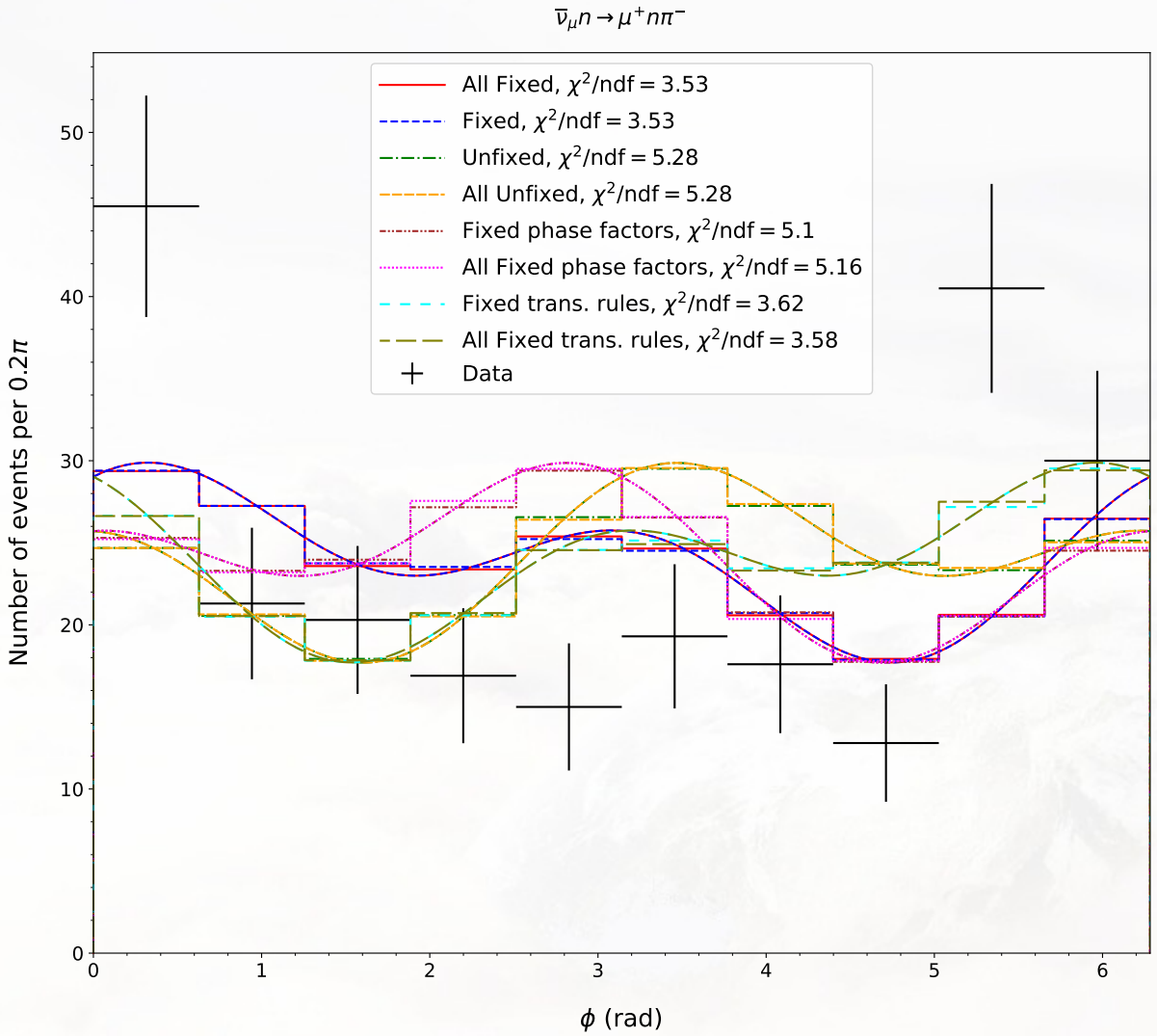

Distribution of pion azimuthal angle in Jackson frame with $W < 1.4$ GeV. Neutrino spectrum is restricted by $5.0 < E_\nu < 200.0$ GeV. Model predictions are area-normalized. Predictions with all resonances (All)/without resonance F17(1970) with fixed phase factor and with fixed neutrino to antineutrino transition rules. Data are taken from Ref. [19]. Neutrino spectrum is taken from [36].

Next topic

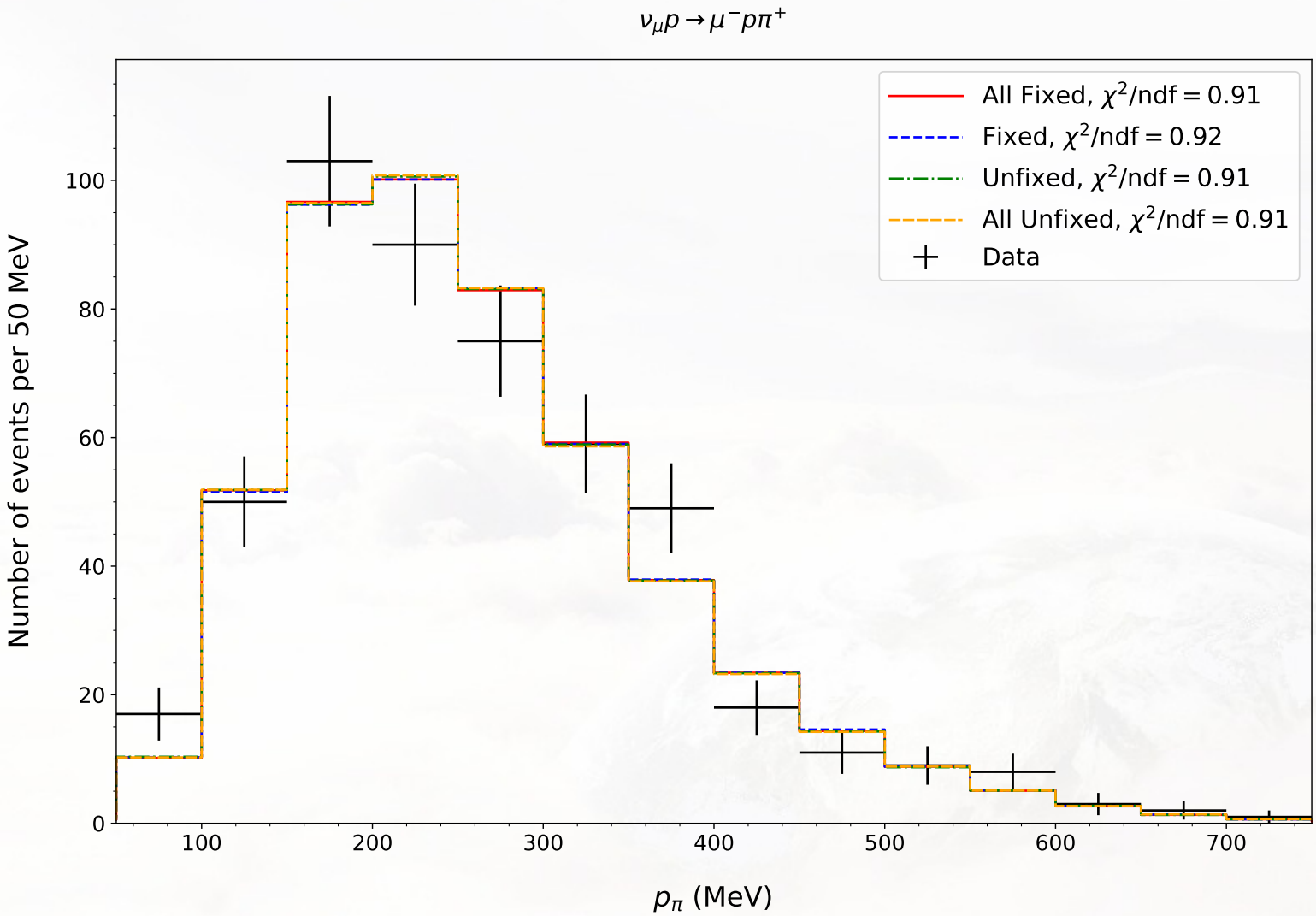

Distribution of pion momentum with $W < 1.4$ GeV. Neutrino spectrum is restricted by $E_\nu < 1.5$ GeV. Model predictions are area-normalized. Predictions with all resonances (All)/without resonance F17(1970) and with fixed and unfixed bugs are shown. Data are taken from Ref. [39]. Neutrino spectrum is taken from [34]. Cf Fig. 9 left from Ref. [1]

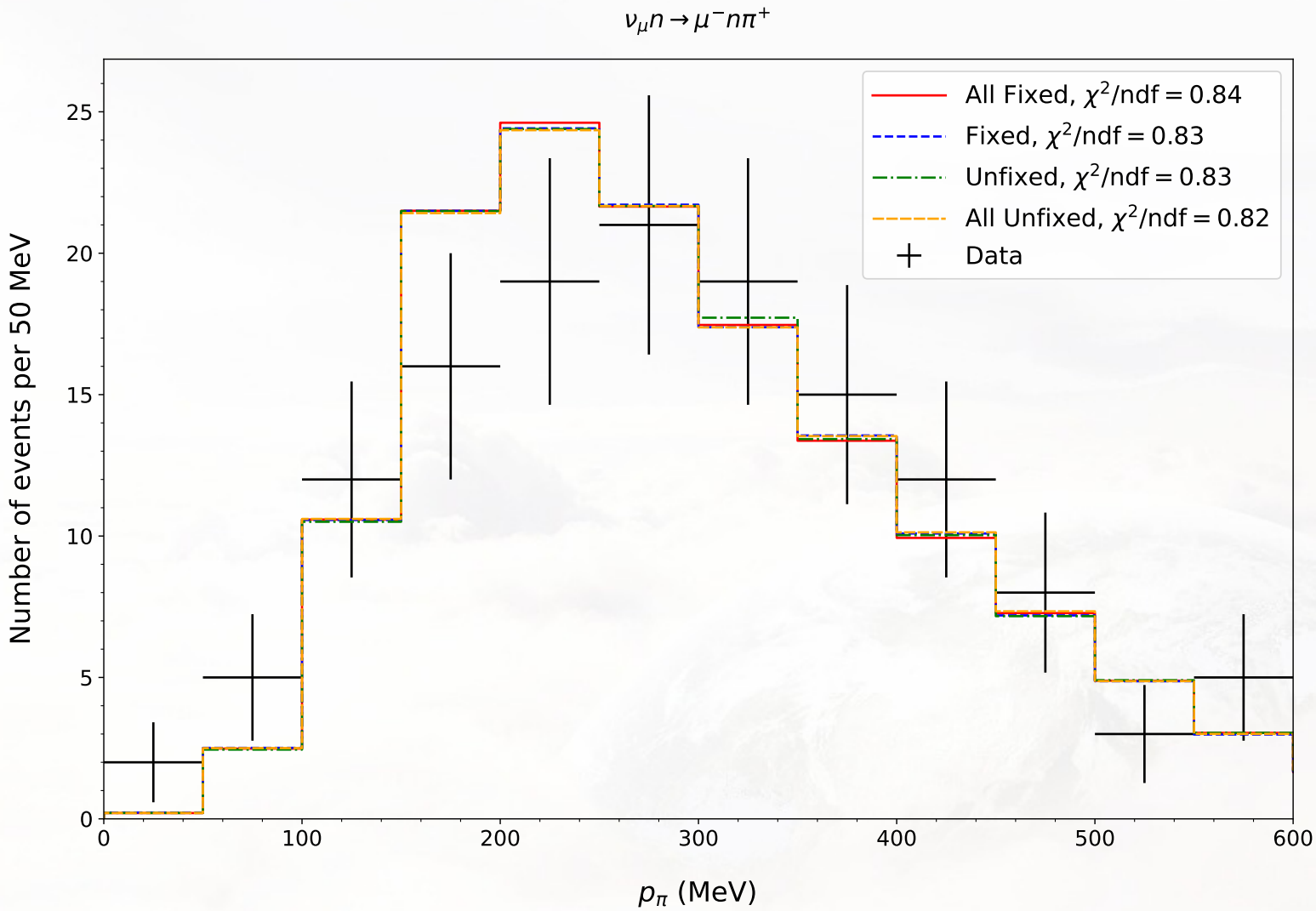

Distribution of pion momentum with $W < 1.4$ GeV. Neutrino spectrum is restricted by $E_\nu < 1.5$ GeV. Model predictions are area-normalized. Predictions with all resonances (All)/without resonance F17(1970) and with fixed and unfixed bugs are shown. Data are taken from Ref. [39]. Neutrino spectrum is taken from [34]. Cf Fig. 9 right from Ref. [1]

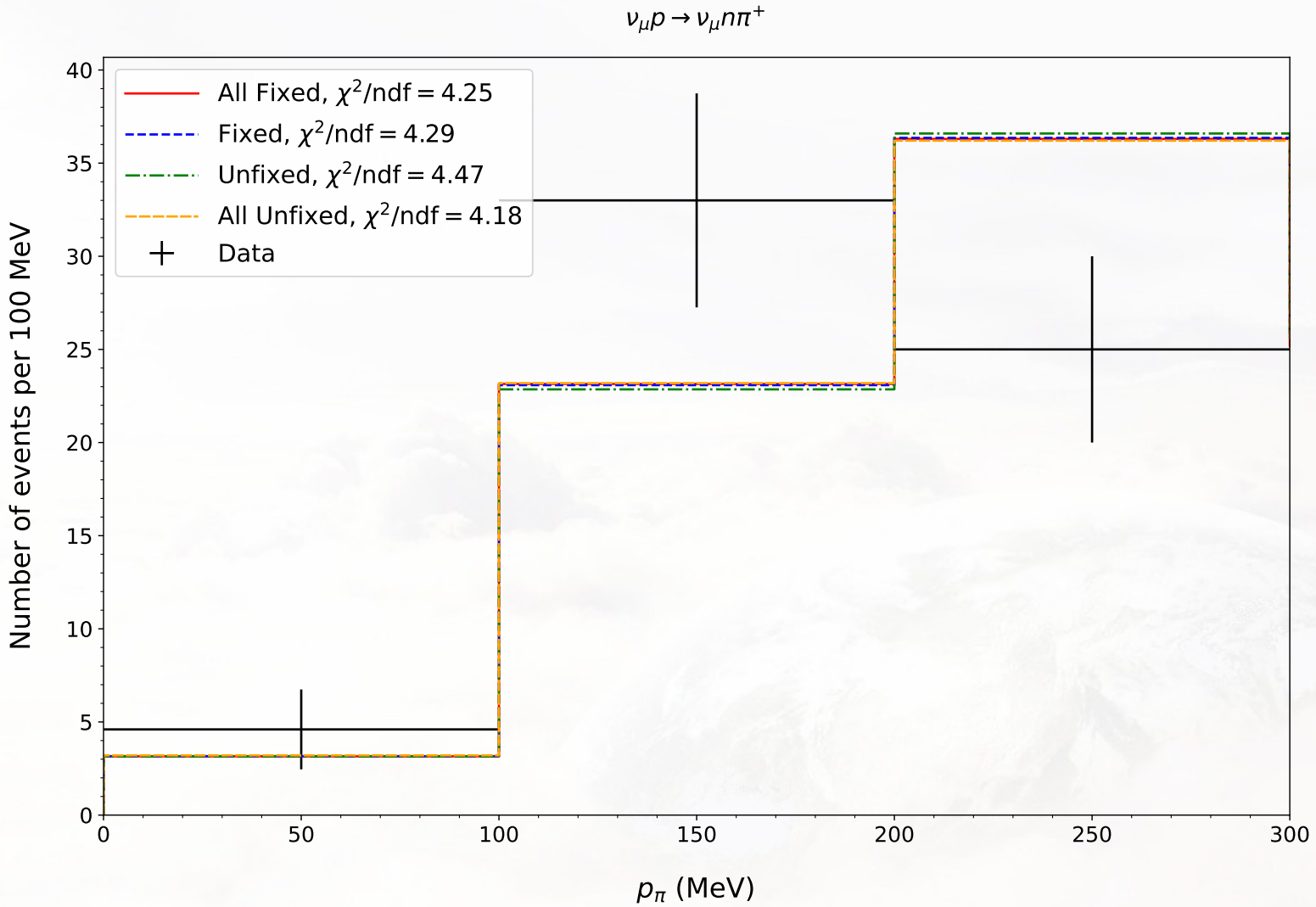

Distribution of pion momentum with no W_{cut}. Neutrino spectrum is restricted by $E_\nu < 6.0$ GeV. Model predictions are area-normalized. Predictions with all resonances (All)/without resonance F17(1970) and with fixed and unfixed bugs are shown. Data are taken from Ref. [39]. Neutrino spectrum is taken from [34].

Next topic

Conclusions

- The original MK code and its implementation are consistent.
- Difference between **All Fixed** and **All Unfixed** versions (as well as between **Fixed** and **Unfixed**) are important only for distributions over ϕ. Although the relevant data are very uncertain, we can conclude that (on average) they support the corrected (**All fixed**) version.

Bibliography I

[1] M. Kabirnezhad, Phys. Rev. D **97**(1), 013002 (2018), arXiv:1711.02403 [hep-ph]

[2] K.M. Graczyk, J.T. Sobczyk, Phys. Rev. D **77**(5), 053001 (2008), [Erratum: *ibid.* **79**, 079903 (2008)], arXiv:0707.3561 [hep-ph]

[3] S.J. Barish et al. (1975), aNL-HEP-PR-75-36

[4] G.T. Jones et al. (Birmingham–CERN–Imperial College–München (MPI)–Oxford University College (WA21 Collaboration)), Z. Phys. C **43**(4), 527 (1989)

[5] D.H. Perkins, *Review of neutrino experiments*, in *Proceedings of the International Symposium on Lepton and Photon Interactions at High Energies, Leland Stanford Junior University, Stanford, California, USA, August 21–27, 1975*, edited by T.W. Kirk (SLAC National Accelerator Laboratory, Stanford, California, USA, 1975), pp. 571–603

[6] G.M. Radecky et al., Phys. Rev. D **25**(5), 1161 (1982), [Erratum: *ibid.* **26**, 3297 (1982)]

[7] W. Lerche et al., Phys. Lett. **78 B**(4), 510 (1978)

[8] V.E. Barnes et al., *Study of the isospin properties of single-pion production by neutrinos*, in *Proceedings of the 6th International Conference on Neutrino Physics (Neutrino 1978), Purdue University, West Lafayette, Indiana, USA, April 28 – May 2, 1978*, edited by E.C. Fowler (Purdue University Press, West Lafayette, Indiana, USA, 1978), pp. C56–C63

[9] R.T. Ross (Fermilab–Hawaii–Berkeley–Michigan Collaboration), *A study of the reaction* $\nu p \to \mu^- p \pi^+$, in *Proceedings of the 6th International Conference on Neutrino Physics (Neutrino 1978), Purdue University, West Lafayette, Indiana, USA, April 28 – May 2, 1978*, edited by E.C. Fowler (Purdue University Press, West Lafayette, Indiana, USA, 1978), pp. 929–938

Bibliography II

[10] S.J. Barish et al., Phys. Lett. B **91**(1), 161 (1980)

[11] T. Kitagaki et al., Phys. Rev. D **34**(9), 2554 (1986)

[12] S.J. Barish et al., Phys. Rev. D **19**(9), 2521 (1979)

[13] P. Allen et al. (Aachen–Bonn–CERN–München–Oxford Collaboration), Nucl. Phys. B **176**(2), 269 (1980)

[14] J. Bell et al., Phys. Rev. Lett. **41**(15), 1008 (1978)

[15] S.J. Barish et al., Phys. Rev. Lett. **36**(4), 179 (1976)

[16] P. Rodrigues, C. Wilkinson, K. McFarland, Eur. Phys. J. C **76**(8), 474 (2016), arXiv:1601.01888 [hep-ex]

[17] S.J. Barish et al., Phys. Rev. D **18**(7), 2205 (1978)

[18] T. Bolognese, J.P. Engel, J.L. Guyonnet, J.L. Riester, Phys. Lett. **81 B**(3–4), 393 (1979)

[19] D. Allasia et al. (Amsterdam–Bergen–Bologna–Padova–Pisa–Saclay–Torino Collaboration), Z. Phys. C **20**(2), 95 (1983)

[20] H.J. Grabosch et al. (SKAT Collaboration), Z. Phys. C **41**(4), 527 (1989)

[21] V.I. Efremenko et al., ITEP-83-1981 (1981)

[22] P. Allen et al. (Aachen–Birmingham–Bonn–CERN–London–Munich–Oxford Collaboration), Nucl. Phys. B **264**, 221 (1986)

[23] S.J.M. Barlag, Ph.D. thesis, Amsterdam U. (1984)

[24] D. Allasia et al., Nucl. Phys. B **343**(2), 285 (1990)

Bibliography III

[25] E.A. Hawker, *Single pion production in low energy neutrino-carbon*, in *Proceedings of the 2nd International Workshop on Neutrino-Nucleus Interactions in the Few GeV Region (NuInt 2002), Irvine, California, USA, December 12–15, 2002*, edited by J.G. Morfin (North Holland Publishing Co., Amsterdam, The Netherlands, 2002)

[26] I. Budagov et al., Phys. Lett. **29 B**(8), 524 (1969)

[27] J. Campbell et al., Phys. Rev. Lett. **30**(8), 335 (1973)

[28] M. Derrick, *Charged current neutrino reactions in the resonance region*, in *Proceedings of the 17th International Conference on High-Energy Physics (ICHEP 1974), London, England, UK, July 1–10, 1974*, edited by J.R. Smith (Science Research Council, Rutherford Laboratory, Chilton, England, UK, 1975), pp. II.166–170

[29] W. Krenz et al. (Gargamelle Neutrino Propane, Aachen–Brussels–CERN–Ecole Poly–Orsay–Padua Collaborations), Nucl. Phys. B **135**(1), 45 (1978)

[30] A.A. Aguilar-Arevalo et al. (MiniBooNE Collaboration), Phys. Rev. D **81**(1), 013005 (2010), arXiv:0911.2063 [hep-ex]

[31] M. Derrick et al., Phys. Lett. **92 B**(3–4), 363 (1980), [Erratum: *ibid.* **95 B**, 461 (1980)]

[32] H. Faissner et al., Phys. Lett. B **125**, 230 (1983)

[33] C.A.P.D.B. Licciardi, Ph.D. thesis, Regina U. (2012)

[34] S.J. Barish et al., Phys. Rev. D **16**(11), 3103 (1977)

Bibliography IV

[35] K. Furuno et al., *BNL 7-foot bubble chamber experiment: Neutrino deuterium interactions*, in *Proceedings of the 2nd International Workshop on Neutrino-Nucleus Interactions in the Few GeV Region (NuInt 2002), Irvine, California, USA, December 12–15, 2002*, edited by J.G. Morfin (North Holland Publishing Co., Amsterdam, The Netherlands, 2002)

[36] D. Allasia et al. (Amsterdam–Bergen–Bologna–Padua–Pisa–Saclay–Torino Collaboration), Nucl. Phys. B **239**(2), 301 (1984)

[37] J. Bell et al., Phys. Rev. Lett. **41**(15), 1012 (1978)

[38] G.T. Jones et al. (WA21, Birmingham-CERN-Imperial-Coll-Munich-Oxford-University Coll), Z. Phys. C **43**, 527 (1989)

[39] M. Derrick et al., Phys. Rev. D **23**(3), 569 (1981)

Figures from [1]

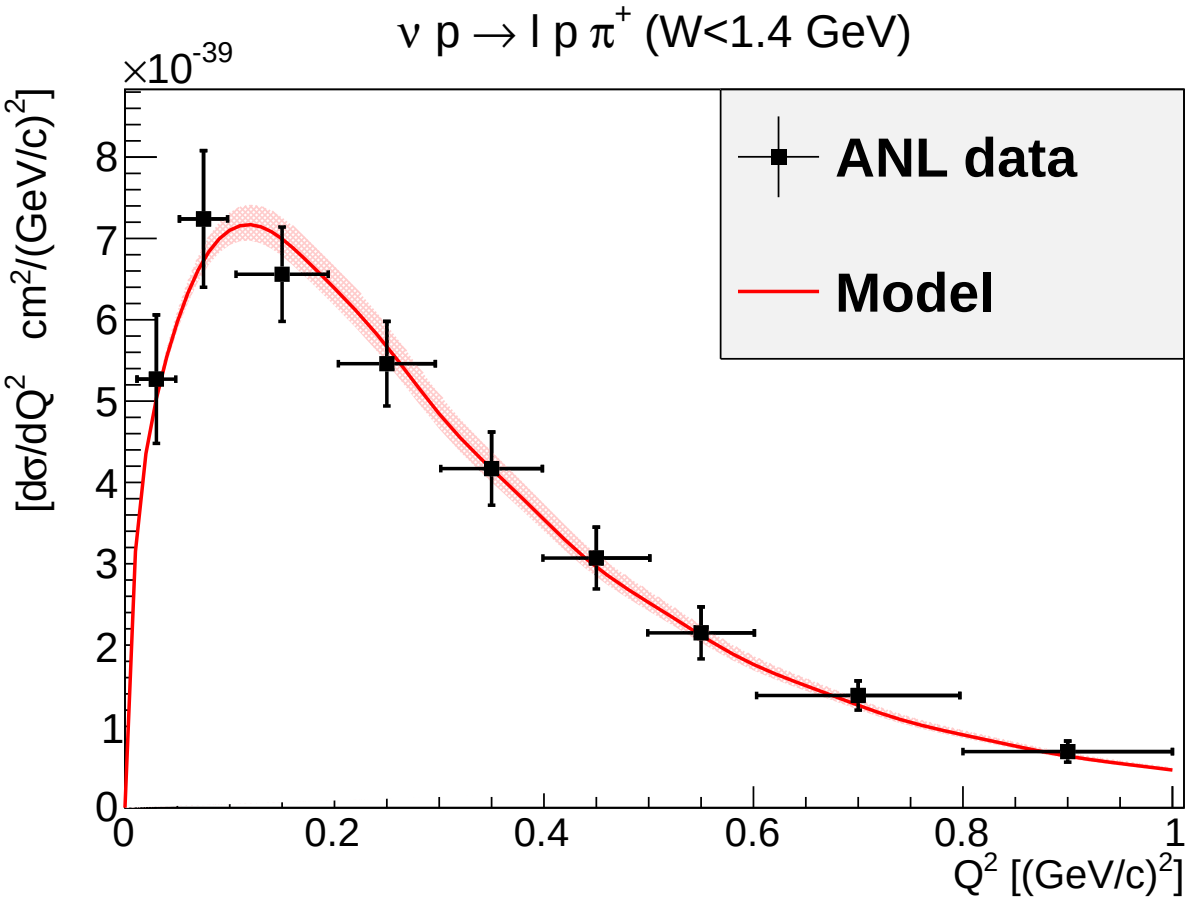

Back Q^2-differential cross section ANL data with invariant mass cut, $W < 1.4$ GeV. The prediction of the model with fitted parameters is shown with a solid red curve. The shaded area accounts for the variation of the results when M_A changes within its error interval.

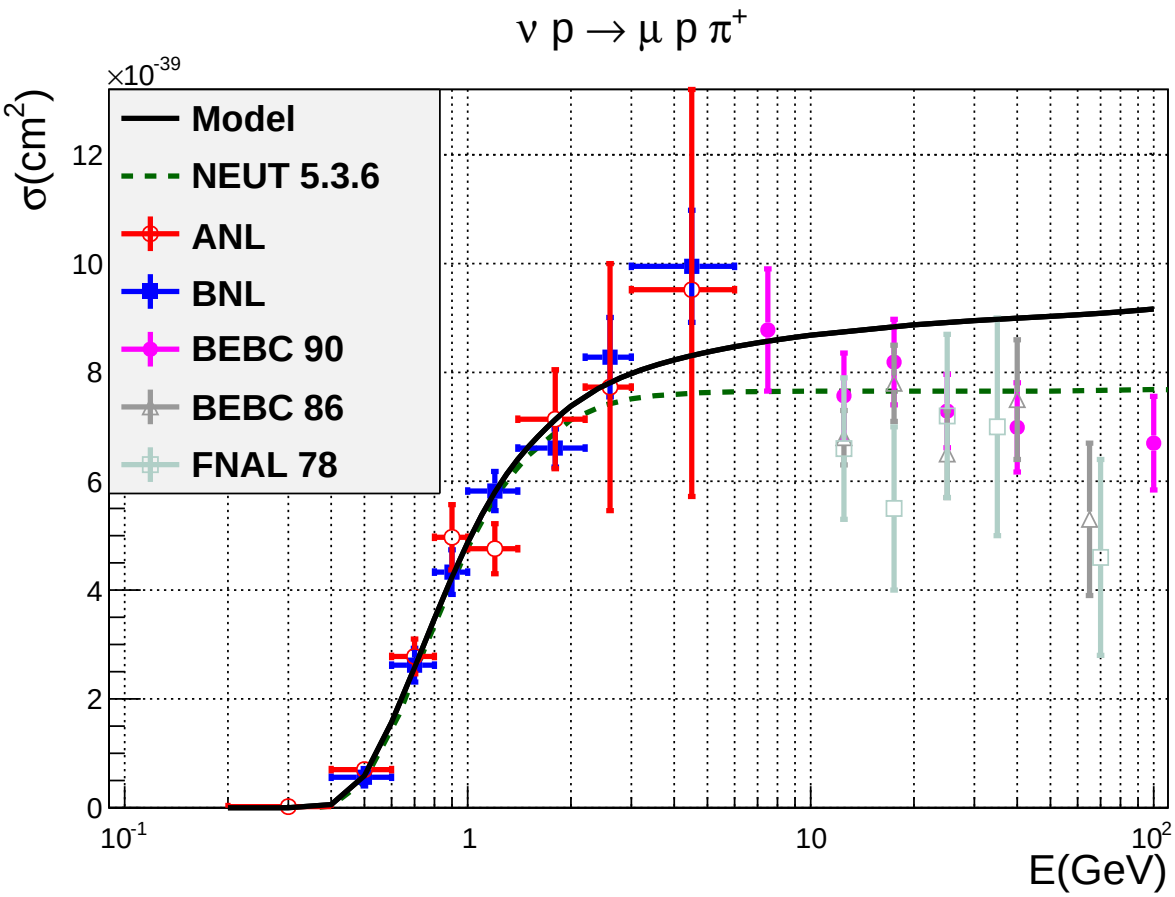

Back Total cross-section with invariant mass cut $W < 2$ GeV, curves are predicted cross sections by the model (solid black) and NEUT 5.3.6 (dashed green), with an invariant mass cut $W < 2$ GeV.

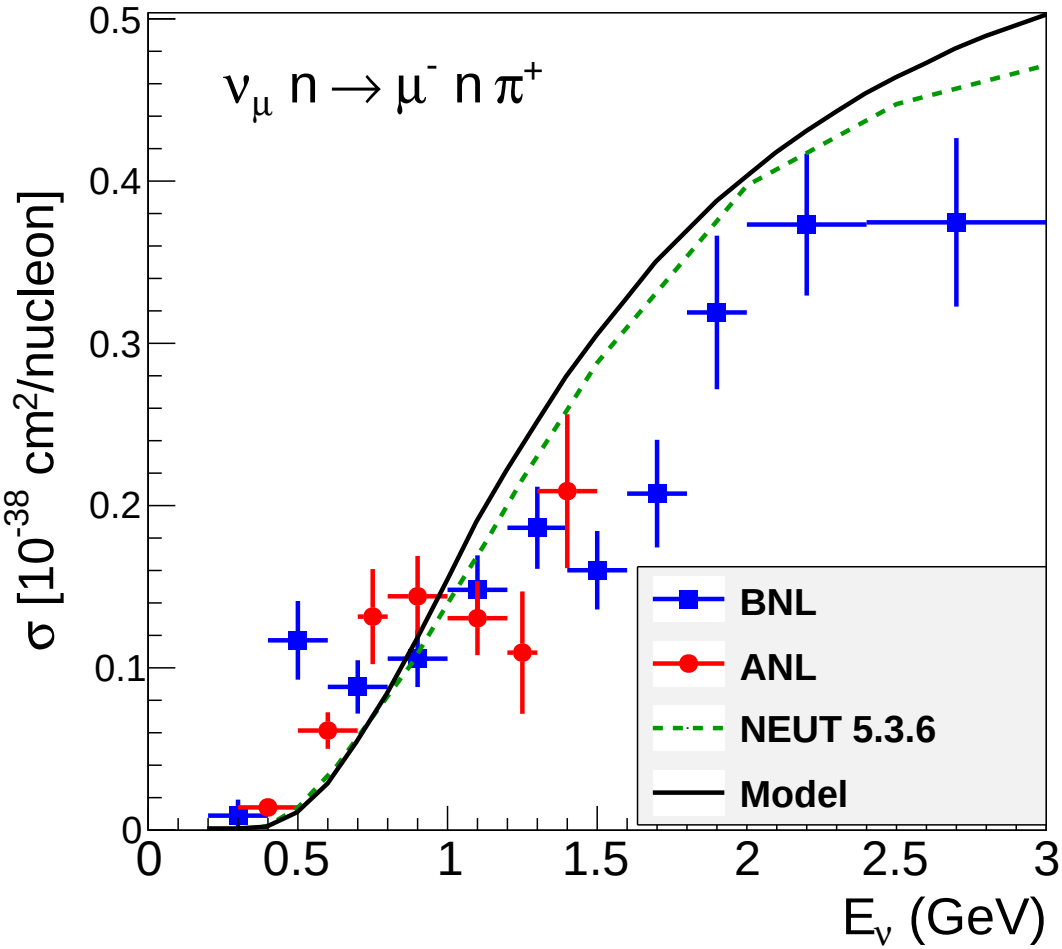

Back Total cross-section with invariant mass cut $W < 2$ GeV, curves are predicted cross sections by the model (solid black) and NEUT 5.3.6 (dashed green), with an invariant mass cut $W < 2$ GeV.

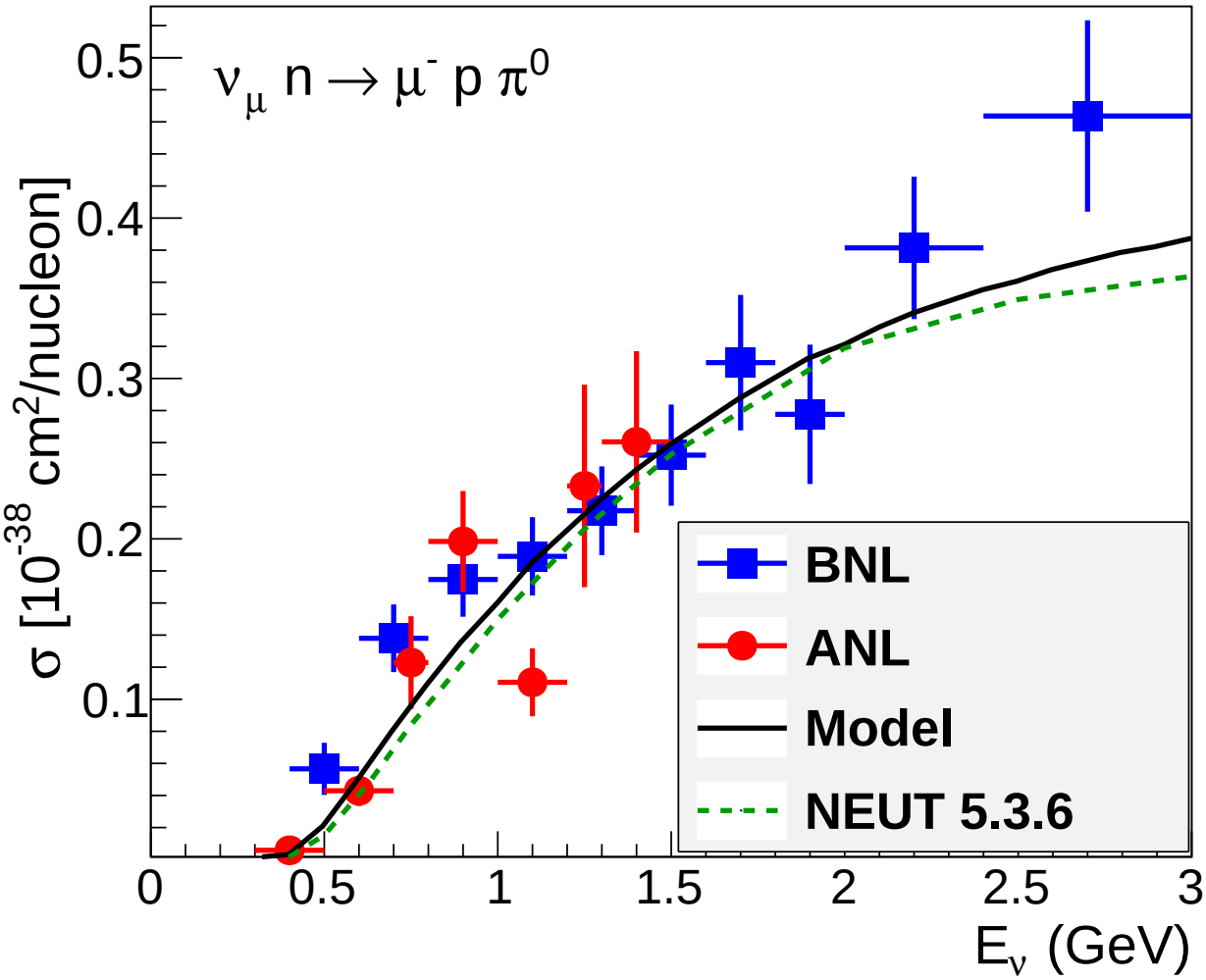

Back Total cross-section with invariant mass cut $W < 2$ GeV, curves are predicted cross sections by the model (solid black) and NEUT 5.3.6 (dashed green), with an invariant mass cut $W < 2$ GeV.

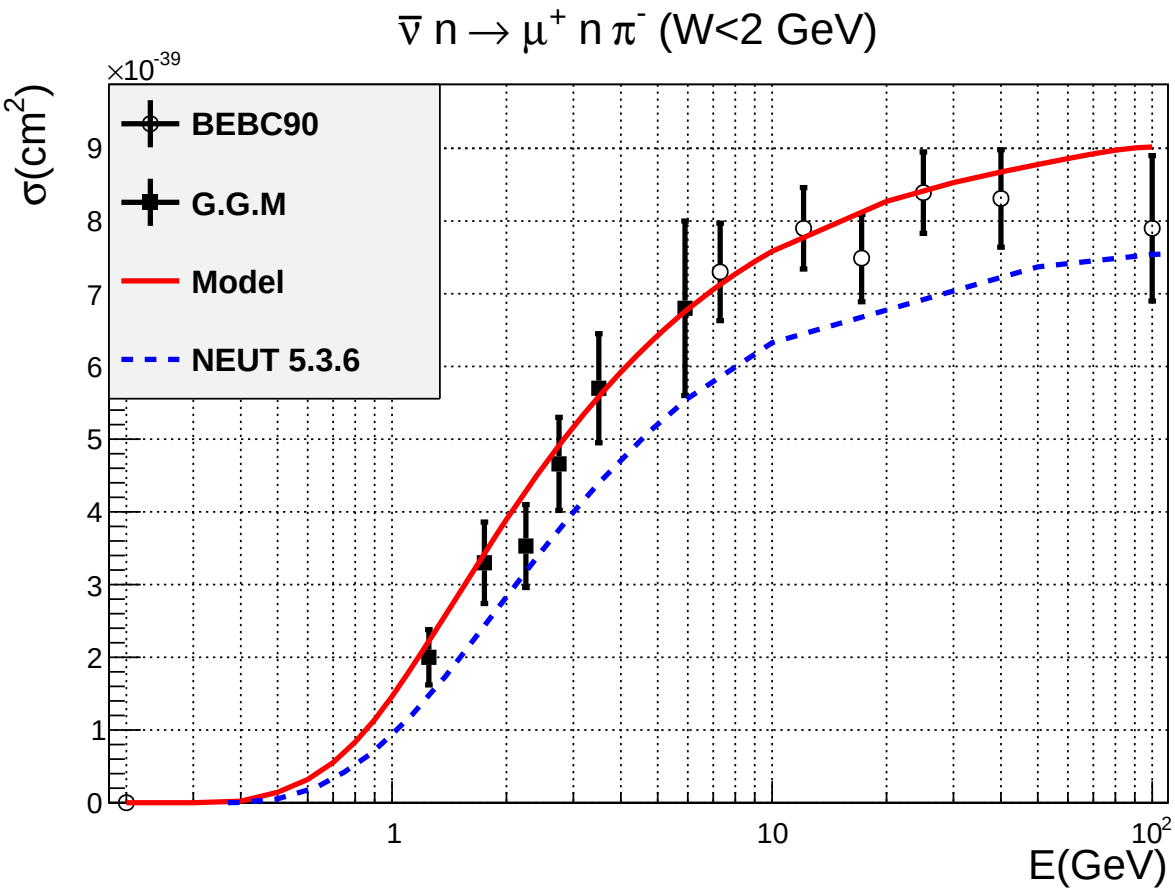

Back Total cross-section with invariant mass cut $W < 2$ GeV, curves are predicted cross sections by the model (solid black) and NEUT 5.3.6 (dashed green), with an invariant mass cut $W < 2$ GeV.

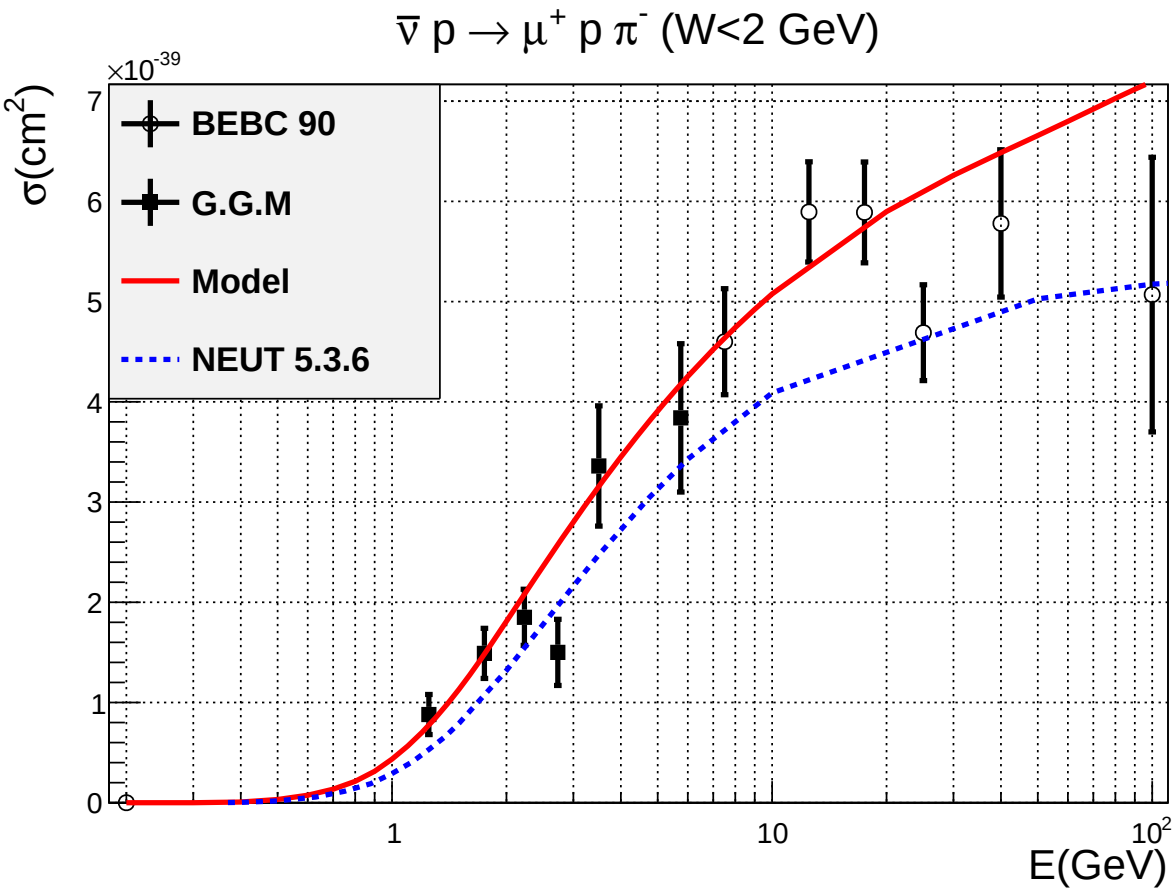

Back Total cross-section with invariant mass cut $W < 2$ GeV, curves are predicted cross sections by the model (solid black) and NEUT 5.3.6 (dashed green), with an invariant mass cut $W < 2$ GeV.

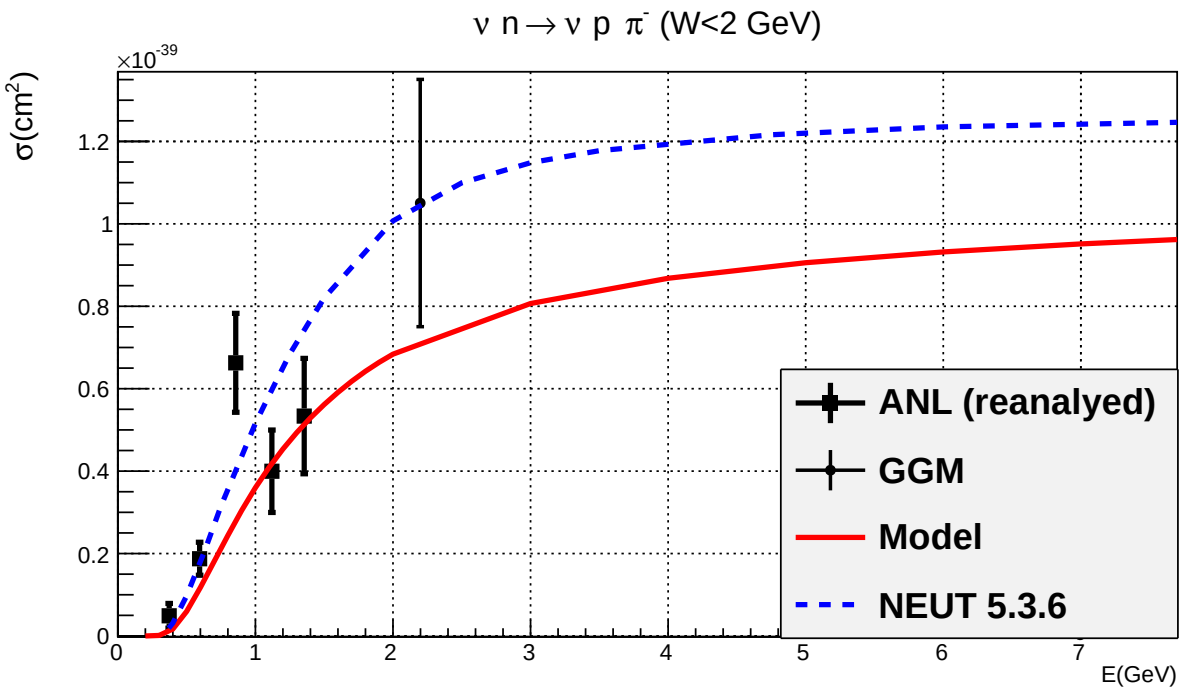

Back Total cross-section with invariant mass cut $W < 2$ GeV, curves are predicted cross sections by the model (solid black) and NEUT 5.3.6 (dashed green), with an invariant mass cut $W < 2$ GeV.

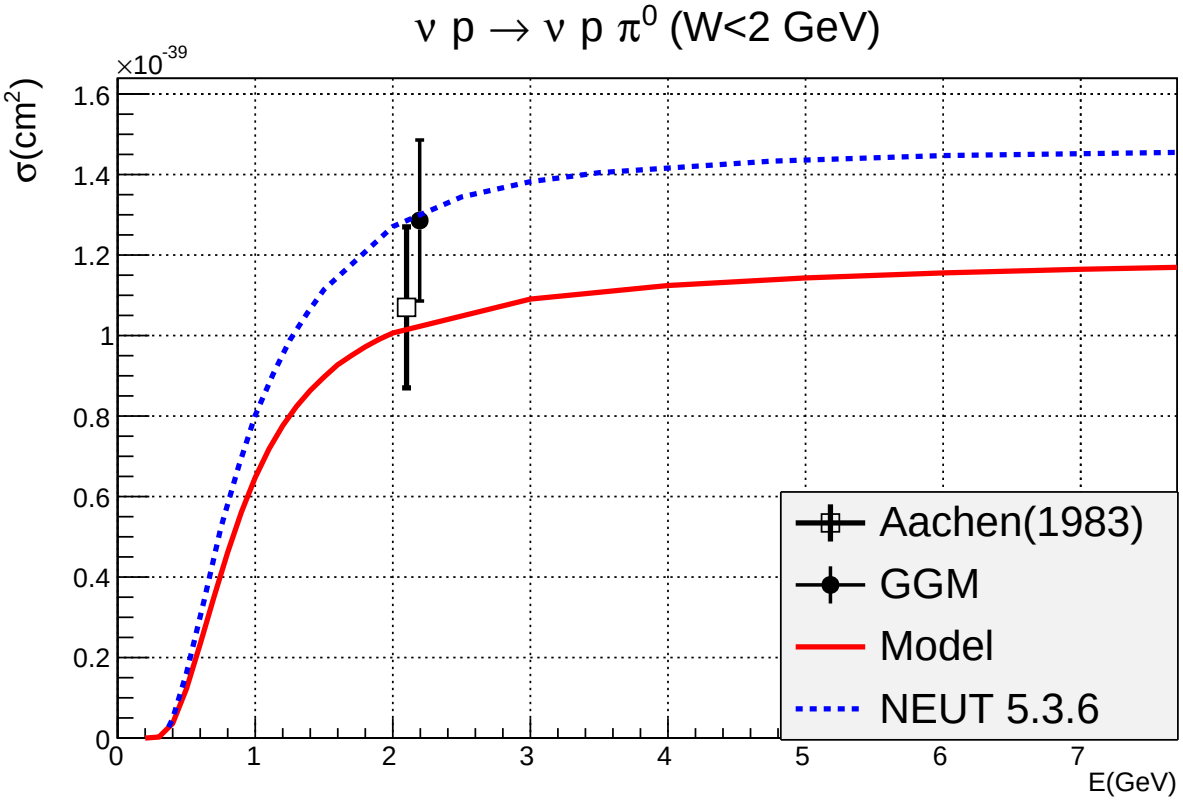

Back Total cross-section with invariant mass cut $W < 2$ GeV, curves are predicted cross sections by the model (solid black) and NEUT 5.3.6 (dashed green), with an invariant mass cut $W < 2$ GeV.

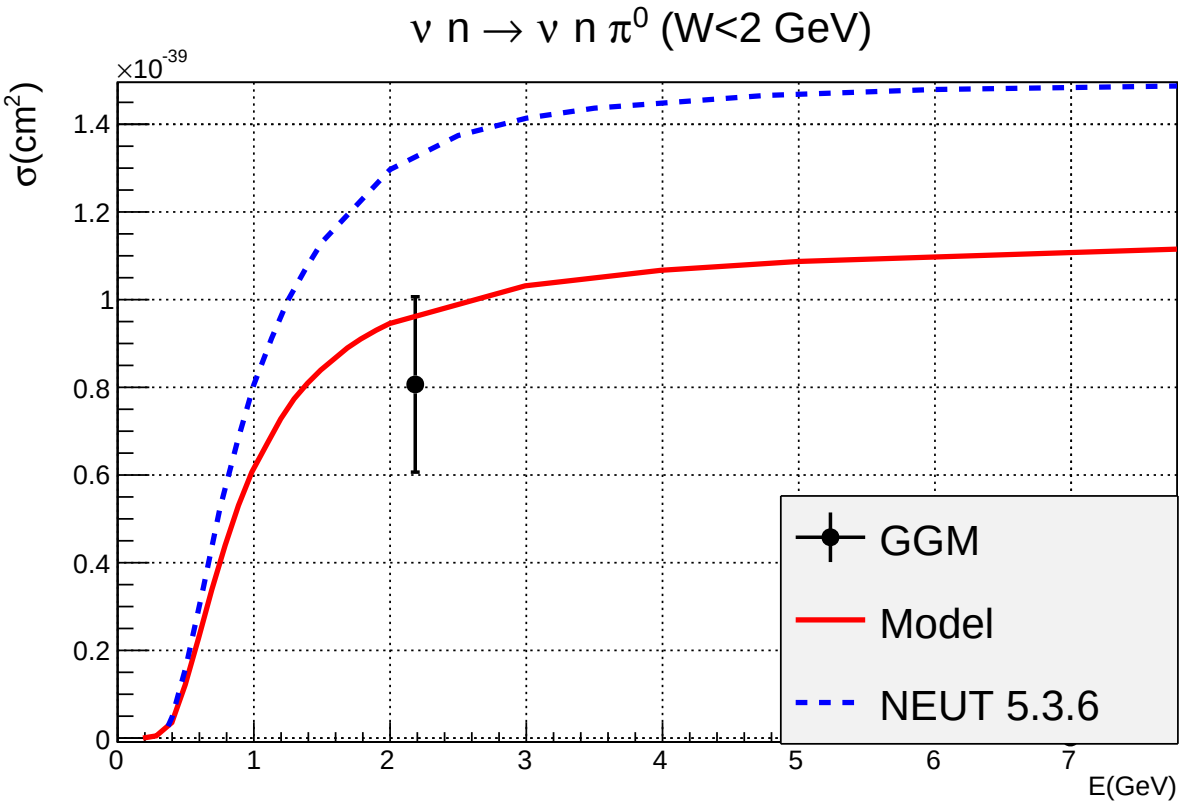

Back Total cross-section with invariant mass cut $W < 2$ GeV, curves are predicted cross sections by the model (solid black) and NEUT 5.3.6 (dashed green), with an invariant mass cut $W < 2$ GeV.

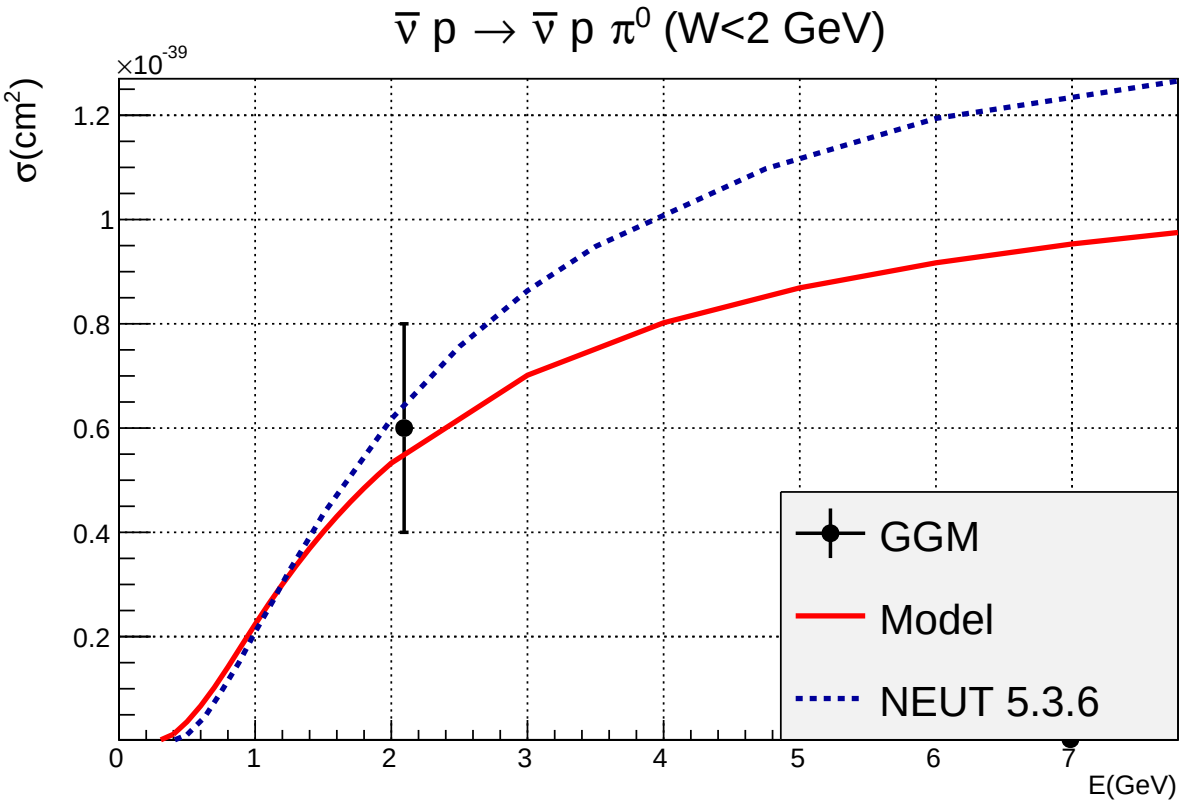

Back Total cross-section with invariant mass cut $W < 2$ GeV, curves are predicted cross sections by the model (solid black) and NEUT 5.3.6 (dashed green), with an invariant mass cut $W < 2$ GeV.

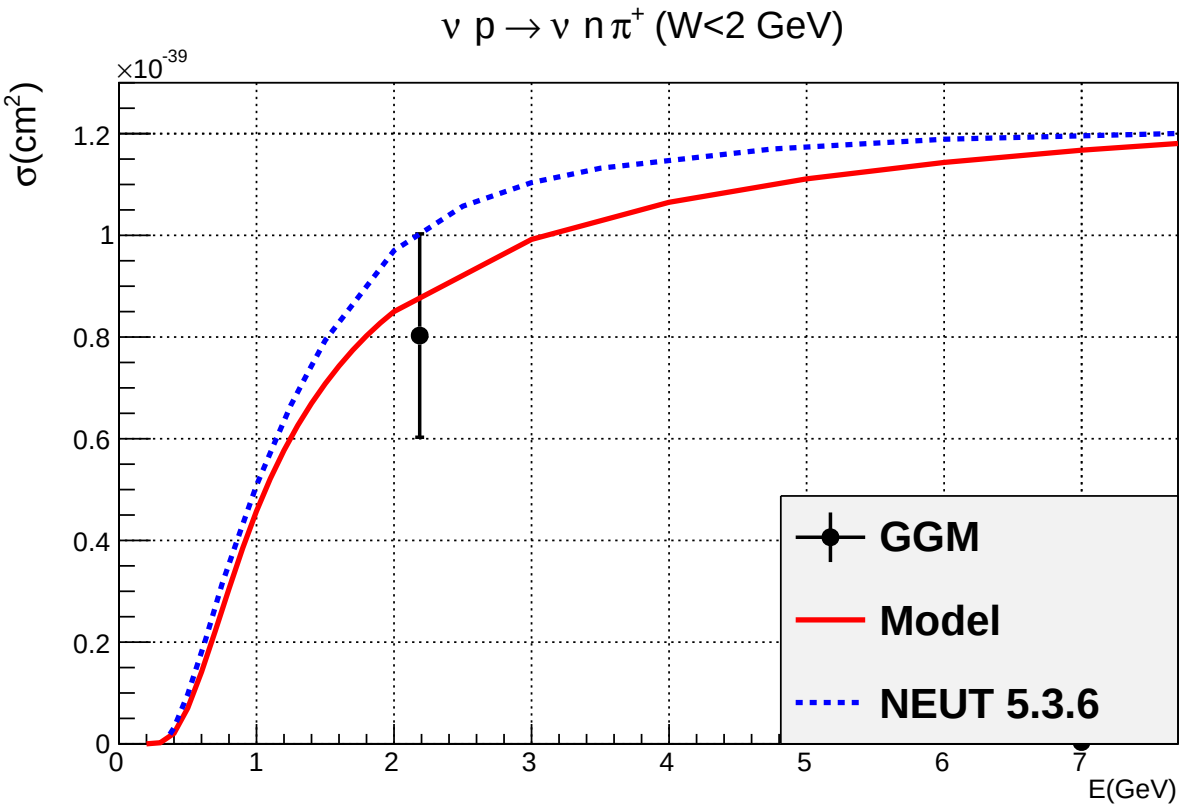

Back Total cross-section with invariant mass cut $W < 2$ GeV, curves are predicted cross sections by the model (solid black) and NEUT 5.3.6 (dashed green), with an invariant mass cut $W < 2$ GeV.

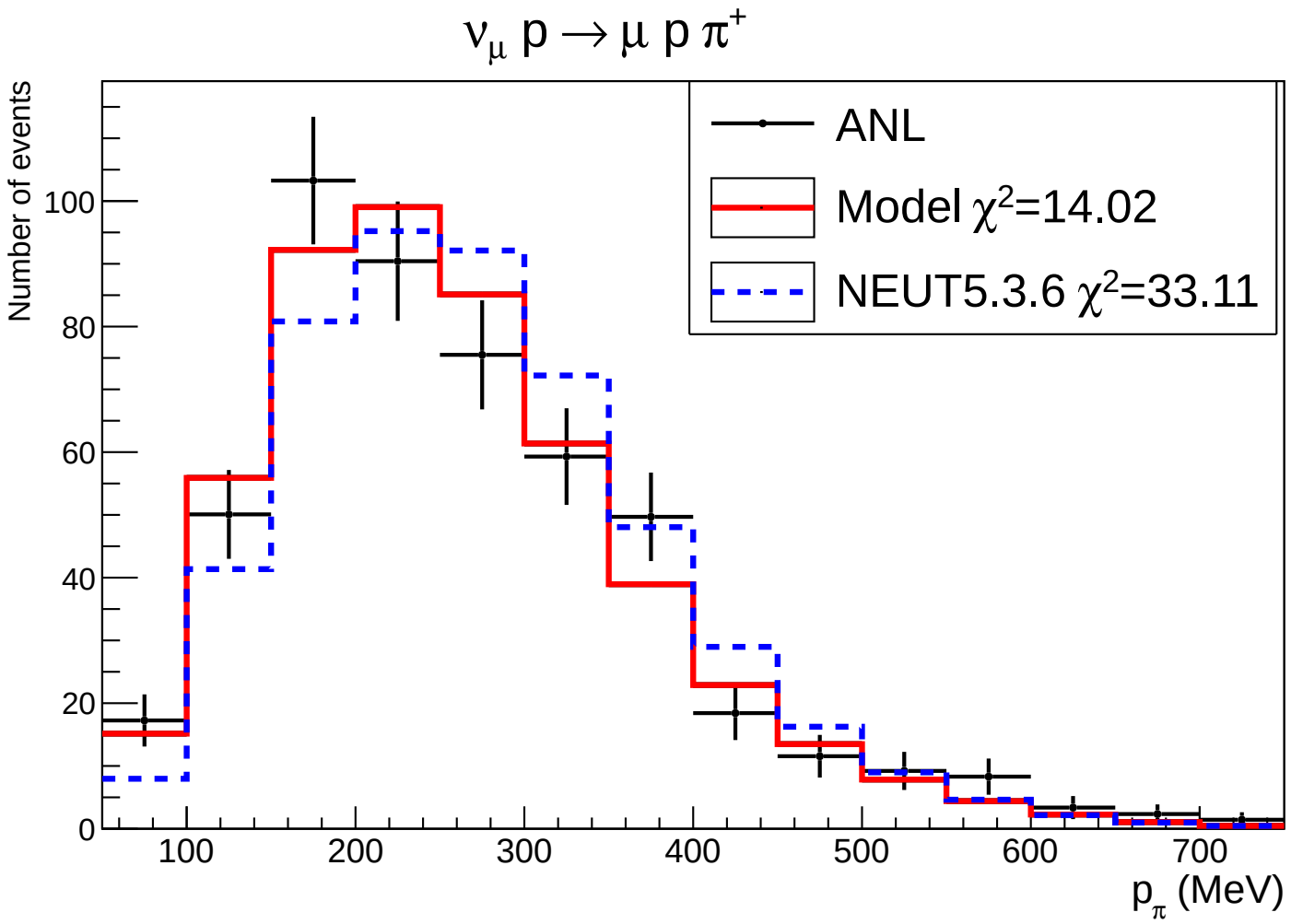

Back Pion momentum distribution from ANL [39]. Model (solid red) and RS model (dashed blue) predictions of flux-averaged p_π-differential cross sections (with $W < 2$ GeV cut) are normalized to data.

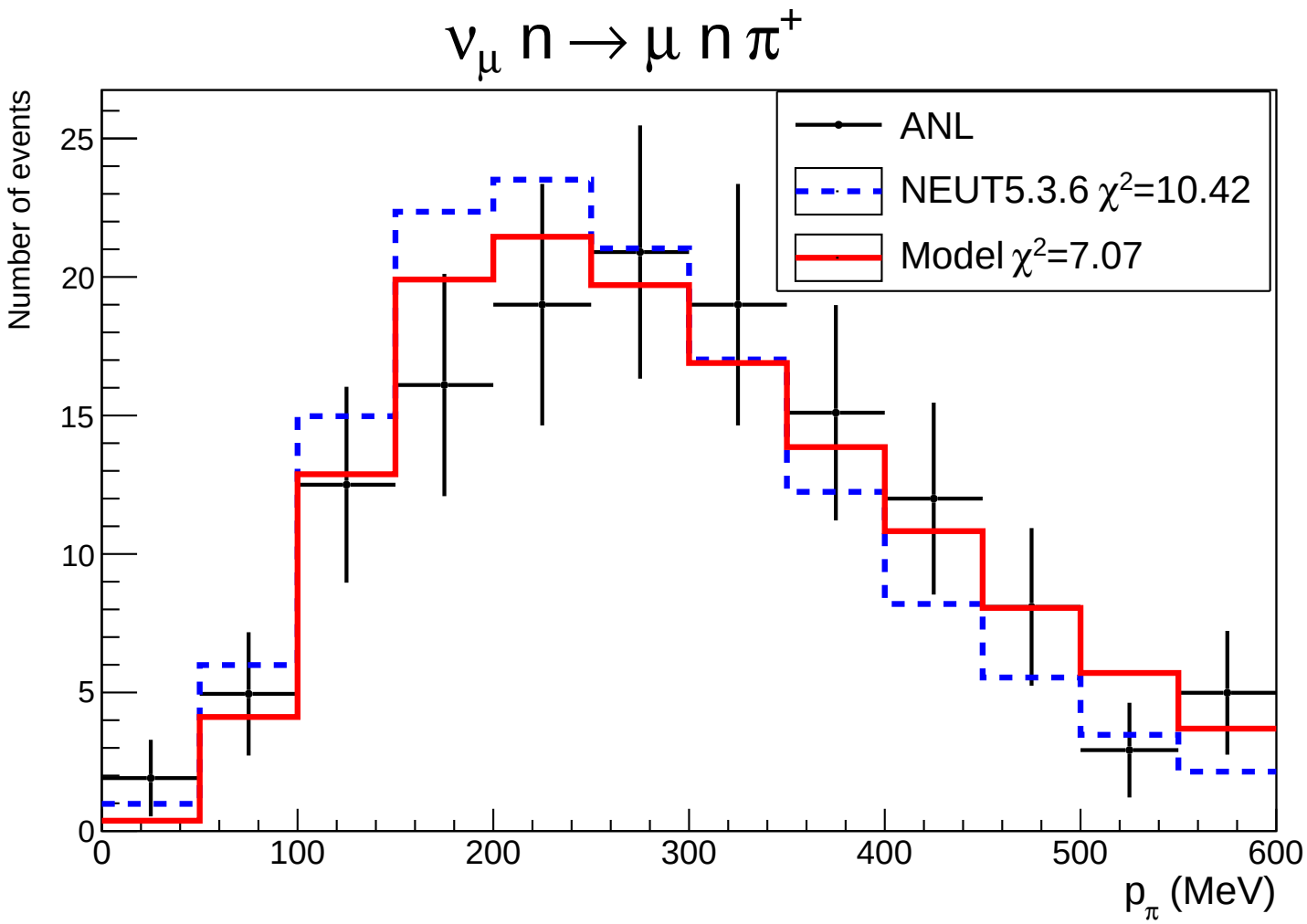

Back Pion momentum distribution from ANL [39]. Model (solid red) and RS model (dashed blue) predictions of flux-averaged p_π-differential cross sections (with $W < 2$ GeV cut) are normalized to data.

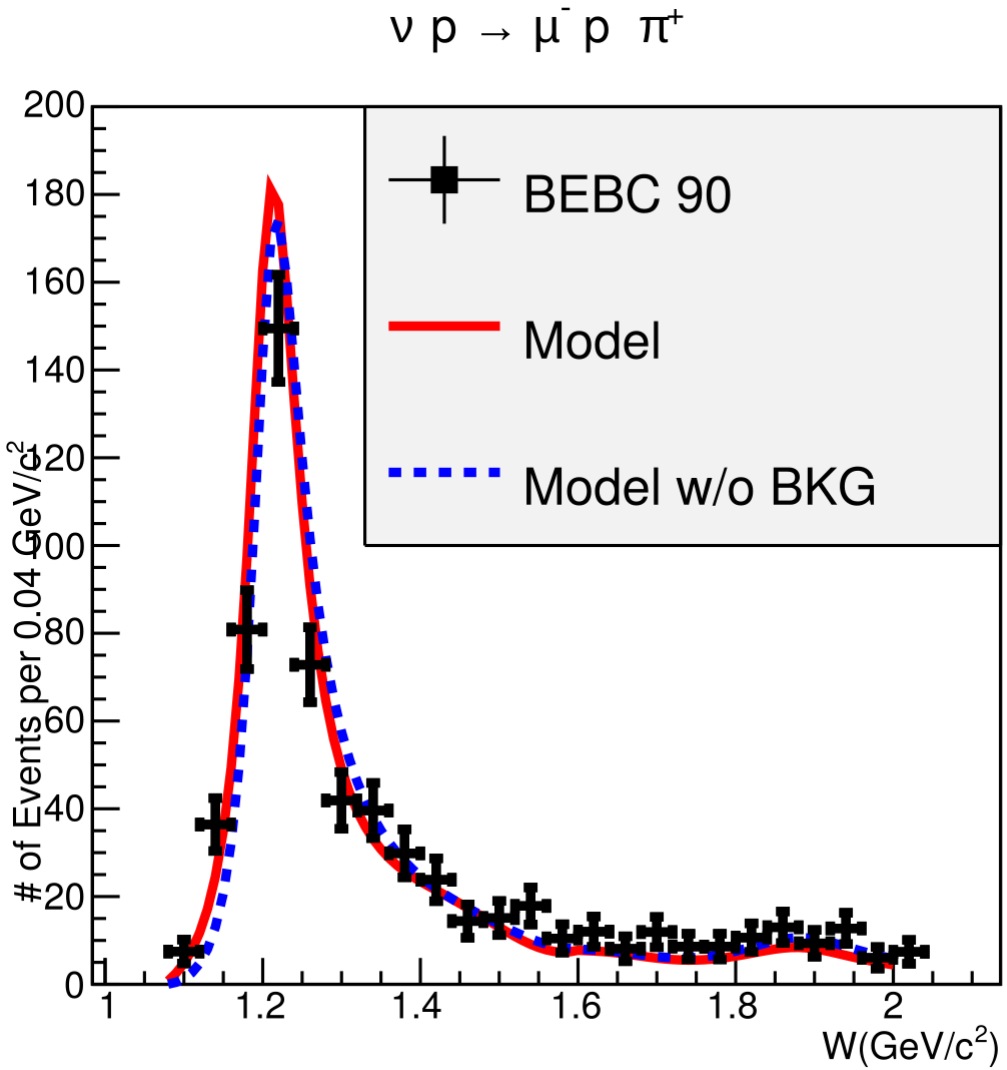

Back W distribution from Ref. [24]. Curves are the model predictions with (solid red) and without (dashed blue) background.

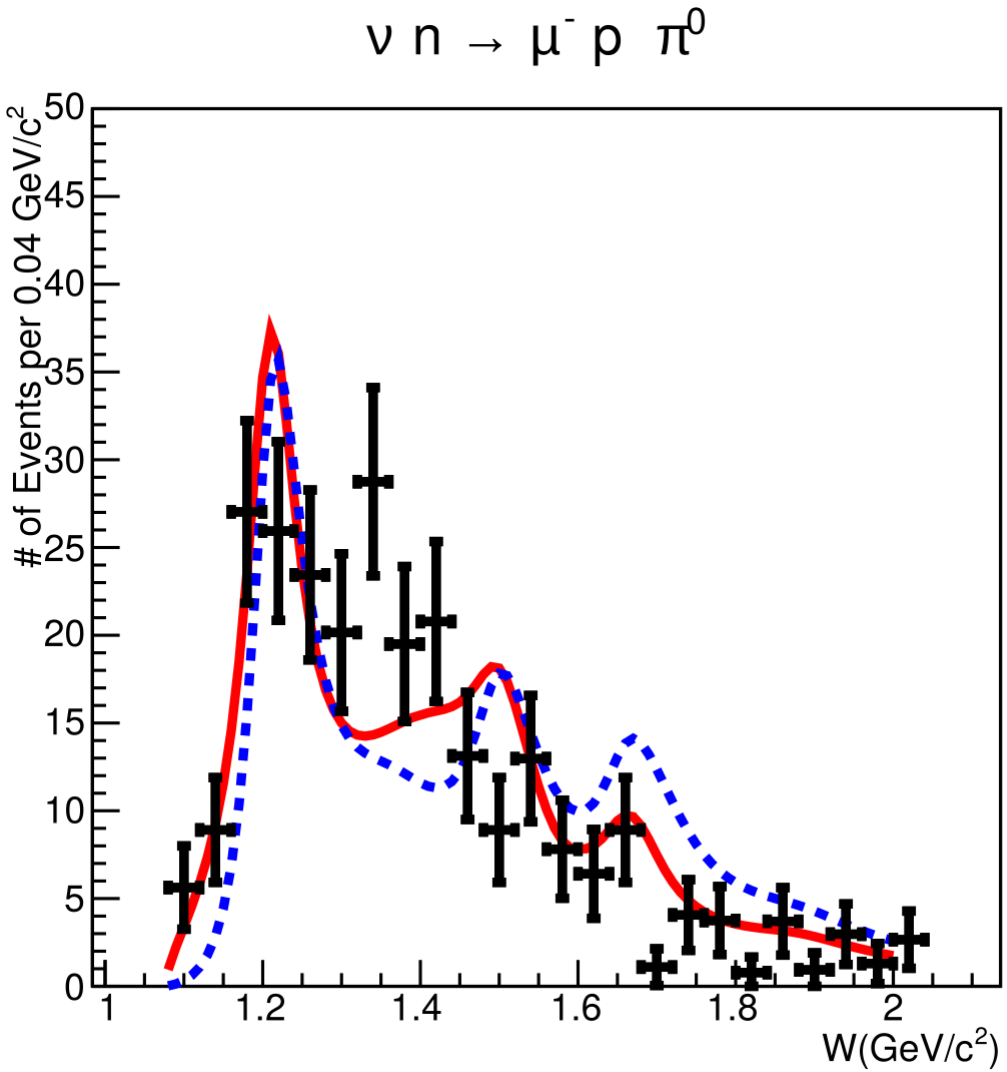

Back W distribution from Ref. [24]. Curves are the model predictions with (solid red) and without (dashed blue) background.

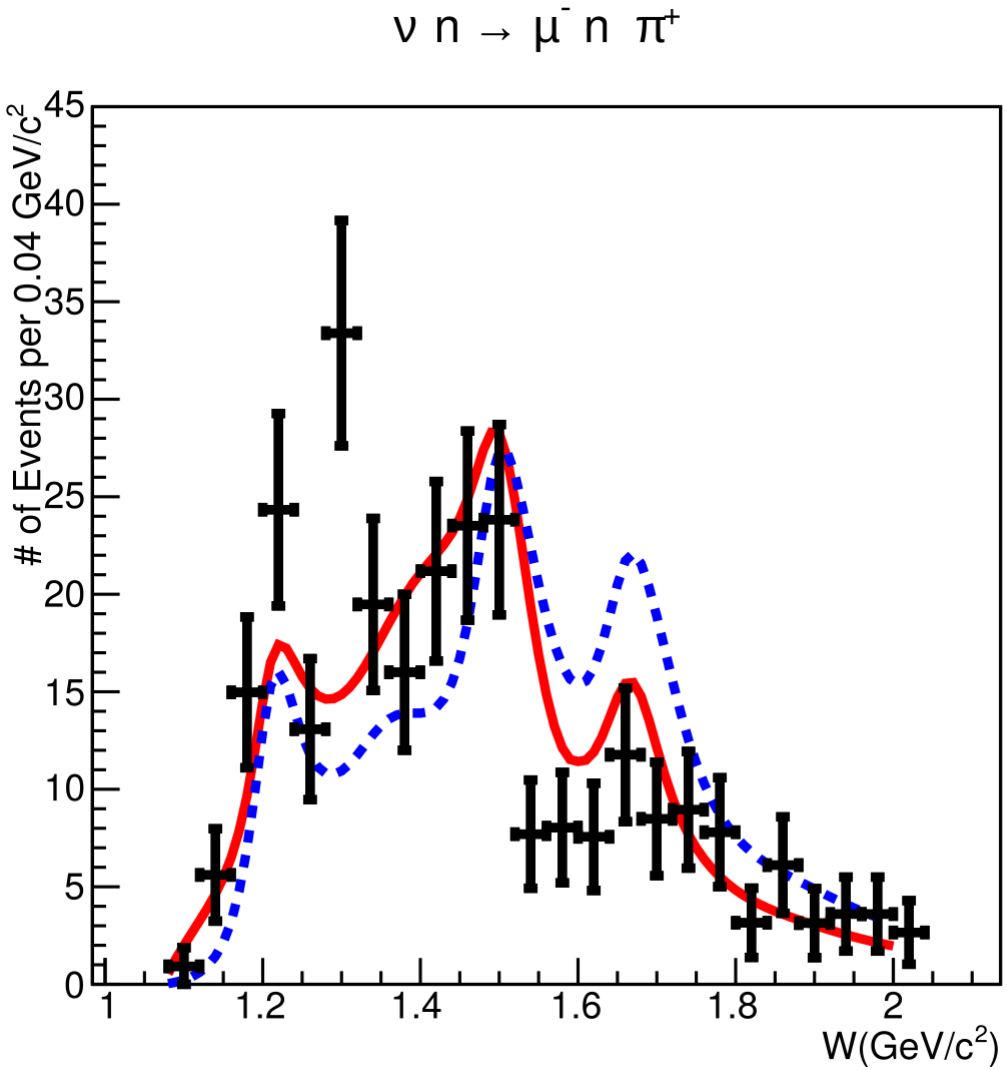

Back W distribution from Ref. [24]. Curves are the model predictions with (solid red) and without (dashed blue) background.

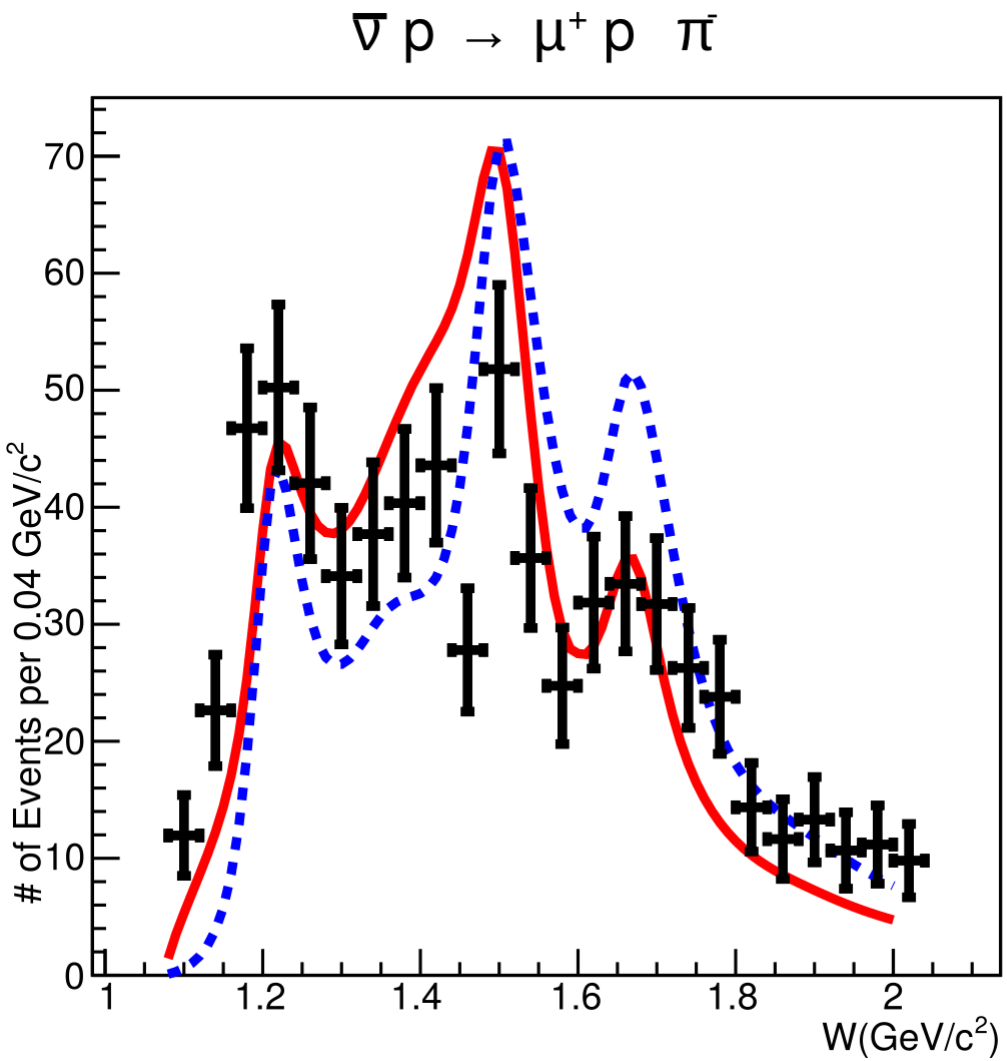

Back W distribution from Ref. [24]. Curves are the model predictions with (solid red) and without (dashed blue) background.

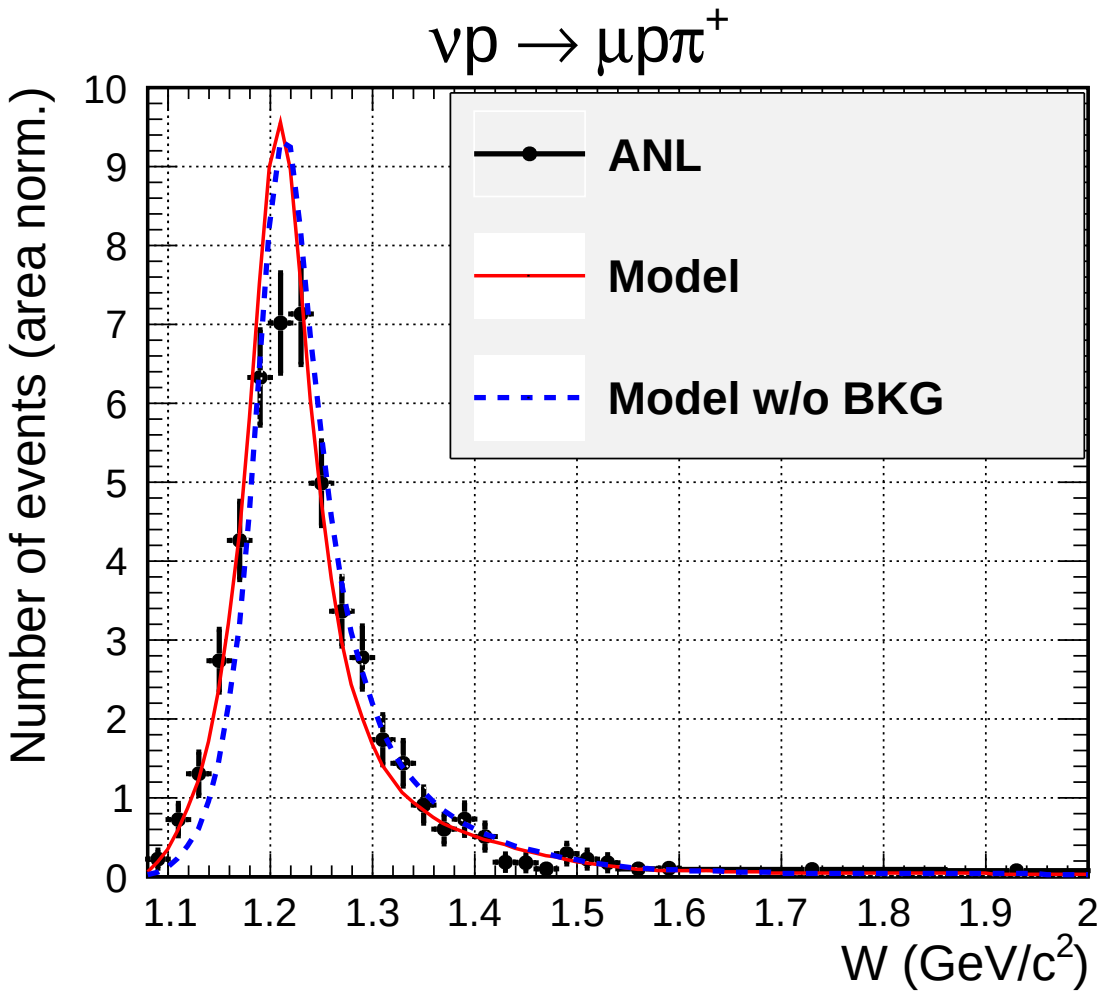

Back W distribution from Ref. [6]. Curves are the model predictions with (solid red) and without (dashed blue) background.

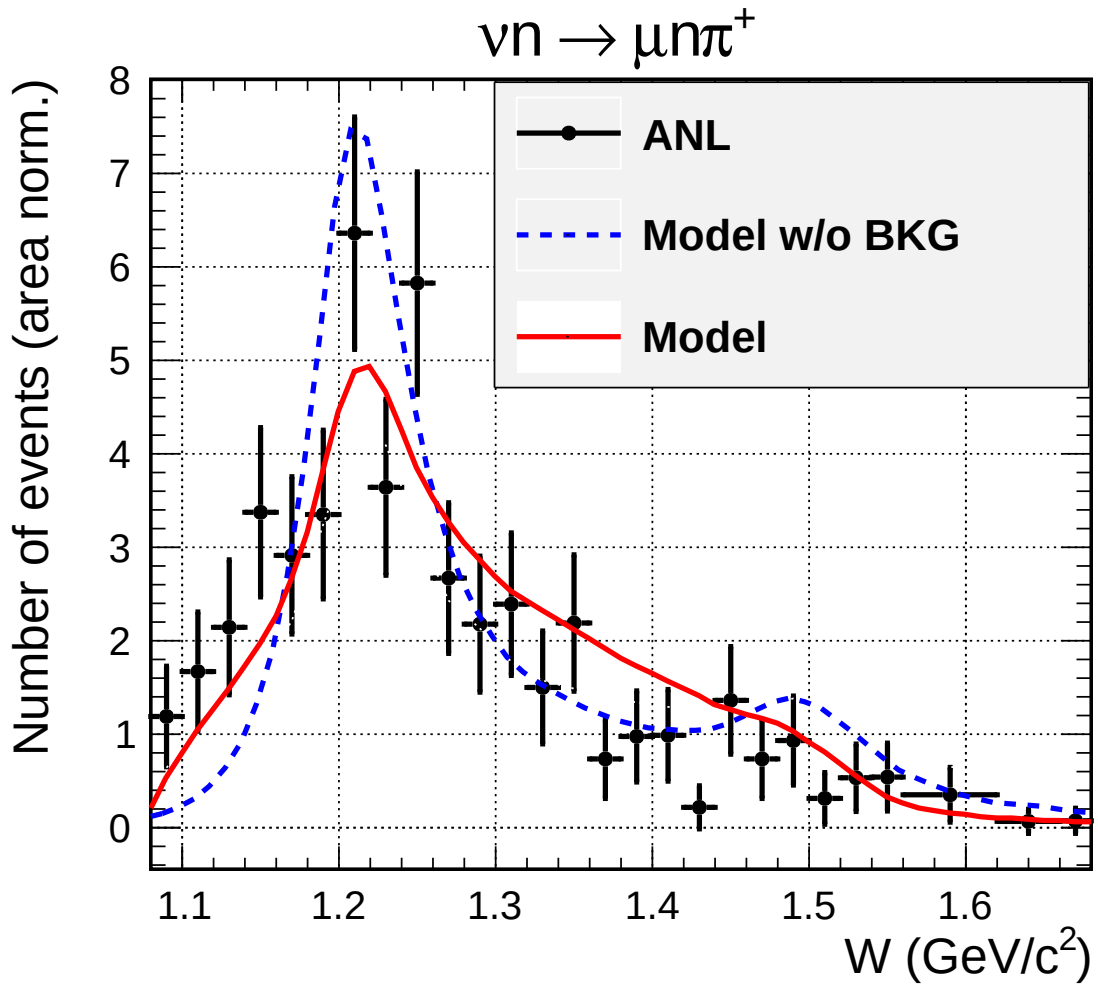

Back W distribution from Ref. [6]. Curves are the model predictions with (solid red) and without (dashed blue) background.

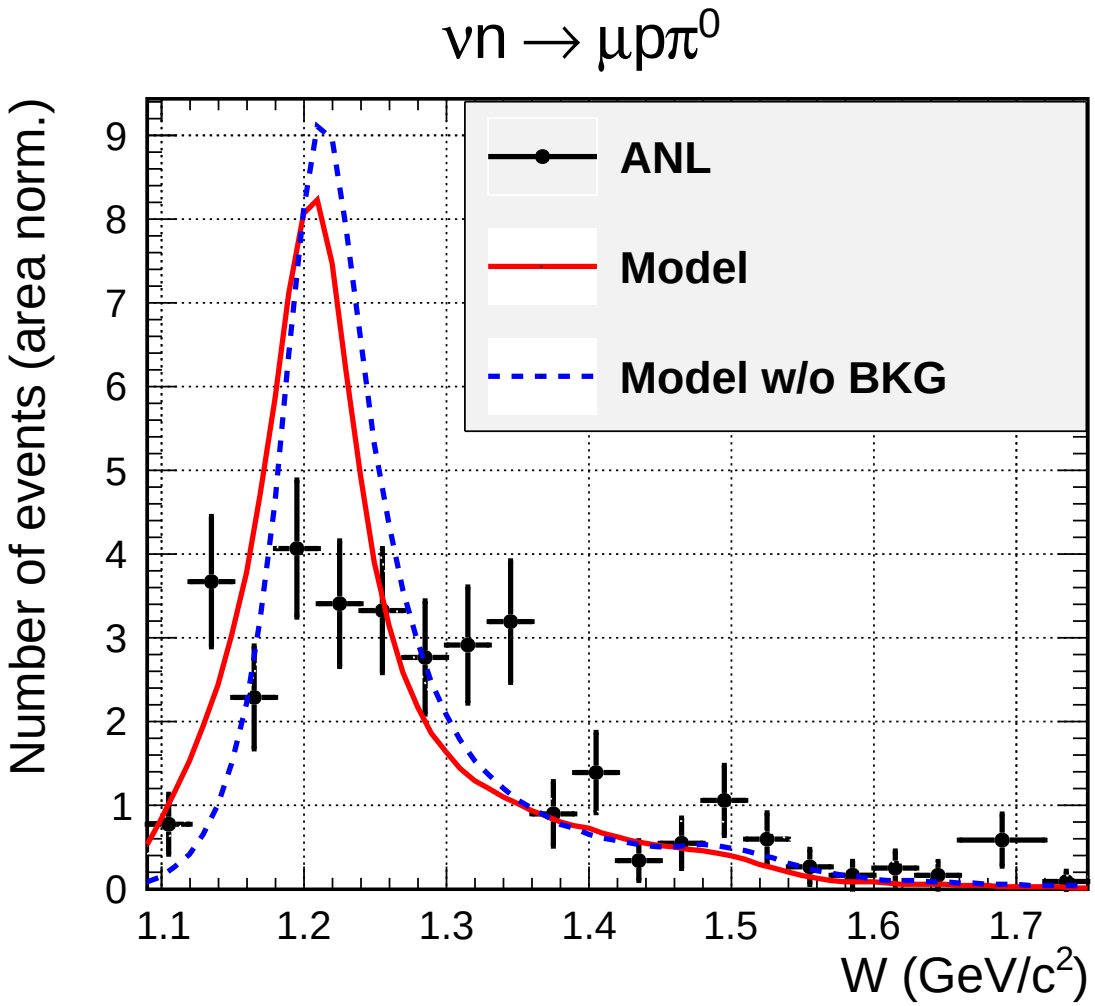

Back W distribution from Ref. [6]. Curves are the model predictions with (solid red) and without (dashed blue) background.

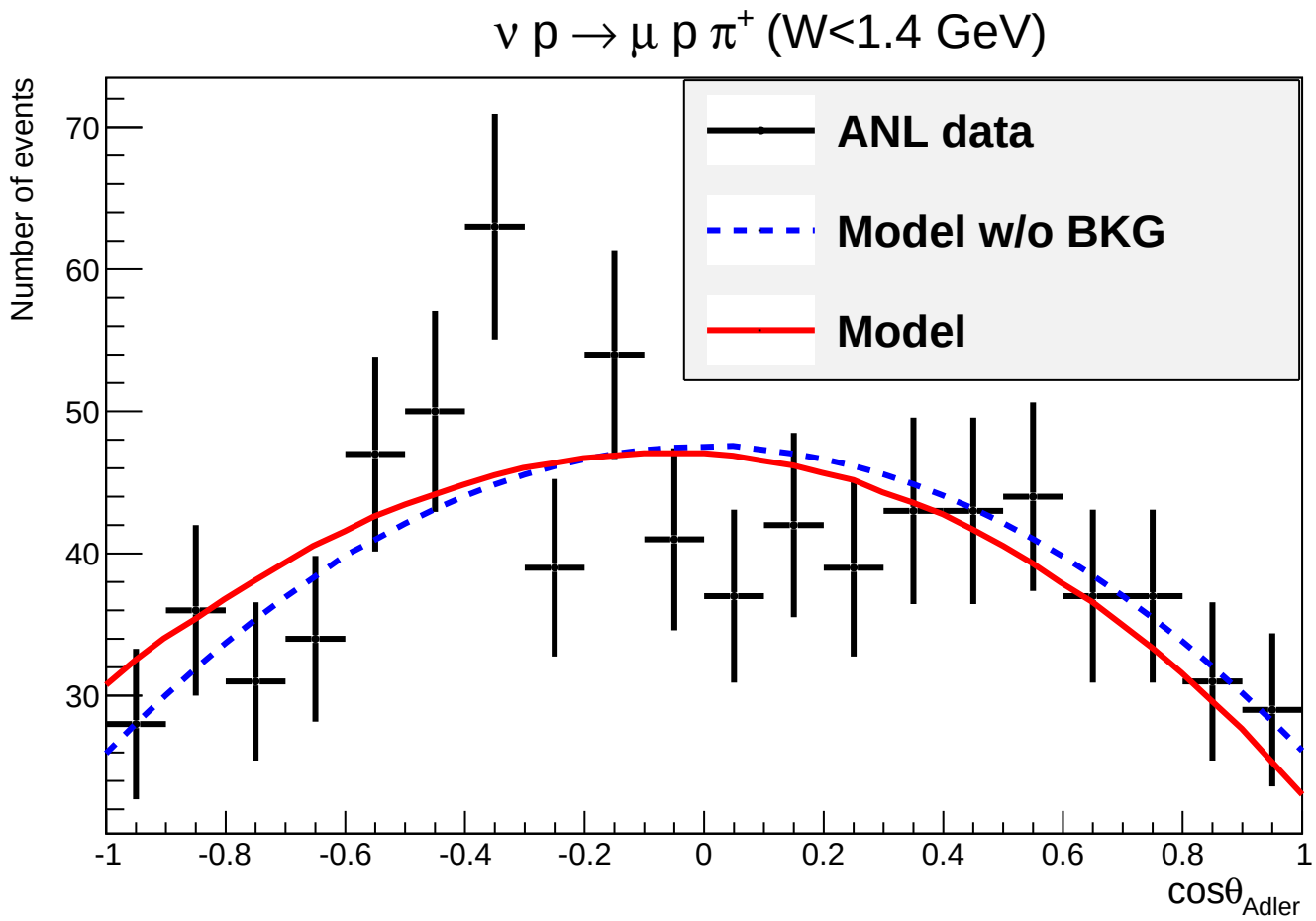

Back Event distribution in the pion polar angle for ANL with invariant mass cut, $W < 1.4$ GeV, from Refs. [6]. Curves are flux-averaged, area-normalized prediction of the model (solid red) and the model without background (dashed blue).

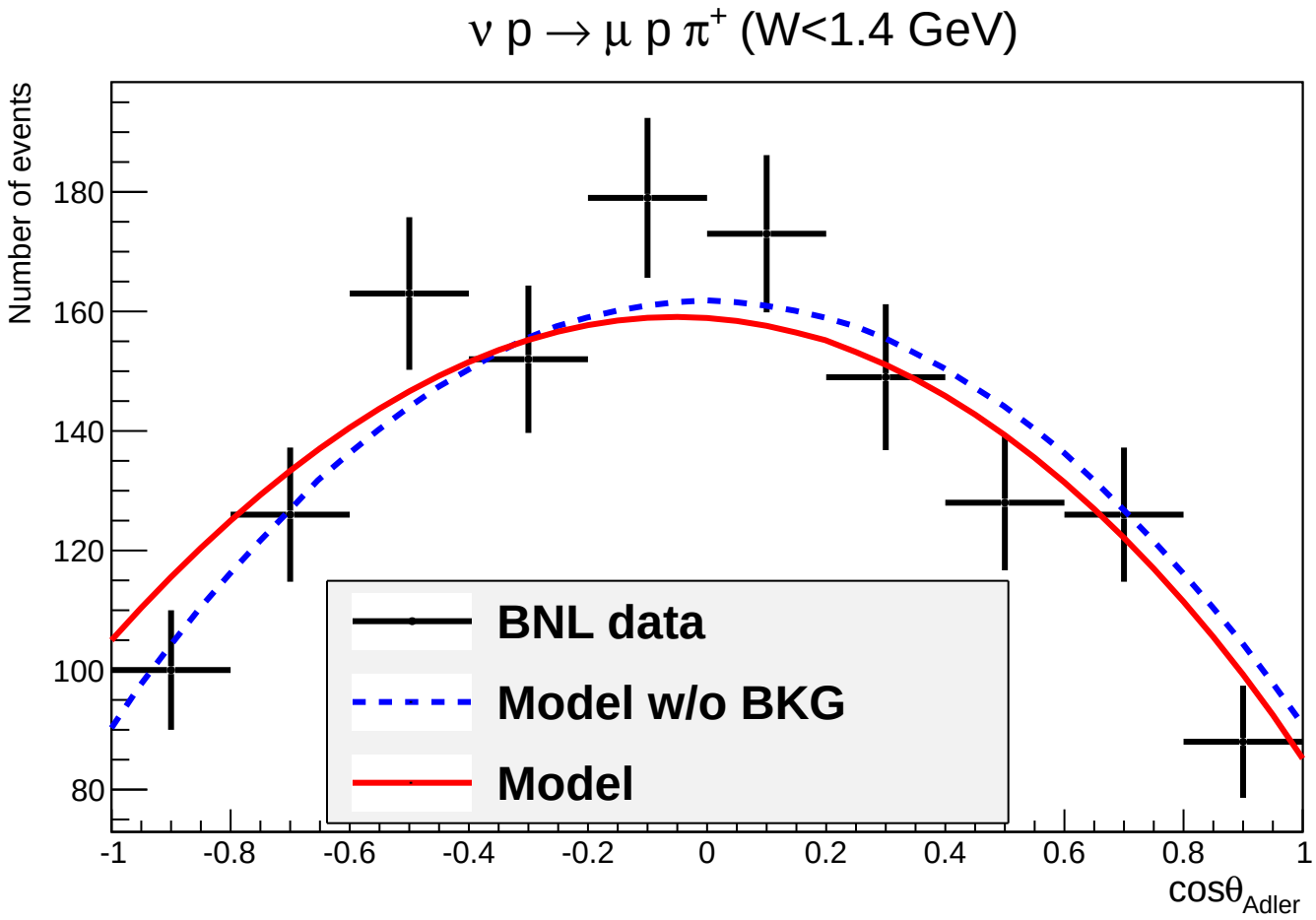

Back Event distribution in the pion polar angle for BNL with invariant mass cut, $W < 1.4$ GeV, from Refs. [11]. Curves are flux-averaged, area-normalized prediction of the model (solid red) and the model without background (dashed blue).

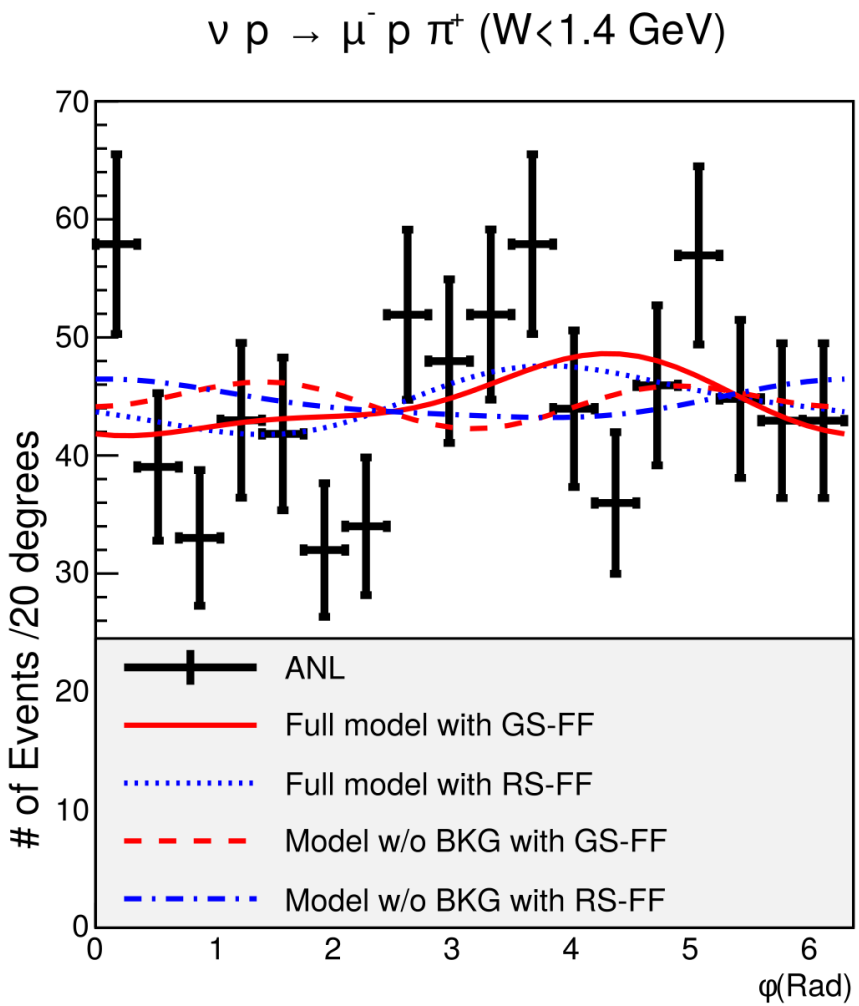

Back ANL distribution of events in the pion azimuthal angle in the πN rest frame with $W < 1.4$ GeV for the $\mu^- p \pi^+$ final state. Curves are flux-averaged, area-normalized prediction of the model for $d\sigma/d\phi$.

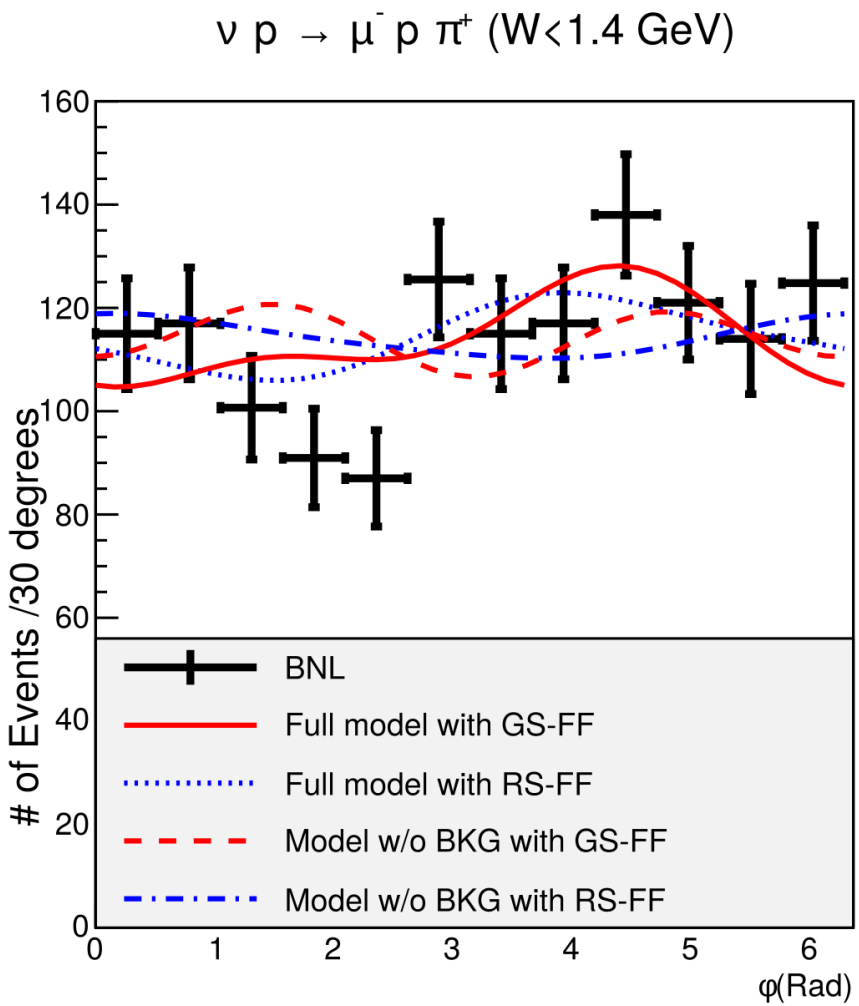

Back BNL distribution of events in the pion azimuthal angle in the πN rest frame with $W < 1.4 GeV$ GeV for the $\mu^- p \pi^+$ final state. Curves are flux-averaged, area-normalized prediction of the model for $d\sigma/d\phi$.

Backup

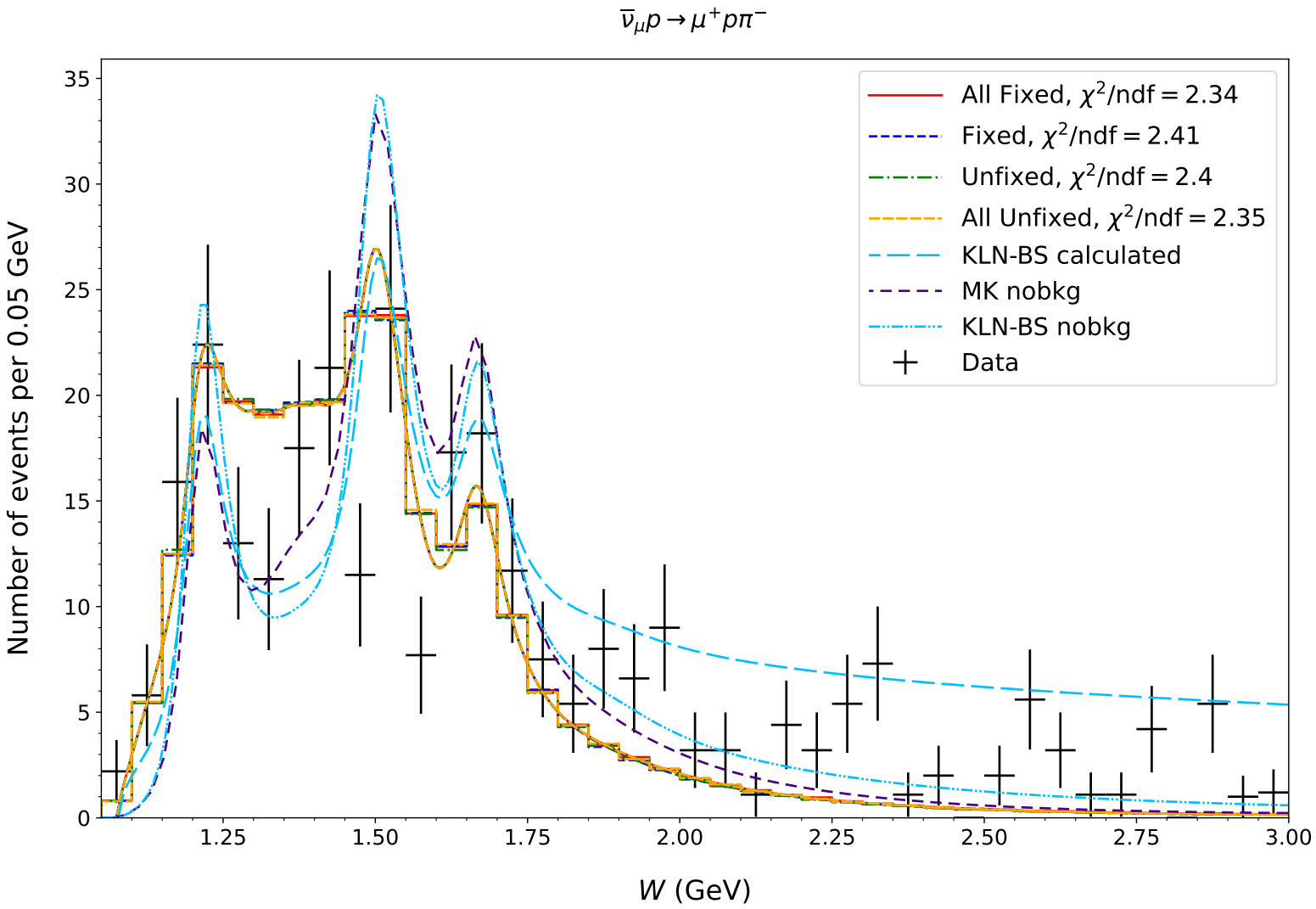

W distribution with no W_{cut}. Neutrino spectrum is restricted by $5.0 < E_\nu < 200.0$ GeV. Model predictions are area-normalized. Predictions with all resonances (All)/without resonance F17(1970) and with fixed and unfixed bugs are shown. Data are taken from Ref. [19]. Only $W < 2.0$ GeV used for area renormalization calculation. Neutrino spectrum is taken from [36].

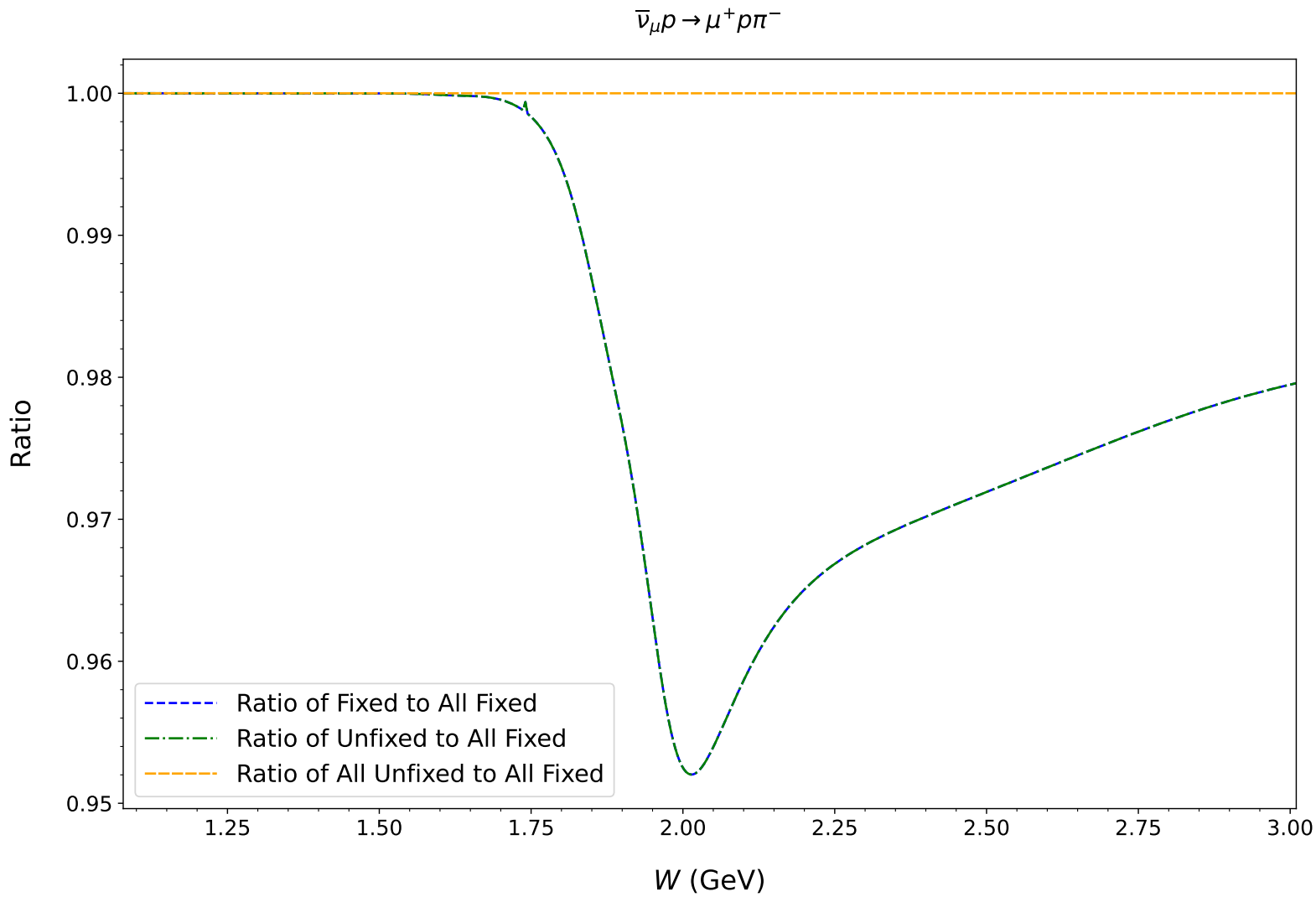

Ratio of $d\sigma/dW$ with no W_{cut}. Neutrino spectrum is restricted by $5.0 < E_\nu < 200.0$ GeV. Data are taken from Ref. [19]. Neutrino spectrum is taken from [36].

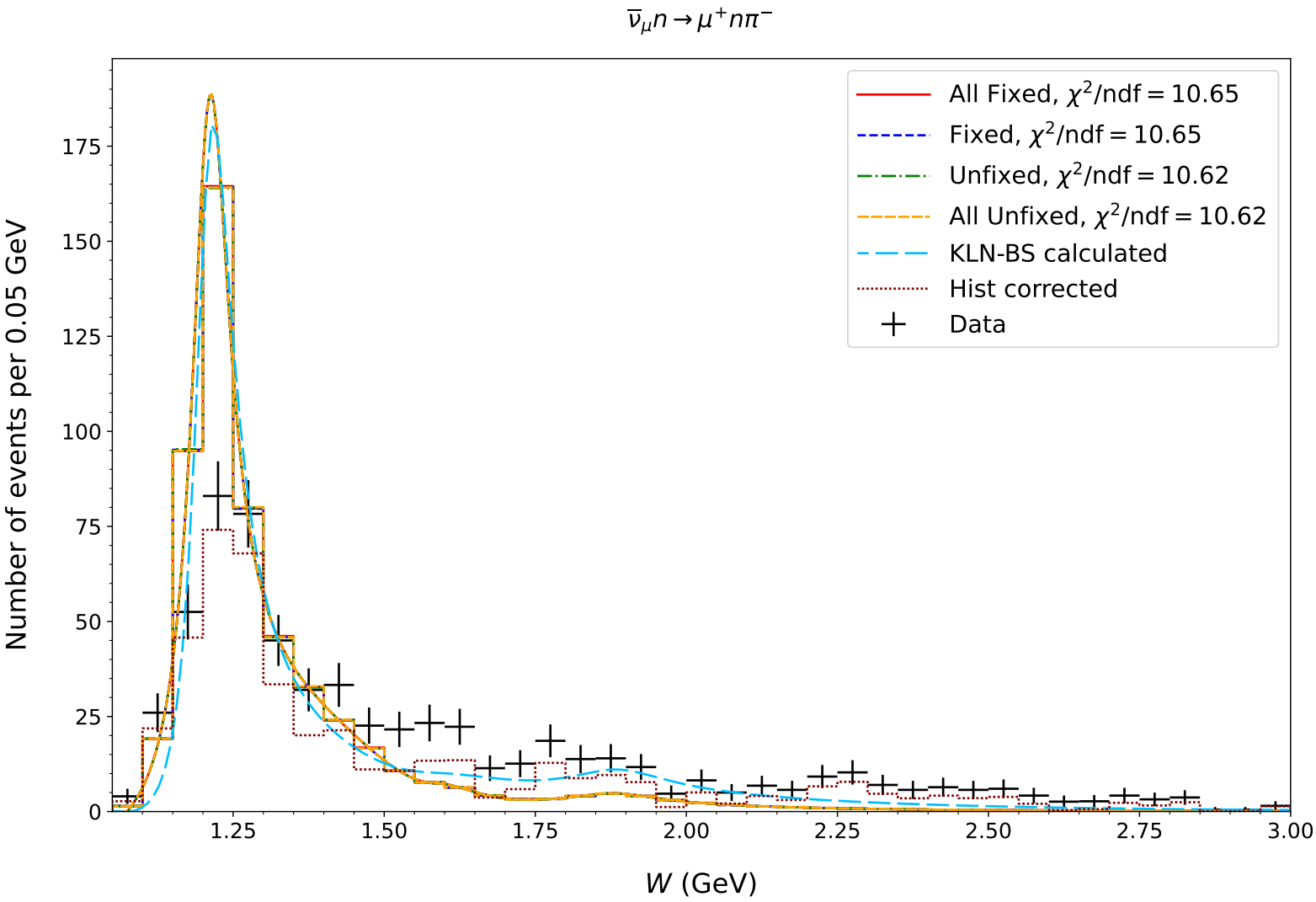

W distribution with no W_{cut}. Neutrino spectrum is restricted by $5.0 < E_\nu < 200.0$ GeV. Model predictions are area-normalized. Predictions with all resonances (All)/without resonance F17(1970) and with fixed and unfixed bugs are shown. Data are taken from Ref. [19]. Only $W < 2.0$ GeV used for area renormalization calculation. Neutrino spectrum is taken from [36].

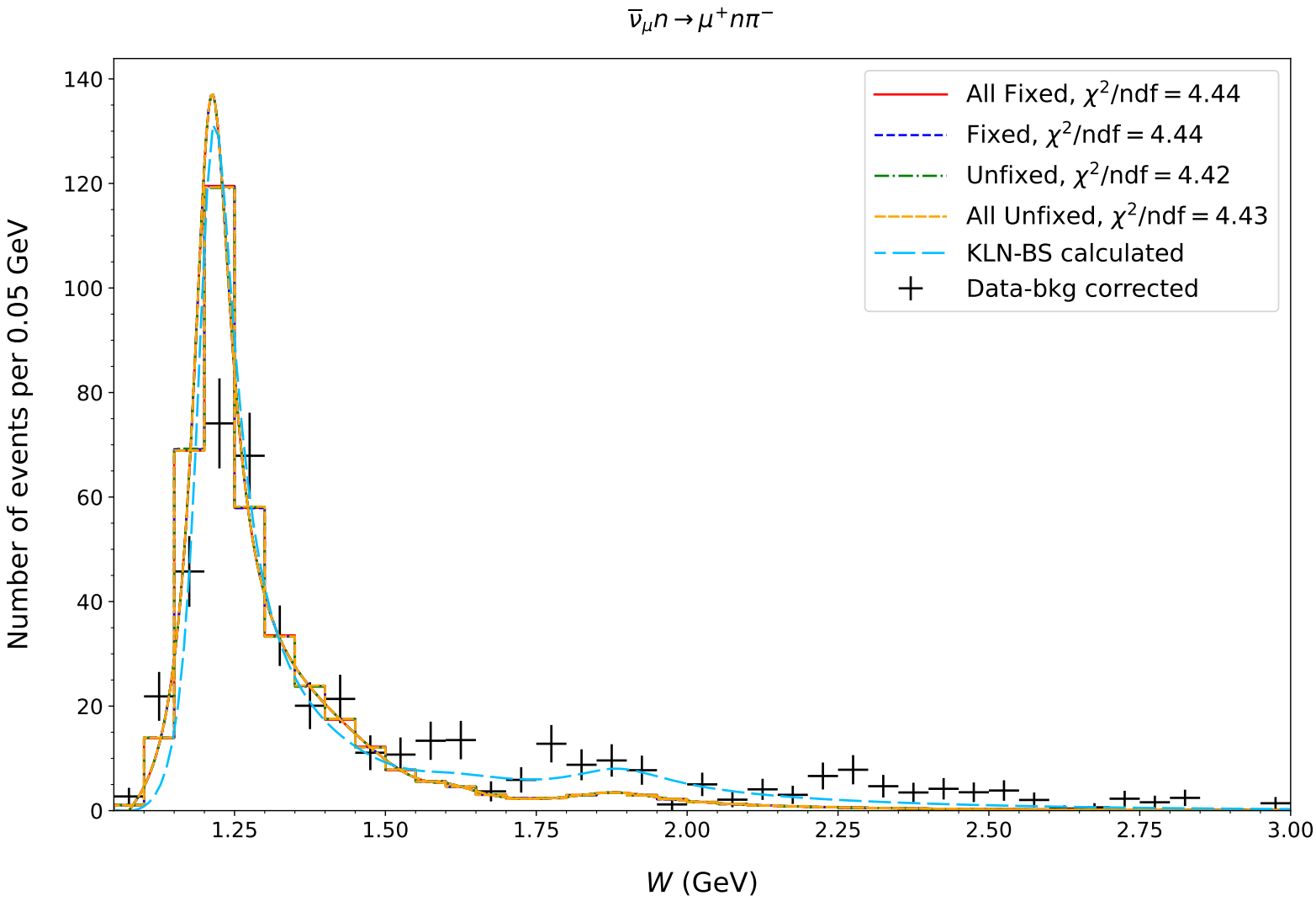

W distribution with no W_{cut}. Neutrino spectrum is restricted by $5.0 < E_\nu < 200.0$ GeV. Model predictions are area-normalized. Predictions with all resonances (All)/without resonance F17(1970) and with fixed and unfixed bugs are shown. Data are taken from Ref. [19]. Only $W < 2.0$ GeV used for area renormalization calculation. Neutrino spectrum is taken from [36].

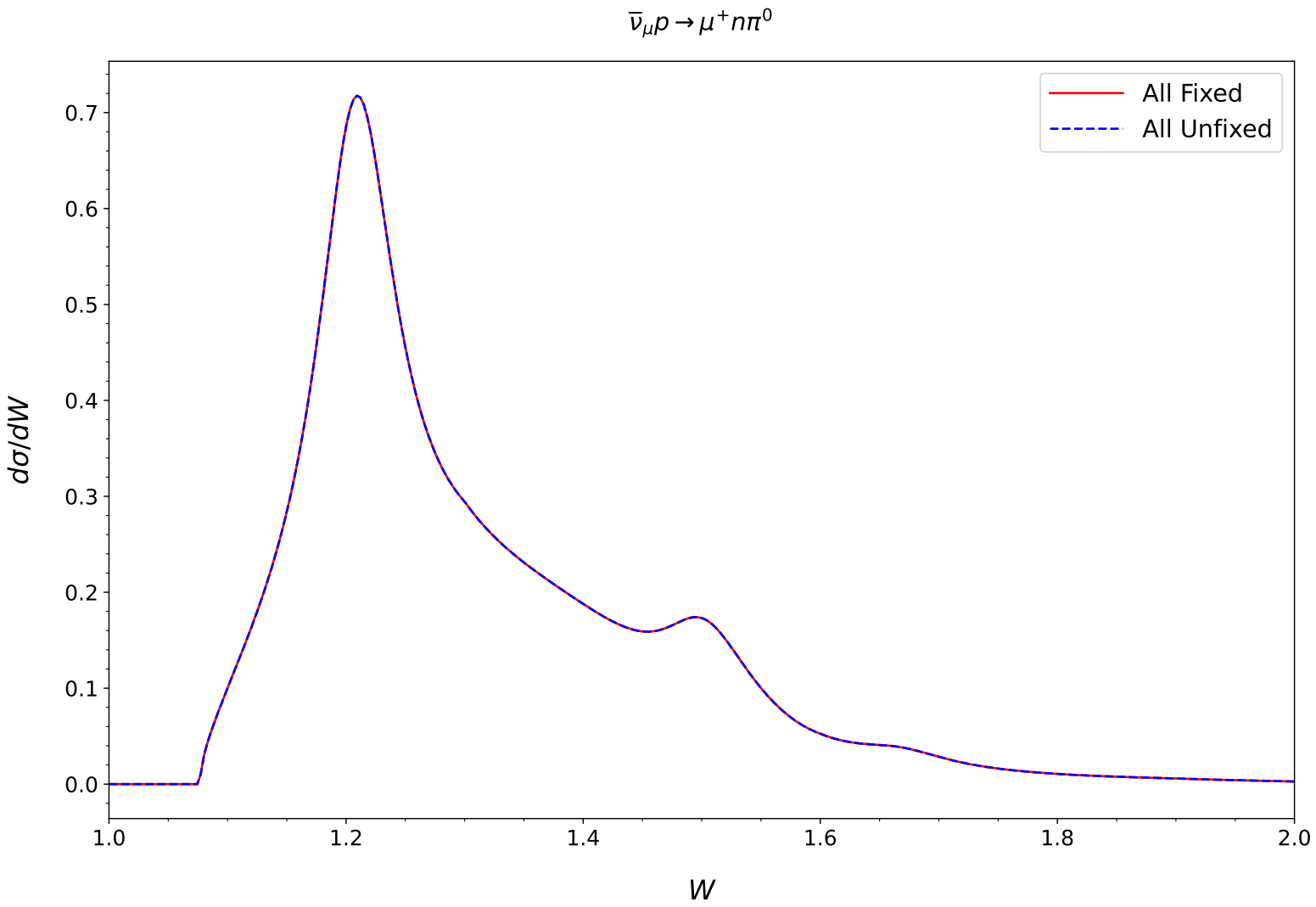

$d\sigma/dW$ with no W_{cut}. Neutrino energy is 2.0 GeV.

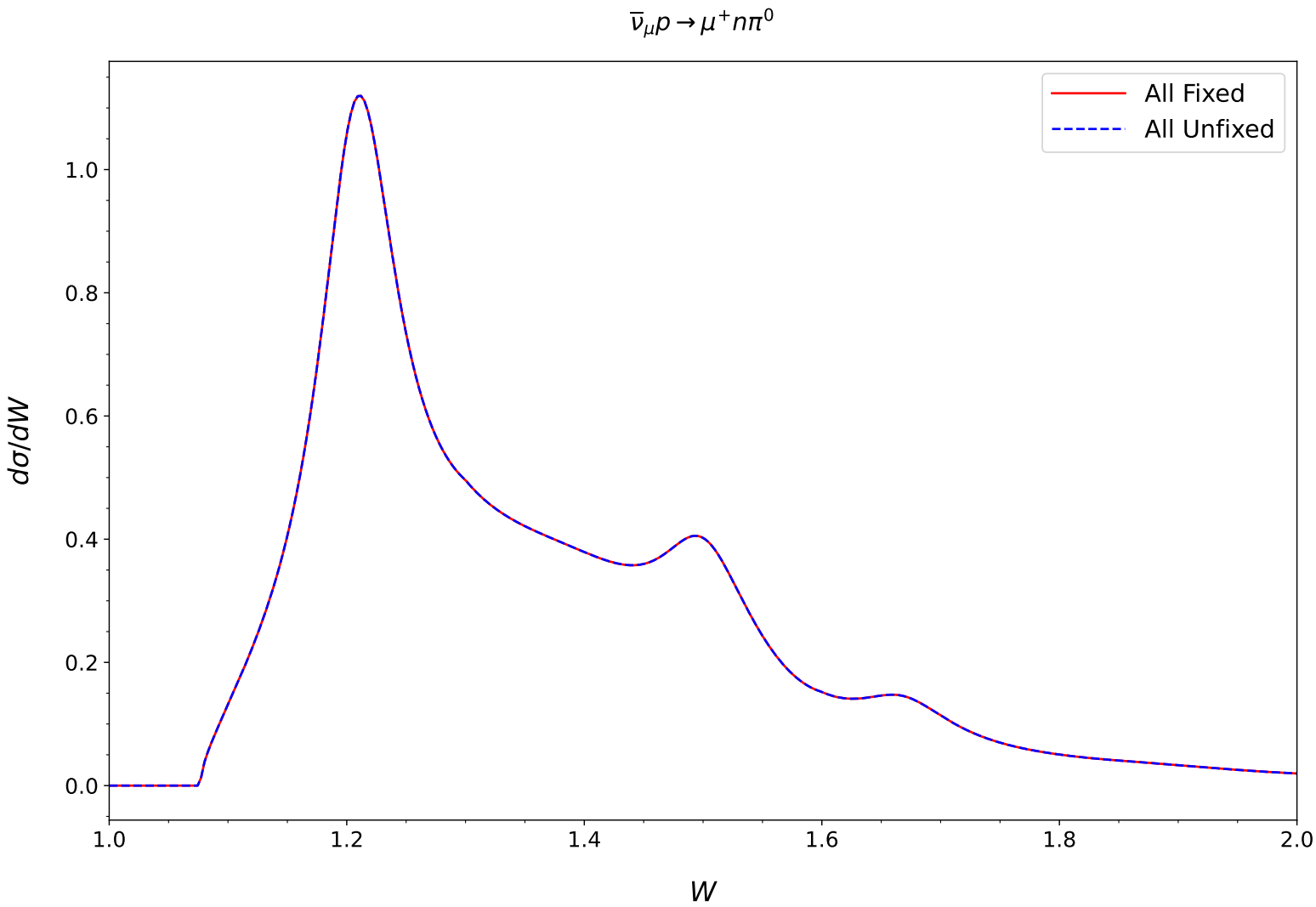

$d\sigma/dW$ with no W_{cut}. Neutrino energy is 5.0 GeV.

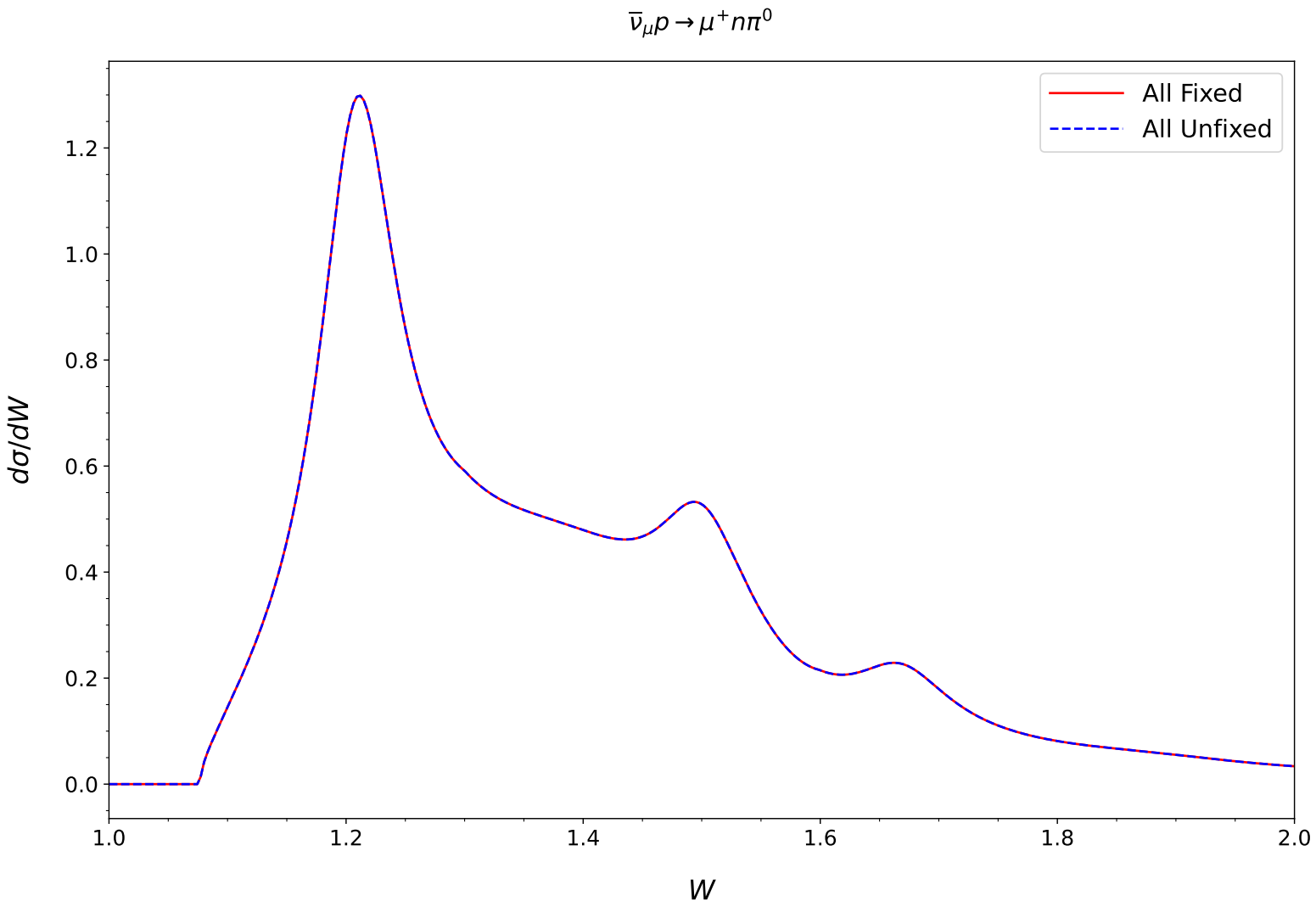

$d\sigma/dW$ with no W_{cut}. Neutrino energy is 10.0 GeV.

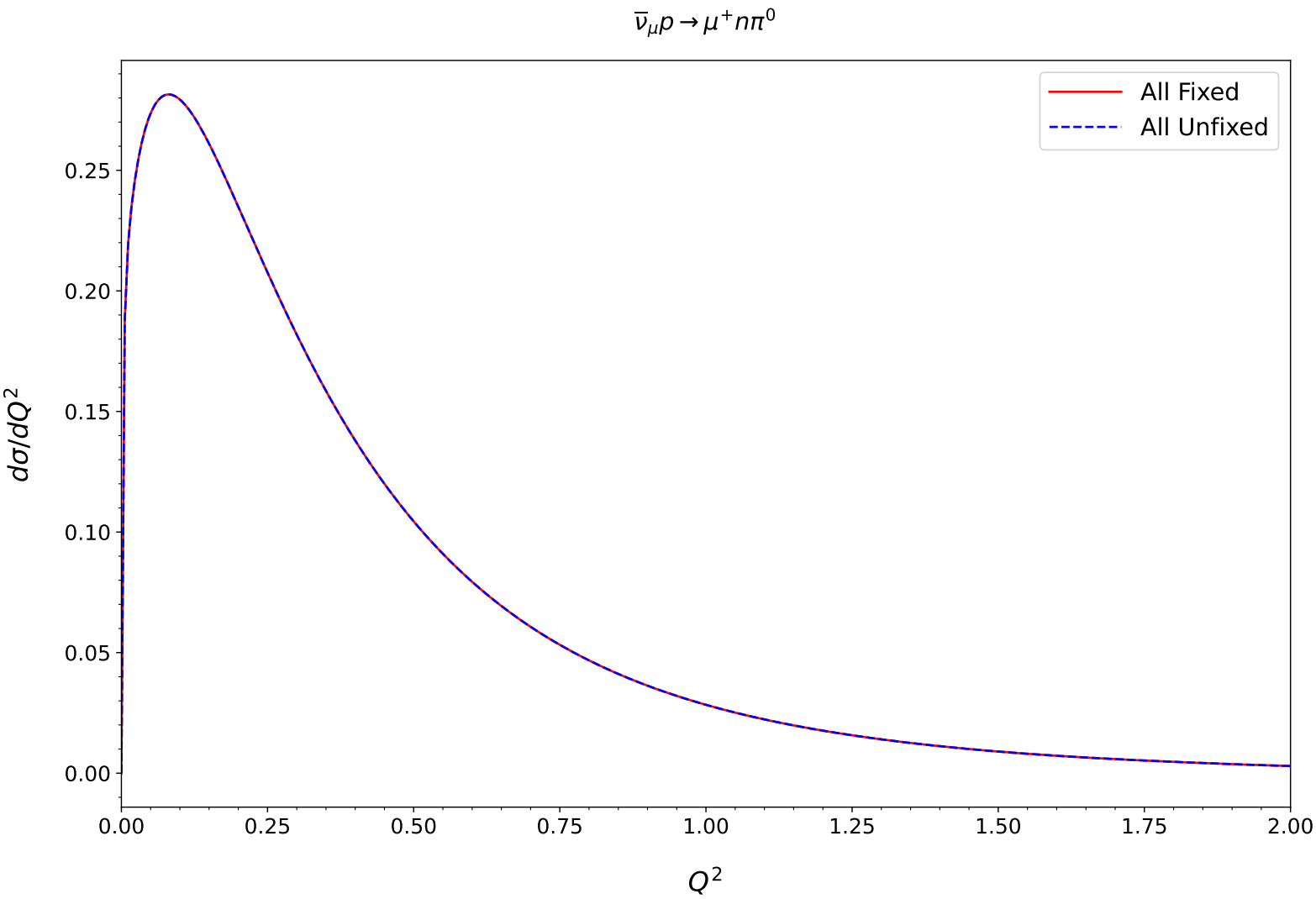

$d\sigma/dQ^2$ with no W_{cut}. Neutrino energy is 2.0 GeV.

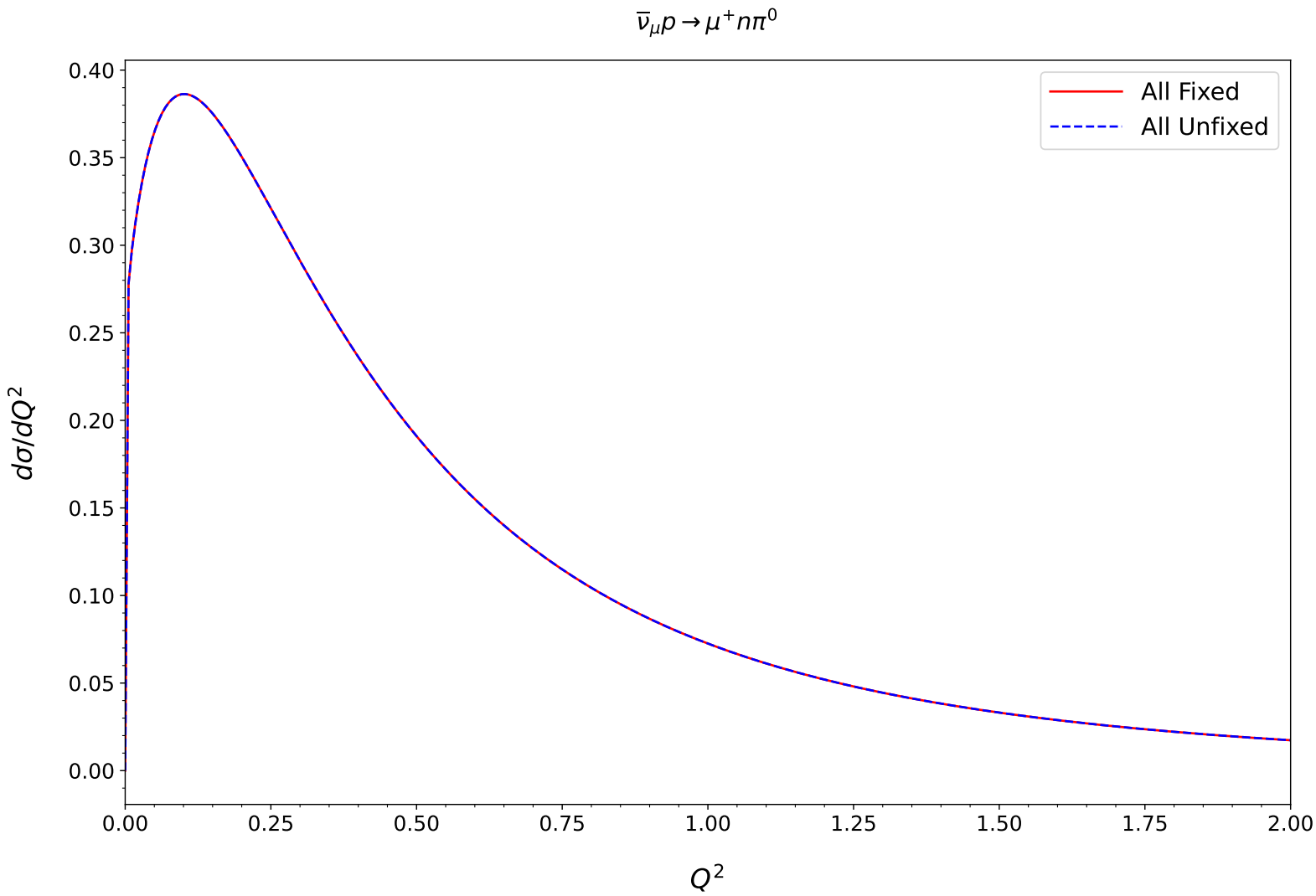

$d\sigma/dQ^2$ with no W_{cut}. Neutrino energy is 5.0 GeV.

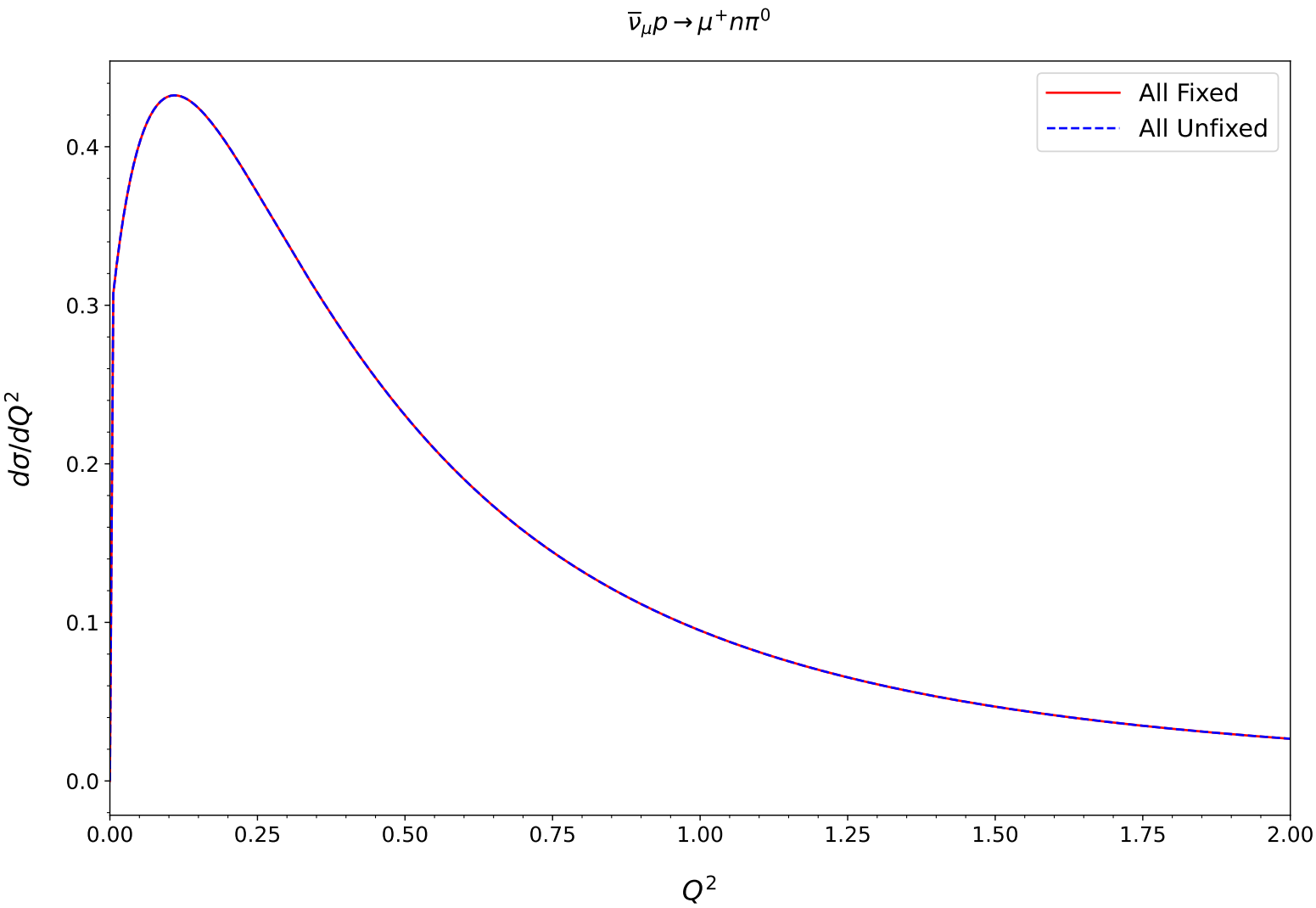

$d\sigma/dQ^2$ with no W_{cut}. Neutrino energy is 10.0 GeV.

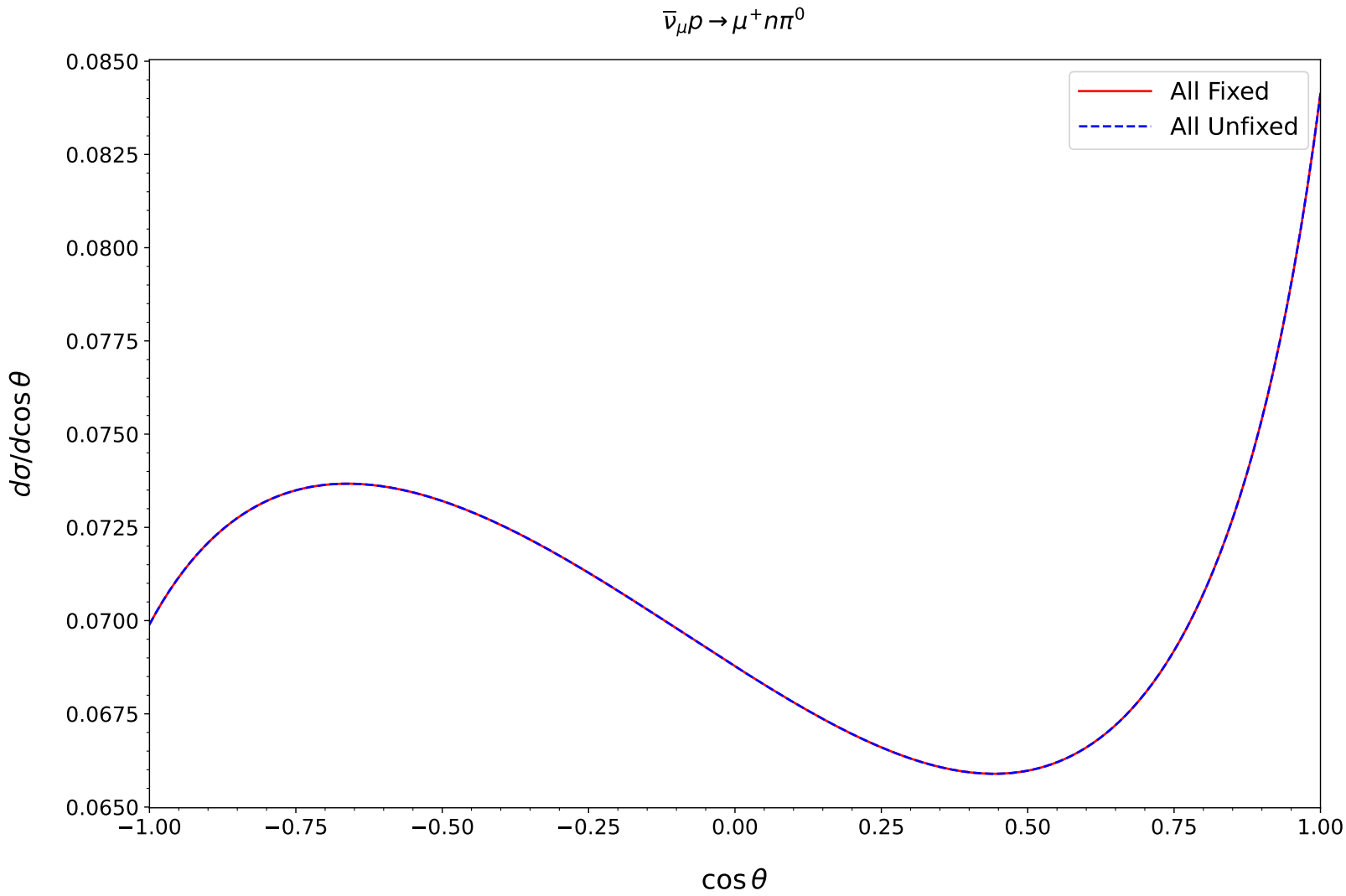

Cosine of pion zenith angle in Adler frame with no W_{cut}. Neutrino energy is 2.0 GeV.

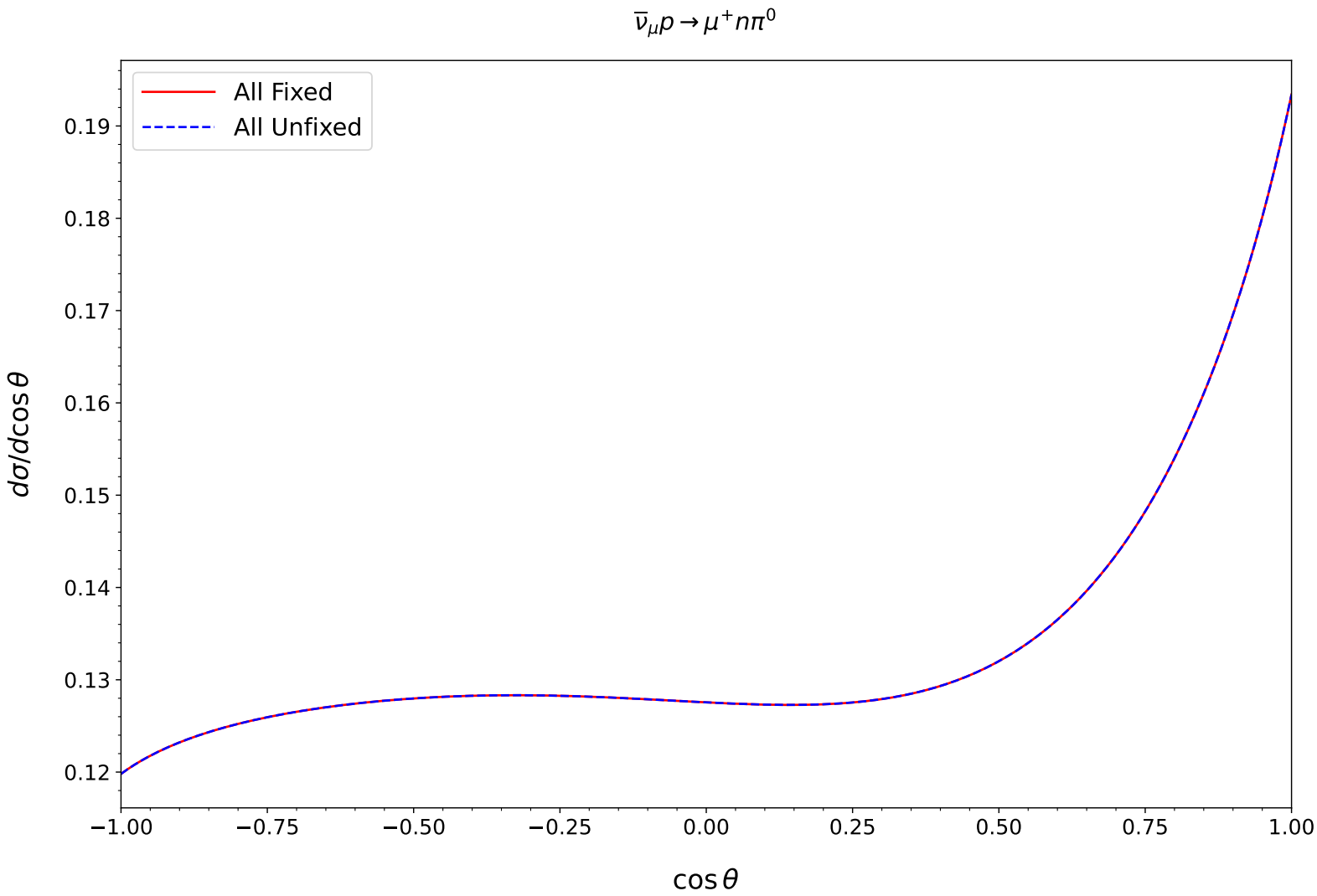

Cosine of pion zenith angle in Adler frame with no W_{cut}. Neutrino energy is 5.0 GeV.

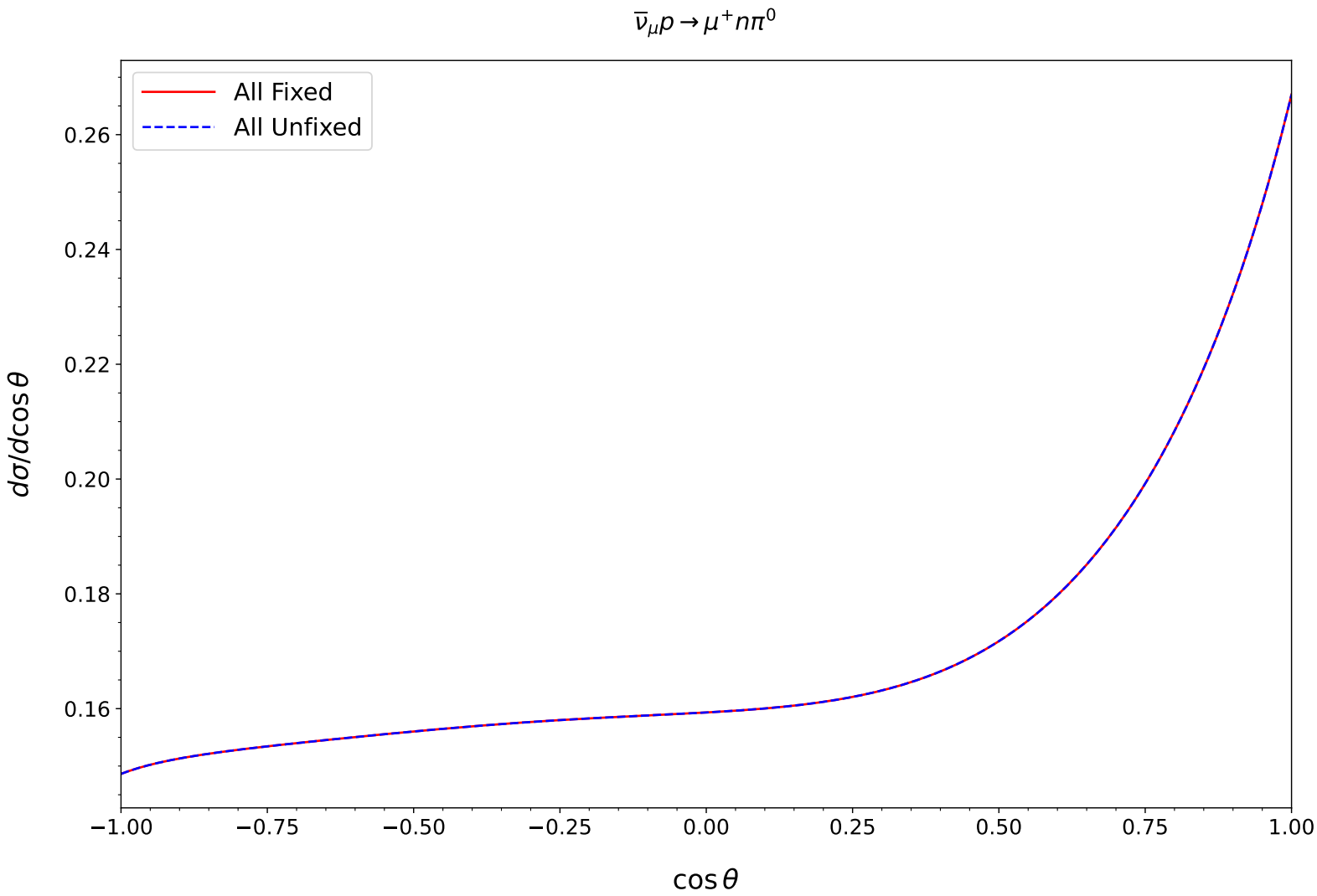

Cosine of pion zenith angle in Adler frame with no W_{cut}. Neutrino energy is 10.0 GeV.

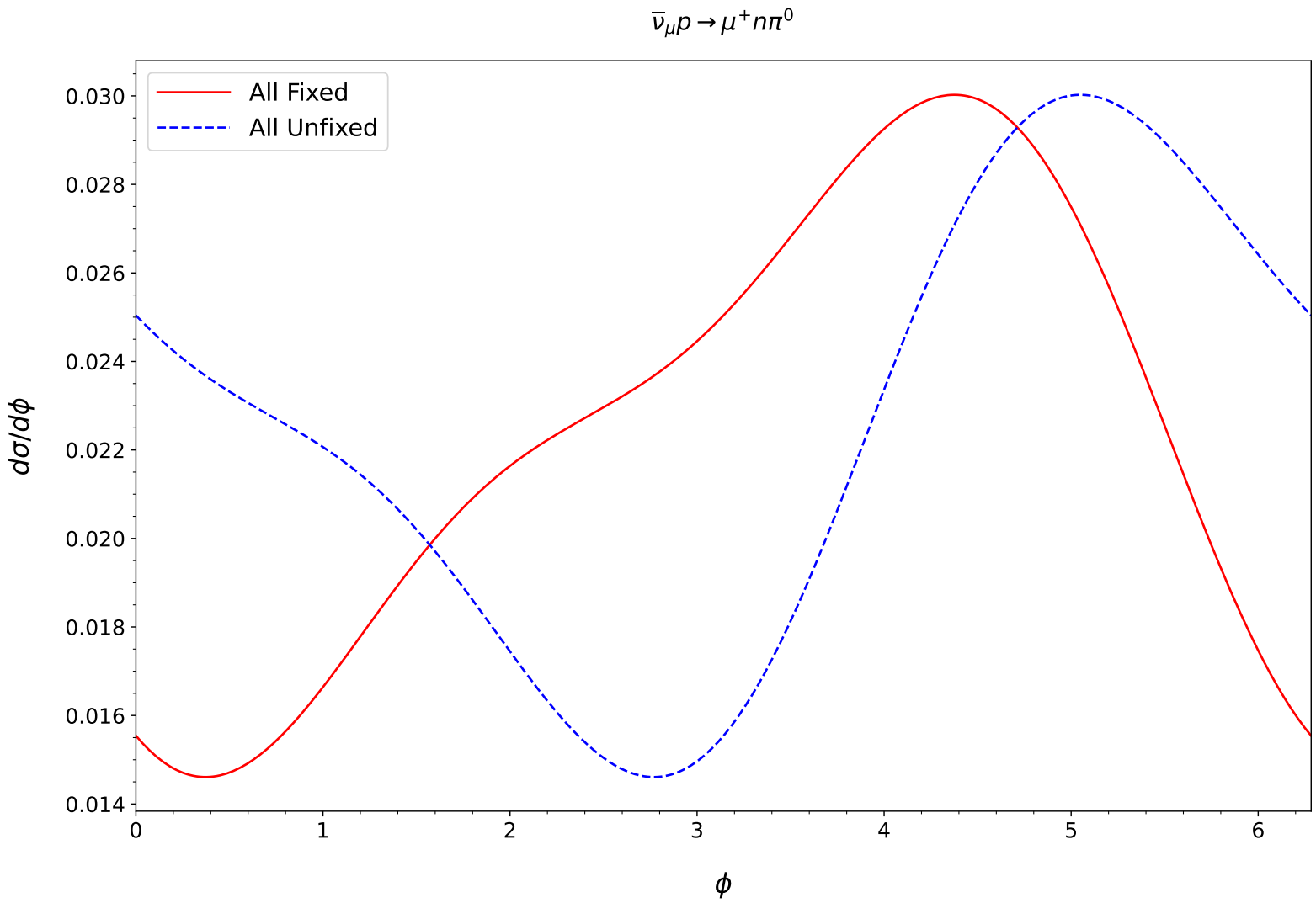

Pion azimuthal angle in Adler frame with no W_{cut}. Neutrino energy is 2.0 GeV.

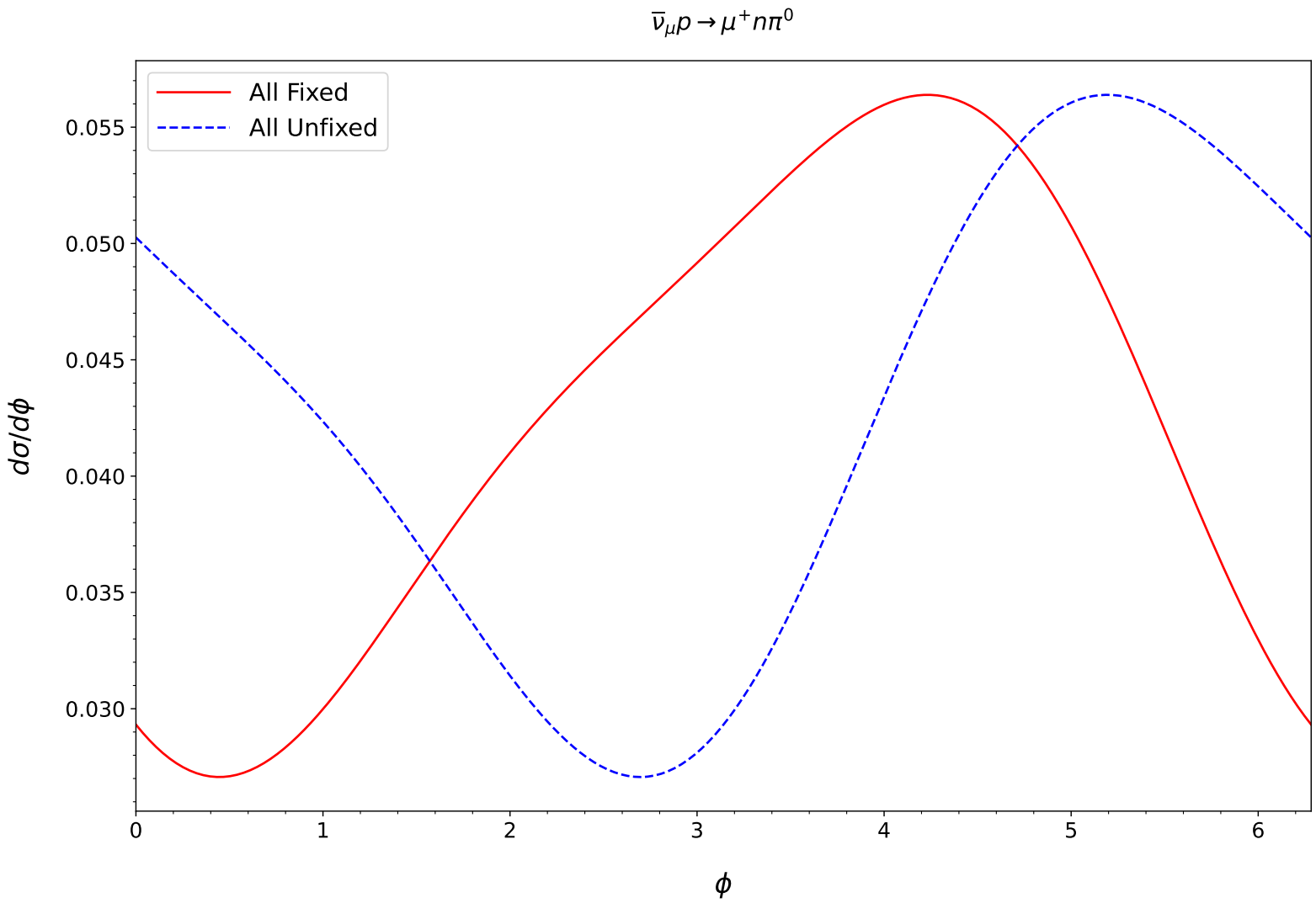

Pion azimuthal angle in Adler frame with no W_{cut}. Neutrino energy is 5.0 GeV.

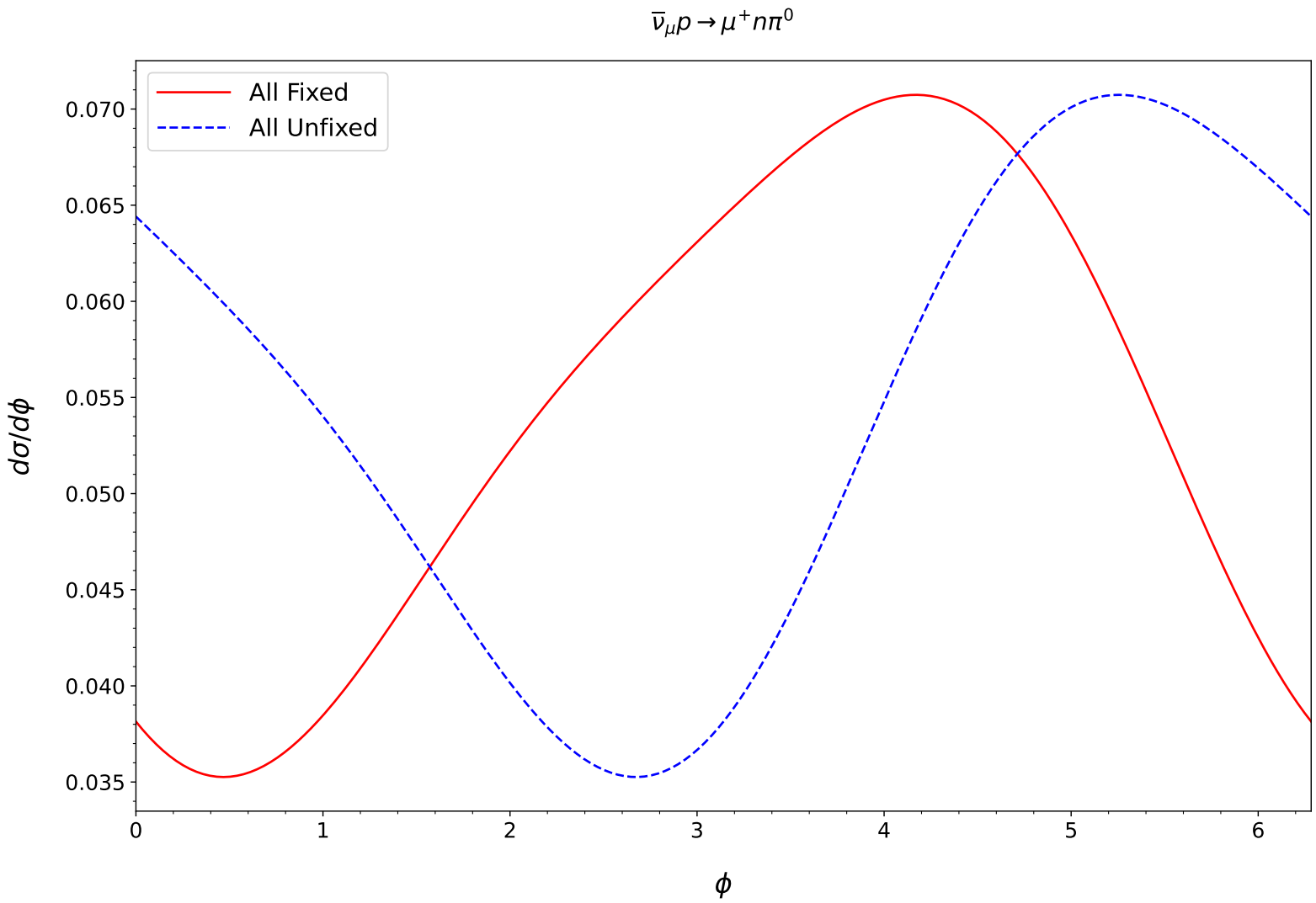

Pion azimuthal angle in Adler frame with no W_{cut}. Neutrino energy is 10.0 GeV.